Helsinki University of Technology Control Engineering Laboratory

Espoo 2001 Report 127

MEASURING, MODELLING AND CONTROLLING THE pH VALUE AND THE DYNAMIC CHEMICAL STATE

Jean-Peter Ylén

TEKNILLINEN KORKEAKOULU
TEKNISKA HÖGSKOLAN
HELSINKI UNIVERSITY OF TECHNOLOGY
TECHNISCHE UNIVERSITÄT HELSINKI
UNIVERSITE DE TECHNOLOGIE D´HELSINKI

Helsinki University of Technology Control Engineering Laboratory

Espoo November 2001 Report 127

MEASURING, MODELLING AND CONTROLLING THE pH VALUE AND THE DYNAMIC CHEMICAL STATE

Jean-Peter Ylén

Dissertation for the degree of Doctor of Science in Technology to be presented with due permission of the Department of Automation and Systems Technology for public examination and debate in Council Room at Helsinki University of Technology (Otakaari 1 F, Espoo, Finland) on the 14th of December, 2001, at 12 noon.

Helsinki University of Technology

Department of Automation and Systems Technology

Control Engineering Laboratory

Distribution:
Helsinki University of Technology
Control Engineering Laboratory
P.O. Box 5400
FIN-02015 HUT, Finland
Tel. +358-9-451 5201
Fax. +358-9-451 5208
E-mail: control.engineering@hut.fi
http://www.control.hut.fi/

ISBN 951-22-5782-3
ISSN 0356-0872

Picaset Oy
Helsinki 2001

HELSINKI UNIVERSITY OF TECHNOLOGY
P.O. BOX 1000, FIN-02015 HUT
http://www.hut.fi

ABSTRACT OF DOCTORAL DISSERTATION

Author Jean-Peter Ylén

Name of the dissertation

Measuring, modelling and controlling the pH value and the dynamic chemical state

Date of manuscript 10.09.2001 | Date of the dissertation 14.12.2001

☑ Monograph ☐ Article dissertation (summary + original articles)

Department Department of Automation and Systems Technology
Laboratory Control Engineering Laboratory
Field of research Process Control
Opponent(s) Professors Dale E. Seborg and Pentti Lautala
Supervisor Professor Heikki Koivo
(Instructor)

Abstract

pH value is a challenging quantity to measure, model and control. In fact, pH value is a mere one-dimensional projection of a multi-dimensional quantity called chemical state and measuring, modelling and controlling the chemical state is much more challenging.

This thesis contributes to all aspects of pH processes. A new method for measuring the pH value under difficult conditions (pressure and flow variations in thick pulp) is presented. Classical physico-chemical modelling of chemical systems is extended with a concept of population principle which is a new formulation of the "reaction invariant – reaction variant" structure. Self-organising fuzzy controller (SOC) is modified to suit pH-processes better (high frequency noise and oscillations are damped more efficiently).

All the methods described above were tested with practical applications that include a pilot neutralisation process, an industrial ammonia scrubber and a paper machine wet end. The new methods showed such a significant improvement that they were installed permanently on the industrial applications.

Keywords self-organising fuzzy control, industrial control, pH modelling, pH measurement, adaptive control, pH control

UDC 66.012:681.5:541.132.3:519.8 | Number of pages 145

ISBN (printed) 951-22-5782-3 | ISBN (pdf) 951-22-5783-1

ISBN (others) | ISSN 0356-0872

Publisher Helsinki: University of Technology, Control Engineering Laboratory

Print distribution Helsinki: University of Technology, Control Engineering Laboratory

☑ The dissertation can be read at http://lib.hut.fi/Diss/

Glenties (pl.n.)

Series of small steps by which someone who has made a serious tactical error in conversation or argument moves from complete disagreement to wholehearted agreement. [1]

Inverinate (vb.)

To spot that both people in a heated argument are talking complete rubbish. [1]

Douglas Adams & John Lloyd: *The Deeper meaning of liff – A dictionary of things that there aren't any words for yet [1]*.

Preface

Clackavoid (n.)
The technical term for a single page of script from an Australian soap opera. [1]
Querrin (n.)
A person that no one has ever heard of who unaccountably manages to make a living writing prefaces. [1]

The research work for this thesis was carried out at the Control Engineering Laboratory, Helsinki University of Technology in the turn of the millennium. There are many people and institutions who deserve a special thank

- My supervisor, professor Heikki Koivo for his help, support and guidance.
- The staff of control engineering laboratory in Helsinki University of Technology for creating an encouraging and absurd surrounding which is very fertile for research.
- Pentti Jutila for introducing me to the world of pH measurement, modelling and control. His expertise and guidance throughout the research has been irreplaceable and he also pushed me into working day and night at odd hours.
- Kai Zenger for ridiculing and shooting down every idea I had (or indeed, any idea anyone ever has). He is a constant source of progress as he makes people excel themselves.
- Professor Heikki Koivo and Seppo Ahokas for their constant nagging and asking when my thesis will be ready. Without them this thesis would still be in progress.
- Pauli Sipari for the laboratory manager jokes.
- Sari Ahokas for encouragement (she made it clear that I have to thank her in the thesis and she is rather intimidating).
- My mother Helena Ylén, to whom I owe everything.
- The people who worked with me in the research projects, especially Isto Niemi, Pasi Koskela, Veli-Pekka-Jutila, Pekka Komulainen and Terhi Ylöstalo deserve a special thanks.
- My family and friends for understanding that social life is greatly overrated at the final stage of writing thesis.
- Professor Heikki Hyötyniemi just for being Heikki Hyötyniemi (truly unique individual – they broke the mold after he was made – and that is not necessarily a bad thing).

- Professors Jouko Virkkunen and Antti Niemi for introducing feedback in my life.
- My co-workers at InterQuest for putting up with me when I showed up in the mornings weary-eyed after writing the thesis during long nights.
- Mikael Maasalo for singing Mombasa (and the world was never the same).
- The reviewers of this thesis, professors Dale Seborg and Raimo Ylinen for their constructive comments how to improve the thesis.
- Jani Tuuri for services rendered.
- Professor Pentti Lautala who had to read carefully every page of the thesis (and he complained that there were plenty).
- Neles Foundation and the Finnish Society of Automation for the financial support, which is greatly appreciated.
- The Academy of Finland and Tekes, the National Technology Agency, for funding research projects, the results of which are presented in this thesis.

Seriously (if I can), I may crack a joke or two, but the raw fact is, that you guys have been, are and will be a constant source of support and I am truly grateful.

Helsinki, 23rd November, 2001 Jean-Peter Ylén

Contents

Great Wakering (ptcpl. vb.)

Panic which sets in when you badly need to go to the lavatory and cannot make up your mind about what book or magazine to take with you. [1]

Symbols, notations and abbreviations

Cafu (n.)
The frustration of not being able to remember what an acronym stands for. [1]
Pen tre-tafarn-y-fedw (n.)
Welsh word which literally translates as "leaking-biro-by-the-glass-hole-of-the-clerk-of-the-bank-has-been-taken-to-another-place-leaving-only-the-special-inkwell-and-three-inches-of-tin-chain. [1]

$[i]$	Concentration of *i*, reference to bibliography
$\overline{[i]}$	Equilibrium concentration of *i*
$[i]^*$	Flow concentration of *i*, Takes the flow/mixing characteristics but the reaction into consideration
$[i]_0$	Initial concentration of *i*
$[i]_T$	Total concentration of *i*
$\{i\}$	Activity of *i*
$\overline{\{i\}}$	Equilibrium activity of *i*
^	Fuzzy vector containing the membership function activation levels
A	Generally an arbitrary component, Specifically (strong) acid A
a	Genarally an arbitrary stoichiometric coefficient,
a	Weak acid
α	Variance weighting factor
α	Weak acid
α_i	Distribution of component *i*
B	Generally an arbitrary component, Specifically (strong) base B
b	Genarally an arbitrary stoichiometric coefficient
b	Weak base
β	Buffer index, weak base
β	Weak base
C	Chemical content
C	Generally an arbitrary component
CSTR	Continuous stirred tank reactor
C	Generally control, concentration
c	Genarally an arbitrary stoichiometric coefficient, pH-model structure
D	Generally an arbitrary component, derivative action
DCS	Distributed control system

d	Genarally an arbitrary stoichiometric coefficient
d^*	Distance from the optimal line
Δe	Change of error
Δd^*	Change of distance from the optimal line
Δd	Diminishing of distance from the optimal line
E	Standard potential
e	Error signal
F	Faraday constant, flow
f	Activity coefficient, generally an arbitrary function
G	Gibbs free energy
G_e	Gain for error
$G_{\Delta e}$	Gain for the change of error
H	Hydrogen ion, proton
H	Enthalpy, disturbance
h	Sampling time
I	Integral action
ISFET	Ion-sensitive field effect transistor
K	Chemical equilibrium constant
K_a	Acid constant
K_b	Base constant
K_D	Derivative gain
K_I	Integral gain
K_P	Proportional gain
K_{SP}	Solubility product
K_w	Ion product of water
k	Discrete time instant, generally a running integer, bypass coefficient
k_i	Reaction rate constant of the advancing reaction i
k_{-i}	Reaction rate constant of the inverse reaction $-i$
λ	Forgetting factor
M,m	Generally a measurement, Number of membership functions, model in SOC
MIMO	Multiple input – multiple output
μ	Membership function
N	Number of membership functions, Number of samples
n	Number of electrons in a cell reaction, charge number, molar amount, limitation of self-organisation in SOC, generally a running integer
$\bar{n}_\tau$	Average time constant in discrete time instances
P	Pressure, Help variable in recursive variance calculation, generally process
P	Proportional action
p	Vector containing the positions of the membership functions
p(i)	"power" operator, defined as $-\log_{10}(i)$
p	Output correction in SOC
q	Performance criterion, required diminishing of distance
q_v	Performance criterion for variance, maximum allowed variance level
R	Gas constant, Resistance
r	Input correction in SOC
r_i	Reaction rate of the advancing reaction i
r_{-i}	Reaction rate of the inverse reaction i
REF,ref	Reference value
S	Entropy, Generally a system

SISO	Single input – single output
SAE	Strong acid equivalent
SASB	Strong acid - Strong base
SOC	Self-organising fuzzy controller
Σe	Sum of error
$\sigma^2_{\Delta d}$	Variance of Δd
T	Absolute temperature, Total component (sum of the partial components)
T_D	D-time (derivative time), time delay
T_I	I-time (integral time)
TOT	Total
U,u	Voltage, Control signal, generally an input in block diagrams
u_0	Control signal operating point
u^*	Required control signal in SOC
V	Volume
WAWB	Weak acid - weak base
Y,y	Controlled variable, generally an output in block diagrams
x	An arbitrary variable, specifically valve opening

Chapter 1

Introduction

Pulverbatch (n.)

The first paragraph on the blurb of a dust-jacket in which famous authors claim to have had a series of menial jobs in their youth. [1]

pH value is a very common chemical on-line measurement in process industry. Even though it is not an unequivocal measure it is often considered essential in controlling the process as many chemical, physical and biological phenomena are, if not directly, at least indirectly connected to the pH value. The pH value can be used as a quality indicator, a manipulated variable or, as in many cases, a controlled variable.

In the end, everything in this thesis revolves around pH control; a good pH control performance is the final target in every application that is presented. However, there are many different elements that all contribute to pH control problem, including the basic understanding of what pH value actually is, pH measurement, pH modelling and simulation and finally the actual pH control. All these elements are looked into, at least superficially, in the thesis.

What new does this thesis contribute to pH systems? There is a minor contribution to practical pH measurement but the main contribution is in developing the population principle for pH modelling and self-organising fuzzy controller modification for pH control. All the methods developed are applied to industrial pH processes successfully and these practical applications give important insight to three very different pH problems from the practical point of view. The applications show that the ideas and methods introduced in this thesis are not only of academic interest but they can easily be adapted to industrial pH processes as well.

The thesis is divided into two sections; the first part deals with definitions, measurement, modelling and simulation as well as control of pH value. The approach is rather general and the results can be applied to an arbitrary pH process. Most of the theoretical contribution of the thesis is included in this part. The second part contains practical applications in three different pH processes: a pilot neutralisation plant, an industrial ammonia scrubber and acidification of thick de-inked pulp.

In order to understand better the principles of measuring, modelling and controlling the pH value, one has to be familiar with the basic properties of liquids, ionic reactions and what is their relation to pH value. In chapter 2 the concept of pH is looked upon with some detail. The terminology and symbols used in this thesis are also mainly introduced in this chapter.

In many cases the quality of the pH measurement is the reason for poor pH control performance. Different pH measuring principles, solutions and weaknesses are presented in chapter 3. Many of the pH measurement problems are due to the lack of understanding the measurement principle and consequently they can usually be easily solved. This thesis contains a minor contribution to a specific measurement problem in chapter 6.

Modelling and simulation issues of a pH process are studied in chapter 4. The traditional pH-models: Wiener models, reaction invariants and physico-chemical models that separate the dynamics and highly nonlinear static pH mapping are extended with the introduction of population principle. In population principle the difficult system of stiff differential equations is converted into two parts: a part that includes the quick reactions and a part containing an ordinary non-stiff dynamic model that includes the slow limiting phenomena.

The basic control paradigms, including feedback and feedforward structures, applied to pH process are presented in chapter 5. Adaptive and nonlinear control is used in pH processes and therefore a short introduction to them is included as well. More details of the modified self-organising control algorithm (SOC) is given. SOC is used in two practical applications and, in fact, the modified algorithm is a significant part of the contribution of this thesis.

Practical applications, including a laboratory neutralisation process, an industrial ammonia scrubber and deinked pulp acidification in a paper machine, are presented in chapter 6. Neutralisation pilot plant is a small, versatile, laboratory-scale process. It is an excellent test bench for different modelling and control approaches because the process is well known (both the equipment and the source materials in the flows) and any number of load and buffer changes are easily created. With different raw materials an arbitrary difficult control problem can be created.

An industrial ammonia scrubber is a much more difficult process to control. There are numerous unknown disturbances and there is only a limited amount of knowledge of the reacting components, which change constantly. As a pH process the ammonia scrubber is a highly nonlinear and time-variant system that forms a challenging control problem. From modelling point of view the system is not the most difficult one as it can be described with a time-variant Wiener model. The only problem is that all the reacting components are not known in the actual process. The modified SOC-algorithm was used successfully to control the pH value in this application.

Acidification of thick de-inked pulp is a difficult process to model and the pH measurement is problematic. Once the pH measurement problem is solved the pH control problem is not too difficult. However, there is a different kind of pH control problem altogether as a new question arises: What is an optimal pH-value for the de-inked pulp under different conditions? When a satisfactory answer is found the actual pH control is easily performed. Experimental and theoretical modelling is used for clarifying this question and the population principle proved to be beneficial in this process as there are several slow limiting phenomena present. The limiting phenomena include phase change (evaporation, dissolution, precipitation) and mass transfer between liquid phase and fibres.

This thesis requires very little prior knowledge on the subject from the reader; most of the basics are explained in the first chapters. The reason for this is the fact that people who are familiar with the chemistry behind the pH value are not often experts in control engineering and control engineers who understand the principles of nonlinear and adaptive control seldom grasp what pH value actually stands for. The reader who is experienced in both aspects of pH control can easily omit the first chapters.

Chapter 2

General properties of liquids and the pH value

Tulsa (n.)
A slurp of beer which has accidentally gone down your shirt collar. [1]
Tomatin (n.)
The chemical from which tinned tomato soup is made. [1]

This chapter explains what pH value stands for and how it is related to chemical properties of a liquid system. Much of the terminology and symbols used in the thesis are introduced within this chapter as well. From chemical point of view some basic definitions are reviewed mainly from the areas of ionic equilibrium, reaction kinetics and thermodynamics.

2.1 Liquids

Liquid phase systems consist of a solvent and dissolved components. The most typical solvent is water, the properties of which are well known. Most of the chemical constants related to pH are connected to systems where water is used as a solvent.

When solid compounds are introduced to water, there is an upper limit how much substance can be dissolved. This limit is called solubility. When the solvent contains the maximum amount of dissolved component or more (solid phase contains the excess component) the solution is called saturated.

The concentration of a solution $[\cdot]$, is defined as the amount of dissolved substance per the amount of solvent. Concentration is usually given in moles/litre (sometimes mol/ft^3, g/l and also mass- or volumetric percentages, etc.).

The compounds that form ionic bonds dissolve into ions in water. A typical example is dissolving of sodium chloride:

$$\mathrm{NaCl} \Leftrightarrow \mathrm{Na}^+ + \mathrm{Cl}^- . \tag{2.1}$$

Many physical phenomena are related to the activity $\{\cdot\}$ of a given ion. In dilute solutions the activity coincides with the concentration but in more concentrated solutions there can be significant

differences. In literature the activity is sometimes described as the efficient concentration. The relation between concentration and activity of a substance *i* is often assumed to be as follows:

$$\{i\} = f_i \cdot [i]. \tag{2.2}$$

The activity coefficient *f* is assumed to be one in very dilute solutions. For somewhat more concentrated solutions the activity coefficient can be estimated with the help of ionic strength. For very concentrated solutions the calculation of *f* becomes rather complicated.

There are many excellent books on the field of ionic equilibrium and pH systems. The notations used in this thesis are similar to those of Butler [8] and Bates [5]. These books are also recommended, if a more detailed treatment on the subject is required.

2.2 Chemical reactions

Most chemical reactions are reversible. There are always two reactions taking place simultaneously; advancing reaction and inverse reaction. Consider the general case:

$$a\mathrm{A} + b\mathrm{B} \Leftrightarrow c\mathrm{C} + d\mathrm{D}. \tag{2.3}$$

The reversible reaction consists of the advancing reaction $a\mathrm{A} + b\mathrm{B} \rightarrow c\mathrm{C} + d\mathrm{D}$ and the inverse reaction $c\mathrm{C} + d\mathrm{D} \rightarrow a\mathrm{A} + b\mathrm{B}$.

The reaction that takes place with a single step is called a unit reaction. For unit reactions the rate of reaction depends on the activities of the participating components. For advancing reaction the reaction rate is as follows:

$$r_1 = k_1 \cdot \{\mathrm{A}\}^a \cdot \{\mathrm{B}\}^b \tag{2.4}$$

Correspondingly for the inverse reaction:

$$r_{-1} = k_{-1} \cdot \{\mathrm{C}\}^c \cdot \{\mathrm{D}\}^d \tag{2.5}$$

The reaction rate constants k_1 and k_{-1} have a very notable dependency on temperature. In some cases the dependency can be described with the Arrhenius equation.

At equilibrium, the reaction rates of the advancing and the inverse reaction are the same ($r_1 = r_{-1}$) and the overall reaction does not advance in either direction.

$$k_1 \cdot \overline{\{\mathrm{A}\}}^a \cdot \overline{\{\mathrm{B}\}}^b = k_{-1} \cdot \overline{\{\mathrm{C}\}}^c \cdot \overline{\{\mathrm{D}\}}^d. \tag{2.6}$$

The ratio of the reaction rate constants is called the equilibrium constant *K* as follows

$$\frac{k_1}{k_{-1}} = \frac{\overline{\{\mathrm{C}\}}^c \cdot \overline{\{\mathrm{D}\}}^d}{\overline{\{\mathrm{A}\}}^a \cdot \overline{\{\mathrm{B}\}}^b} = K. \tag{2.7}$$

A large value of the equilibrium constant indicates that the overall reaction tends to go to the right towards the reaction products and a small value that the overall reaction tends to go to the left towards the source materials. Similarly to the reaction rate constants the equilibrium constant also depends on the temperature.

2.3 Acids and bases

Acids contain hydrogen that can be released under certain conditions. Acids can be monoprotic or polyprotic (diprotic, triprotic, etc.) depending on the number of hydrogen ions H^+ that they can donate. The hydrogen ion H^+ forms different compounds with the water molecule, but usually in acid-base systems all the hydrogen ion combinations (e.g. H_3O^+, $H_9O_4^+$) are symbolised with a simple hydrogen ion H^+ or an oxonium ion H_3O^+.

$$HA + H_2O \Leftrightarrow A^- + H_3O^+ \quad \text{(monoprotic acid).} \tag{2.8}$$

$$H_3A + 3H_2O \Leftrightarrow A^{3-} + 3H_3O^+ \quad \text{(triprotic acid).} \tag{2.9}$$

Polyprotic acids donate the hydrogen ions in several stages and therefore reaction (2.9) can be separated into three unit reactions.

$$\begin{cases} H_3A + H_2O \Leftrightarrow H_2A^- + H_3O^+ \\ H_2A^- + H_2O \Leftrightarrow HA^{2-} + H_3O^+ \\ HA^{2-} + H_2O \Leftrightarrow A^{3-} + H_3O^+ \end{cases}. \tag{2.10}$$

Bases can accept hydrogen ions and similarly to acids they can be called monoprotic or polyprotic as well

$$B + H_2O \Leftrightarrow HB^+ + OH^-. \tag{2.11}$$

The hydrogen ion is actually a mere proton and therefore in literature the acids are defined as proton donors and the bases as proton acceptors. Every acid HA has a corresponding base A^- and together they form an acid-base pair. Substance that can either accept or donate a proton is called an ampholyte. The most important ampholyte is water (as can be seen from all the previous examples).

2.3.1 Acid-base constants

The equilibrium constants can also be written for acids and bases. For monoprotic acids, that obey the reaction (2.8) the equilibrium constant is defined as follows

$$K = \frac{\overline{\{A^-\}} \cdot \overline{\{H_3O^+\}}}{\overline{\{HA\}} \cdot \overline{\{H_2O\}}}. \tag{2.12}$$

The reaction takes place in an aqueous solution and the activity (and the concentration) of water can be considered as a constant and combined to the equilibrium constant

$$K_a = K \cdot \overline{\{H_2O\}} = \frac{\overline{\{A^-\}} \cdot \overline{\{H_3O^+\}}}{\overline{\{HA\}}}. \tag{2.13}$$

The modified equilibrium constant is called the acid constant. For bases a corresponding base constant is developed. For reaction (2.11) the base constant is given by the relation:

$$K_b = \frac{\overline{\{HB^+\}} \cdot \overline{\{OH^-\}}}{\overline{\{B\}}}. \tag{2.14}$$

Polyprotic acids and bases have equilibrium constants for each dissociation step. The acid constants of a triprotic acid, which follows the reaction mechanism (2.10) are as follows

$$K_{a1} = \frac{\overline{\{H_2A^-\}} \cdot \overline{\{H_3O^+\}}}{\overline{\{H_3A\}}},\ K_{a2} = \frac{\overline{\{HA^{2-}\}} \cdot \overline{\{H_3O^+\}}}{\overline{\{H_2A^-\}}},\ K_{a3} = \frac{\overline{\{A^{3-}\}} \cdot \overline{\{H_3O^+\}}}{\overline{\{HA^{2-}\}}}. \tag{2.15}$$

The acid and base constants describe the strength of the acids and bases. A large acid constant indicates a strong acid that donates practically all the protons. The concentration of hydrogen ions is the same as the concentration of the dissolved acid. Weak acids have a small acid constant and only some of the protons that could be released are actually donated.

The equilibrium of weak acids and bases can be moved to either side of the reaction by adding or removing reaction products or source materials. A typical method of removing reaction products is the neutralisation of a solution by adding bases to acids and vice versa.

2.3.2 Neutralisation

The oxonium ion H_3O^+ (hydrogen ion H^+) and the hydroxide ion OH^- neutralise each others producing water

$$H_3O^+ + OH^- \Leftrightarrow 2H_2O. \tag{2.16}$$

Consider an example where sodium hydroxide and hydrochloride acid are mixed together:

$$\begin{cases} NaOH \Leftrightarrow Na^+ + OH^- \\ HCl + H_2O \Leftrightarrow Cl^- + H_3O^+ \\ H_3O^+ + OH^- \Leftrightarrow 2H_2O \end{cases}. \tag{2.17}$$

The overall reaction can be presented as follows:

$$NaOH + HCl \Leftrightarrow Na^+ + Cl^- + H_2O. \tag{2.18}$$

The result of mixing equal amounts of sodium hydroxide and chloride acid is a neutral solution containing table salt and water.

2.3.3 Ionic product of water

The neutralisation reaction (2.16) is also reversible. The inverse reaction is called the autoprotolysation of water

$$2H_2O \Leftrightarrow H_3O^+ + OH^-, \qquad K = \frac{\overline{\{H_3O^+\}} \cdot \overline{\{OH^-\}}}{\overline{\{H_2O\}}^2}. \tag{2.19}$$

The equilibrium constant is modified similarly to the acid and base constants

$$K_w = K \cdot \overline{\{H_2O\}}^2 = \overline{\{H_3O^+\}} \cdot \overline{\{OH^-\}} . \tag{2.20}$$

The modified equilibrium constant is called the ionic product of water (at 25 °C $K_w = 1.0 \cdot 10^{-14}$ $(mol/l)^2$).

2.3.4 Definition of pH

In acidic solutions there are more oxonium ions than hydroxide ions present, and vice versa for alkalinic solutions. If the system is neutral, there are equal amounts of both ions. Section 2.3.3 stated that the product of oxonium and hydroxide ion activities (efficient concentrations) is constant. The definitions of acidic and alkalinic liquids are therefore, as follows

$\{H_3O^+\} > \{OH^-\}$	acidic,
$\{H_3O^+\} = \{OH^-\} = \sqrt{K_w} = 1.0 \cdot 10^{-7}$, (at 25°C)	neutral,
$\{H_3O^+\} < \{OH^-\}$	alkalinic.

For practical reasons the logarithmic scale is more appealing. The pH-value is defined as:

$$\mathrm{pH} = -\log_{10}\{H_3O^+\} = -\lg\{H_3O^+\}. \tag{2.21}$$

At 25°C the neutrality of a solution is given as (the pH varies usually between 1 and 14 but higher or lower values are also possible.):

pH < 7	acidic,
pH = 7	neutral,
pH > 7	alkalinic.

Weak acids and bases have equal amounts of dissociated and undissociated forms when the oxonium ion concentration is equal to the equilibrium constant as can be seen from formulas (2.13) - (2.15). There are important practical phenomena when this happens (such as maximum buffering that is explained in the next chapter) and therefore the corresponding pH-value is significant. Often the equilibrium constants K_a and K_b are given in pK_a and pK_b values the definitions of which are identical to (2.21)

$$\mathrm{p}\,K_a = -\lg K_a\,,\ \mathrm{p}\,K_b = -\lg K_b\,. \tag{2.22}$$

pK_a and pK_b values indicate directly important pH ranges that have practical significance.

2.3.5 Buffer solutions

In many practical situations the pH-value should be close to an optimal value. This is typically the case for biochemical processes. The solution should be insensitive to small additions of acids or bases and if this applies the solution is called a buffer solution. Many natural systems contain buffer solutions (e.g., blood) but buffers can be produced artificially as well from weak acids and bases and their salts.

A typical buffer solution can be produced from acetic acid (HAc) and sodium acetate (NaAc). The resulting solution contain both acetic acid and acetic ion (Ac^-). The reactions are as follows:

$$HAc + H_2O \Leftrightarrow Ac^- + H_3O^+ . \tag{2.23}$$

If acid is added, the free hydrogen ion (oxonium ion) reacts with the excess acetic ion forming acetic acid (inverse reaction). The pH is not significantly affected until the buffer solution runs out of acetic ions. Correspondingly, if base is added, the free hydroxium ions react with hydrogen ions forming water. The acetic acid dissociates more (advancing reaction) in order to satisfy the equilibrium condition. The pH changes only little until the buffer solution runs out of acetic acid. The buffer solution can be considered as a reservoir of ions that are released when needed in the reaction. The efficiency of a buffer solution is described with the buffer index β that is defined in the next chapter.

2.4 Gibbs free energy

Deep understanding of the chemical equilibrium can only be achieved by means of thermodynamics but that is out of the scope of this thesis A good reference book for thermodynamics can be found in [68]. The elementary principles relay on the Gibbs free energy that is defined by the relation

$$G = H - TS \tag{2.24}$$

where H is the enthalpy, T the absolute temperature and S the entropy. Any free system is autonomously moving towards small values of G and it will not stop until is has reached the minimum Gibbs free energy, i.e., the equilibrium.

The practical significance of this fundamental truth is in the fact that many parameters and constants related to Gibbs free energy are tabled or easily calculated enabling the determination of the equilibrium constants in changing situations such as varying temperatures. The free energy of any substance X can be calculated as follows:

$$G_X = G_X^0 + RT \ln\{X\} \tag{2.25}$$

where G_X^0 is standard free energy and R is the gas constant. For reaction $a\mathrm{A} + b\mathrm{B} \Leftrightarrow c\mathrm{C} + d\mathrm{D}$ the change of Gibbs free energy is

$$\Delta G = cG_C + dG_D - aG_A - bG_B = G^0 + RT \ln \frac{\{C\}^c \{D\}^d}{\{A\}^a \{B\}^b} . \tag{2.26}$$

The change in the free energy is equal to the negative of the maximum work.

2.5 Chemical energy and electrical energy

Chemical energy can be transformed into electrical energy in a galvanic element that is founded on two electrodes with liquid contact. If a metallic element is introduced to ionised salt liquid containing the same metal ion, there is an equilibrium. The electrons and metal ions remain in different phases close to each others creating an electrical potential difference.

The potential of the galvanic element is a direct measure of the cell work and correspondingly also of the change in the free energy. The free energy change can be calculated as follows:

$$\Delta G = -nFE\,, \tag{2.27}$$

where n is the number of electrons transferred in the cell reaction, F is the Faraday constant and E is the cell potential. By combining equations (2.26) and (2.27) the Nernst equation is obtained

$$E = E^0 - \frac{RT}{nF} \ln \frac{\{\mathrm{C}\}^c \{\mathrm{D}\}^d}{\{\mathrm{A}\}^a \{\mathrm{B}\}^b} \tag{2.28}$$

where standard potential of the cell E^0 is defined as follows:

$$E^0 = -\frac{G^0}{nF}\,. \tag{2.29}$$

The standard potential of any electrode can be determined by combining it with a reference electrode in a galvanic cell. The standard hydrogen electrode (shown in Fig. 2.1) is arbitrarily chosen as a general reference electrode with a zero potential. The standard hydrogen electrode consists of a platinum plate that is constantly kept saturated with hydrogen by a continuous hydrogen gas stream.

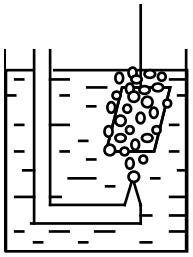

Fig. 2.1: Standard hydrogen electrode

The standard potentials of electrodes measured against standard hydrogen electrode can be found from numerous tables.

Chapter 3

pH measurement

Nad (n.)

Measure defined as the distance between a driver's out-stretched fingertips and the ticket machine in an automatic car-park.

1 nad = 18.4 cm [1]

Ostwaldtwistle (n.)

(Old Norse) Small brass wind instrument used for summoning Vikings to lunch when they're off on their longships, playing. [1]

When constructing pH control the pH measurement is often assumed to be ideal and omitted from controller performance evaluation. From practical point of view this may be the wrong course of action as in several real life applications it is the quality of the pH measurement that is the major hindrance for good controller performance.

pH measurement is unlike most of the on-line measurements in the aspect that it can not be "installed and forgotten". It requires constant maintenance including cleaning, calibration and fault diagnosis and even if the maintenance is performed to the last detail, the pH probe has a process dependent life-span after which it has to be replaced.

The correct installation of the probe is also essential; correct angle, correct depth, different kind of installation if there are solid particles or if the system contains only clear liquid phase. Adequate distance from any components can generate flow and pressure variations, etc.

There are even many cases in which the control performance has been excellent; pH value has shown a straight line for years and the reason for it is that the measurement had had no relation to the actual pH value due to broken connection between the pH-electrode and the reference electrode or between the pH probe and the process liquid. All this emphasises the importance of good quality pH measurement.

This chapter concentrates on the pH sensitive glass electrode that is the most common pH probe in industry. Glass electrode was also used in all practical applications discussed in Chapter 6. A practical application in which the controller performance was limited by the poor measurement is presented in section 6.3. The pH measurement problem is discussed with some detail in [145].

3.1 Measuring of pH value

Almost all practical pH measurements can be divided into three main categories: pH sensitive electrodes (including glass, antimony and enamel electrodes), pH sensitive transistors (ISFET) and pH sensitive optical phenomena. The most common measuring electrode for pH value is the pH sensitive glass electrode that is looked into in the next section.

3.2 pH sensitive glass electrode

Around 1906 Cremer found that some types of glass gave a potential difference, the magnitude of which depended on the acidity of the liquid in which the glass was immersed, [11]. Later Haber and Klemensiewics proved that this potential difference, within a fixed pH range, followed Nernst´s potential in the same way as the hydrogen electrode, [31]. Corning Glass Works Inc. developed a well known glass material named Corning 015. It included 72.2 mole-% SiO_2, 6.4 mole-% CaO and 21.4 mole-% Na_2O. This glass type can be used for the pH measurement in the range from 0 to 9. Since that, glass types including in addition LiO_2, Cs_2O, BaO and La_2O_3 were developed. With these also more alkalinic pH values could be measured.

Glass can be considered as an "undercooled" electrolyte consisting of an irregular SiO_2 structure including other components, which move in the interspace. These components give an electron balance of the membrane, see Fig. 3.1. When immersed in aqueous solution, glasses exchange the metal ions of the glass texture with the H^+ ions of the solution. As a result of this reaction a "gel-layer" will be formed on the surface of the glass membrane. This gel-layer is the equivalent of the metal ion layer in the Nernst´s theory and therefore essential for the operation of the glass electrode. After one or two days the electrode reaches an equilibrium, and the resulting gel-layer has a thickness between 10 and 100 nanometers. This mechanism depends on several factors such as the composition of the glass and the temperature in which the glass is immersed. Many theories have been developed on the subject of the gel-layer formation, e.g., [5].

It is to be noted that the electrical potential with a glass electrode is generated in a different way than the one with metal electrodes. In glass electrodes only the charged ions change placements not the electrons.

3.2.1 Construction of the glass electrode

The construction principle of the glass electrode is shown in Fig. 3.2. The electrode consists of a glass tube body, into which a bulb shape membrane of a specific pH glass is welded. The electrode is filled with a buffer solution containing Cl^- ions. Usually the pH value of this electrolyte is 7. An inner electrode, which is constructed of a metal pin covered by its sparingly soluble salt, is connected to the output cable of the electrode. The inner electrode is immersed in the electrolyte containing anions of the salt.

One typical inner electrode is the silver-silver chloride electrode, in which AgCl salt covers the Ag-pin. When the electrolyte contains Cl^- ions, the following electrode reaction occurs:

$$AgCl + e^- \Leftrightarrow Ag + Cl^- . \tag{3.1}$$

A potential difference between the inner electrode pin and the electrolyte is formed as a redox reaction, see Fig 3.2. The value of the potential difference can be calculated from the Nernst equation (2.28).

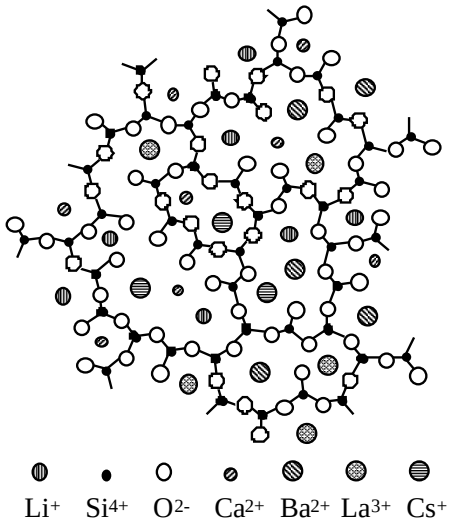

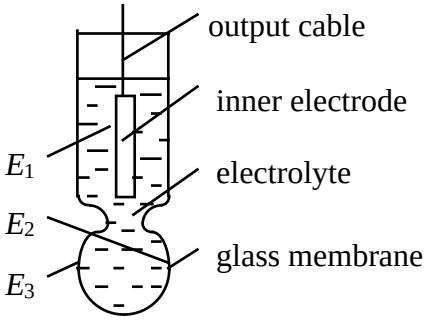

Fig. 3.1: Texture of the pH glass. Fig. 3.2: The construction principle of the glass electrode.

Another common inner electrode is the calomel electrode in which the output cable is in a galvanic connection with mercury, which is in connection with mercury chloride Hg_2Cl_2. This compound is known by the name calomel. The electrode reaction is as follows:

$$Hg_2Cl_2 + 2e^- \Leftrightarrow 2Hg + 2Cl^-. \tag{3.2}$$

The potential difference between the inner electrode and the electrolyte can be calculated from Nernst equation. Thallium amalgam-thallium inner electrode is used especially, when the temperature of the process liquid to be measured is high. In the electrode, thallium amalgam is in connection with thallium chloride.

As mentioned earlier the pH-sensitive membrane is produced from special glass. Its thickness is usually 50-200 μm, but in the measurement of very aggressive solutions it can be even 1 mm. After the immersion in water the glass electrode can measure the process solution. A potential difference between the process liquid and the glass surface is created, and this difference is a function of the activity of H_3O^+ ions and thus also a function of the pH value. Fig. 3.3 shows the structure of a typical glass electrode with a calomel inner electrode.

As shown in figure 3.2 the following three potential differences (source voltages) are created in the glass electrode:

-E_1 between the inner electrode and the electrolyte
-E_2 between the inner surface of the glass electrode and the electrolyte
-E_3 between the outer surface of the glass electrode and the liquid to be measured.

As mentioned earlier E_1 is a constant potential difference. The potential difference E_3 is a significant indicator of the pH value. The Nernst equation holds quite well:

$$E_3 = E_0 + (RT/F)\ln\{H_3O^+\}_{OUTER}, \tag{3.3}$$

where E_0 is constant in a certain temperature, and $\{H_3O^+\}_{OUTER}$ is the activity of the H_3O^+ ions in the process liquid. The pH-sensitive gel-layer will also be developed in the inner surface of the glass membrane. The potential difference E_2 also obeys Nernst equation:

$$E_2 = E_0 + (RT/F)\ln\{H_3O^+\}_{INNER}, \tag{3.4}$$

where $\{H_3O^+\}_{INNER}$ is the activity of the H_3O^+ ions in the electrolyte inside the electrode. Because the electrolyte is a buffer solution, the potential difference E_2 is constant. At constant temperature only E_3 is a variable, and it changes when the H_3O^+ content changes in the measured process liquid.

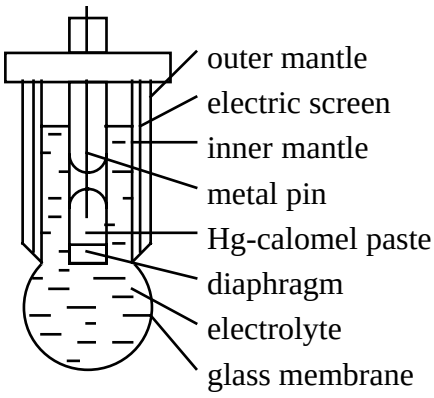

Fig. 3.3: The construction of the glass electrode.

By noting that $\ln\{H_3O^+\} = \ln 10 \lg\{H_3O^+\}$ and $pH = -\lg\{H_3O^+\}$, equation (3.3) can be rewritten as:

$$E_3 = E_0 - (RT \ln 10 / F)\mathrm{pH}_{OUTER}. \tag{3.5}$$

and equation (3.4) as:

$$E_2 = E_0 - (RT \ln 10 / F)\mathrm{pH}_{INNER}. \tag{3.6}$$

The total potential in output cable of the electrode is:

$$E_M = E_1 - E_2 + E_3. \tag{3.7}$$

Equation (3.7) can now be rewritten as:

$$E_M = E_{M0} - (RT \ln 10 / F)\mathrm{pH}_{OUTER}, \text{ where} \tag{3.8}$$

$$E_{M0} = E_1 + (RT(\ln 10)/F)\mathrm{pH}_{INNER}. \tag{3.9}$$

Equation (3.8) shows, that the potential of the glass electrode is a function of the pH value and the temperature. If the glass electrode potential obeys equation (3.8), it is said to be ideal.

3.2.2 Resistance of the glass membrane

The definition of the pH value requires the potential difference of the measuring and the reference electrodes. If it is measured using a semiconductor converter, a small electric current is created through the electrodes. The current penetrates the pH-sensitive membrane, the resistance of which is quite high (about 10 - 500 MΩ in the room temperature), and which varies as a function of the temperature. For instance the resistance of a membrane produced from the Corning 015 glass is about 200 MΩ in the room temperature and 1000 MΩ in the temperature 10°C.

The high resistance of the glass electrode causes practical problems in the construction of the measuring circuits. Different kinds of glass types are developed for different measurement conditions. The important aspects are the acidity and temperature ranges of the liquids to be

measured. However, the resistance of the glass membrane should in all cases be as small as possible.

3.2.3 The asymmetry potential

The reason for the asymmetry potential is the difference in the behaviour of the outer and inner surfaces of the glass membrane. If the inside and outside liquids are identical, and there are identical electrodes on both sides, there still exists a potential difference between the electrodes that is called the asymmetry potential. It is only some millivolts, but it changes slowly during the ageing of the electrode. The reasons for asymmetry potential are:

- different strains in the inner and outer surface of the electrode
- during production thermal effects decrease the amount of cations of the outer surface of the membrane, and that is why the penetration of water is different on different sides of the membrane.
- the outer surface is a vulnerable for mechanical and chemical effects
- the fouling of the membrane

3.2.4 Alkaline and acid errors

The pH measurement error in strong alkalinic liquids is called the alkaline error or sometimes the sodium error. In alkalinic solutions above pH value 9 other monovalent cations such as Na^+ and Li^+ etc. have influence on the electrode potential causing too low measured values. The alkaline error increases with high temperatures. Nowadays special electrodes with a small alkaline error are available. They are well suited for the measurement under strong alkalinic conditions.

In very concentrated acid solutions the output voltage will not completely obey Nernst law. Tests show, that the gel-layer absorbs acid molecules and consequently the hydrogen ion concentration (and activity) increases resulting an increase in pH value. The acid error is significant only at very low pH values and it is relatively small as compared to the alkaline error. Acid error does not depend on the temperature very much.

3.3 Reference electrode

A pH measurement requires both a measuring electrode and a reference electrode giving the reference potential with which the potential of the measuring electrode is compared. The reference potential has to stay constant, when the properties of the process liquid change. On the other hand, the reference electrode constructs a galvanic contact from the process liquid to the pH converter.

3.3.1 Ag-AgCl electrode

This electrode is named after its inner electrode. The inner electrode has the same structure as the corresponding measuring electrode i.e. silver electrode coated with silver chloride immersed in KCl solution. The structure of the electrode is shown in Fig 3.4. In the glass mantle of the reference electrode is a diaphragm, through which the galvanic contact is created. The diaphragm is produced from ceramics, teflon or different kinds of fibres. The KCl solution flows very slowly through the diaphragm and this is why care must be taken, that the KCl solution never runs out. The pressure inside the electrode has to always overcome the pressure of the process liquid at all times. Otherwise the flow through the diaphragm changes direction and the electrode becomes poisoned.

In the diaphragm, the concentration of the KCl solution decreases and a diffusion potential exists. This potential disturbs the measurement and its value must be minimised. KCl solution has been chosen as the electrolyte for this particular reason. The sizes and thus the mobilities of K^+ and Cl^- ions are almost equal, and the diffusion potential is very small. The usual electrolytes are 1-molal, 3-3.5-molal or saturated KCl solutions.

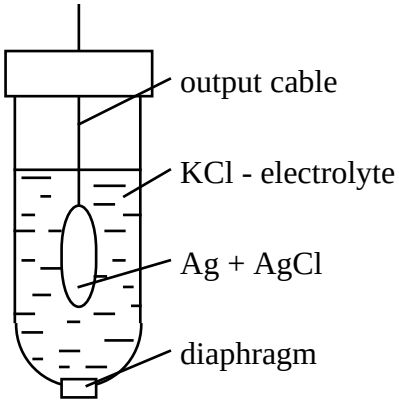

Fig. 3.4: The structure of the Ag-AgCl reference electrode.

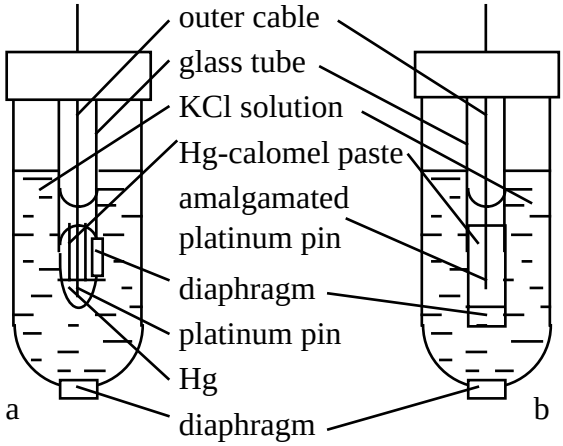

Fig. 3.5: Constructions of the calomel reference electrode.

3.3.2 Calomel electrode

Another commonly used reference electrode is the calomel electrode, which is also named after its inner electrode. Fig. 3.5 shows two different calomel electrode constructions The inner electrode is again immersed in KCl solution. In the construction of Fig. 3.5.a the body of the inner electrode consists of a closed glass tube with mercury on the bottom. A platinum pin connected to the output cable is immersed into mercury, which is further connected to a paste prepared from mercury, calomel and KCl. The electric contact with the KCl solution is realised with a diaphragm on the side of the inner glass tube. Fig. 3.5.b shows another construction. An amalgamated platinum pin is connected with Hg-calomel paste, and the electric connection is realised with a diaphragm. In both cases the electrode constitutes of calomel and mercury. The potential difference is the same as in the calomel measuring electrode.

3.3.3 Tl-TlCl electrode

The Ag-AgCl-electrode operates up to 100°C temperatures and the calomel electrode up to 80°C. With higher temperatures the Tl-TlCl-electrode can be used. It measures pH up to 135°C or even 150°C temperatures. The construction of the electrode is analogous to the other reference electrodes. The potential difference is created according to the reaction equation:

$$TlCl + e^- \Leftrightarrow Tl + Cl^- . \qquad (3.10)$$

3.3.4 Special constructions

The steady KCl solution flow out from the electrode is essential. The amount of the flow can be decreased by adding gel ingredient into the KCl solution, [124], [149], [40]. Another technique is to impregnate the KCl solution into a wood piece, [124]. Both these techniques decrease the possibility of the electrode fouling.

If the process liquid includes compounds which can react with the KCl solution, an additional chamber can be constructed between the KCl chamber and the process liquid. It is connected with a diaphragm on both ends (one end to the inner chamber and the other towards the liquid to be measured) and filled with a special electrolyte, [149]. In drossy circumstances the diaphragm must be constructed large enough to assure good operation. In very drossy circumstances the diaphragm can be replaced by a capillary flow tube, [149], [32]. Then the consumption of the KCl solution is increased, but the fouling effect is avoided. One manufacturer produces a special electrode which controls the pressure of the KCl solution chamber with a bellows connected to the pressure of the process liquid. The elasticity of the bellows controls the pressure of the KCl solution chamber to a slightly higher value than the process pressure thus avoiding the fouling of the diaphragm. Also pressures below atmosphere are possible, [149].

3.4 Combined electrode construction

As an alternative to the normal configuration with separated glass and reference electrodes a combined system may be used, which combines both electrodes into one unit. With this construction the high-ohmic glass electrode is screened by the electrolyte of the reference electrode, and the metal screen can be omitted. The advantage of the combined electrode is the ease of the maintenance and the ability to measure very small quantities of liquid. Also the construction of the joint junctions into pressurised flow tubes is simpler. A major disadvantage is that due to the construction of the electrode it is not possible to provide the selection of glass types for many applications. Figure 3.6 shows the construction of a combined electrode.

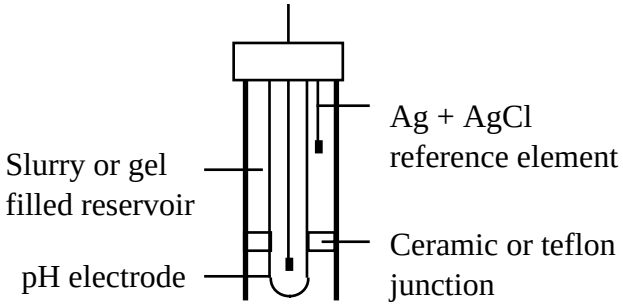

Fig. 3.6: A combined electrode structure

3.5 The electric measurement circuit

The measurement circuit includes a measuring electrode, a reference electrode and a signal converter, Fig. 3.7. The electrodes construct the voltage source, and if the measurement signal is a standard signal, say 4-20 mA, the converter is a pH transmitter. The following potential differences exist:

-E_3 between the outer surface of the glass electrode and the process liquid
-E_2 between the inner surface of the glass electrode and the electrolyte

-E_1 between the inner electrode of the glass electrode and the electrolyte
-E_4 between the inner electrode of the reference electrode and the electrolyte
-E_5 the diffusion potential of the reference electrode.

An electric circuit shown in figure 3.8 is created in the measurement system. The source voltage of the system is the sum of all the voltage sources:

$$E_S = E_1 - E_2 + E_3 - E_4 - E_5. \tag{3.11}$$

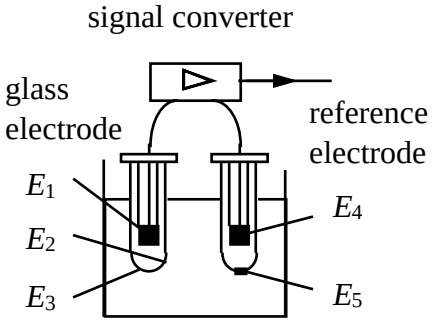

Fig. 3.7: The pH measurement circuit.

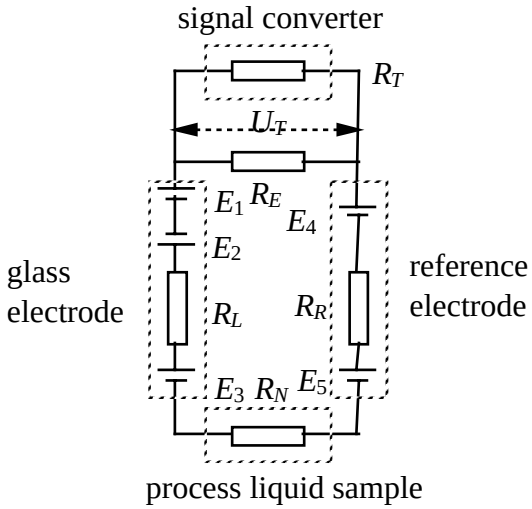

Fig. 3.8: The electric circuit of the pH measurement.
U_T is the voltage in the poles of the signal converter
R_T is the input resistance of the signal converter
R_E is the isolation resistance between the connecting cables
R_R is the resistance of the reference electrode
R_N is the resistance of the process liquid
R_L is the resistance of the membrane of the glass electrode

Usually the inner electrodes and the electrolytes of the both electrodes are identical, and thus $E_1 = E_4$. In usual constructions E_5 is so small, that it can be neglected and thus:

$$E_S = E_3 - E_2 . \tag{3.12}$$

The membrane resistance R_L is 10 - 1000 MΩ, and the resistances R_R and R_N are much smaller and therefore they are neglected. The isolation resistance R_E between the connecting cables must be very large. If the decrease of the isolation resistance, caused by moisture, can be avoided, its value can be assumed insignificantly large in the circuit. With these assumptions the voltage in the input cables obeys equation:

$$U_T = (R_T /(R_L + R_T))E_S . \tag{3.13}$$

Because the value of the voltage U_T should be as identical as possible with E_S, the input resistance must be very large, about 1 - 10 TΩ.

3.6 The effect of the temperature

By substituting equations (3.8) and (3.9) into equation (3.12) the following form is obtained:

$$E_S = ((RT\ln 10)/F)(\mathrm{pH}_{INNER} - \mathrm{pH}_{OUTER}) = k(\mathrm{pH}_{INNER} - \mathrm{pH}_{OUTER}). \quad (3.14)$$

The electrolyte of the measuring electrode is a buffer solution and thus pH_{INNER} is a constant, and the usual value is 7. The coefficient k in equation (3.14) is a function of the absolute temperature T. When the temperature is constant, equation (3.14) defines a straight line with a negative slope. The values of the coefficient k as a function of the temperature are listed in Table 1.

Table 3.1: Values of the coefficient *k*.

t/°C	*k*/(mv/pH-unit)
0	54.20
25	59.16
50	64.12
75	69.08
100	74.04

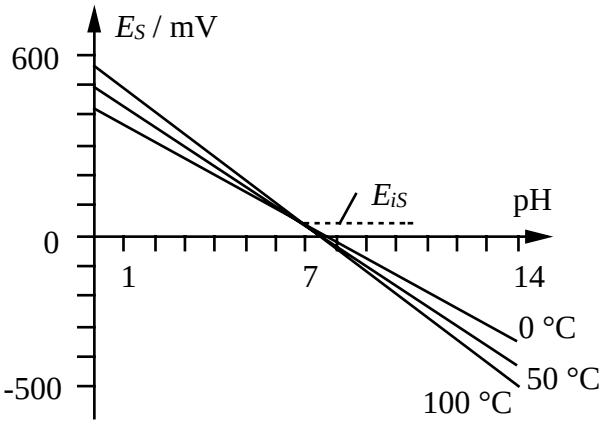

Fig. 3.9: $E_S = f(\mathrm{pH}_{OUTER})$ of the real electrodes in different temperatures.

Fig. 3.9 shows the source voltage as a function of the temperature in the case $\mathrm{pH}_{INNER} = 7$. The lines intersect in the isopotential point. Ideally this should be: $E_S = 0$, $\mathrm{pH}_{INNER} = 7$, as seen in equation (3.14). In the real case with existing electrodes the isopotential voltage differs from zero as shown in Fig. 3.9. Also the pH value of the intersection point can differ from 7. The following factors have an effect on the creation of the isopotential voltage:

- small differences between the inner electrodes
- the asymmetry potential of the glass electrode
- the diffusion potential of the reference electrode
- the fouling of the glass membrane

The temperature dependence of the electrodes can be compensated using a Pt 100 or a termistor sensor which is immersed in the process liquid. The sensor gives the knowledge of the temperature, and based on this knowledge the compensation is made in the signal converter. The temperature sensor can act as a third electrode in the conventional assembly, or it can be integrated in the same body as the two other electrodes in the combined electrode construction.

More serious problem is caused by the temperature dependence of the pH value of the process liquid to be measured. That can not be compensated easily, because the effect is a function of the liquid composition. That is why it is usually omitted.

3.7 Signal converter

The special properties of the pH measurement circuit lay some minimum requirements on the signal converter or the transmitter, e.g. high input impedance, temperature compensation, and the elimination of the ageing of the electrodes. Cheaper transmitters are realised with analogue technique and the more sophisticated ones digitally with microprocessors. In both cases high input impedance is easy to realise with semiconductor techniques. Besides the temperature dependence, the isopotential voltage must be compensated. The automatic temperature compensation is included in almost all applications, and only in laboratory devices the compensation is realised with a potentiometer. The output signal of the transmitter is usually the standard 4 - 20 mA in industrial applications. If PC-computers are used in the on-line control applications, a voltage output signal is needed, e.g. 0/1 - 5 V or 0/2 - 10 V.

Digital implementation with microprocessors improves the operability of the transmitters in many ways:

- the measurement scale can be changed during the continuous use
- advanced diagnostics are available
- the hold function of the signal during the maintenance is possible
- better possibilities for the temperature compensation
- improved measurement accuracy
- digital signal transfer is possible.

The diagnostics can include the functions of both the transmitters and the electrodes. By measuring, e.g., the resistance of the glass membrane, the resistance of the reference electrode, the change of the isopotential voltage, and some other properties, conclusions can be made, whether the electrodes are broken, fouled, aged, or that they are not immersed in the process liquid, [149], [32], [20], [125]. In some special cases, when the composition of the process liquid is accurately known, also the change of the pH value of the liquid as a function of the temperature can be compensated. This is e.g. the case in the alkalinic turbine water including one base and demineralised water, [149].

3.8 Special constructions

If the process liquid is very drossy or contains glass etching substances (e.g. hydrofluoric acid, HF), an antimony measuring electrode can be used. When the antimony electrode is immersed in the process liquid, a potential which obeys Nernst law is created. The applicable pH value range is only from 2 to 9, but the antimony electrode measurement is much faster than that of the glass electrode. Antimony electrode is easy to clean because of its metallic structure.

For avoiding the non-ideal features with the conventional measurement-reference electrode pair a differential pH measurement method was developed, [25]. This method uses two identical glass electrodes, and one of these measures the process liquid, and the other is immersed in a buffer solution with a connection to the process liquid via a salt bridge. A metallic reference electrode is also immersed in the process liquid. The resulting source voltage is gained as a difference of these two measuring electrode source voltages against the same reference potential, and thus the actual reference potential value is suppressed. Thus the fouling of the reference electrode and the small

leakage currents existing in the liquid because of the inaccuracy of the isolation between the reference electrode and the liquid earth are avoided.

One manufacturer has developed sensors using semiconductor technology. The product is ion-sensitive field effect transistor (ISFET). A conventional reference electrode can be used. The response time of this electrode is about 1 second. The size of the system is small and the maintenance is easier than that of a glass electrode, [40].

Commercially available pH electrodes also include a combined enamel electrode which consists of the enamel measuring electrode and an enamel Na-selective electrode, which is used as the reference electrode. With this electrode the pH value of dough mass can be measured up to 15 % thicknesses .

An emerging technique is the optical glass fibre measurement. The colour of the light shows the pH value. The fibre optics sensor can measure the resulting mean value from a large region and not only pointwise. At the moment this technique is not yet suitable for reliable pH measurement, and it is only used for the moisture alarm of concrete structures.

3.9 Practical pH measurement

3.9.1 Calibration of the pH measurement

The calibration is made using two or three different standard buffer solutions. A buffer with pH value near 7 will be always used, because at that value the theoretical voltage value is about zero. When the measurement range is on the acidic side, a buffer solution with pH value near 4 is used, and with the alkalinic side a buffer with pH value near 10 is needed. Alternatively all three buffers can be used. The buffer and the process liquid sample must have the same temperature. The sensors must be rinsed with ion-changed water between the immersions in the different buffers. The zero point and the slope of the calibration line are found by using the buffers. Specific electrical calibrators are sometimes used, but they do not take the individual differences of the electrodes into account .

3.9.2 Practical definition of the pH value

The idea of the practical definition of the pH value is to compare the measured value of the process sample with that of the buffer solution. When these voltages are denoted as E_S and E_{SB}, the definition can be constructed using equation (3.14):

$$\mathrm{pH}_{OUTER} = \mathrm{pH}_{BUFFEROUTER} - F(E_S - E_{SB})/(RT\ln 10)\,. \tag{3.15}$$

3.9.3 Installation, use and maintenance of the electrodes

In industrial environment the electrodes must be protected against breakage with robust mounting chambers. The most common types, the immersing chamber and the by-pass flow chamber, are shown in Fig. 3.10. In pulp and paper industry the combined electrode assembly shown in figure 3.11 is often used. In this case the pulp flowing in the pipes can have even 15 % thickness and in such a case the measurement is possible from the thin liquid film formed on the tube wall. Under extreme circumstances an automated sample system must be used. The system automatically takes the sample, measures the pH value, pushes out the sample, washes the electrodes, and takes a new sample. In the mounting, the earthing of the process liquid is important. In mountings made from steel no problems exist. Otherwise a special earth electrode is often used.

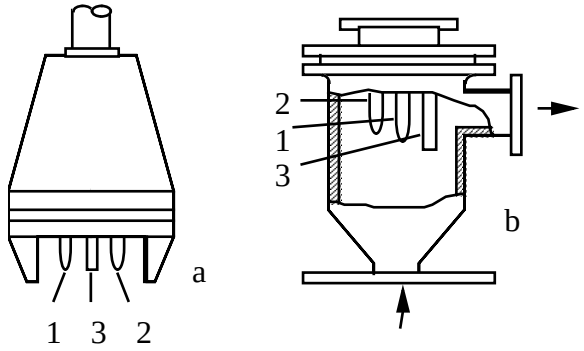

Fig. 3.10: Immersion chamber (a) and by-pass flow chamber (b).
1 = Measuring electrode
2 = Reference electrode
3 = Temperature compensator

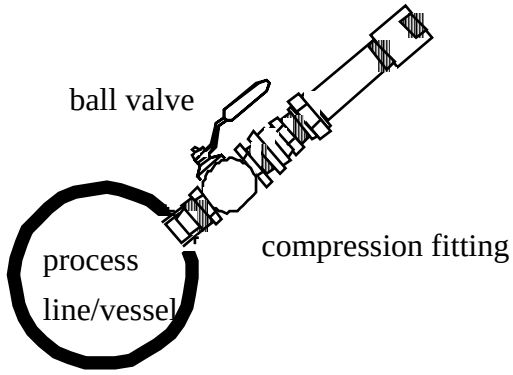

Fig. 3.11: A combined electrode assembly in a tube line.

Cleaning is important in the industrial measurement. It can be automated to function periodically but in more demanding situations also manual maintenance is needed. From the automated cleaning methods the following can be mentioned:

- mechanical spherical brushing of the sensor head
- water spraying periodically
- chemical spraying periodically
- ultrasonic washing

The electrodes can be washed manually with different chemicals depending on the reason of the fouling. Sterilisation can be made if needed either chemically or physically with hot steam. The sensor head form has an important role in the fouling properties. The flat sensor head is suitable for the pH measurement of thick samples in pipes. Other sensor head profiles are beneficial for other reasons, e.g. spherical sensor head makes it possible to measure very small liquid samples.

The reference electrode consumes KCl solution, and additional solution must be added periodically. Microprocessor based transmitters with diagnostics help in the planning of the sensor maintenance. When the glass electrode is not used in measurement, it is usually kept in the buffer with value 4. If it is stored dry, it must be soaked in distilled or ion-changed water for at least 24 hours before use.

Chapter 4

pH modelling

Papcastle (n.)
Something drawn or modelled by a small child which you are supposed to know what it is. [1]
Fritham (n.)
A paragraph that you get stuck on in a book. The more you read it, the less it means to you. [1]

pH models are crudely divided into static and dynamic models and similarly the modelling methods are divided into theoretical and experimental. The borders of these divisions are vague at the best and many models combine static and dynamic model structures (Wiener models) and use both theoretical and experimental methods. The applications in Chapter 6 show the benefits of these kinds of models.

This chapter gives a short review of the most important static models (such as titration curves, buffer index diagrams and distribution diagrams) and then concentrates on dynamic modelling. Dynamic modelling problem is first presented with arbitrary components without any mention to pH value and only after the introduction of population principle the models are applied to pH processes. The section containing dynamic modelling is very detailed and illustrated with several simulations.

Traditional dynamic pH models are of Wiener type where dynamic flow and mixing chracteristics are combined to instantaneous chemical equilibrium. There are two different schools of dynamic pH modelling: The classical physico-chemical modelling approach presented by McAvoy *et al.*, [84] and the reaction invariant formulation of the physico-chemical approach presented by Gustafsson and Waller, [30]. Both approaches are based on the same idea of separating the chemical reaction (equilibrium) from the reaction invariant dynamics; the resulting models are identical but the problem formulation is different. This thesis uses the problem formulation of the classical physico-chemical approach.

4.1 Static modelling

Static models are valid when the system has reached the equilibrium. The acid-base unit reactions can be considered instantaneous and therefore static modelling is a very natural approach. Static models include titration curves and distribution diagrams. Experimental static models are

often basic tools for product quality control as well as process state indicators. Experimental methods have been used for both qualitative and quantitative analysis.

4.1.1 Titration curve

Titration curves are traditional classical pH-models. They describe the pH-value as a function of acid-base content difference. Experimental titration curves usually present the pH-value as a function of added acid or base volume; the only difference is in the scaling. The shape of the titration curve is determined by the participating chemical components. A group of typical titration curves are shown in Fig. 4.1 (mixtures of acetic acid HAc, ammonia NH_3 and water are treated with strong acids and bases). The solutions containing HAc have a titration bump at the pK_a of acetic acid, the solutions containing NH_3 have a titration bump at the pK_b of ammonia and the pure water shows a typical strong acid - strong base titration curve. Polyprotic acids donate more than one hydrogen ion and the titration curves have correspondingly more than one step as shown in Fig. 4.2 (Titration curve for phosphoric acid H_3PO_4).

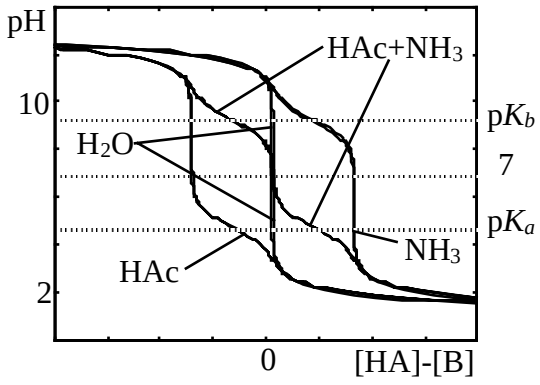

Fig. 4.1: Typical monoprotic titration curves

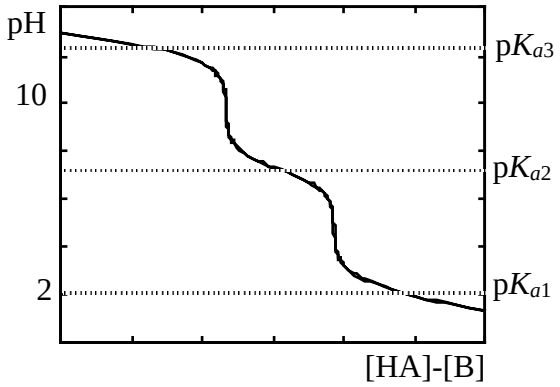

Fig. 4.2: A polyprotic (H_3PO_4) titration curve

Theoretical titration curves require the knowledge of the equilibrium constants and the total concentrations of acids and bases. Experimental curves, on the other hand, only require a sample.

Theoretical titration curves can be generated from the charge balance (also known as electro-neutrality equation) that takes into account all the charged ions of the solution. The solution has no overall charge and therefore the sum of all particular charges must be zero

$$\sum_n \pm z_n \cdot \left[x^{\pm z_n} \right] = 0 \,. \tag{4.1}$$

The ions are usually divided into components of water (oxonium and hydroxide ions), components of strong acids (H_zA) and bases (B) and components of weak acids (H_za) and bases (b).

$$\left[H_3O^+ \right] - \left[OH^- \right] + \sum_i z_i \left[H_{z_i} B_i^{+z_i} \right] - \sum_i z_i \left[A_i^{-z_i} \right] + \sum_i \sum_n z_{ni} \left[H_{z_{ni}} b_i^{+z_{ni}} \right] - \sum_i \sum_n z_{ni} \left[a_i^{-z_{ni}} \right] = 0 \,. \tag{4.2}$$

Index *i* corresponds to particular acids and bases whereas index *n* refers to charge levels, e.g. strong acids HCl and HNO_3 appear in equation (4.2) as completely dissociated charged ions Cl^- and NO_3^-, i.e., A_1^- and A_2^-, whereas weak acid H_3PO_4 appears in equation (4.2) with different charge levels: $H_2PO_4^-$, HPO_4^{2-} and PO_4^{3-}, i.e., a_1^-, a_1^{2-} and a_1^{3-}.

Titration curve shows the dependency between pH (function of oxonium ion activity) and acid/base concentration. Strong acids and bases dissociate completely and their ion concentrations

are total concentrations as well. Weak components only dissociate partially and their ion concentrations have to be calculated from equilibrium constants. Each weak acid or base ion concentration can be replaced in equation (4.2) with a function of oxonium, hydroxide and total ion concentrations calculated from the equilibrium equations such as equations (2.13)-(2.15). The hydroxide ion concentration is then replaced with a function of oxonium ion concentration and ionic product of water in accordance to equation (2.20). After all this manipulation equation (4.2) contains only total acid and base concentrations and oxonium ion concentration (from which the pH-value can be calculated in accordance to (2.21)).

4.1.2 Buffer index

The steepness of the titration curve is closely connected to the sensitivity of the process at the corresponding pH range. The sensitivity (and correspondingly the buffering of a liquid system) can be evaluated even better from buffer index β that is further derived from a titration curve.

$$\beta = \frac{d[\overline{\mathrm{B}}]}{d\mathrm{pH}} = -\frac{d[\overline{\mathrm{A}}]}{d\mathrm{pH}}. \tag{4.3}$$

The differential change in the concentration of a strong base B vs. the differential change in the pH-value (or negative differential change in the concentration of a strong acid A vs. the differential change in the pH-value) corresponds to the inverse of the titration curve slope. In Fig. 4.3 the buffering index of the acetic buffer solution described earlier is presented as a function of pH-value. The maximum buffering is reached at pH = pK_a = 4.75. The curve (buffer solution) is compared to the corresponding curve of a solution (no buffering) that contains only water and strong acids and bases.

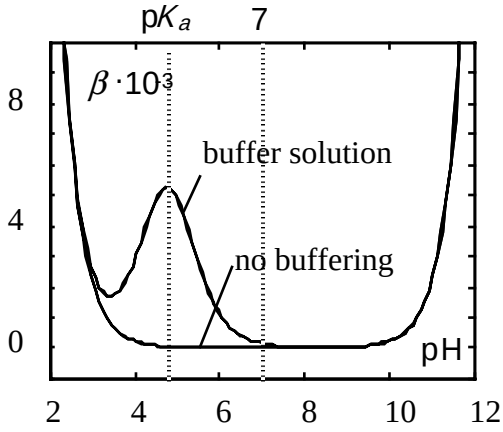

Fig. 4.3: The buffer index of acetic acid solution

4.1.2 Distribution diagram

Distribution diagrams give more information than titration curves. They are generated for specific compounds and they describe the distribution of different forms of a compound as a function of pH. In Fig. 4.4 is the distribution diagram of a pure phosphoric acid (H_3PO_4) solution and in Fig. 4.5 the same diagram on a logarithmic scale.

Distribution diagrams are generated from the total balances of a substances. Consider the phosphoric acid

$$\overline{[\mathrm{P}]}_{TOT} = \overline{[\mathrm{H_3PO_4}]} + \overline{[\mathrm{H_2PO_4^-}]} + \overline{[\mathrm{HPO_4^{2-}}]} + \overline{[\mathrm{PO_4^{3-}}]}. \tag{4.4}$$

Each concentration in equation (4.4) is replaced with a function of equilibrium constants, oxonium ion concentrations and total phosphoric concentrations. The distribution for component X is defined as follows

$$\alpha_i = \frac{\overline{[\mathrm{X}_i]}}{\overline{[\mathrm{X}]}_{TOT}}. \tag{4.5}$$

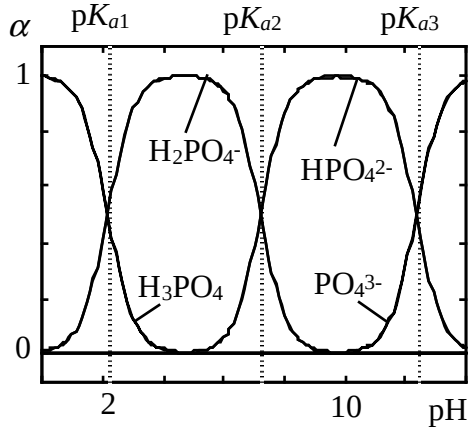

Fig. 4.4: Distribution diagram of H_3PO_4.

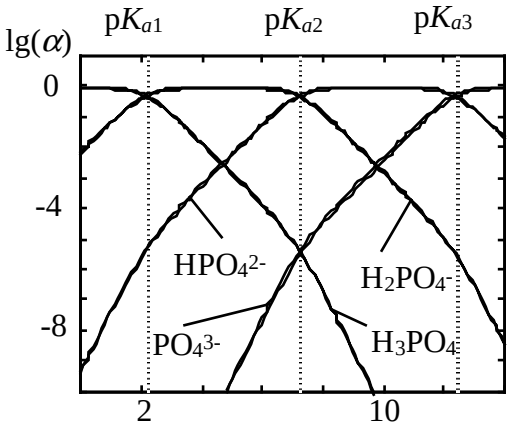

Fig. 4.5: Logarithmic distribution diagram of H_3PO_4.

The distribution diagrams are useful for evaluating optimal pH-ranges for particular reactions, e.g. separation processes. In separation processes the distribution diagram is often made for different phases of the compound. Fig. 4.6 displays the distribution of calcium to solid and liquid phases in a calcium/carbonate solution. A similar distribution diagram could be constructed for carbonate in the same solution. That would be a three-phase diagram (carbon dioxide in gaseous phase, calcium carbonate in solid phase and all carbonate states in liquid phase: soluted carbon dioxide, carbonic acid, hydrocarbonate-ions, calciumbicarbonate-ions and carbonate-ions).

The distribution diagrams including reactions with different compounds do not usually reach the maximum value 1 with each fraction. In Fig. 4.6 the maximum value of $CaCO_3$ fraction is determined by both the total calcium concentration and the total carbonate concentration. It is to be noted that in Fig. 4.6 there is more calcium than carbonate and therefore there is excessive aqueous Calcium even under alkalinic conditions.

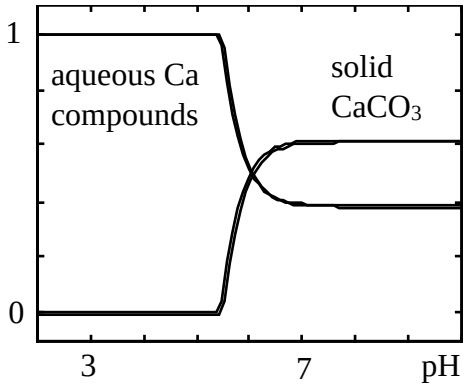

Fig. 4.6: Solid-Aqueous distribution diagram of $CaCO_3$.

4.2 Dynamic pH process modelling

Dynamic modelling is fundamentally more difficult than static modelling. Static modelling concentrates only on the equilibrium state where the system does not change as a function of time. In the dynamic modelling procedure the behaviour of pH and related phenomena are considered as functions of time; they change autonomously even though the changes in the input have already passed.

The dynamic pH-systems can be divided into two categories; the systems where chemical phenomena are significantly faster than flow and mixing phenomena and the systems where this is not the case. These categories are treated in more detail in the following sections.

4.2.1 Background

4.2.1.1 Equilibrium modelling and reaction invariants

The principle of physico-chemical dynamic modelling of a pH-process was first stated by McAvoy *et al.* in 1972, [84]. They used the model (acetic acid and sodium hydroxide) for simulating the behaviour of a simple pH-process in a time-optimal control loop. Richter *et al.,* [106] presented a model including the electro-neutrality condition for many 1-valued acids and bases two years later.

Gustafsson and Waller, [30] and Jutila and Orava, [51] developed more complex models, closer to practical processes. The term "reaction invariant" was originally introduced by Fjeld *et al.,* [19] but the pH process formulation of reaction invariants was presented by Gustafsson and Waller, [30] as a systematic matrix formulation of the physico-chemical modelling procedure. The stoichiometric chemical reactions and the charge balance form together a set of equations that can be used for determining the reaction invariants with the help of simple linear algebra. The practical determination of the reaction invariants is discussed in [27], [30] and [29]. More elaborate chemical systems including complex formation and two-phase systems (solid/liquid) are presented by Gustafsson *et al.,* [28].

The concept of reaction invariants is not a new idea; it is just a name for applying "the conservation of substance" on concentrations. For instance Orava and Niemi, [93] and McAvoy *et al.,* [84] used these kind of sums of concentrations before they were named "reaction invariants". An early review of the reaction invariants and their use was presented by Waller and Mäkilä, [128].

A recent paper by Gadewar *et al.,* [22] in 2001 extended the concept of reaction invariants to mole numbers. A set of reaction invariants that are linear transformations of the species mole numbers were identified. With this set of reaction invariants the consistency of experimental data and the reaction chemistry can be checked easily and the material balances of complex chemical reactions can be written in simple collected matrix structure. The method was illustrated with a toluene to benzenhydrodealkylation, dehydrocyclization of propane, methanol and formaldehyde oxidation and synthesis of 2-methylpyrazine. The key benefit of this method is the automation of mole balances in the conceptual design of chemical processes.

pH neutralisation process with different chemical contents (i.e. different titration curves) was modelled experimentally with three different fuzzy-neural approaches by Junhong *et al.,* [48]. They used a simple fuzzy logic system as the pH model, the rule base of which was learned with the help of different artificial neural networks. They used unsupervised and supervised self-organising counter-propagation networks as well as a self-growing adaptive vector quantization. Three case studies were presented: a strong acid – strong base system, a weak acid – strong base system and a system with changing buffering. All case examples were learned reasonably well, but, on the other hand, all the case examples were simulated processes.

Emara-Shabaik *et al.*, [18] used cumulant/bispectrum model structure identification on a pilot scale pH process. They used this strategy to pinpoint the nonlinearity in the process, the results showed that in the pilot pH process with pH-value and level as state variables the level height was weakly nonlinear (a linear model could be used) whereas the pH-value was strongly nonlinear and that a Wiener-Hammerstein model would be appropriate for it. This is hardly a surprise, but the emphasis on this research was to show that the cumulant/bispectrum method works.

Many researchers have modelled the nonlinear pH model with several linear submodels, (e.g., Ylöstalo and Hyötyniemi, [147], Nyström et al., [91] and Johansen, [44]). Johansen and Foss, [45] applied the operating regime based modelling they developed for the pH process simulator presented by Hall and Seborg, [34]. Later they developed the operating regime based modelling scheme into a general modelling and identification toolkit ORBIT, [46].

Wiener-model identification is also been widely used for pH-modelling. E.g., Pajunen, [94] and Kalafatis et al., [55], [56] identified a pH process with Wiener-models and also used the models they developed for pH-control.

4.2.1.1 Stiff chemical systems and combination of instantaneous and slow limiting phenomena.

Most real processes are stiff by nature but in many cases the stiffness can be ignored. If base reagent is added to a well mixed open vessel containing municipal water the pH value will rise immediately (instantaneous reaction) but in the course of hours and days the pH value will slowly drop until equilibrium is reached (slow limiting phenomena, dissolution of CO_2). At the same time the liquid in the vessel becomes cloudy as carbonates precipitate. If the test period is very short the slow dissolution of carbon dioxide and the precipitation of calcium carbonate can be ignored as their effect can be seen only gradually in the long run.

On the other hand, there are numerous examples of processes in which the stiffness can not be ignored. The stiffness can cause problems in the process operation and control as well as in the product quality. A good example is deinked pulp that is produced for paper machines. The qualifications of the produced pulp are well within acceptable levels, that is, at least for a short time after the production. The fibres in the pulp have gone through many mechanical and chemical operations during the production cycle and they have not reached equilibrium. The final state of the product is the result of a complex chain of variables containing the properties of raw materials and each mechanical and chemical operation in the production.

However, in most cases when the problems of stiffness are discussed, the emphasis is on the modelling, identification and simulation problems. The earlier papers also dealt with the efficiency of algorithms and the saved computer time with respect to acceptable integration errors. With the rapid development of modern computers and calculation efficiency, the efficiency of algorithms is not such an issue any longer.

Tyreus *et al.*, [126] presented robust integration algorithms for large binary distillation columns. The stiffness is mainly caused by columns with high product purities of low relative volality. This is a typical case, where the algorithm efficiency is the key problem.

Martinez and Drozdowicz, [83] also had the algorithm efficiency as their target, but in this case the reason for it was that the stiff system was used in a real-time training simulator. They used time-scale decomposition based on singular perturbation method. The large system was divided into smaller subsystems that were suitable for explicit numerical methods.

Ashour and Hanna, [4] developed an implicit, second order method (based on the general mid-point rule) for the integration of highly stiff ordinary differential equations. If low or intermediate accuracy is desired, the method is shown to be more efficient than classical implicit mid-point rule. In addition, it has good stability characteristics (in terms of damping).

All the cases presented above [126], [83] and [4] are mere separate examples of research on stiff chemical systems and there are many more. The common feature is that they all concentrate on

algorithms (principally on different integration methods). The fact that the methods are applied on chemical systems is a minor point as a priori knowledge on chemistry is not crucial.

A different approach to modelling and simulating stiff chemical systems is to take a closer look at the chemical phenomena in the process and to modify, approximate or formulate the system in a way to avoid the stiffness. The method of approximation has been widely used in chemical reaction engineering. Traditionally the slow limiting reactions are pinpointed and an approximate model is created that consider only a few kinetic constants. Many examples of this approach can be found in, e.g., Levenspiel, [73].

Sun *et al.*, [120] developed a method for solving stiff ordinary differential equations in a chemical system. The method consisted of dividing the variables into a fast kinetic subgroup and a slow kinetic subgroup. The fast variables are solved using the implicit backward-differentiation formulas but the dimension of the Jacobian is considerably smaller than the one of the original stiff system. The slow kinetic subgroup is solved with a simple explicit Adams-Bashforth method. The authors claimed that, when compared to traditional methods used for stiff systems, they reached the same accuracy but with only one-third of the execution time.

The concept of using detailed kinetic models for the re-formulation of the stiff system has been explored by, e.g., Knio and Najm, [64] and Joshi *et al.*, [47]. Knio and Najm presented two different simulation schemes for stiff diffusion flow system. The first scheme consists of implicit integration of the reaction source terms with a second-order predictor-corrector treatment of advection and diffusion whereas the second scheme relies on operator-split formulation, in which the implicit integration of reaction source terms is combined with an explicit fractional step update of the diffusion source terms.

Joshi *et al.* developed a transformation from stiff differential algebraic equations to stiff ordinary differential equations, which are easier to solve. They used kinetic steady-state approximation ([73]) for eliminating intermediate species of the complex kinetic model and flowing surface species approximation for converting differential algebraic equations into ordinary differential equations. The benefit of this approximation is that it becomes more accurate as the system gets stiffer. They applied the method to a catalytic reforming process.

In most cases the differences between different chemical and physical phenomena are so great that some of the chemical reaction seem to take place instantaneously and the kinetic constants are close to infinity. If all phenomena apart from flow and mixing characteristics can be considered instantaneous, the process can be modelled with classical reaction invariant approach, [30] or classical physico-chemical approach, [51]. However, if there are slow phenomena that limit the chemical equilibrium, the classical approaches have to be extended.

The reaction invariant approach has been extended to include reaction variants (slow forming or deforming components; in the examples of [28] complex ions and solid precipitates). This method is well documented in Gustafsson *et al.*, [28] and in Sandström and Gustafsson, [109]. In this approach the state vector containing reaction invariants is extended to also include reaction variants, which are in this case the solid phase concentrations. The kinetic reaction rates are added as new factors to the traditional reaction invariant state equation. A very detailed practical application of this approach in given in [117].

Slightly different formulation of the reaction invariant approach is given by Wright and Kravaris, [134] and Wright *et al.*, [138]. Their approach is closer to the classical physico-chemical approach [51] with the definition of total concentrations and a modified charge balance. The major difference when compared to the classical physico-chemical modelling, is that the model is still formulated in a matrix equation.

Wright and Kravaris, [137] also extended their approach to systems that contain slow forming or deforming compounds and they applied their approach to a precipitation process (only computer simulation, no experimental data). The extended approach contained separate reaction rate equations for dissolution and precipitation which was connected to the original model by

introducing a separate transfer variable, which described the mass transfer between solid and liquid state.

There are many practical cases, in which the slow forming or deforming component enters the system with the reagent. In pH control systems this is a very typical situation when hydrated lime is used as a base reagent. Hydrated lime is a rather inexpensive reagent and therefore widely used in industrial applications. It also has a low solubility but when introduced to acidic system the hydroxyl groups of lime react with the acids neutralising the system and as hydroxide groups are consumed in neutralisation, the demand for equilibrium boosts up the solubility as well. As a result, the base reagent slowly releases more hydroxide groups to the solution and the limiting reaction is the dissolution of lime.

The slow dynamics is a severe practical problem that has to be taken into consideration whenever lime is used as a reagent. Several researchers have presented different ideas, solutions and applications from the control point of view. E.g., Docherty, [14] described in great detail the required equipment, achievable time constant, scale-up problem, sedimentations, controller structure, etc.

Relatively few authors have looked this problem from the modelling point of view trying to understand the phenomena behind the obvious slow behaviour. Kässer, [54] and [67] neutralised waste water (pilot process) and used the pilot data to validate a model and parameters of the kinetic model. He identified the slope of the titration curve and used it in a conventional PI-controller. The kinetic model was described with a simple first order dynamic equation with only one fixed time constant, but nevertheless, the results were rather good with lime.

Walsh and Perkins, [129] took much more ambitious approach and modelled the dissolution with a distributed parameter model. They used the particle radius as a changing parameter that described the dissolution. They developed a tanks-in-series model that had pH and particle radius as variables (the model contained different kinetic constants for different pH-regions).

Ala-Kaila, [2] studied the slow phenomena limited pH systems from a different angle. He developed a dynamical model for pH-value in kraft pulp, in which the limiting slow phenomenon is the material transport between the fibres and the surrounding liquid. The application is very interesting in view of this thesis and the dynamic chemical state of deinked pulp presented in section 6.3.2. Ala-Kaila studied closely the mass transfer film (i.e., the fibre wall) and the particular ions inside the fibres and in the surrounding liquid. The model he developed was a two compartment model (one compartment is the liquid within the fibres and the other the surrounding liquid), in which a perfect mixing was assumed for both compartments.

The pH and ion concentration calculation procedure was presented in detail in [3]. It is based on sequential computing, in which the mass transfer is calculated from integrating the differential equations of mass transport and diffusion (receiving the mobile ion fluxes between phases) after which the static equilibrium was calculated in both compartments. Two examples were given: the O_2 delignified kraft pulp entering the bleaching apparatus and the acidified kraft pulp undergoing a displacement washing with alkaline wash water. The results in both examples are very good.

The film model structure by Ala-Kaila concentrates on the properties of the kraft pulp fibres and the film separating the compartments whereas the population principle of this thesis takes a much more general approach to systems with several limiting phenomena (carbon dioxide – gas, calcium carbonate – precipitates, material inside the fibres). The model given by Ala-Kaila describes very accurately the material transport phenomena between the fibres and the surrounding liquid but it requires ca. 10 parameters as well as the mobile ion concentrations in the immobile liquid that are very difficult to define theoretically or experimentally. The population principle requires only one kinetic constant and one concentration for each ion that transports between fibres and the surrounding but correspondingly the model is much more approximate and does not even try to describe the actual micro phenomena of the material transport.

A combination of the two approaches could have several advantages, namely containing the robust structure for combining several slow phenomena and equilibria to a very accurate model of

one of the slow limiting phenomena. That would require a lot of experiments, though, as Ala-Kaila studied kraft pulp and in this thesis the population principle was applied to deinked pulp. The different raw materials and processes make the two pulps very different from each others, but the structures and modelling principles of one application can be applied to the other.

In this thesis the classical physico-chemical approach has been extended for arbitrary many different slowly forming or deforming compounds, with the introduction of population principle. The method developed here is a simple trick of formulating the system equations in a way that the integration of the stiff system variables is avoided. The population principle can also be applied to other than chemical systems; the only requirement is that the application is a population system and that the stiffness is resulted by the transfer phenomena from one population to another. Hence the name: population principle. Chemical systems are very typical population models (one component changes into another) but the method suits equally well to, e.g., animal populations.

The population principle introduced in this thesis is a logical extension of the dynamic physico-chemical modelling of equilibrium reactions. It can be seen as a hybrid structure between instantaneous chemical equilibrium and slow reaction kinetics. Its use is advantageous when chemical equilibrium creeps as a result of slow reactions or other limiting phenomena, such as slow dissolution/precipitation kinetics. The models created with the population principle avoid stiffness that is typical for systems containing combined fast and slow dynamics. The population principle is first illustrated with a general example of chemical reactions and the pH-value is included in the models only at the very end of the chapter.

4.2.2 Introduction to dynamic chemical processes

4.2.2.1 Fluid and mixing dynamics

Two basic processes are used as simple examples. An ideal mixer with fixed flow rates F_i and volume V stands for a continuously operating process (shown in Fig.4.7). Only concentrations $[\cdot]$ change in this system. The key feature in continuous chemical reactors of this kind is that for slow reactions the steady state is reached but not the equilibrium.

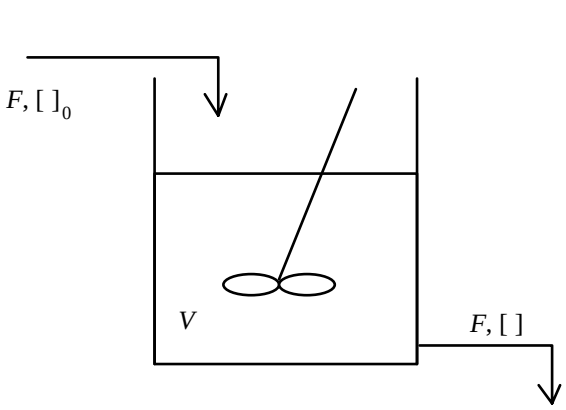

Fig. 4.7: Continuous flow reactor.

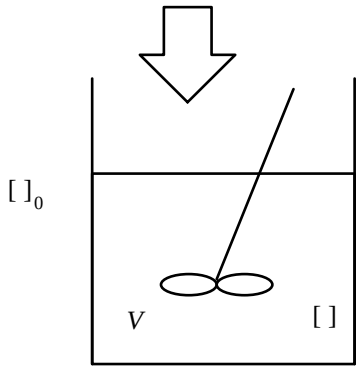

Fig. 4.8: Batch reactor.

In the batch process shown in Fig. 4.8 there are no flows in or out of the tank. The concentrations in the tank are affected by solid material additions. The components dissolve immediately and the volume increase is assumed to be negligible. As there are no flows, the steady-state and the equilibrium describe the same chemical phenomenon. The volume of both tanks is 1 m^3 and the volumetric flow in and out of the continuous reactor is 1 m^3/min.

4.2.2.2 One unit equilibrium reaction in one phase

The first chemical reaction is the simplest of them all. Component A is consumed and component B formed. The equilibrium conditions are indicated with a dash above the symbol (B in brackets is the concentration of B; B in brackets with a dash above is the equilibrium concentration of B).

$$\mathrm{A} \underset{k_{-1}}{\overset{k_1}{\Leftrightarrow}} \mathrm{B}, \qquad K_1 = \frac{k_1}{k_{-1}} = \frac{\overline{[\mathrm{B}]}}{\overline{[\mathrm{A}]}} = 0.75 \tag{4.6}$$

If the reaction is instantaneous, the batch process becomes completely static and the continuous process can be described with separate flow dynamics and static mapping (reaction). The total concentration is divided between A and B with respect to the equilibrium constant. The two static equations (below left) describe the batch process. The flow dynamics in the continuous flow process is described with partial material balances (below right).

$$\begin{cases} \overline{[\mathrm{A}]} = \dfrac{1}{1+K_1}\left([\mathrm{A}]+[\mathrm{B}]\right) \\ \overline{[\mathrm{B}]} = \dfrac{K_1}{1+K_1}\left([\mathrm{A}]+[\mathrm{B}]\right) \end{cases} \qquad \begin{cases} \dfrac{d[\mathrm{A}]}{dt} = \dfrac{1}{V}\cdot\left(F[\mathrm{A}]_0 - F[\mathrm{A}]\right) \\ \dfrac{d[\mathrm{B}]}{dt} = \dfrac{1}{V}\cdot\left(F[\mathrm{B}]_0 - F[\mathrm{B}]\right) \end{cases} . \tag{4.7}$$

The SIMULINK simulation model of the batch process is presented in Appendix1, Fig. A1.1, the step response results are in Figs. 4.9 – 4.11.

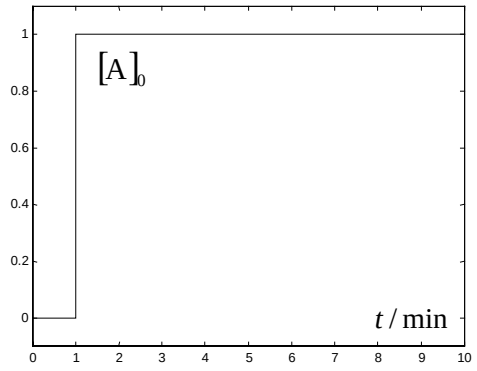

Fig. 4.9: Step input for the batch process.

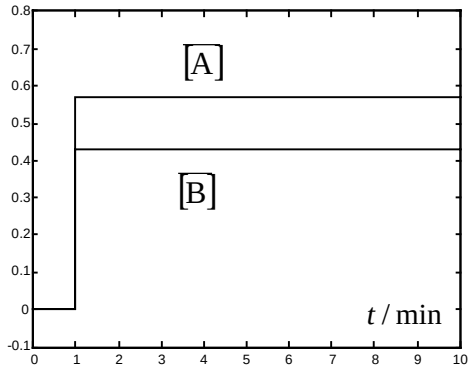

Fig. 4.10: Response for the batch process.

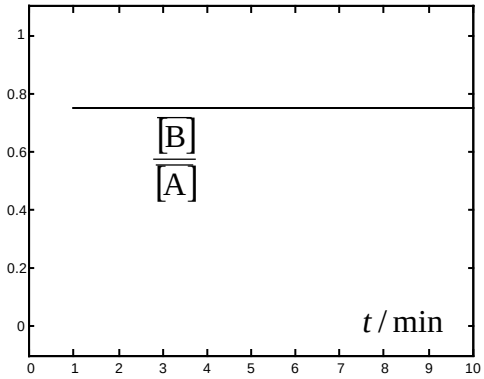

Fig 4.11: The concentration ratio of batch process.

Figs. 4.9 and 4.10 show that there is no dynamics present. The equilibrium condition can be also checked. The concentration ratio is shown in Fig. 4.11.

The same simulation is repeated for the continuous flow reactor. The simulation model is given in Appendix 1, Fig. A1.2, the step responses in Fig. 4.12 and the concentration ratio in Fig. 4.13.

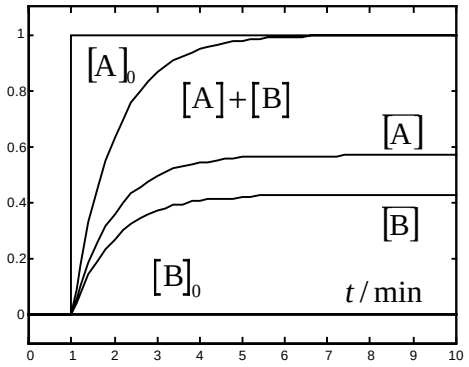

Fig 4.12: The unit step response of the continuous flow process.

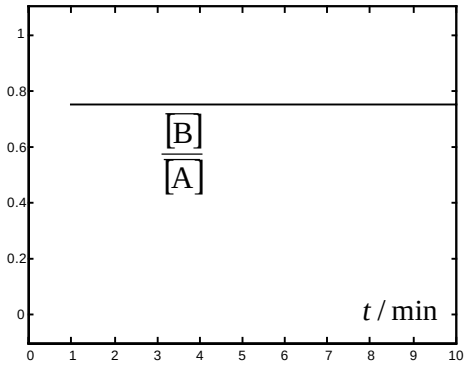

Fig 4.13: The concentration ratio of the continuous flow process.

Now there is dynamic behaviour in the reactor (Fig. 4.12), but it is caused entirely by the flow dynamics. The chemical reaction is at equilibrium at every time instant as can be seen from Fig. 4.13. The same simulations are repeated again, but this time the reactions are slow. The equilibrium constant is still 0.75, but this time the reaction rate constants have to be taken into consideration. The batch reactor model consists of reaction rates (no dilution or washout)

$$\begin{cases} \dfrac{d[\mathrm{A}]}{dt} = -k_1[\mathrm{A}] + k_{-1}[\mathrm{B}] \\ \dfrac{d[\mathrm{B}]}{dt} = k_1[\mathrm{A}] - k_{-1}[\mathrm{B}] \end{cases}. \tag{4.8}$$

The continuous flow process model has the flow dynamics and chemical kinetics interconnected

$$\begin{cases} \dfrac{d[\mathrm{A}]}{dt} = \dfrac{1}{V}\left(F[\mathrm{A}]_0 - F[\mathrm{A}]\right) - k_1[\mathrm{A}] + k_{-1}[\mathrm{B}] \\ \dfrac{d[\mathrm{B}]}{dt} = \dfrac{1}{V}\left(F[\mathrm{B}]_0 - F[\mathrm{B}]\right) + k_1[\mathrm{A}] - k_{-1}[\mathrm{B}] \end{cases}. \tag{4.9}$$

The simulation model for the continuous flow process is shown in Appendix 1, Fig. A1.3 and the model for the batch process in Appendix 1, Fig. A1.4.

It is to be noted that derivatives of the state variables in Fig. A1.4 are output signals that are saved. This is due to the fact that the actual input to the batch in an impulse. The step input was used because an ideal impulse can not be simulated. For linear systems an impulse response can be generated by taking derivative of the step response. Input signals Ai and Bi in Fig. A1.4 are in fact integrals of the actual inputs; they describe the sum of all components that have been fed to the system. The simulation results are presented in Fig. 4.14.

The equilibrium is reached after ca. 3 minutes has passed from the initial chemical addition. For the continuous flow process the equilibrium is not necessarily reached as can be seen from the

simulation results in Fig. 4.15. In continuous flow process the steady state is reached but not the equilibrium due to the washout. The steady state can be calculated from the partial material balance

$$\frac{[\mathrm{B}]_S}{[\mathrm{A}]_S} = \frac{k_1[\mathrm{A}]_{0S} + \left(\frac{F}{V} + k_1\right)[\mathrm{B}]_{0S}}{\left(\frac{F}{V} + k_{-1}\right)[\mathrm{A}]_{0S} + k_{-1}[\mathrm{B}]_{0S}} = K_1 \frac{[\mathrm{A}]_{0S} + \left(\frac{F}{Vk_1} + 1\right)[\mathrm{B}]_{0S}}{\left(\frac{F}{Vk_{-1}} + 1\right)[\mathrm{A}]_{0S} + [\mathrm{B}]_{0S}}. \tag{4.10}$$

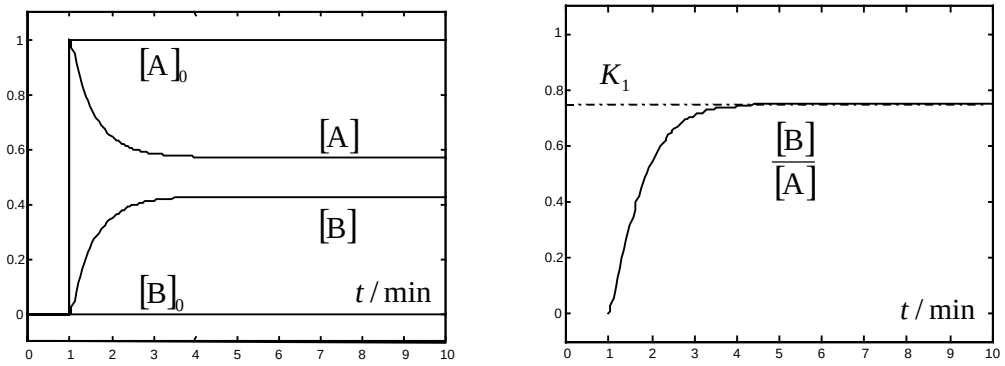

Fig. 4.14: The batch process concentrations and their ratio (slow reactions).

The steady state obviously differs from the equilibrium with any real values for flow, volume and reaction rate constants. The limit value of steady state concentration ratio approaches the equilibrium constant when either reaction rate constants go to infinity (instantaneous reactions), the flow rate drops to zero (batch process, no washout, infinitely slow fluid dynamics) or the volume goes to infinity (infinitely slow fluid dynamics). This point is illustrated by repeating the same simulations with lower flow rates. In Fig. 4.15 the flow rate is 1.0 m^3/min, in Fig. 4.16 0.1 m^3/min and in Fig. 4.17 0.01 m^3/min.

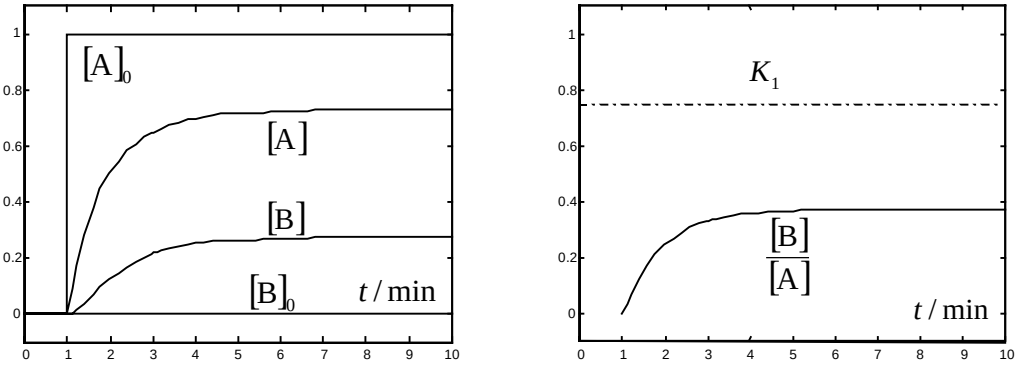

Fig. 4.15: The continuous flow concentrations and their ratio (slow reactions, F = 1).

The stiffness of the model becomes apparent when flow rate is dropped as can be seen from an enlargement of the concentration ratio of Fig. 4.17 (Fig. 4.18). The simulation problem can be overcome by changing the integration routine from Runge-Kutta type to Adams-Gear type. The same simulation is made in SIMULINK with Dormand-Prince-method (Runge-Kutta type for regular differential equations) and NDF15-method (Gear type for stiff differential equations); the results are shown in Fig. 4.18.

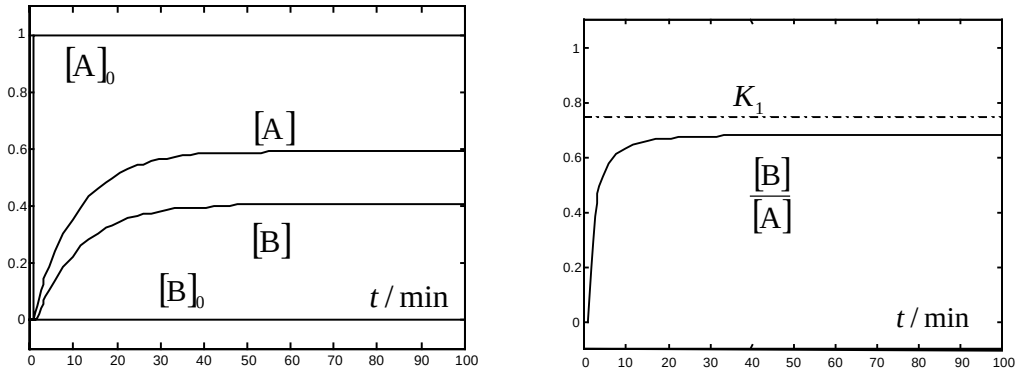

Fig. 4.16: The continuous flow concentrations and their ratio (slow reactions, F = 0.1).

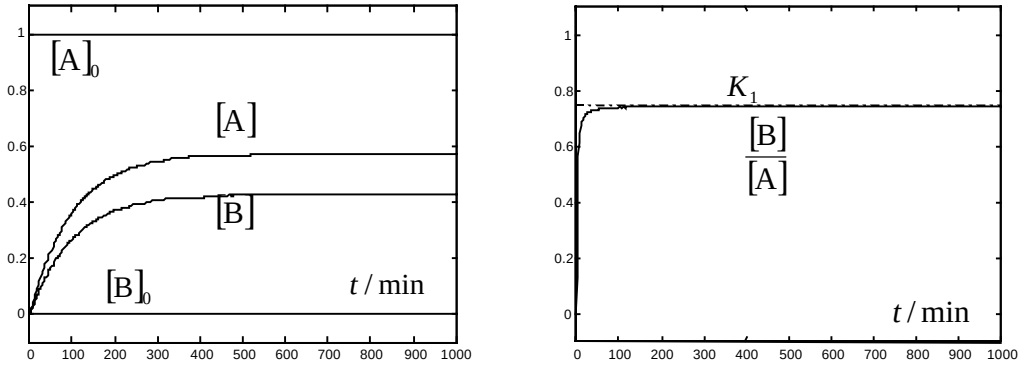

Fig. 4.17: The continuous flow concentrations and their ratio (slow reactions, F = 0.01).

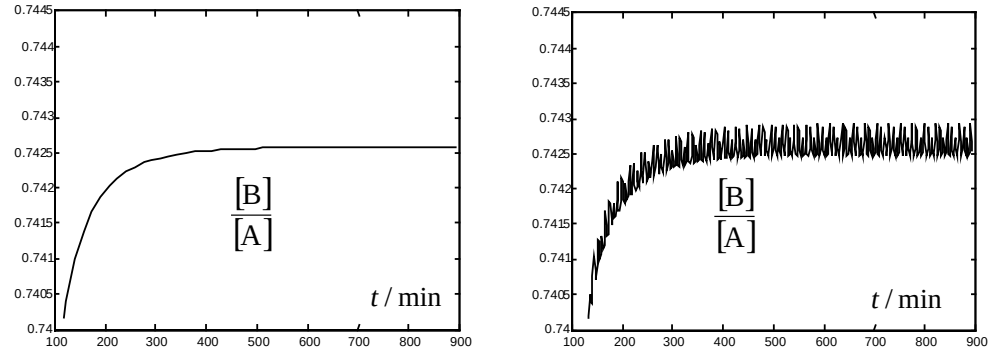

Fig. 4.18: The concentration ratio simulation with Dormand-Prince-method (left) and NDF15-method (right), F = 0.01.

All the processes, models and simulations in this chapter are very simple, but they serve as a platform when more complex systems are generated. The same basic features of chemical reaction modelling (such as the combination of fluid dynamics and chemical kinetics, steady state vs. equilibrium conditions and the stiffness problems) are encountered with complex systems as well.

4.2.2.2 Equilibrium chain reactions in one phase

Let us enlarge the model slightly. The original reaction from A to B still takes place, but now there is a further reaction in which B reacts into C

$$\begin{cases} \mathrm{A} \underset{k_{-1}}{\overset{k_1}{\Leftrightarrow}} \mathrm{B}, & K_1 = \dfrac{k_1}{k_{-1}} = \dfrac{[\mathrm{B}]}{[\mathrm{A}]} = 0.75 \\ \mathrm{B} \underset{k_{-2}}{\overset{k_2}{\Leftrightarrow}} \mathrm{C}, & K_2 = \dfrac{k_2}{k_{-2}} = \dfrac{[\mathrm{C}]}{[\mathrm{B}]} = 0.5 \end{cases} . \tag{4.11}$$

If all reactions are instantaneous, the equilibrium is easily determined. The total concentration [T] is constant and all concentrations can be written as functions of the total concentration.

$$[\mathrm{T}] = [\mathrm{A}] + [\mathrm{B}] + [\mathrm{B}] = [\mathrm{A}] + [\mathrm{B}] + [\mathrm{C}] = \text{constant} . \tag{4.12}$$

$$\begin{cases} [\mathrm{A}] = x \cdot [\mathrm{T}] \\ [\mathrm{B}] = K_1 \cdot [\mathrm{A}] = K_1 \cdot x \cdot [\mathrm{T}] \\ [\mathrm{C}] = K_2 \cdot [\mathrm{B}] = K_2 \cdot K_1 \cdot [\mathrm{A}] = K_2 \cdot K_1 \cdot x \cdot [\mathrm{T}] \end{cases} . \tag{4.13}$$

$$[\mathrm{T}] = [\mathrm{A}] + [\mathrm{B}] + [\mathrm{C}] = (1 + K_1 + K_1 K_2) \cdot x \cdot [\mathrm{T}] \quad \Rightarrow \quad x = \frac{1}{1 + K_1 + K_1 K_2} \tag{4.14}$$

$$\Rightarrow \quad \begin{cases} [\mathrm{A}] = \dfrac{1}{1 + K_1 + K_1 K_2} \cdot [\mathrm{T}] \\ [\mathrm{B}] = \dfrac{K_1}{1 + K_1 + K_1 K_2} \cdot [\mathrm{T}] . \\ [\mathrm{C}] = \dfrac{K_1 K_2}{1 + K_1 + K_1 K_2} \cdot [\mathrm{T}] \end{cases} \tag{4.15}$$

Both batch and continuous flow processes use the same equilibrium condition (for instantaneous reactions); the only difference is that in the continuous flow process the total concentration is not an external variable that can be directly manipulated (it is determined by the flow dynamics). The simulation models are analogous to those shown in Appendix; Figs. A1 and A2 (with the addition of component C) and they are not repeated here.

The simulation results for batch process is shown in Fig. 4.19 and for continuous flow process in Fig. 4.20.

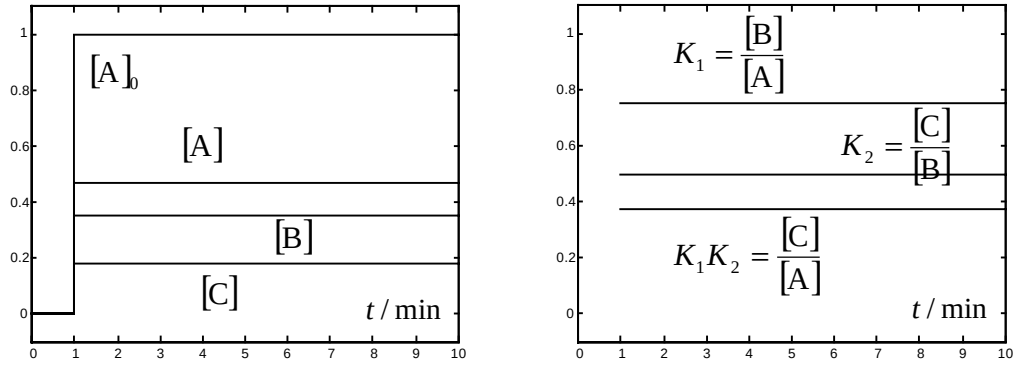

Fig. 4.19: The batch process concentrations and their ratios (instantaneous reactions).

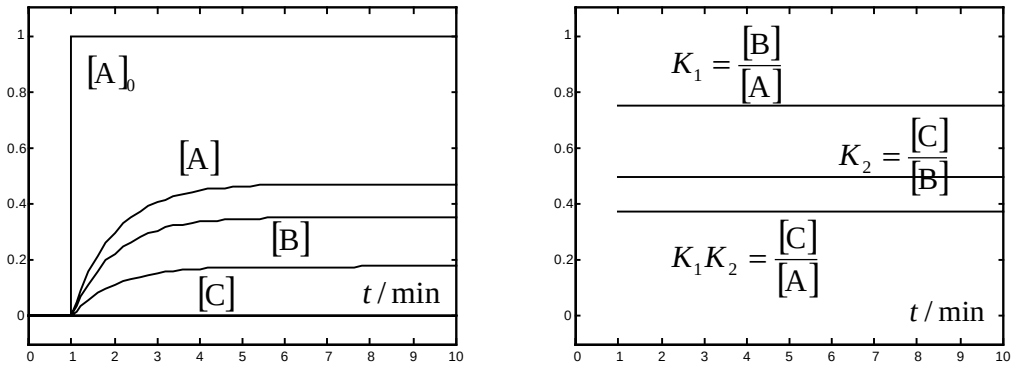

Fig. 4.20: The continuous flow concentrations and their ratios (instantaneous reactions).

The simulation results show that the concentration ratios always obey the equilibrium condition which is no surprise because the models are created based on it. The modelling and simulation was not more difficult than with only one reaction.

If slow reaction kinetics are present there are two possibilities; either both reactions have slow kinetics or one reaction has slow kinetics while the other has instantaneous kinetics. The first simulations illustrated the simpler case, all reactions are slow. The reaction rate constants are chosen as $k_1 = 1.5$, $k_{-1} = 2$, $k_2 = 0.25$ and $k_{-2} = 0.5$. The simulation results for the batch process is shown in Fig. 4.21 and for continuous flow process in Fig. 4.22.

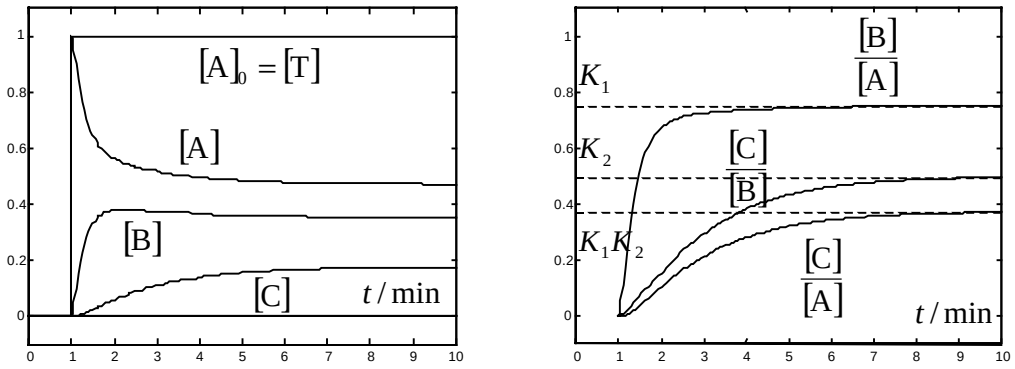

Fig. 4.21: The batch process concentrations and their ratios (slow reactions).

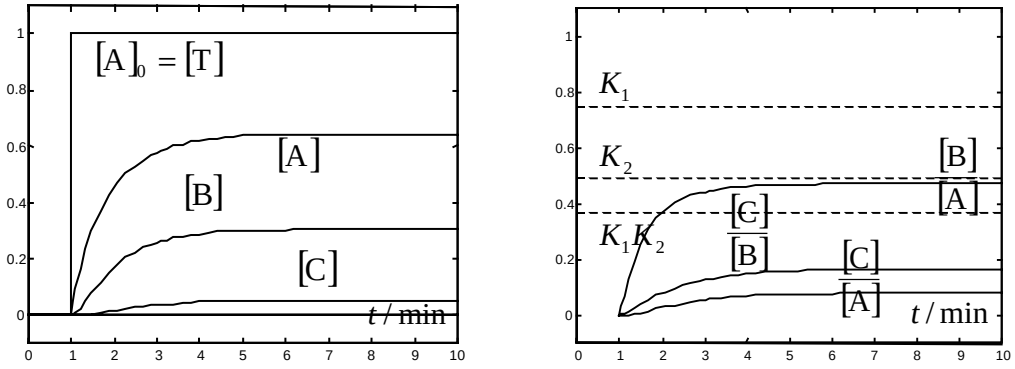

Fig. 4.22: The continuous flow concentrations and their ratios (slow reactions).

The continuous flow process does not reach equilibrium in the reactor but the batch reactor converges to the equilibrium (similarly to the one-reaction case). The modelling and simulation are no more difficult than with one reaction case.

Significant problems arise when one of the reactions can be considered instantaneous (large rate constants) and the other is relatively slow (small rate constants) compared to the flow dynamics. In the simulation example the first reaction (A → B) is instantaneous (k_1, $k_{-1} \to \infty$, K_1 = 0.75) and the second reaction (B → C) is relatively slow (k_2 = 0.25, k_{-2} = 0.5).

One method of solving the modelling and simulation problem is to give an arbitrary large value to one of the instantaneous reaction rate constants and determining the other rate constant from the equilibrium condition

$$k_1 = K_1 \cdot k_{-1}. \tag{4.16}$$

Reaction rates for the slower reaction were kept at k_2 = 0.25 and k_{-2} = 0.5 while different values for k_1 and k_{-1} were tried. The reaction rate constants were increased from the initial values (k_1 = 1.5, k_{-1} = 2) to (k_1 = 15, k_{-1} = 20), (k_1 = 150, k_{-1} = 200) and (k_1 = 1500, k_{-1} = 2000). No significant changes could be detected when larger values than (k_1 = 150, k_{-1} = 200) were used. The simulation results of the batch process are presented in Fig. 4.23 and the continuous flow in Fig. 4.24. (arrows point towards larger kinetic constants)

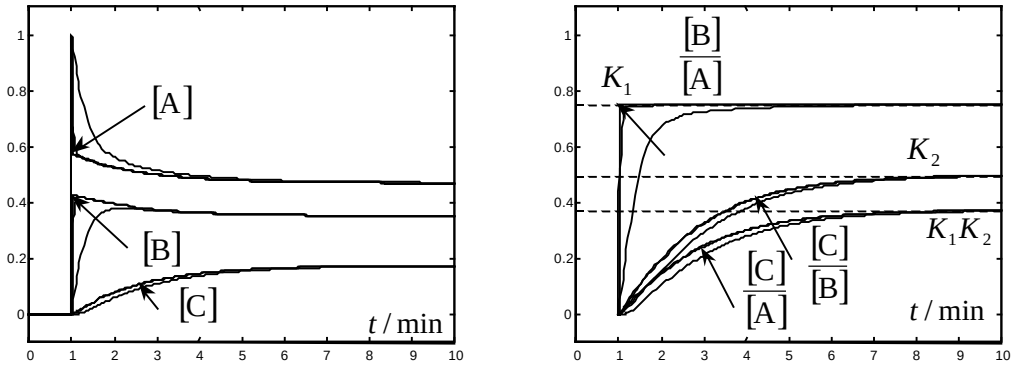

Fig. 4.23: The batch process concentrations and their ratios (combined slow – fast reaction kinetics, different reaction rates for the fast reaction).

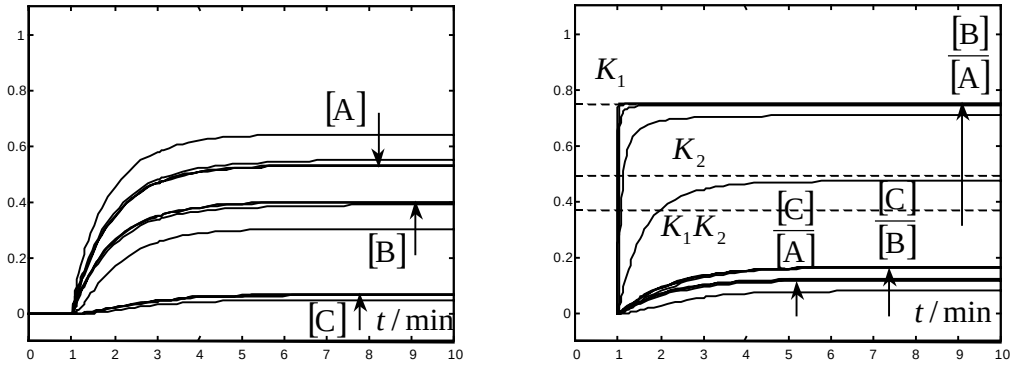

Fig. 4.24: The continuous flow concentrations and their ratios (combined slow – fast reaction kinetics, different reaction rates for the fast reaction).

The simulations prove that this method works for simultaneous fast and slow reaction kinetics. Unfortunately it also makes the modeling and simulation more complex. In most cases there are numerous reactions of which only one or two are determining the overall reaction rate (bottleneck reactions). A static equilibrium mapping can make large systems more efficient and easier to simulate. The problem of static – dynamic modeling is studied in detail in the next section.

4.2.2.4 Equilibrium mapping with slow side reactions

Equilibrium mapping is easily performed, even though it can be an iterative procedure. Adding slow reaction kinetics to fluid dynamics is an equally simple task. Combining these two ideas together is not as straightforward as it might seem. Different combination structures were tested with the same simple chain reaction that was used in the previous section. The batch and continuous flow process responses with the new method should respond to those received with the fast – slow reaction method in the previous section. The responses are shown in Figs. 4.25 and 4.26.

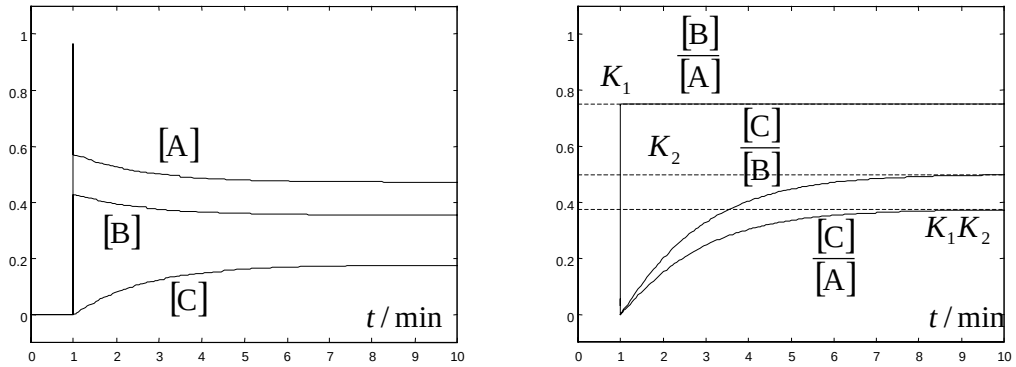

Fig. 4.25: The batch process concentrations and their ratios (combined slow – fast reaction kinetics, different reaction rates for the fast reaction).

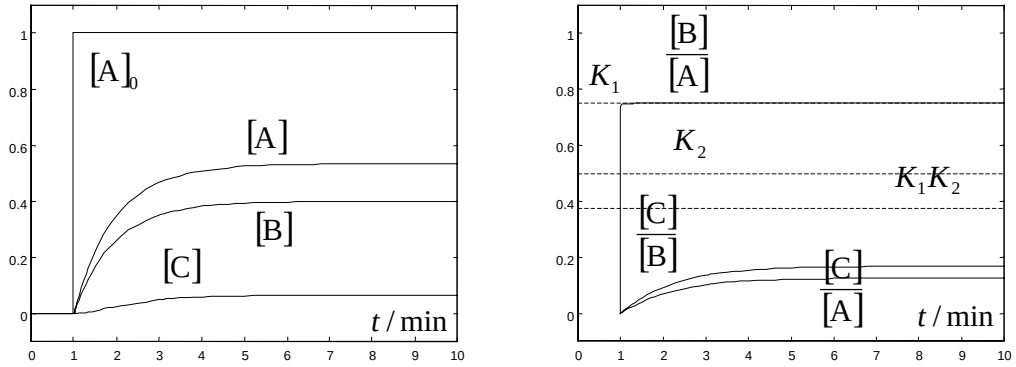

Fig. 4.26: The continuous flow concentrations and their ratios (combined slow – fast reaction kinetics, different reaction rates for the fast reaction).

The intermediate component B causes problems in the modelling procedure. B is at equilibrium at every time instant with A but not necessarily with C. The sum of all concentrations is determined by the total concentration [T] at every time instant.

$$\frac{[\mathrm{B}]}{[\mathrm{A}]} = K, \qquad [\mathrm{T}] = [\mathrm{A}] + [\mathrm{B}] + [\mathrm{C}]. \tag{4.17}$$

If these two criteria are not satisfied at every time instant, the simulation model is not adequate. Because material can not be created from nothing the total concentration is the same whether there are reactions or not. This fact can be used for avoiding numerically sensitive and ill-behaving differential equations. For instance in the example the partial material balance of B is problematic.

$$\frac{d[\mathrm{A}]}{dt} = \underbrace{\frac{1}{V}(F[\mathrm{A}]_0 - F[\mathrm{A}])}_{\text{slow dynamics}} + \underbrace{(-k_1[\mathrm{A}] + k_{-1}[\mathrm{B}])}_{\text{fast kinetics}}$$

$$\frac{d[\mathrm{B}]}{dt} = \underbrace{\frac{1}{V}(F[\mathrm{B}]_0 - F[\mathrm{B}])}_{\text{slow dynamics}} + \underbrace{(k_1[\mathrm{A}] - k_{-1}[\mathrm{B}])}_{\text{fast kinetics}} + \underbrace{(-k_2[\mathrm{B}] + k_{-2}[\mathrm{C}])}_{\text{slow kinetics}}. \qquad (4.18)$$

$$\frac{d[\mathrm{C}]}{dt} = \underbrace{\frac{1}{V}(F[\mathrm{C}]_0 - F[\mathrm{C}])}_{\text{slow dynamics}} + \underbrace{(k_2[\mathrm{B}] - k_{-2}[\mathrm{C}])}_{\text{slow kinetics}}$$

The first equation (partial material balance of A) can be divided into dynamic flow characteristics and static reaction kinetics, the last equation (partial material balance of C) contains interconnected dynamic characteristics from fluid and reaction kinetics but as there are no instantaneous reactions it is well-behaving (Fig. 4.27). An imaginary concept of "flow concentration" is introduced (indicated with a star index in the upper right corner). It is a concentration of a given substance assuming that no reactions would take place.

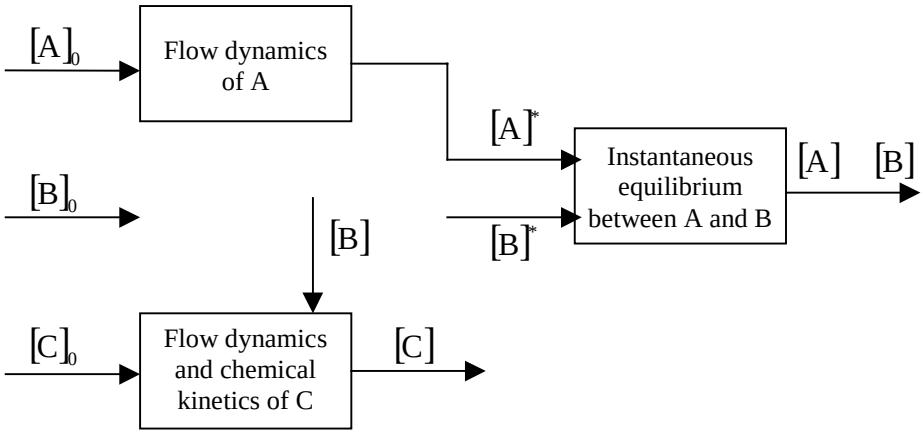

Fig. 4.27: The model structure for components A and C.

Intuitively the second equation could be divided into slow and instantaneous parts but this approach would lead to many practical problems as the concentration of B would be determined both by the equilibrium and the slow kinetics.

$$\begin{aligned} &\frac{d[\mathrm{B}]^*}{dt} = \frac{1}{V}(F[\mathrm{B}]_0 - F[\mathrm{B}]) + (-k_2[\mathrm{B}] + k_{-2}[\mathrm{C}]) \qquad \text{(dynamic part)} \\ &([\mathrm{A}],[\mathrm{B}]) = f([\mathrm{A}]^*,[\mathrm{B}]^*) \qquad \text{(static equilibrium)} \end{aligned} \quad . \qquad (4.19)$$

These problems can be avoided by using the concept of total concentration [T]. All material available at certain point of the process is determined entirely by the total concentration. At that particular point of process the individual concentrations have been affected by various reactions but the total concentration is unaffected by individual reactions (e.g. as B reacts to C there is a decrease in [B] and a corresponding increase in [C] so that [B] + [C] stays constant).

However, it is to be noted that the total molar amount is not constant if the stoichiometric constants are not equal. This problem is easily avoided by using normalised total concentration where the individual concentrations are weighted with the inverses of the stoichiometric constants.

For instance, if the reaction mechanisms were as follows

$$\begin{cases} A \Leftrightarrow 4B \\ 3B \Leftrightarrow 2C \end{cases} \quad => \quad A \Leftrightarrow 4B \Leftrightarrow \tfrac{8}{3}C \quad => \quad \tfrac{1}{8}A \Leftrightarrow \tfrac{1}{2}B \Leftrightarrow \tfrac{1}{3}C. \tag{4.20}$$

One mole of A would produce four moles of B (if only the first reaction would take place and the reaction would be complete) and 8/3 moles of C (if also the second reaction would take place and the reaction would be complete). In this case the normalised total concentration could be e.g.

$$\begin{aligned} &[T]_A = [A] + \frac{[B]}{4} + \frac{3[C]}{8} \quad \text{or} \quad [T]_B = 4[A] + [B] + \frac{3[C]}{2} \quad \text{or} \\ &[T]_C = \frac{8[A]}{3} + \frac{2[B]}{3} + [C] \quad \text{or} \quad [T] = 8[A] + 2[B] + 3[C]. \end{aligned} \tag{4.21}$$

Despite of any reactions and no matter to what extent the reactions take place the total normalised total concentration is constant.

The original problem does not contain any stoichiometric inbalances so all concentrations can be added together directly (or each term is divided by one; procedure that does not change anything). The fluid dynamics of each component determine the total concentration everywhere in the process.

$$\begin{cases} \dfrac{d[A]^*}{dt} = \dfrac{1}{V}\left(F[A]_0 - F[A]^*\right) \\ \dfrac{d[B]^*}{dt} = \dfrac{1}{V}\left(F[B]_0 - F[B]^*\right) \\ \dfrac{d[C]^*}{dt} = \dfrac{1}{V}\left(F[C]_0 - F[C]^*\right) \end{cases}, \qquad [T] = [A]^* + [B]^* + [C]^*. \tag{4.22}$$

The concentrations of the individual components carry no essential information and the number of derivates can be reduced by constructing the differential equation for the total concentration.

$$\frac{d[T]}{dt} = \frac{d[A]^*}{dt} + \frac{d[B]^*}{dt} + \frac{d[C]^*}{dt}. \tag{4.23}$$

In this simple example where all components have identical fluid dynamics the differential equation for the total concentration is as follows

$$\begin{aligned} \frac{d[T]}{dt} &= \frac{1}{V}\left(F[A]_0 - F[A]^* + F[B]_0 - F[B]^* + F[C]_0 - F[C]^*\right) \\ &= \frac{1}{V}\left(F[A]_0 + F[B]_0 + F[C]_0 - F[T]\right) = \frac{1}{V}\left(F[T]_0 - F[T]\right). \end{aligned} \tag{4.24}$$

The fluid dynamics and the chemical kinetics can not be completely separated (as was the case when all chemical reactions were instantaneous). The fluid model has to be included in the partial material balance of C but as explained earlier, this equation is well-behaving.

$$\frac{d[\mathrm{C}]}{dt} = \underbrace{\frac{1}{V}(F[\mathrm{C}]_0 - F[\mathrm{C}])}_{\text{slow dynamics}} + \underbrace{(k_2[\mathrm{B}] - k_{-2}[\mathrm{C}])}_{\text{slow kinetics}}. \tag{4.25}$$

The formation of C is a function of the concentration [B] that is the equilibrium concentration (the equilibrium between A and B, not the equilibrium between B and C that may not necessarily be achieved).

The equilibrium concentrations of A and B can be determined once the sum of A and B is known. The concentration $[\mathrm{T}]^*$ describes the sum of all components that take part in the instantaneous equilibrium reactions

$$[\mathrm{T}]^* = [\mathrm{A}] + [\mathrm{B}]. \tag{4.26}$$

Instead of creating complicated algebraic loops for the behaviour of [B], the well-behaving partial material balance of [C] can be used.

$$[\mathrm{T}] = [\mathrm{A}]^* + [\mathrm{B}]^* + [\mathrm{C}]^* = [\mathrm{A}] + [\mathrm{B}] + [\mathrm{C}] \quad \Rightarrow \quad [\mathrm{T}]^* = [\mathrm{A}] + [\mathrm{B}] = [\mathrm{T}] - [\mathrm{C}] \tag{4.27}$$

This model structure is very practical for simulation. The dynamical part consists of total concentration fluid model and parallel model for slow reactions. The total concentration is divided into components that participate in the instantaneous equilibrium and to components that do not. The parallel slow reaction models determine the non-participating components and by subtracting these components from the total concentration, the fraction used for equilibrium mapping is resulted. The concentrations after the equilibrium mapping are used in parallel slow reaction models in reaction rate terms. The improved model structure is shown in Fig. 4.28.

$$\begin{cases} \dfrac{d[\mathrm{T}]}{dt} = \dfrac{1}{V}(F[\mathrm{A}]_0 + F[\mathrm{B}]_0 + F[\mathrm{C}]_0 - F[\mathrm{T}]) \\ \dfrac{d[\mathrm{C}]}{dt} = \dfrac{1}{V}(F[\mathrm{C}]_0 - F[\mathrm{C}]) + (k_2[\mathrm{B}] - k_{-2}[\mathrm{C}]) \end{cases} \quad \Rightarrow \quad [\mathrm{T}]^* = [\mathrm{T}] - [\mathrm{C}]. \tag{4.28}$$

$$([\mathrm{A}], [\mathrm{B}]) = f([\mathrm{T}]^*)$$

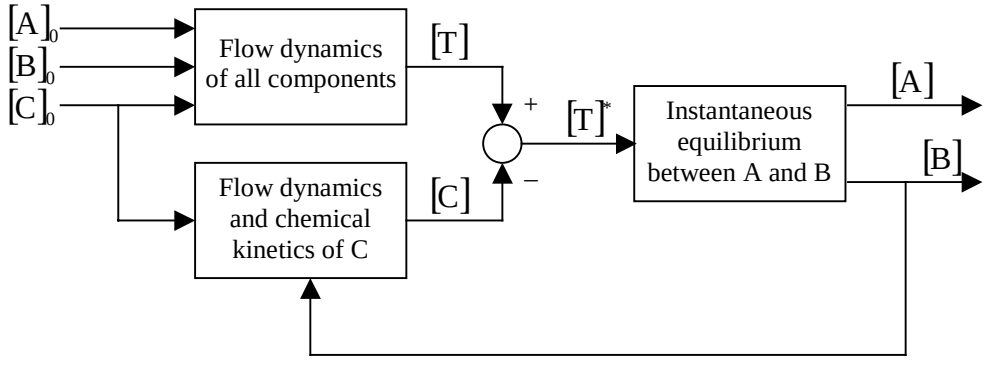

Fig. 4.28: The model structure for the example process.

For the batch process that does not contain any fluid dynamics the simulation model is shown in Appendix 1, Fig. A1.5 and the simulation results in Fig. 4.29.

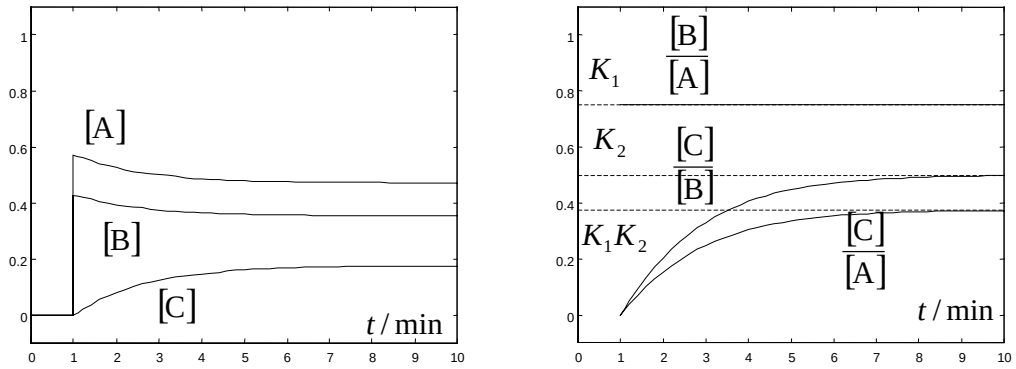

Fig. 4.29: Simulation results for the batch process with combined instantaneous and slow dynamics.

For the continuous flow the simulation model is shown in Appendix 1, Fig. A1.6 and the simulation results in Fig. 4.30.

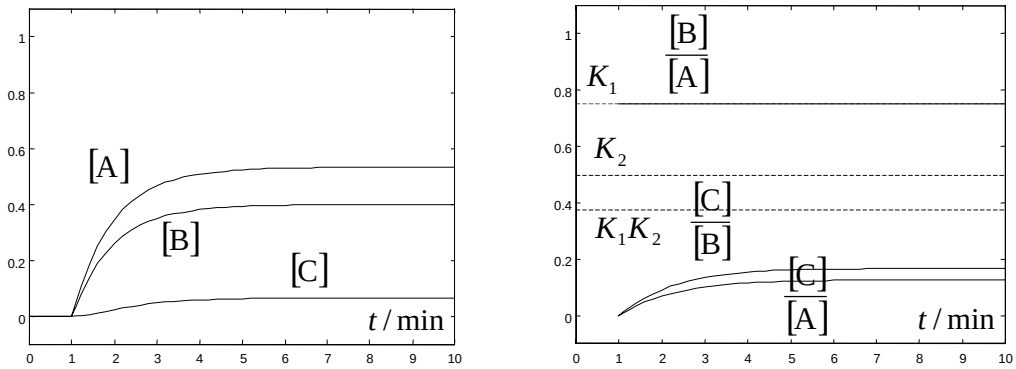

Fig. 4.30: Simulation results for the continuous flow process with combined instantaneous and slow dynamics.

The results shown in Figs. 4.29 and 4.30 correspond to those obtained by using stiff models with arbitrary fast reaction kinetics. However, with these models there are obvious benefits; the model stiffness is avoided (the models are not as sensitive to integration routine selection), no arbitrary rate constants have to be invented (well known equilibrium constants can be used) and models are fast and easy to simulate. In many practical cases there are only one or two bottleneck reactions that determine the overall rate of reaction and the modelling effort can be concentrated on these reactions. The temperature dependency is better known for equilibrium constants than for rate constants and in many cases Gibbs free energy can be used for modelling the effects of temperature changes on the equilibrium reactions.

4.2.2.5 pH processes

pH processes always contain instantaneous reaction kinetics. The protolysation reactions are very fast in general, but there can be slow side reactions that limit the overall speed of reaction kinetics. There is always equilibrium between hydroxide and oxonium ions (ion product of water). The oxonium and hydroxide ions participate in numerous separate reactions and instead of chain reactions there is a net of reactions with the neutralisation or the autoprotolysation reaction as the connecting link.

$$H_3O^+ + OH^- \Leftrightarrow 2H_2O, \qquad K_W = \left[H_3O^+\right]\cdot\left[OH^-\right] = 10^{-14}\ (\text{mol}/\text{l})^2 \quad , \text{ at } 25^\circ\text{C}. \tag{4.29}$$

Instead of forming balances for oxonium and hydroxide a more practical solution is to use the charge balance (electro-neutrality equation) and the ion product of water for combining pH-phenomena to other reactions. The pH-value is defined as

$$\text{pH} = -\log_{10}\{H_3O^+\} \approx -\log_{10}\left[H_3O^+\right]. \tag{4.30}$$

The pH-modelling procedure is illustrated with the help of an example. Weak acid HA and reagent C are fed to the inlet of an ideal mixer as shown in Fig. 4.31.

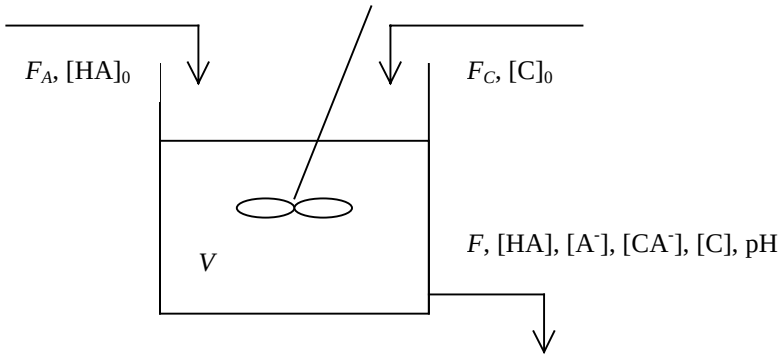

Fig. 4.31: The example pH-process

The following reactions take place

$$\begin{cases} HA + H_2O \Leftrightarrow A^- + H_3O^+, \qquad K_A = 0.5\cdot 10^{-5}\ (\text{mol/l}) \\ A^- + C \underset{k_{-1}}{\overset{k_1}{\Leftrightarrow}} AC^-, \qquad \begin{cases} k_1 = 0.2\ (\text{l}^2/(\text{mol}\cdot\text{s})) \\ k_{-1} = 0.1\ (\text{l/s}) \end{cases} \\ H_3O^+ + OH^- \Leftrightarrow 2H_2O, \qquad K_W = 10^{-14}\ (\text{mol/l})^2 \end{cases} . \tag{4.31}$$

The following concentrations are defined

$$\begin{cases} \left[A\right]_T = \left[HA\right] + \left[A^-\right] + \left[AC^-\right] \quad , \quad \left[C\right]_T = \left[C\right] + \left[AC^-\right] \quad , \quad \left[T\right] = \left[A\right]_T + \left[C\right]_T \\ \left[T\right]^* = \left[HA\right] + \left[A^-\right] = \left[A\right]_T - \left[AC^-\right] = \left[T\right] - \left[C\right]_T - \left[AC^-\right] = \left[T\right] - \left[C\right] - 2\left[AC^-\right] \end{cases} \tag{4.32}$$

The material balances are

$$\begin{cases} \dfrac{d\left[A\right]_T}{dt} = \dfrac{1}{V}\left(F_A\left[A\right]_0 - F\left[A\right]_T\right) \\ \dfrac{d\left[C\right]_T}{dt} = \dfrac{1}{V}\left(F_A\left[A\right]_0 - F\left[C\right]_T\right) \\ \dfrac{d\left[C\right]}{dt} = \dfrac{1}{V}\left(F_C\left[C\right]_0 - F\left[C\right]\right) + \left(-k_1\left[C\right]\left[A^-\right] + k_{-1}\left[AC^-\right]\right) \\ \left[AC^-\right] = \left[C\right]_T - \left[C\right], \qquad \left[T\right]^* = \left[A\right]_T - \left[AC^-\right] \end{cases} . \tag{4.33}$$

The charge balance is $[H_3O^+] - [OH^-] - [A^-] - [AC^-] = 0$. (4.34)

The three first terms of the charge balance describe the instantaneous equilibrium phenomena and the last term slow chemical reaction. pH-value is a direct function of the oxonium ion concentration and therefore the second and the third terms of the balance should be modified. The ion product of water determines the relationship between oxonium and hydroxide ions and the equilibrium constant K_A defines the fraction ion A^- from the total concentration.

$$\begin{cases} K_W = [H_3O^+] \cdot [OH^-] \\ K_A = \dfrac{[H_3O^+] \cdot [A^-]}{[HA]} = \dfrac{[H_3O^+] \cdot [A^-]}{[T]^* - [A^-]} \end{cases} \quad => \quad \begin{cases} [OH^-] = \dfrac{K_W}{[H_3O^+]} \\ [A^-] = \dfrac{K_A}{K_A + [H_3O^+]} [T]^* \end{cases} \tag{4.35}$$

With these modifications, the charge balance can be presented as follows

$$[H_3O^+] - \frac{K_W}{[H_3O^+]} - \frac{K_A}{K_A + [H_3O^+]} [T]^* - [AC^-] = 0, \quad pH = -\log_{10}[H_3O^+] \tag{4.36}$$

This is the static equation that defines the pH-value. The oxonium ion concentration has to be iterated at each simulation step. The dynamic process model consists of the following equations

Dynamic part:

$$\begin{cases} \dfrac{d[A]_T}{dt} = \dfrac{1}{V}(F_A[A]_0 - F[A]_T) \\ \dfrac{d[C]_T}{dt} = \dfrac{1}{V}(F_C[C]_0 - F[C]_T) \\ \dfrac{d[C]}{dt} = \dfrac{1}{V}(F_C[C]_0 - F[C]) + (-k_1[C][A^-] + k_{-1}[AC^-]) \end{cases} . \tag{4.37}$$

Static part:

$$\begin{cases} [AC^-] = [C]_T - [C], \qquad [T]^* = [A]_T - [AC^-] \\ [H_3O^+] - \dfrac{K_W}{[H_3O^+]} - \dfrac{K_A}{K_A + [H_3O^+]} [T]^* - [AC^-] = 0 \\ pH = -\log_{10}[H_3O^+], \qquad [A^-] = \dfrac{K_A}{K_A + [H_3O^+]} [T]^* \end{cases} . \tag{4.38}$$

The same model also applies to a batch processes (simulation model shown in Fig. 4.38). When all flows are set to zero the model becomes as follows:

$$\begin{cases} [A]_T = \int \dfrac{n_A}{V} \quad , \quad [C]_T = \int \dfrac{n_C}{V} \\ \dfrac{d[C]}{dt} = \dfrac{n_C}{V} + (-k_1[C][A^-] + k_{-1}[AC^-]) \end{cases}, \tag{4.39}$$

$$\begin{cases} [\mathrm{AC^-}] = [\mathrm{C}]_T - [\mathrm{C}], \qquad [\mathrm{T}]^* = [\mathrm{A}]_T - [\mathrm{AC^-}] \\ [\mathrm{H_3O^+}] - \dfrac{K_W}{[\mathrm{H_3O^+}]} - \dfrac{K_A}{K_A + [\mathrm{H_3O^+}]}[\mathrm{T}]^* - [\mathrm{AC^-}] = 0 \\ \mathrm{pH} = -\log_{10}[\mathrm{H_3O^+}], \qquad [\mathrm{A^-}] = \dfrac{K_A}{K_A + [\mathrm{H_3O^+}]}[\mathrm{T}]^* \end{cases} . \tag{4.40}$$

The calculation of concentrations $[A]_T$, $[C]_T$, [C], $[AC^-]$ and $[T]^*$ is performed with SIMULINK blocks. The iteration of $[H_3O^+]$ and the pH-value and the $[A^-]$ concentration determination are done in a MATLAB-function named `pHvalue`, the script of which is as follows

```
function y = pHvalue (u)
global T C
T=u(1);
C=u(2);
z=fzero('charg(x)',[1e-20;100000]);
y(1)=-log10(z);
y(2)=(0.5e-5)/(z+0.5e-5);
```

The iteration routine of `pHvalue` is `fzero` that finds the value (`z`) of $[H_3O^+]$ (`x`) that satisfies the charge balance (`'charg(x)'`). The charge balance is another MATLAB-function (named `charg`); as follows

```
function y=charg(x)
global T C
y=x-(1e-14)/x-(0.5e-5)*T/((0.5e-5)+x)-C;
```

The simulation model for the batch pH-process is shown in Appendix 1, Fig. A1.7. The concentrations of the weak acid HA and the reagent C were increased during the simulations as shown in Fig. 4.32. The initial concentration of HA was 1e-6 mol/l and C was 0 mol/l. The total concentration of the acid ($[A]_T$ = [HA] + $[A^-]$ + $[AC^-]$) was increased to 3.25e-6 mol/l at time instant 10 s and to 10e-6 mol/l at time instant 140 s. At t = 70 s reagent C was added so that the total concentration of the reagent ($[C]_T$ = [C] + $[AC^-]$) was 1e-4 mol/l.

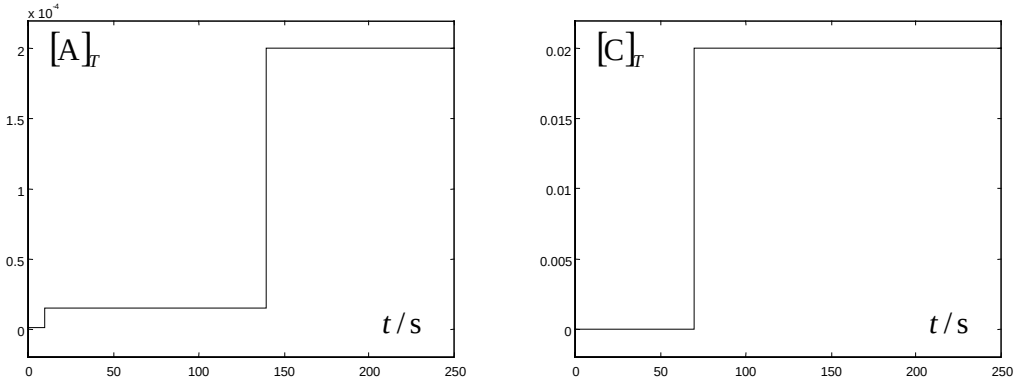

Fig. 4.32: The total concentrations of acid HA and reagent C in the batch pH process.

The responses to the acid and reagent additions are shown in fig. 4.33. A dashed line in Fig. 4.33 (left figure) shows how the pH-value would behave if there were no reagent C additions. The reaction rates are shown in Fig. 4.34.

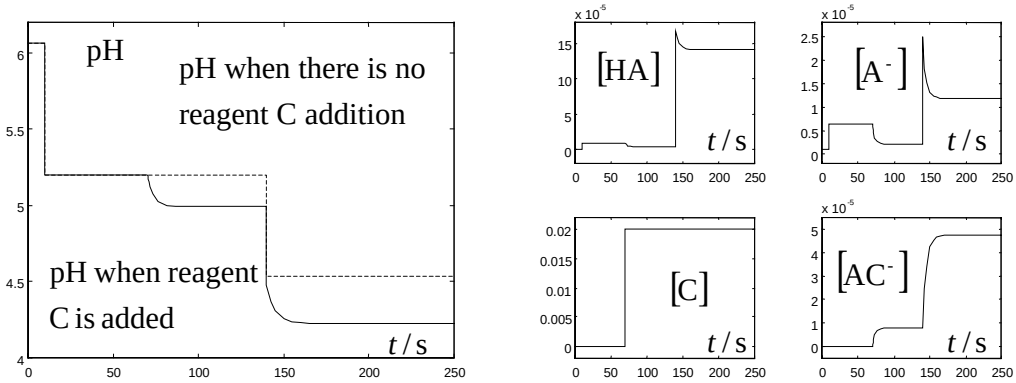

Fig. 4.33: The pH and concentration responses in the batch pH-process.

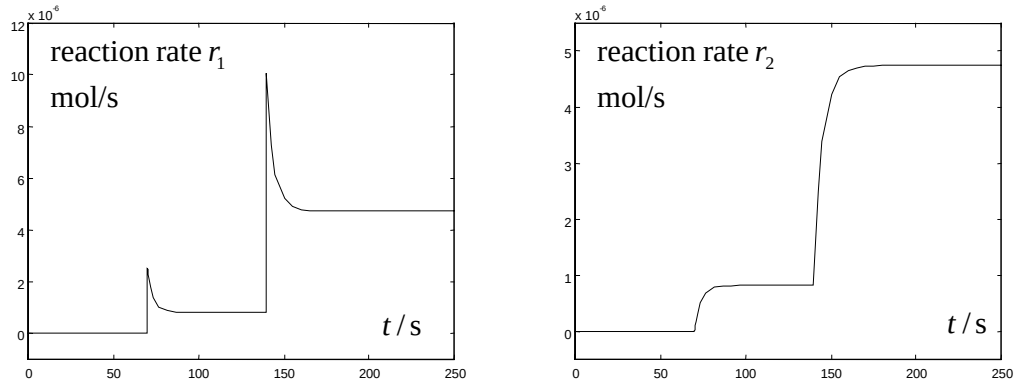

Fig. 4.34: The reaction rates in the batch pH-process.

The results show that the batch pH process is dynamic only if there is reagent C present in the vessel. The batch process is an idealisation of a titration vessel and the dynamic behaviour can be a problem during titration experiments. The reactions in the example are relatively fast but in many real cases they can be very slow. As a result of the slow reaction kinetics there can be a long waiting period after each acid/base addition in titration.

Dissolution/precipitation reactions are typical slow side reactions that can have a very slow effect on the pH-value. The mechanisms of these reactions are more complicated than the example given in this section. The dissolution/precipitation reactions are treated in more detail in the next section.

4.2.2.6 pH process with slow dissolution/precipitation phenomena

Dissolution and precipitation consist of complex molecular micro phenomena that are difficult to model. The phase change is governed by e.g. the surface area between the two phases (the porosity of the solid particles, the size distribution of the particles and the relative mixing of the two phases).

In the thick de-inked pulp application presented in Chapter 6 calcium carbonate precipitation/dissolution took place and therefore calcium carbonate is given as an example already in this section. The kinetics concerning other precipitates have similar if not identical structure to that of calcium carbonate.

Instead of using complex micro models, in many cases simple macro models will describe the behaviour of the process adequately. There are many articles on precipitation and dissolution kinetics in general and specifically on calcium carbonate dissolution/precipitation. Sjöberg [116] suggested a very simple macro model that has been also verified by other researchers, e.g. Compton and Daly [10].

$$\frac{d[\mathrm{CaCO_3}]}{dt} = k \cdot A \cdot \left(\sqrt{[\mathrm{Ca^{2+}}] \cdot [\mathrm{CO_3^{2-}}]} - \sqrt{K_{SP}} \right). \tag{4.41}$$

Here k is a rate constant, A is the surface area between the two phases and K_{SP} is the solubility product of calcium carbonate. The equation has many benefits such as guaranteed equilibrium condition and minimal number of free parameters. The equilibrium condition is guaranteed in the sense that dissolution and precipitation do not take place if the ionic product and the solubility product are equal or the physical boundaries are reached.

A serious drawback in the model is the required a priori information of the surface area between the solid and liquid phases. It is very reasonable that the surface area affects the dissolution/precipitation phenomena but the determination of the area is not possible in many practical processes. In some cases the actual surface area can be replaced with an average surface area that can be considered constant.

A simple simulation example is constructed from a weak acid HA and dissolution/precipitation phenomena of CA which is a salt that dissolves under acidic conditions.

$$\begin{cases} \mathrm{HA} + \mathrm{H_2O} \Leftrightarrow \mathrm{A^-} + \mathrm{H_3O^+}, & K_A = 0.5 \cdot 10^{-5} \ (\mathrm{mol/l}) \\ \mathrm{A^-} + \mathrm{C^+} \underset{k}{\overset{k}{\Leftrightarrow}} \mathrm{CA\ (s)}, & kA = 0.1 \ (\mathrm{l/s}), \quad K_{SP} = 3.162 \cdot 10^{-8} \ (\mathrm{mol/l})^2 . \\ \mathrm{H_3O^+} + \mathrm{OH^-} \Leftrightarrow 2\mathrm{H_2O}, & K_W = 10^{-14} \ (\mathrm{mol/l})^2 \end{cases} \tag{4.42}$$

Similarly to the example in the previous section, following concentrations are defined

$$\begin{cases} [\mathrm{A}]_T = [\mathrm{HA}] + [\mathrm{A^-}] + [\mathrm{CA}] \\ [\mathrm{C}]_T = [\mathrm{C^+}] + [\mathrm{CA}] \\ [\mathrm{T}] = [\mathrm{A}]_T + [\mathrm{C}]_T \\ [\mathrm{T}]^* = [\mathrm{HA}] + [\mathrm{A^-}] = [\mathrm{A}]_T - [\mathrm{CA}] = [\mathrm{T}] - [\mathrm{C}]_T - [\mathrm{CA}] = [\mathrm{T}] - [\mathrm{C^+}] - 2[\mathrm{CA}] \end{cases} . \tag{4.43}$$

The material balances are

$$\begin{cases} \dfrac{d[\mathrm{A}]_T}{dt} = \dfrac{1}{V}\left(F_A[\mathrm{A}]_0 - F[\mathrm{A}]_T\right) \\ \dfrac{d[\mathrm{C}]_T}{dt} = \dfrac{1}{V}\left(F_A[\mathrm{C}]_0 - F[\mathrm{C}]_T\right) \\ \dfrac{d[\mathrm{CA}]}{dt} = \dfrac{1}{V}\left(F_C[\mathrm{CA}]_0 - F[\mathrm{CA}]\right) + \left(kA\left(\sqrt{[\mathrm{C^+}][\mathrm{A^-}]} - \sqrt{K_{SP}} \right) \right) \\ [\mathrm{C^+}] = [\mathrm{C}]_T - [\mathrm{CA}], \quad [\mathrm{T}]^* = [\mathrm{A}]_T - [\mathrm{CA}] \end{cases} . \tag{4.44}$$

There is additional feed of strong acid and base that is used for controlling the pH value. It is assumed that the concentrations of these components in the vessel can be manipulated freely and therefore no dynamic equations are needed for the strong acid-base behaviour. The only place where the strong components have any effect on the system is the charge balance that is as follows

$$\begin{cases} [H_3O^+] - [OH^-] - [A^-] + [C^+] + [X] = 0 \\ [X] = [\text{Strong Base}] - [\text{Strong Acid}] \end{cases}, \tag{4.45}$$

$$\begin{cases} K_W = [H_3O^+] \cdot [OH^-] \\ K_A = \dfrac{[H_3O^+] \cdot [A^-]}{[HA]} = \dfrac{[H_3O^+] \cdot [A^-]}{[T]^* - [A^-]} \end{cases} \Rightarrow \begin{cases} [OH^-] = \dfrac{K_W}{[H_3O^+]} \\ [A^-] = \dfrac{K_A}{K_A + [H_3O^+]} [T]^* \end{cases}. \tag{4.46}$$

With these modifications, the charge balance can be presented as follows

$$\begin{cases} [H_3O^+] - \dfrac{K_W}{[H_3O^+]} - \dfrac{K_A}{K_A + [H_3O^+]} [T]^* + [C^+] + [X] = 0 \\ \text{pH} = -\log_{10}[H_3O^+] \end{cases}. \tag{4.47}$$

This is the static equation that defines the pH-value. The oxonium ion concentration has to be iterated at each simulation step. The dynamic process model consists of the following equations

Dynamic part:

$$\begin{cases} \dfrac{d[A]_T}{dt} = \dfrac{1}{V}\left(F_A[A]_0 - F[A]_T\right) \\ \dfrac{d[C]_T}{dt} = \dfrac{1}{V}\left(F_A[C]_0 - F[C]_T\right) \\ \dfrac{d[CA]}{dt} = \dfrac{1}{V}\left(F_C[CA]_0 - F[CA]\right) + \left(kA\left(\sqrt{[C^+][A^-]} - \sqrt{K_{SP}}\right)\right) \end{cases}. \tag{4.48}$$

Static part:

$$\begin{cases} [C^+] = [C]_T - [CA], \qquad [T]^* = [A]_T - [CA] \\ [H_3O^+] - \dfrac{K_W}{[H_3O^+]} - \dfrac{K_A}{K_A + [H_3O^+]} [T]^* + [C^+] + [X] = 0 \\ \text{pH} = -\log_{10}[H_3O^+], \qquad [A^-] = \dfrac{K_A}{K_A + [H_3O^+]} [T]^* \end{cases}. \tag{4.49}$$

The process was simulated in batch mode (all flows were set to zero). Initially there is 0.001 mol/l of weak acid HA, 0.001 mol/l of C^+-ion and 0.0015 mol/l of strong acid. Strong base was added every minute so that its concentration increased 0.00042 mol/l with every addition. With

these definitions the process mimics a titration procedure. The simulation model is shown in Appendix1, Fig. A1.8.

The static iteration is almost identical to that presented in the previous chapter. The script of the Matlab functions `pHvalue2` and `charg2` are as follows

```
function y = pHvalue2 (u)
global T C
T=u(1);
C=u(2);
z=fzero('charg2(x)',[1e-20;100000]);
y(1)=-log10(z);
y(2)=(0.5e-5)/(z+0.5e-5);

function y=charg2(x)
global T C
y=x-(1e-14)/x-(0.5e-5)*T/((0.5e-5)+x)+C;
```

The simulation results are shown in Figs. 4.35 – 4.36. Fig. 4.35a shows the strong base/strong acid concentration difference and Fig. 4.35b the behaviour of the pH-value. Fig. 4.36a shows the concentrations of individual components and Fig. 4.36b compares the ion product to the solubility product.

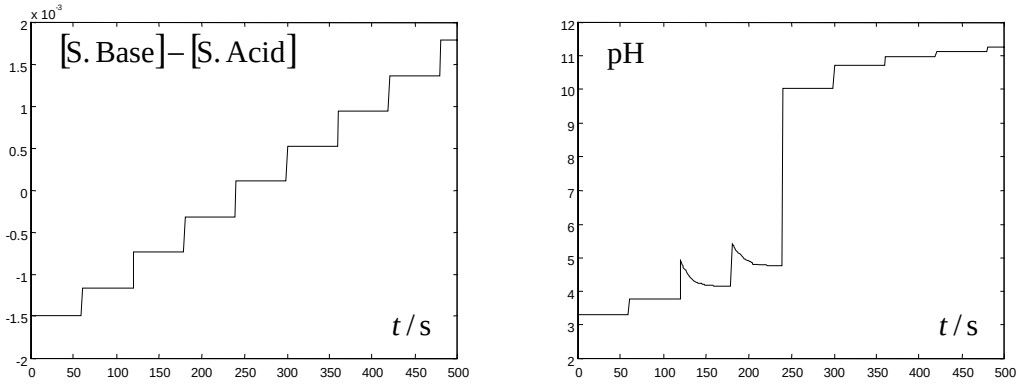

a b

Fig. 4.35: The total concentrations of acid HA and reagent C in the batch pH process.

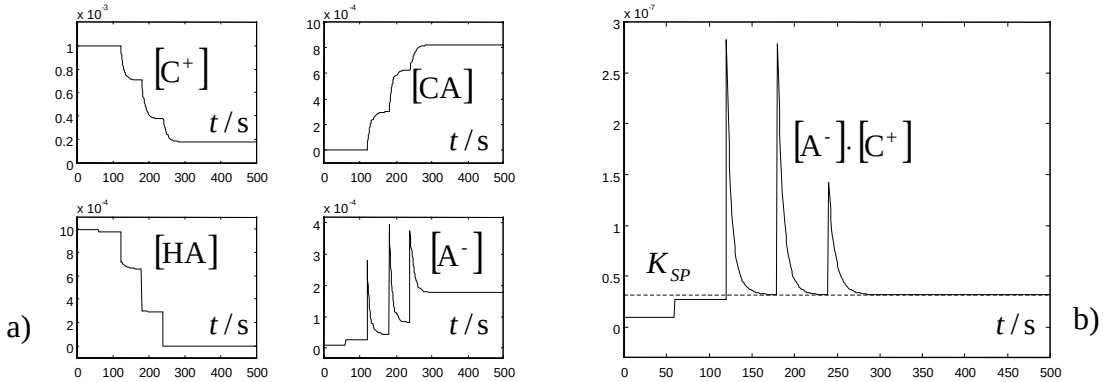

a) b)

Fig. 4.36: The concentrations and the ion product in the titration process.

The results show that the model satisfies the precipitation/dissolution assumptions and the static gains of the model are accurate. The precipitation/dissolution kinetics have an effect on the

titration process only conditionally. Nothing happens if there are no precipitates and the ionic product is lower than the solubility product; the system behaves as if there were no slow reactions present. When there are precipitates present, the system is trying to satisfy the solubility product. In batch processes solubility product is satisfied at steady state and in continuous flow processes this is not necessarily true. Nevertheless the system is always aiming for the solubility product.

The results show that the process is dynamic only at certain pH-region. This is both true and misleading; at low pH-values there are no precipitates present and at high pH-values the system is running out of participating ions. The system would have dynamic responses if at low pH-values solid CA were added or at high pH-values the concentration of either of the participating ions were changed.

It is to be remembered that in this approach the precipitates were evenly spread into the liquid phase by vigorous mixing (ideal mixer) and that the surface characteristics of the precipitates were omitted. The hydrophobic particles that tend to precipitate on the vessel walls are not able to react freely in the vessel and additional kinetics has to be considered in these cases.

4.2.2.7 Gas – liquid phase equilibrium and kinetics

Solid – liquid slurries are usually relative easy to mix into homogeneous mass especially if the solid percentage is not too high. For gas – liquid mixtures the problem is much more severe. The kinetic models for phase change are usually much more clearly governed by the surface area and the transport phenomena than for the liquid – solid systems. There is usually a reaction mechanism similar to that shown below present

$$\mathrm{D\,(aq)} \underset{k_{-1}}{\overset{k_1}{\Leftrightarrow}} \mathrm{D\,(g)}, \qquad K_1 = \frac{P_\mathrm{D}}{[\mathrm{D\,(aq)}]}\,(\mathrm{atm \cdot l/mol}), \tag{4.50}$$

where P_D is the partial pressure of D. Simple kinetic models that can be used for this include, e.g.

$$\frac{d[\mathrm{D\,(aq)}]}{dt} = k \cdot A \cdot \left(P_\mathrm{D} - K_1[\mathrm{D\,(aq)}]\right). \tag{4.51}$$

This equation describes the gas formation more accurately than the gas absorption that is affected more by the surface area and transportation kinetics.

4.2.2.8 Calcium – carbonate model

All the structures developed in the earlier sections are used in the calcium – carbonate reaction chain modelling. A slightly simplified reaction chain is presented below

$$\mathrm{CO_2(\uparrow g)} \underset{k_{g-1}}{\overset{k_{g1}}{\Leftrightarrow}} \mathrm{CO_2}(aq), \quad K_g = \frac{k_{g1}}{k_{g-1}}$$

$$\mathrm{CO_2}(aq) + \mathrm{H_2O} \underset{k_{h-0}}{\overset{k_{h0}}{\Leftrightarrow}} \mathrm{H_2CO_3}\ K_{h0} = \frac{k_{h0}}{k_{h-0}}$$

$$\mathrm{H_2CO_3} + \mathrm{H_2O} \underset{k_{h-1}}{\overset{k_{h1}}{\Leftrightarrow}} \mathrm{HCO_3^-} + \mathrm{H_3O^+}\ K_{h1} = \frac{k_{h1}}{k_{h-1}}$$

$$HCO_3^- + H_2O \underset{k_{h-2}}{\overset{k_{h2}}{\Leftrightarrow}} CO_3^{2-} + H_3O^+ \quad K_{h2} = \frac{k_{h2}}{k_{h-2}}. \tag{4.52}$$

$$CO_3^{2-} + Ca^{2+} \underset{k_{s-1}}{\overset{k_{s1}}{\Leftrightarrow}} CaCO_3(\downarrow s) \quad K_{s1} = \frac{k_{s1}}{k_{s-1}}$$

$$H_3O^+ + OH^- \underset{k_{w-1}}{\overset{k_{w1}}{\Leftrightarrow}} 2H_2O \quad K_w = \frac{k_{w1}}{k_{w-1}}$$

The model is created assuming that the phase change phenomena are the only ones that have slow kinetics. All other reactions are assumed to be instantaneous. There is an additional flow of strong acids and bases that is used for controlling the pH-value. The concentrations of strong components can be freely manipulated and they have no effect on the volume of the system. Furthermore it is assumed that the temperature inside the reactor is constant and that the reactor is closed (the gas phase does not interact with the surrounding). The reactor is shown in Fig. 4.37.

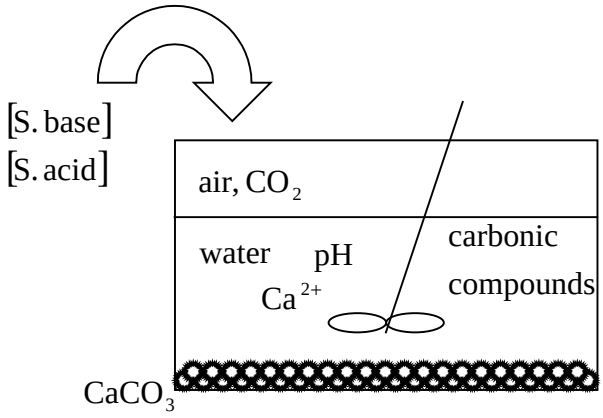

Fig. 4.37: The calcium – carbonate process.

The following concentrations have been defined

$$\begin{cases} [Ca]_T = [Ca^{2+}] + [CaCO_3] \\ [CO]_T = [CO_2(g)] + [CO_2(aq)] + [H_2CO_3] + [HCO_3^-] + [CO_3^{2-}] + [CaCO_3] \\ [T] = [Ca]_T + [CO]_T \\ [T]^* = [CO_2(aq)] + [H_2CO_3] + [HCO_3^-] + [CO_3^{2-}] = [CO]_T - [CaCO_3] - [CO_2(g)] \end{cases}. \tag{4.53}$$

The concept of concentration applies only for liquid components. Because most of the reactions take place in liquid phase it is convenient to use artificial concentrations for solid and gaseous phases as well.

$$[CaCO_3] = \frac{n_{CaCO_3}}{V_L}, \quad [CO_2(g)] = \frac{n_{CO_2(g)}}{V_L} = \frac{P_{CO_2} V_g}{RTV_L}. \tag{4.54}$$

Equilibrium constants for the process are

$$K_g = \frac{[CO_2(aq)]}{P_{CO_2}} = 0.0316 \text{ mol/(l} \cdot \text{atm)}, \qquad K_{h0} = \frac{[H_2CO_3]}{[CO_2(aq)]} = 1.047 \cdot 10^{-3}$$

$$K_{h1} = \frac{[H_3O^+][HCO_3^-]}{[H_2CO_3]} = 4.074 \cdot 10^{-4} \text{ mol/l}, \quad K_{h2} = \frac{[H_3O^+][CO_3^{2-}]}{[HCO_3^-]} = 5.6 \cdot 10^{-11} \text{ mol/l}.$$
$$K_{s1} = [Ca^{2+}][CO_3^{2-}] = 4.96 \cdot 10^{-9} \text{ (mol/l)}^2, \quad K_w = [H_3O^+][OH^-] = 1 \cdot 10^{-14} \text{ (mol/l)}^2 \qquad (4.55)$$

The vessel is filled with water and air. Both air and water contain carbon dioxide:

$$P_{CO_2} = 3.162 \cdot 10^{-4} \text{ atm}, \quad P = 1 \text{ atm}, \quad V_{air} = 1 \text{l}$$
$$[CO]_{liquid} = 5.261 \cdot 10^{-5} \text{ mol/l} \quad V_{liquid} = 1 \text{l}, \quad \text{T} = 25 \text{ °C}.$$

The carbon dioxide concentration is calculated from the partial pressure of carbon dioxide

$$[CO_2\,(g)] = \frac{P_{CO_2} V_{air}}{RTV_{liquid}} = \frac{(3.162 \cdot 10^{-4} \text{ atm}) \cdot (1 \text{ l})}{(0.0821 \text{ atm} \cdot \text{l} \cdot \text{mol}^{-1} \cdot \text{K}^{-1}) \cdot (298.15 \text{ K}) \cdot (1 \text{l})} \approx 1.29 \cdot 10^{-5} \frac{\text{mol}}{\text{l}}. \qquad (4.56)$$

Similarly the equilibrium constant is modified for concentrations instead of partial pressures

$$K_g = \frac{[CO_2(aq)]}{P_{CO_2}} = \frac{V_{air}}{RTV_{liquid}} \cdot \frac{[CO_2(aq)]}{[CO_2(g)]}$$
$$\Rightarrow \quad K_{g^*} = \frac{[CO_2(aq)]}{[CO_2(g)]} = \frac{RTV_{liquid}}{V_{air}} \cdot K_g = 0.7735. \qquad (4.57)$$

0.1 grams of solid calcium carbonate is added to the vessel

$$n_{CaCO_3} = \frac{m_{CaCO_3}}{M_{CaCO_3}} = \frac{0.1 \text{ g}}{100.09 \text{ g/mol}} \approx 0.0009991 \text{ mol} \qquad (4.58)$$

The total concentrations in the vessel are as follows

$$\begin{cases} [Ca]_T = 0.0009991 \text{ mol/l} \\ [CO]_T = 0.0009991 \text{ mol/l} + [CO_2(g)] + [CO]_{liquid} \approx 0.001065 \text{ mol/l} \end{cases}. \qquad (4.59)$$

The slow kinetic equations for the phase change phenomena are as follows

$$\begin{cases} \frac{d[CaCO_3]}{dt} = kA_1\left(\sqrt{[Ca^{2+}] \cdot [CO_3^{2-}]} - \sqrt{K_{SP}}\right) \\ \frac{d[CO_2(g)]}{dt} = kA_2\left([CO_2(aq)] - K_{g^*}[CO_2(g)]\right) \end{cases}, \quad \begin{cases} kA_1 = 0.1 \text{ l/min} \\ kA_2 = 0.01 \text{ l/min} \end{cases}. \qquad (4.60)$$

The remaining concentrations and the pH-value result from instantaneous reactions and they can be iterated statically from following equations

$$[H_3O^+] + [OH^-] + [HB^+] - [A^-] - [HCO_3^-] - 2 \cdot [CO_3^{2-}] + 2 \cdot [Ca^{2+}] = 0$$
$$[T]^* = [CO_2(aq)] + [H_2CO_3] + [HCO_3^-] + [CO_3^{2-}]$$
$$[Ca^{2+}] = [Ca]_T - [CaCO_3]$$

$$[OH^-] = \frac{K_w}{[H_3O^+]} \tag{4.61}$$

$$[H_2CO_3] = K_{h0}[CO_2(aq)]$$

$$[HCO_3^-] = K_{h1}\frac{[H_2CO_3]}{[H_3O^+]} = K_{h0}K_{h1}\frac{[CO_2(aq)]}{[H_3O^+]}$$

$$[CO_3^{2-}] = K_{h2}\frac{[HCO_3^-]}{[H_3O^+]} = K_{h0}K_{h1}K_{h2}\frac{[CO_2(aq)]}{[H_3O^+]^2}$$

All concentrations of the components that take place in the instantaneous equilibrium can be written as functions of the total concentration

$$[T]^* = [CO_2(aq)] + K_{h0}[CO_2(aq)] + K_{h0}K_{h1}\frac{[CO_2(aq)]}{[H_3O^+]} + K_{h0}K_{h1}K_{h2}\frac{[CO_2(aq)]}{[H_3O^+]^2}$$

$$\Rightarrow \quad [T]^* = \left(1 + K_{h0} + \frac{K_{h0}K_{h1}}{[H_3O^+]} + \frac{K_{h0}K_{h1}K_{h2}}{[H_3O^+]^2}\right)\cdot[CO_2(aq)]$$

$$\Rightarrow \quad [CO_2(aq)] = \frac{1}{1 + K_{h0} + \frac{K_{h0}K_{h1}}{[H_3O^+]} + \frac{K_{h0}K_{h1}K_{h2}}{[H_3O^+]^2}}\cdot[T]^*$$

$$[H_2CO_3] = \frac{K_{h0}}{1 + K_{h0} + \frac{K_{h0}K_{h1}}{[H_3O^+]} + \frac{K_{h0}K_{h1}K_{h2}}{[H_3O^+]^2}}\cdot[T]^* . \tag{4.62}$$

$$[HCO_3^-] = \frac{\frac{K_{h0}K_{h1}}{[H_3O^+]}}{1 + K_{h0} + \frac{K_{h0}K_{h1}}{[H_3O^+]} + \frac{K_{h0}K_{h1}K_{h2}}{[H_3O^+]^2}}\cdot[T]^*$$

$$[CO_3^{2-}] = \frac{\frac{K_{h0}K_{h1}K_{h2}}{[H_3O^+]^2}}{1 + K_{h0} + \frac{K_{h0}K_{h1}}{[H_3O^+]} + \frac{K_{h0}K_{h1}K_{h2}}{[H_3O^+]^2}}\cdot[T]^*$$

The charge balance can be written as follows

$$[H_3O^+] + \frac{K_W}{[H_3O^+]} + ([HB^+] - [A^-]) - \frac{\frac{K_{h0}K_{h1}}{[H_3O^+]} + 2\frac{K_{h0}K_{h1}K_{h2}}{[H_3O^+]^2}}{1 + K_{h0} + \frac{K_{h0}K_{h1}}{[H_3O^+]} + \frac{K_{h0}K_{h1}K_{h2}}{[H_3O^+]^2}}\cdot[T]^* + 2\cdot[Ca^{2+}] = 0 . \tag{4.63}$$

($[HB^+]$-$[A^-]$), $[T]^*$ and $[Ca^{2+}]$ are all external variables and the only internal variable $[H_3O^+]$ can be iterated. Once $[H_3O^+]$ is known all other concentrations can be calculated analytically.

The simulation model of the process is shown in Appendix 1, Fig. A1.9 and the simulation results for the process preparation (initially water and air system with carbon dioxide and then solid

calcium carbonate is added) are shown in Figs. 4.38 – 4.40. Fig. 4.38 shows the pH and pressure transients, Fig. 4.39 the behaviour of the individual concentrations and partial pressure of carbon dioxide and Fig. 4.40 the equilibrium characteristics for the evaporation/condensation and precipitation / dissolution processes.

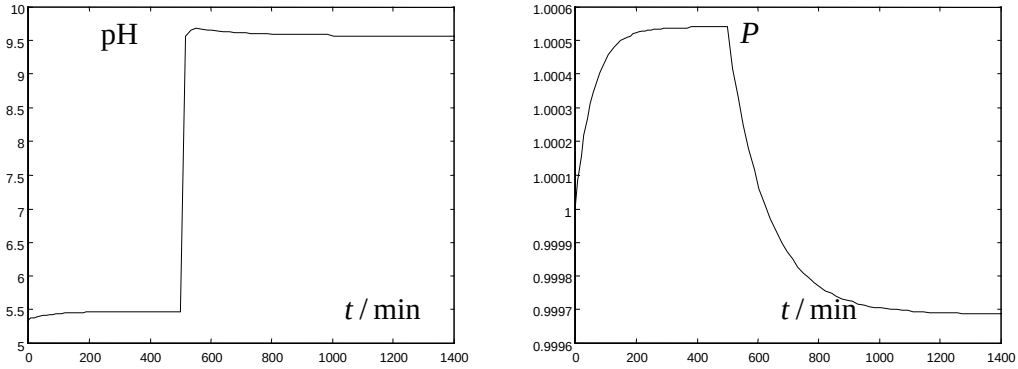

Fig: 4.38. pH value and the total pressure (atm) in the vessel; the initial transients.

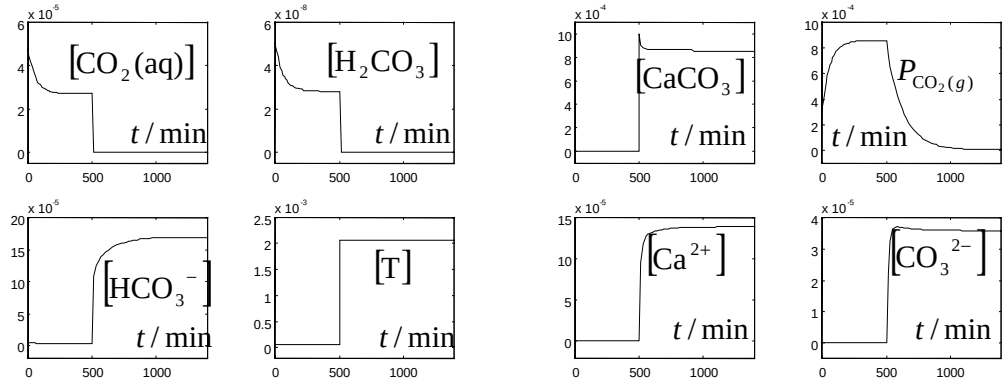

Fig. 4.39: The individual concentrations (mole/l) and partial pressure (atm) of carbon dioxide; the initial transients.

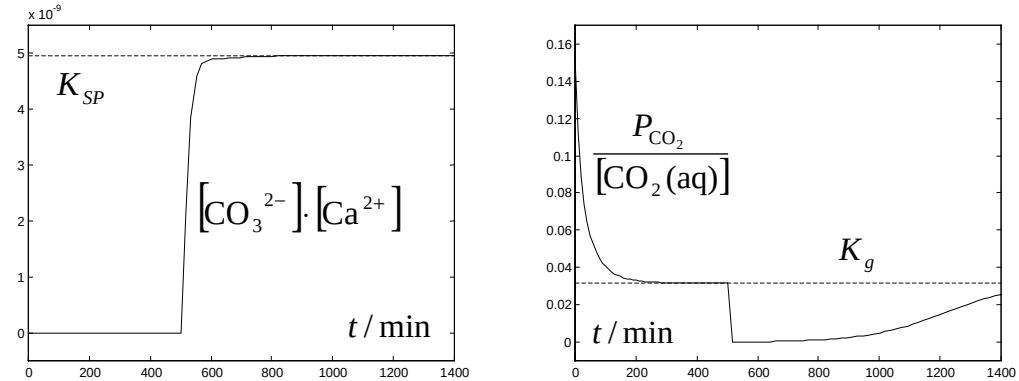

Fig. 4.40: The ion product of calcium carbonate (mol^2/l^2) and the carbon dioxide ratio (atm l/mole); the initial transients.

The results show that the equilibrium between the solid and the aqueous phase is significantly faster than the equilibrium between the gaseous and the aqueous phase. Initially there is more aqueous carbon dioxide in the water than the equilibrium condition allows and the excess slowly evaporates into the gaseous phase. As a result the pressure in the vessel increases. The pH value is also slightly acidic because of the aqueous carbon dioxide and as the excess carbon dioxide leaves the aqueous phase the pH value increases slightly.

At time instant 500 minutes solid calcium carbonate is added to the vessel. As it dissolves there is an increase in the carbonate ion concentration which in turn consumes oxonium ions and forms various aqueous hydro carbonates. When oxonium ion concentration drops, the pH value increases.

The steady state distribution of carbonate compounds depends strongly on the pH-value. Low pH values result in compounds that are in the beginning of the carbonate chain i.e. carbon dioxide and when pH is high there are compounds from the end of the carbonate chain (solid calcium carbonate).

After the initial process preparation equilibrium is reached and a pH-sweep is performed (titration). Strong acid is added every hour until pH value drops close to 3, then the system rests for a couple of hours and after that strong base is added every hour until pH value 11 is reached. The simulation results are shown in Figs. 4.41 – 4.43. Fig. 4.41 shows the pH and pressure behaviour, Fig. 4.42 contains the individual concentrations and Fig. 4.43 the equilibrium level.

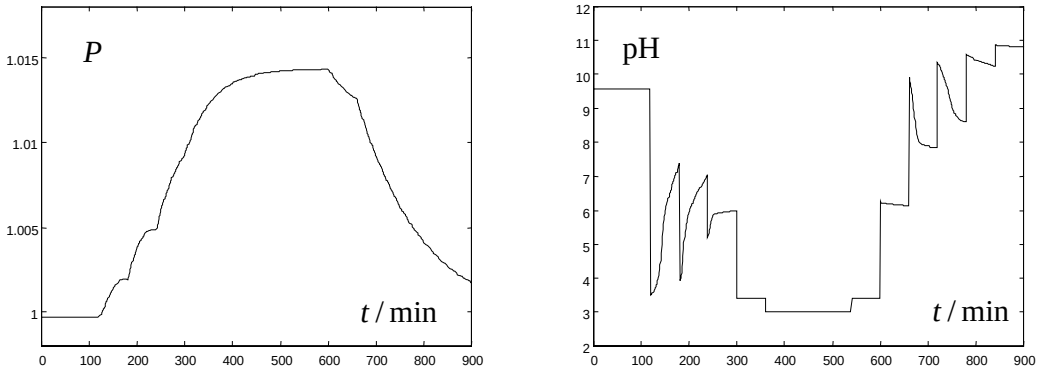

Fig. 4.41: Total pressure (atm) and pH value in the vessel; pH-sweep.

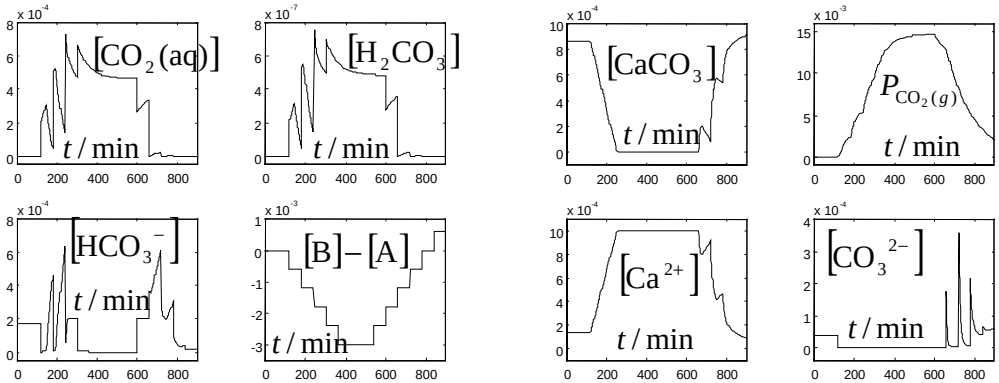

Fig. 4.42: Individual concentrations (mole/l) and CO_2 partial pressure (atm); pH-sweep.

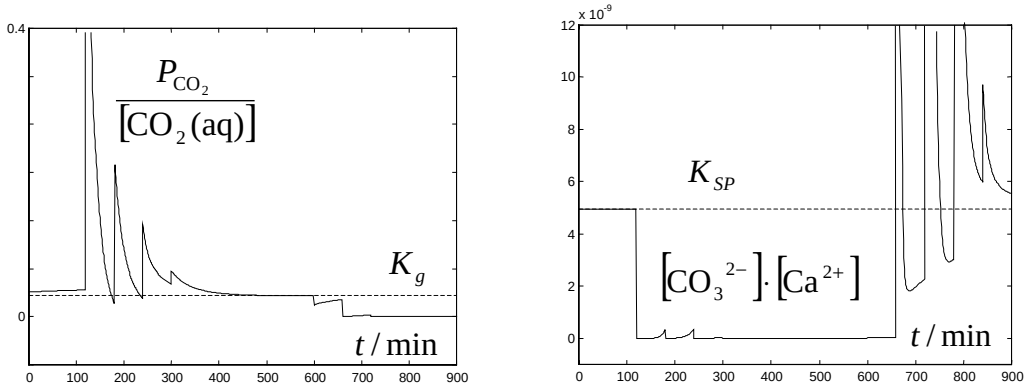

Fig. 4.43: CO_2 ratio (atm l/mole) and ion product of calcium carbonate (mol^2/l^2); pH-sweep.

The results show that the process behaviour corresponds to real situations adequately. No material transport dynamics were considered and the rate constants in this system are more or less arbitrary (they are difficult to determine theoretically and no validation data was available for this example). However, the average relation of the rate constants corresponds to real processes (in many cases the $CaCO_3/CO_3^{2-}$ reaction rates are approximately ten times higher than $CO_2(g)/CO_2(aq)$ rates). The pH transients (pH peaks) are also typical for real processes. The thick deinked pulp acidification application in chapter 6 is good example of this.

Chapter 5

pH control

Alltami (n.)
The ancient art of being able to balance the hot and cold shower taps. [1]
Uttoxeter (n.)
A small but immensely complex mechanical device, which is essentially the "brain" of a modern coffee machine, and which enables the machine to take its own decisions. [1]

This chapter contains a short review of the basic structures and elements of a control loop with special emphasis on the pH process and as nonlinear and adaptive controllers are often used in pH control they are also included. A simple neutralisation process is given as an illustrative example.

pH control is a popular research subject and numerous interesting research papers are written on the subject. A complete review of articles is beyond the scope of one thesis so only selected papers and their main contribution are given in this chapter. A modification of the Self-organising fuzzy controller (SOC) algorithm is part of the contribution of this thesis and that is why SOC is presented with more detail.

5.1 Basics of pH-control

5.1.1 Block diagrams

In control and system theory the interactions between variables are illustrated using block diagrams (Fig. 5.1).

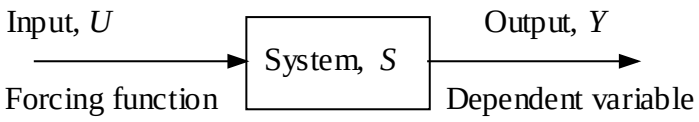

Fig. 5.1: Unit block.

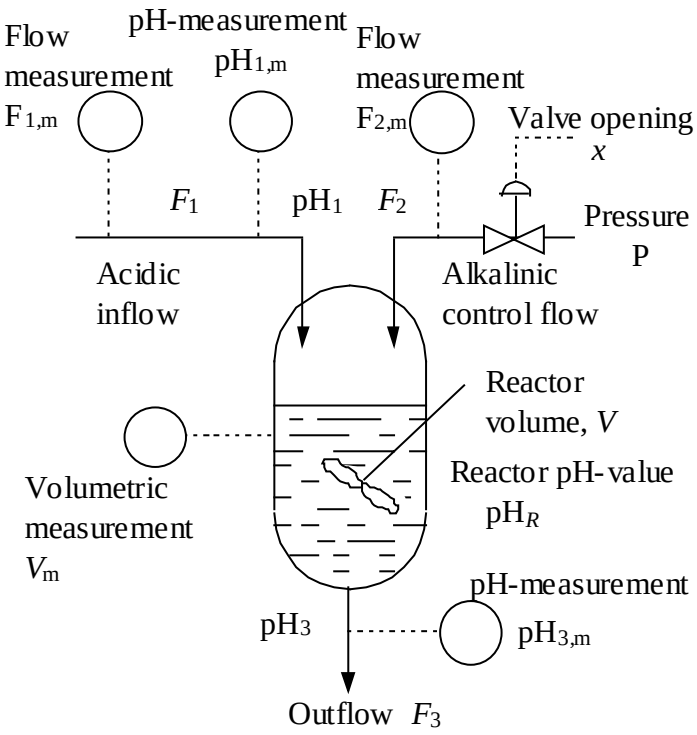

Fig. 5.2: Flow diagram of a neutralisation process.

The components of a general control system as well as the specific features and problems of pH-control are clarified, throughout this chapter, with an example consisting of a simple but excessively instrumented neutralisation process (Fig. 5.2), where strong base (control flow) is used for neutralising acidic liquid (inflow) in order to achieve neutral outflow. The inflow F_1, its contents and the outflow F_3 change in an unpredictable manner and these variations are the main disturbances in the neutralisation process. As a result of the changing flows the reactor volume V also changes (it can be assumed that there are safeguards so that the vessel never overflows or becomes empty).

The available measurements in the system are:

- Inflow ($F_{1,m}$)
- Volume (V_m)
- Inflow pH-value ($pH_{1,m}$)
- Outflow pH-value ($pH_{3,m}$)
- Control flow ($F_{2,m}$)

The only freely manipulated variable (control variable) is the valve opening x. The main disturbances are:

- Inflow (flow changes) (F_1)
- Inflow properties (changes in acidity, buffering, …) (**C**)
- Outflow (flow changes) (F_3)

Other dependent variables are:

- Volume of the neutralisation vessel (V)
- Control flow (F_2)

The control reagent (strong base) concentration can be assumed constant as well as the pressure inside the control flow pipe. The physical limits of the variables are never encountered (inflow is always acidic, there is always liquid in the vessel and it never overflows, the valve is never required to be fully open or closed during the operation, etc.). The reactor can also be considered to be an ideal mixer (CSTR-assumption, continuous stirred tank reactor) and the pipes ideal plug flows without diffusion or dispersion.

The block diagram structure of the neutralisation process can be built up from simple unit blocks. For instance, the inflow acidity (among other properties) has an obvious effect on the pH-value inside the reactor. With crude simplification (ignoring the chemical content and buffering of the inflow), it can be said that the pH-value of the inflow (pH_1) affects the reactor pH-value (pH_R), which, in turn, has an effect on the outflow pH-value (pH_3) (with CSTR and plug flows the effect is a pure time delay). This causal chain is shown in Fig. 5.3.

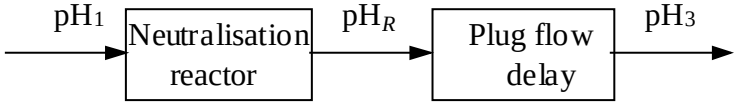

Fig. 5.3: Causality of the pH-values.

Even though the structure in Fig. 5.3 appears, at first glance, to describe the causality of the neutralisation process, it has several problems. Firstly, the inflow pH variations are strictly speaking not the reason for pH variations inside the reactor despite the strong correlation. In fact, the chemical content of inflow (**C**) has a causal effect on the chemical content inside the reactor. pH-value is only an indicator of chemical content and not even an unequivocal one, there are infinite combinations of different components (acids and bases) that produce the same pH-value.

Secondly, the outflow carries components out of the reactor thus changing the chemical content (and pH) inside the vessel but at the same time it changes the time delay caused by the plug flow. There is no reason for separating the pH inside the reactor and at the outflow. A much more natural approach would be to include all flows and the chemical content of the input flow as input variables and pH at the outflow and inside the reactor as well as volume inside the reactor as the output variables. All flows to the reactor and from the reactor contain chemical components that have an effect on the reactor pH. When flow rates change the component balance (and pH) is affected inside the reactor. The flow rate changes also have an effect to the volume inside the vessel that, in turn, have an effect on the time constant of the reactor. This block diagram is shown in Fig. 5.4.

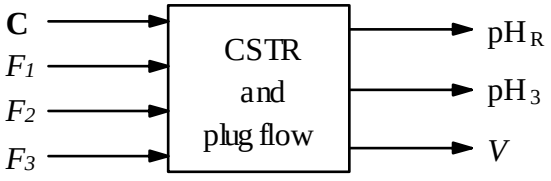

Fig. 5.4: Block diagram of the process.

The block diagram of Fig. 5.4 describes the basic process without the instrumentation, the causality of which is relatively simple. The real quantity in the process is the main input for any properly measured value (other inputs are typically the reason for measurement errors), e.g., if the actual flow rate changes, the measured flow rate should follow the changes in accordance to the flow meter specifications. For actuators the causality is equally clear: if the valve opening changes the flow rate will change as well. The instrumentation block diagrams are shown in Fig. 5.5.

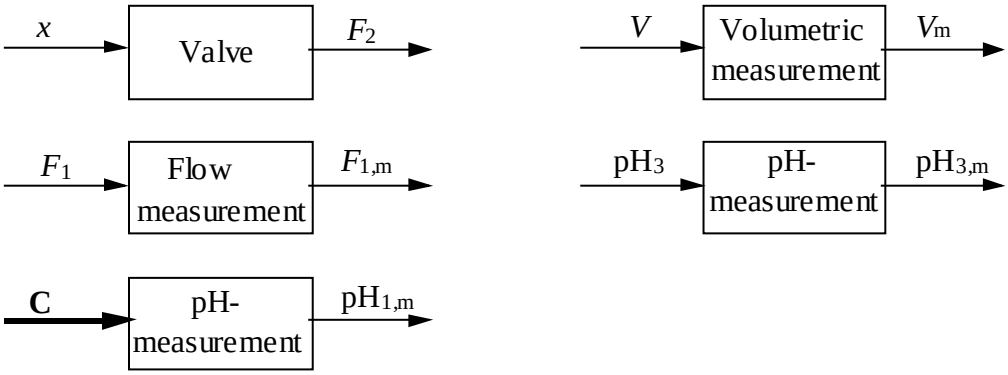

Fig. 5.5: Unit blocks of instrumentation.

Most of the blocks in Fig. 5.5 are self-explanatory but causality of inflow chemical state to pH_1-measurement requires some explanation. The chemical state **C** is a vector quantity (indicated with a thick line) and pH is a scalar that can be considered as a projection from an *n*-dimensional variable space onto one dimensional space. The chemical state defines the process behaviour explicitly whereas pH-value does not. In practice this means that a mere pH-value should not be used as an input to a chemical system.

The block diagram of the instrumented process (Fig. 6) is achieved when the unit blocks of Figs. 5.4 and 5.5 are put together. The manipulated variables, i.e., those variables that can be affected with the control action, remain at horizontal arrows whereas the disturbances that are beyond control enter the process by vertical arrows from the top. In addition, most blocks describing some kind of a measurement are replaced with symbol *M* for simplicity's sake.

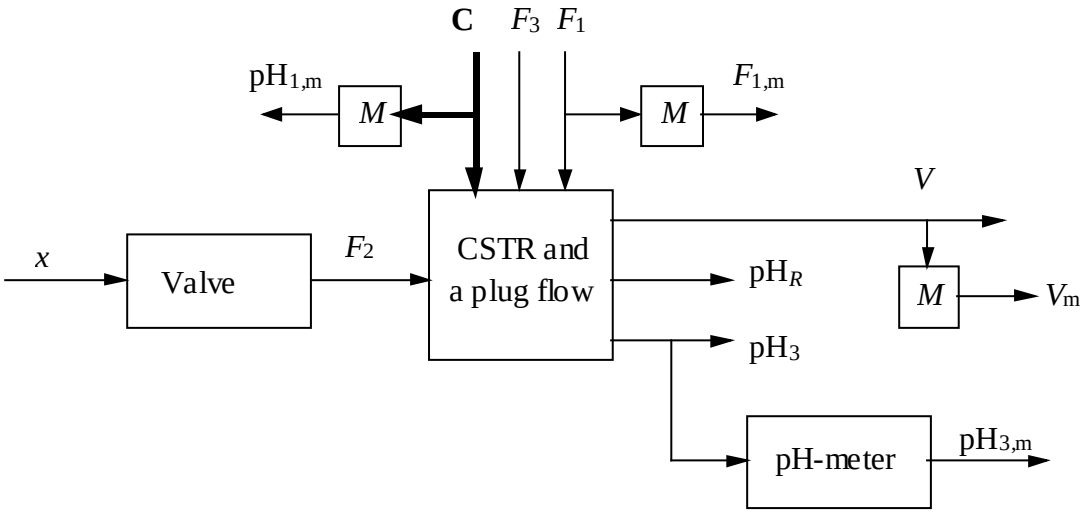

Fig. 5.6: Block diagram of the instrumented process.

The only available method of controlling the outflow pH-value during disturbances is by manipulating the control flow valve. The neutralisation problem focuses on, how to use available information (measurements) for operating the valve in order to get neutral outflow. In the next section, the very basic control methods are presented using the neutralisation process as an example.

5.1.2 Open loop control

Open loop control is the simplest method of controlling the pH-process. No measurements are used and the valve opening is totally independent from any pH-values, flows or volumes. In

practice this means that the process can be operated in accordance to a recipe or that the valve is kept at a fixed value despite of any changes in the pH-value. Open loop control of the neutralisation process is shown in Fig. 5.7 (the desired outflow pH behaviour –target– is indicated with symbol ($pH_{3,t}$)).

Typical application areas include start-ups and shut-downs of the process or sequential neutralisation, in which the pH is neutralised in several consecutive vessels and the first vessels are merely used for pushing the pH-value (with open-loop control) to a vague area where later vessels take care of the fine control of pH. The open loop control strategy can also be suitable for very deterministic systems, where there are practically no disturbances (disturbances are constant and known beforehand).

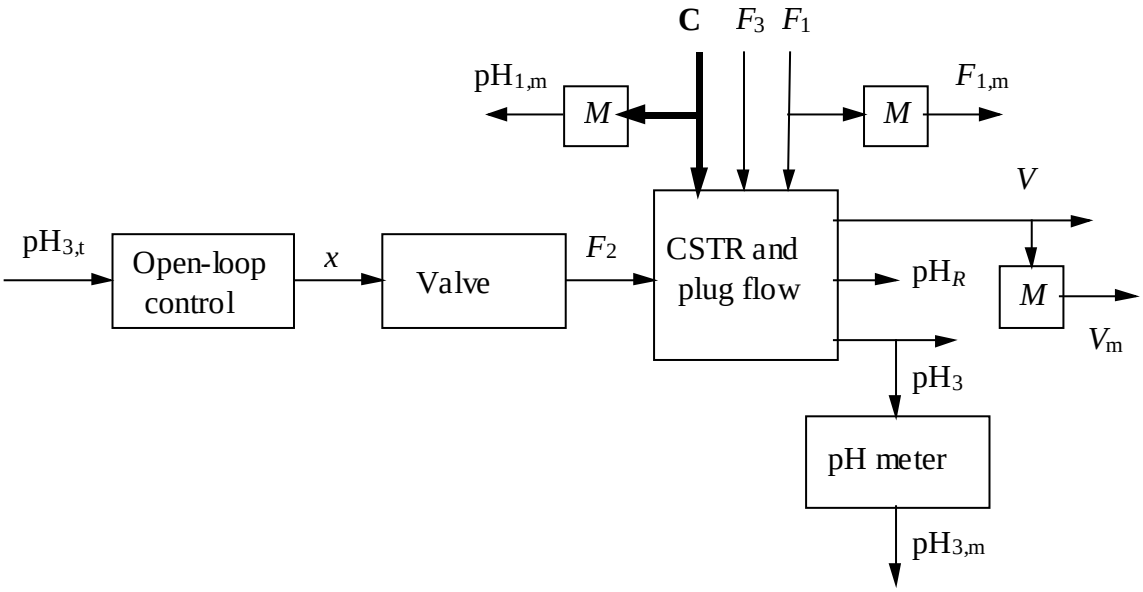

Fig. 5.7: Open-loop control strategy for the neutralisation process.

The benefits of open-loop control include simplicity, ease of maintenance and inexpensivity. No measurements are needed and consequently no questions are raised with respect to disturbances or the performance of the control strategy as there is no evaluation. This is also the weak point of open loop control. If there are significant disturbances in the system, this strategy can not be used.

5.1.3 Feedback control

Feedback control strategy is used, when the controlled output ($pH_{3,m}$) is measured and used in the calculation of the control signal, *x*. The basic structure of feedback control is pure common sense. No matter how the valve is operated, it is still sound to evaluate the outcome and change the valve opening if the output does not behave as it is supposed to do. The very simplest of feedback controllers manipulates the valve according to basic principles: the valve is opened if pH is too high and closed if pH is too low.

How much the valve is opened or closed and how the control signal reacts to dynamic changes in the process is determined by the controller structure and tuning. A controller can be a simple relay-element that understands only two positions for the valve opening (fully open or completely closed), a PID-controller, fuzzy controller, adaptive controller, nonlinear controller, etc. Different controllers are described in more detail in the following chapters. The feedback controlled neutralisation process is shown in Fig. 5.8.

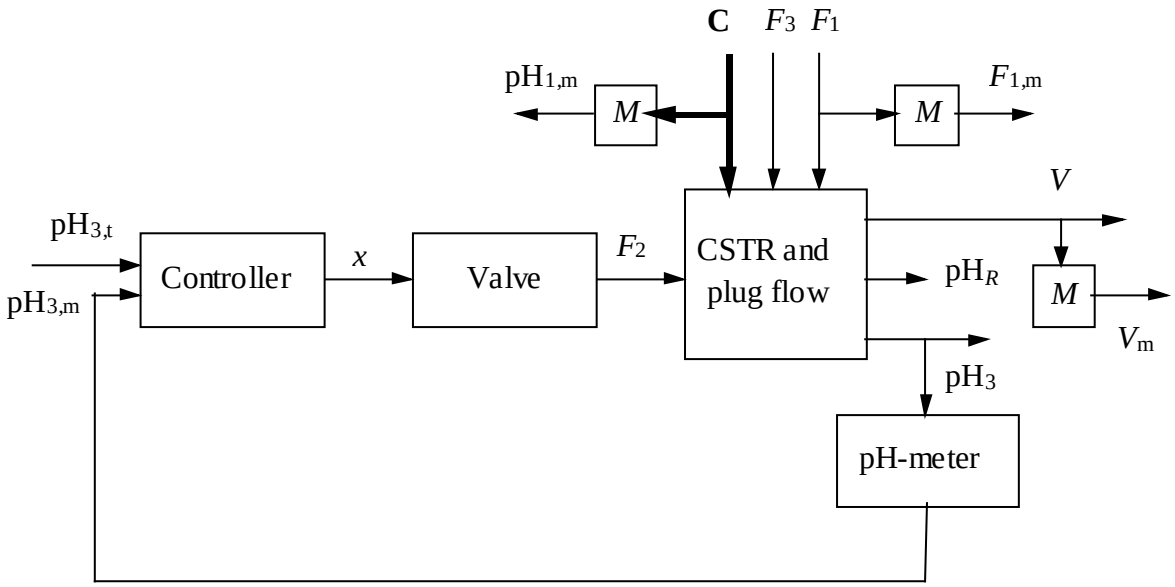

Fig. 5.8: Feedback control system for the neutralisation process.

The main difference between open loop control and feedback (closed loop) control is that in feedback control the errors and variations in the controlled output are measured and acted upon. The basic strategy does not try to prevent errors from taking place, it just tries to correct them once they can be seen in the measurements.

Control system stabilises the neutralisation process. The control actions do not have to be perfect; even the controller itself can make incorrect decisions, but the defining feature of a feedback control system is that no matter how the disturbances are generated the control system will evaluate the output and improve it. The feedback control system is more intelligent compared to open loop control system, but it is more expensive and complex; for one thing, it requires measurement of the controlled output and therefore constant maintenance. Generally pH-transmitter requires more maintenance than most other measurements. The performance of the controlled system relies strongly on the quality of the measurement as the control action is calculated based on the measured value. With poor measurements the control performance is also poor.

The simple feedback control may also be somewhat sluggish. If the pipes are long (long time delays) and the volumes are large (large time constants), it takes a long time to correct errors caused by various disturbances. As there are numerous disturbance measurements in the process it seems inefficient not to use them in the controller, especially, as most of their effects can be evaluated to some extent. Control strategies that take disturbances into consideration are presented in the following section.

5.1.4 Feedforward control

Feedforward control aims to compensate disturbances that affect the process even before their consequences can be seen in the controlled output. For instance, in the neutralisation process, the basic properties of the inflow are measured (flow rate and pH), the effects of which on the outflow pH can be estimated. It seems rather a waste not to use the available information for avoiding poor performance. Consider the following case.

The flows, volume and pH-values are at their nominal values, the outflow is neutralised and everything is operating as planned. Suddenly the inflow rate doubles and as the inflow carries acid to be neutralised also the acid load doubles and if nothing is done the outflow pH will drop. If the

control flow follows the changes in the inflow, i.e. the control flow doubles at exactly the same time instant as the inflow doubles, the disturbance is compensated and there will be no change in the outflow pH-value. Similar kind of compensation can be derived for the inflow acidity (e.g., when the inflow pH increases the control flow has to decrease in order to compensate the drop in the acid load). Feedforward control structure for the neutralisation process is shown in Fig. 5.9.

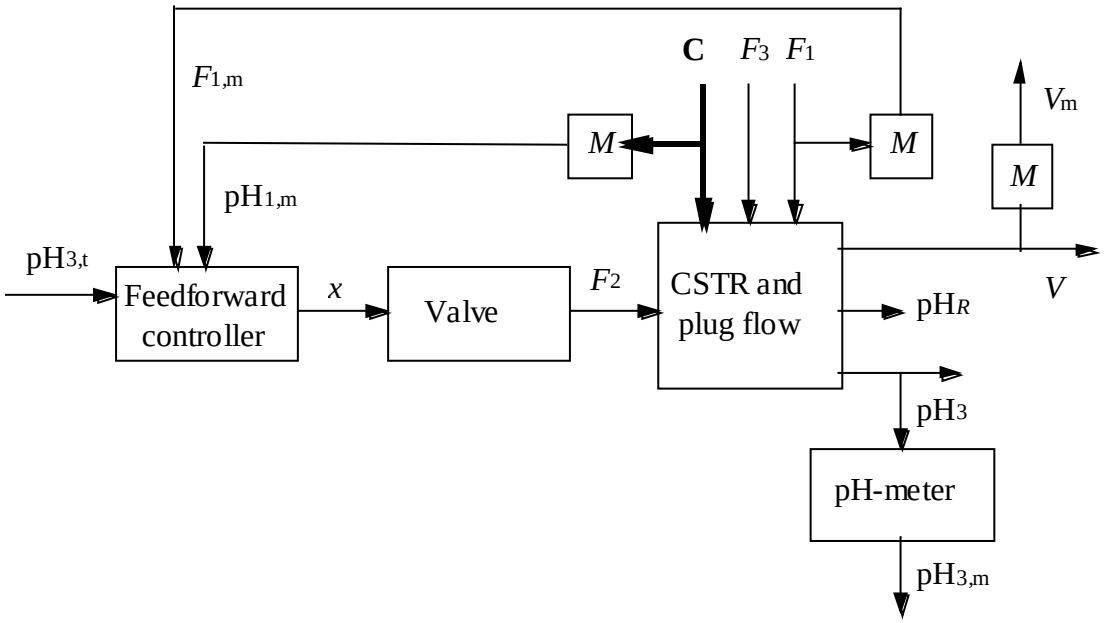

Fig. 5.9: Feedforward control scheme for the neutralisation process.

The basic feedforward strategy uses only disturbance measurement and not the output measurement in the control signal calculation. Perfect compensation is not a realistic concept in practical applications as the effects of measured disturbances are not always completely known and there are several other disturbances that are not considered. The fundamental problem with pure feedforward control is that the control signal is used for trying to compensate the effects of disturbances but there is no evaluation of the performance; maybe the disturbances are compensated or maybe not. If the effects of disturbances are not compensated or if the initial pH-value was incorrect, nothing is done to correct the situation. A more robust performance is achieved by combining the feedback and feedforward elements. The feedforward part will compensate known disturbances (preventive and fast control) and the feedback control will deal with any errors that appear in the output whatever the cause for these errors may be (corrective and slower control). The block diagram for the combined control strategy is shown in Fig. 5.10.

A point of order has to be made on how the volumetric measurement is used in the combined control strategy. The volume of the CSTR is not controlled, even though the control flow affects the volume of the system and there is a “feedback” from the measured volume. The control flow consists of a concentrated strong base and if it would be used for controlling the volume of the CSTR, the pH-value would not be controlled.

On the other hand, the changes in the volume do not have to be compensated in the feedforward strategy that focuses on the compensation of the inflow acidity load changes by introducing a complement change in the base load simultaneously.

Let us consider a case, in which there is a disturbance in the outflow pH-value (too low pH) indicating that the entire CSRT is too acidic. For nominal volume the feedback control corrects the situation, but if the actual volume differs significantly from the nominal volume, the controller will encounter problems without compensation. A small volume requires only a little amount of base

and a large volume drastically more base, i.e. the control action has to be normalised with respect to the volume. (in fact, to the ratio of volume and flow, i.e., time constant)

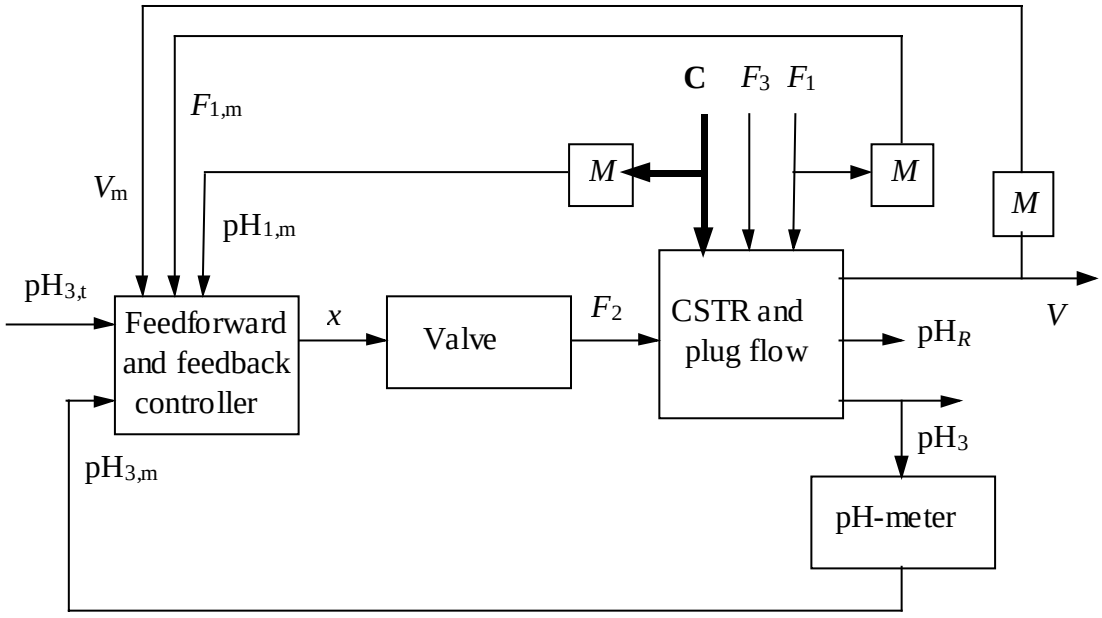

Figure 5.10: Combined feedback and feedforward strategy for the neutralisation process.

5.1.5 Several controllers and control loops

All the control strategies presented in the earlier sections are widely used in the pH-control. A lot can be gained in control performance, productivity and maintenance if a correct strategy is used in the suitable application.

In many cases the pH-value is controlled in several steps and there is more than one controller operating in the system. In the simplest process structure material flows from one unit process to another (e.g., pulp and paper industry) and pH-value can be measured and controlled in several consecutive points in the process. By the second and third pH-measurement there should already be some kind of idea of the incoming flow properties that can be used for feedforward control strategy. When pH is controlled in series, the use of unit controllers is usually well justified at each consecutive point.

pH-value is a key factor in many chemical, physical and biological phenomena and sometimes there are interwoven quantities that are to be controlled under serious interactions. In these cases, multivariable control strategies (such as state control, compensation of interactions, etc.) have to be used. The neutralisation process could create a multivariable system with serious interactions by some modifications, e.g. the pH and volume are controlled together by manipulating both acidic and alkalinic flows with approximately equal concentrations. In this case both flows have significant effect on volume and pH-value.

Cascade control is one of the simplest SISO-control strategies consisting of more than one controller (SISO, Single input – Single output). It can be applied for processes that consist of two subprocesses with measurable medium quantity (the first subprocess should be notably faster than the second subprocess. Cascade control could be beneficial for the process example if the pressure (*P*) in the control flow pipe would vary significantly.

The pressure disturbance has an effect on the valve performance, i.e., the same valve opening results different reagent flows depending on the pressure. As the flow can be measured, it seems rather a waste not to use this measurement for finding out, how much base is actually fed to the

CSTR. The pH-controller calculates the required control flow (actually the corresponding valve opening) and if the control action is not realised because of a pressure disturbance, there is still time to correct the situation before the consequences of the erroneous flow is are seen in the CSTR. The block diagram of cascade-controlled neutralisation process is shown in Fig. 5.11 (some measurements that were not used in the control signal calculation were omitted from the block diagram for simplicity's sake).

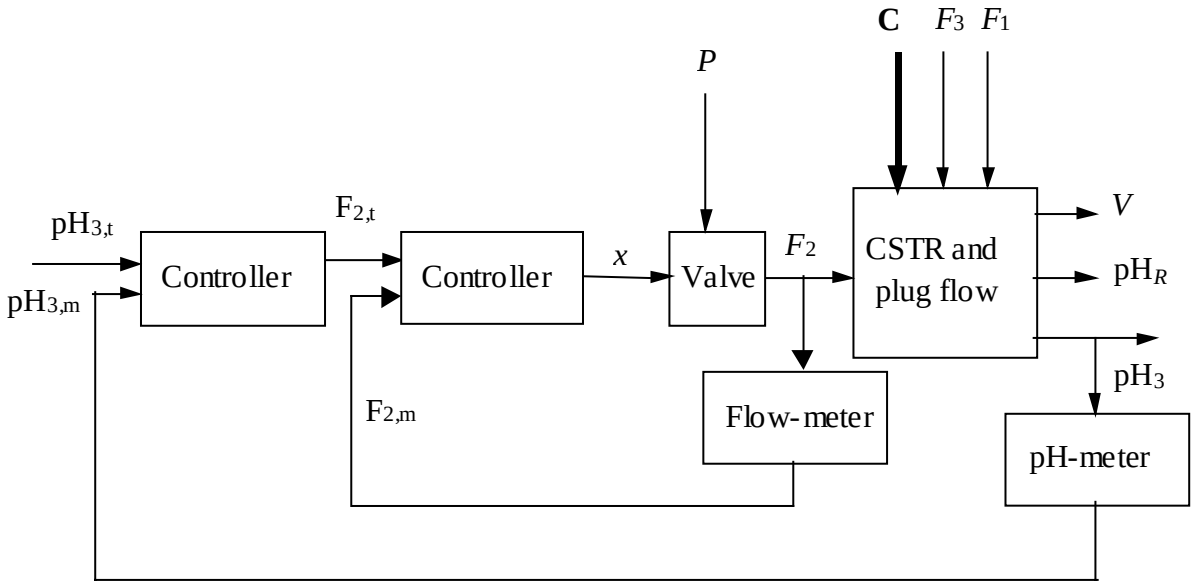

Fig.5.11: Block diagram of a cascade-controlled neutralisation process.

5.1.6. Control of pH by process changes

The previous sections have approached the pH-control problem from the assumption that pH is controlled by feeding acids or bases to the system. A different approach is to change the process conditions to such that the pH-variations diminish.

Mother Nature is an expert on the subject of buffered processes and consequently the same method is widely used in biotechnical processes such as fermentors. By proper buffering the variations in the pH-value can be dropped to a fraction of the original variations and by a suitable selection of buffers the process can be driven to the required pH-range and kept there. Buffering is a property of the chemical system and it is discussed with more detail in the earlier chapters 2 and 4.

The variations in the pH-value can also be decreased by introducing larger vessels that filter all the high frequency dynamics from the process. A further expansion of this idea is to collect acidic or alkalinic wastes from the process at different time instants (batch processes) or different positions (continuous processes) and use them instead of expensive reagents. For instance, a very common practice in food processing industry is to clean the food processing vessels by consecutive acid and base wash sequences. If the wash waters are fed directly to the waste water treatment there will be large variations in the acid and base loads that have to be controlled with expensive reagents. On the other hand, if the used wash waters are combined in a separate vessel first so that they partly neutralise each other, the amount of reagent that is needed is much smaller.

The same concept can be used in the production processes. The acidities and alkalinities of different raw materials can be utilised by careful process planning. There is also need for additional dilution feed and recirculation in many processes. The recirculation feed or the dilution water can be taken from a position in the process that has the required acidity or alkalinity.

5.2. Controllers

The purpose of pH-control is to keep the pH-value at a constant value (regulator problem) or to force the pH-value to follow a pre-specified trajectory (servo problem). These are basically the deterministic goals of the controlled output in all pH-processes. However, depending on the process type there can be variations on the stochastic goals, e.g., in biological processes the large amplitude - high frecuency pH-shocks can be fatal to the micro organisms whereas the small amplitude - low frequency variations are acceptable. The goals can be completely opposite for a high sensitivity low ionic strength systems, where high amplitude variations can not be avoided. In these processes the controller is sometimes tuned for high frequency oscillation that can be filtered with a levelling tank. Lower frequency variations are especially unwanted because filtering would require a larger volume that increases the cost of the equipment.

5.2.1. Relay and PID-controllers

Conventional relay controllers have only two possible values for the control signal $u(t)$: u_{max} and u_{min} (e is the error signal, difference between the target value and the measured value for the controlled output).

$$u(t) = \begin{cases} u_{max} & e(t) > 0 \\ u_{min} & e(t) < 0 \end{cases} \tag{5.1}$$

The conventional relay controller has a tendency for oscillation and coarse control performance. The actuator keeps banging between two extreme values, which can be wearing especially for the mechanical parts in valves. Let us consider the example process of previous section. If the goal is neutralisation, the target value does not change ($pH_{3,t.}$=7). If the measured value ($pH_{3,m}$) is even slightly acidic (e.g., $pH_{3,m}$ = 6.9 => e = 0.1), the valve will open completely. When the measured value will show any sight of alkalinity the valve will close completely (e.g., $pH_{3,m}$ = 7.1 => e = -0.1). As a result the controlled value will oscillate around the neutral value and the amplitude of the oscillation will depend on the delays and measurement errors in the system.

PID-controller and its modifications are the most common controllers in the industry. It is relatively simple, its operation is well known, it has a good noise tolerance, it is inexpensive and it is commercially available. The "text-book" version of the continuous time algorithm can be presented with different parametrisations:

$$u(t) = K_P e(t) + K_I \int_0^t e(t)dt + K_D \frac{de(t)}{dt} \quad \text{or} \quad u(t) = K_P \left(e(t) + \frac{1}{T_I} \int_0^t e(t)dt + T_D \frac{de(t)}{dt} \right) \tag{5.2}$$

K_P = Proportional gain	K_P = Controller gain
K_I = Integral gain	T_I = I-time
K_D = Derivative gain	T_D = D-time

The control action is calculated from the error signal. A graphical interpretation of the different factors of the PID-algorithm is given in fig. 5.12.

The effects of P, I and D terms can be studied one at the time. Mere proportional (P)-control dampens the oscillation when compared to the conventional relay controller. Where the relay controller only recognises two values for the control signal, the P-control has all the values between. With small errors the controller calculates small control signals and with large errors

large values. The drawback with the P-control is that under load changes and stepwise reference changes there will be a steady state error. This is due to the fact that the controller only looks at the error at the present time instant. There is no evaluation of the error history. If the control action does not remove the error caused by a load change, the control signal is not changed and the error remains.

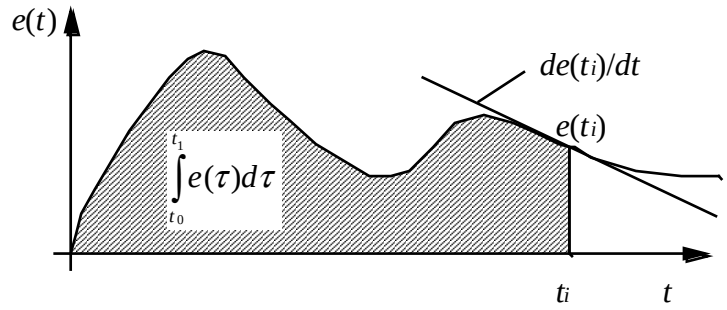

Fig. 5.12: Graphical interpretation of the PID-controller factors.

I-control calculates the integral of the error that corresponds to the error history. If there is an error, the I-controller keeps increasing (or decreasing) the control signal until the error disappears. I-control increases the tendency for oscillation and it might slow down the trajectory slightly but it removes the steady state error. I-action is very robust against high frequency noise.

D-control calculates the current trend of the error, it speeds up the trajectory and stabilises the process. Derivative action amplifies high frequency noise and it should be used with caution for processes with long dead time.

Basic modifications of the PID-controller (e.g., P, PI, PD-controllers) are easily accomplished by selecting the corresponding factors from the general PID-algorithm. There are numerous practical modifications (such as the filtered derivative action) and operational modifications (e.g., antiwindup for integral part under hard signal limits). Naturally, the continuous controller also has a digital counterpart (h is the sample time and k = 1,2,3,...):

$$u(kh) = K_P e(kh) + K_I h \sum_{i=1}^{k} e(ih) + K_D \frac{e(kh) - e(kh-h)}{h} \qquad \text{or}$$

$$u(kh) = K_P \left(e(kh) + \frac{1}{T_I / h} \cdot \sum_{i=1}^{k} e(ih) + T_D / h \cdot \big(e(kh) - e(kh-h) \big) \right) \tag{5.3}$$

5.2.2 Nonlinear control

It has been stated in the earlier chapters 2 and 4 that the pH-process is highly nonlinear. If the nonlinearity is evident in the operation area, a nonlinear control scheme performs better than linear controllers, such as the conventional PID-controller.

If the pH-process consists only of strong acids and bases, its titration curve is very nonlinear and it resembles the one shown in Fig. 5.13 (there is also the operation line of a linear process for comparison). In the nonlinear process (titration curve) the pH-value is very sensitive around the neutral point and insensitive elsewhere, i.e., in the neighbourhood of the neutral point even the smallest amount of reagent can take the pH-value to 4 or 10, whereas for pH-values under 3 or over 11, huge amounts of reagent have to be introduced even for small change in the pH-value. For linear systems a change in the output is always received with the same input change no matter at which point of the operation range the process is.

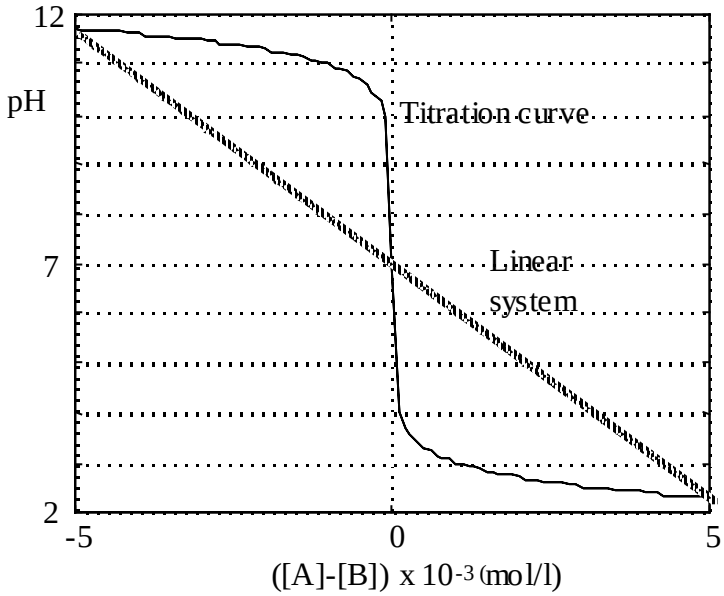

Fig. 5.13: The titration curve of the neutralised sample.

If a linear controller is applied to a highly nonlinear process, the controlled value tends to remain at areas where the process sensitivity is low. For high sensitivity ranges the controller gives much too big control actions that can cause local instability. For low sensitivity range the controller is too weak and impotent, thus careful control actions have practically no effect on the process behaviour.

A nonlinear controller takes the process nonlinearity into account so that in high sensitivity range the controller is careful and in low sensitivity range the controller is efficient. As the pH-process usually follows the Wiener-process structure, this kind of control strategy works perfectly. The buffer index describes the sensitivity of the process and in Fig. 5.14 there is the buffer index of the sample, the titration curve of which was shown in Fig. 5.13. Fig. 5.15 gives the same buffer index in logarithmic scale.

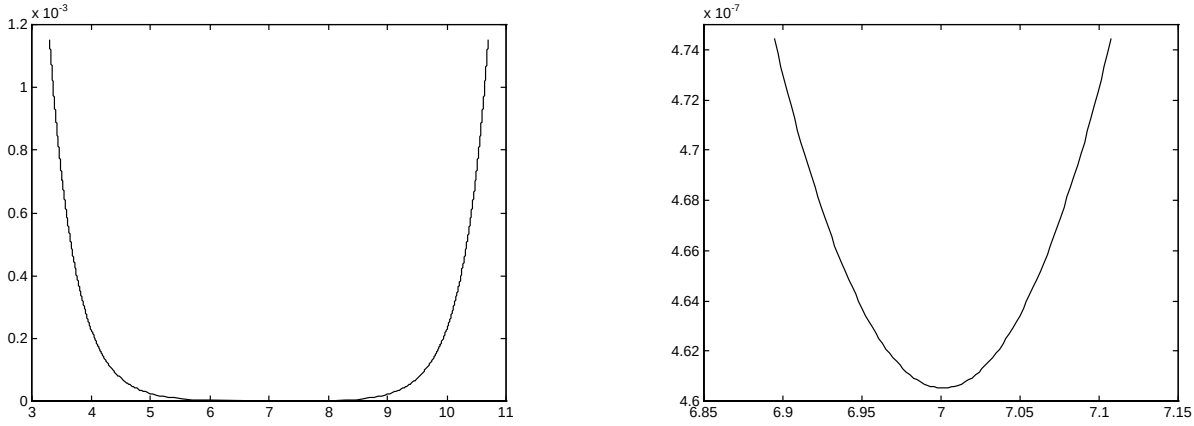

Fig. 5.14: The buffer index of the strong – acid- strong base process.

The simplest method of taking the pH-process nonlinearity into account is to define an experimental titration curve of a process sample. The measured and target values are filtered with the inverse titration curve and if the titration curve does not change in the process the actual process nonlinearity and the inverse titration curve cancel each other out and thus linearising the control

loop. If the chemical content changes in the process, the titration curve will also change and the cancellation is not perfect.

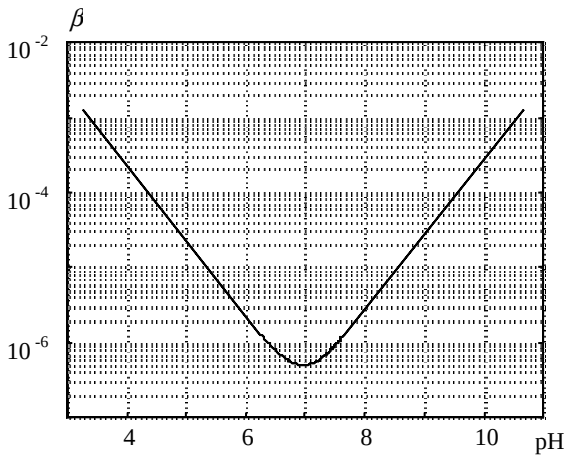

Fig. 5.15: The buffer index of the strong acid – strong base system on a logarithmic scale.

Direct pseudo-linearisation of the control loop is risky, though, if the exact titration curve is not known or if it is timevariant. It has been criticised by, e.g. Gustafsson and Waller [29], Henson and Seborg [37] and Jutila *et al.* [49]. In practical cases the pseudo-linearisation has be performed with utmost caution.

There are numerous other methods that are suitable for a nonlinear mapping from measured to control variables and which are therefore suitable for nonlinear pH-control. Typical methods include neural networks and fuzzy logic to name but a few. It is to be remembered, that if the nonlinearity is not notable in the operation range, linear controllers could be used instead of nonlinear controllers. In any case, the nonlinear controllers require more a priori knowledge, they are more complex and they require more resources than the linear controllers.

5.2.3. Adaptive and learning controllers

5.2.3.1. General principles of adaptivity

The boundary between adaptive and nonlinear control is rather vague. Adaptive controllers adapt to changing circumstances and in the previous section a controller was introduced that operates differently in different pH-ranges, i.e., adapts to different pH-values (adapts to nonlinearity). This is “gain scheduling”-type of adaptation to the letter, if the controller gain follows the changes in the process buffer index. A good source of basic concepts of adaptive control in general can be found in [153] and for process control in particular in [110].

Adaptation only to nonlinearity is somewhat limiting concept as there are other kind of changes that take place as well. Wear and dirt change the process characteristics and inflow can contain random components, which will change the system. These changes take place as functions of time rather than functions of operating point and the processes are time-variant systems.

Adaptivity is usually divided into sub classes of forced (Fig. 5.16), feedforward (Fig. 5.17) and feedback (Fig. 5.18) adaptation. A typical example of a forced adaptation is a grade library, in which there are tuning parameters for each product grade. Whenever there is a grade change at the plant, the controller tuning parameters are automatically replaced with parameters that correspond to that particular grade.

Feedforward adaptation strategy depends on a measurement of a quantity that changes the process characteristics, e.g., the reaction rates of chemical systems depend strongly on the

temperature. When temperature changes, the time constants of a chemical process can change to the extent that different tuning parameters are needed.

Both forced and feedforward adaptation rely heavily on a priori knowledge whereas feedback adaptation does not. In feedback adaptation the controller performance is evaluated online and tuning parameters updated accordingly (direct feedback adaptation) or the process model is identified online and used in a model base controller (indirect feedback adaptation, Fig. 5.19). The common element in both direct and indirect feedback adaptation is that they try to track changing process online without concentrating on, why the process has changed.

Different adaptation mechanisms can also be combined, e.g., feedback adaptation can be forced to adapt to the changed situation faster. For instance, let us consider a case of grade changes with no or poor a priori knowledge. It is a well known fact that every time there is a grade change the controller needs re-tuning. If there are no a priori parameters that can be used, the feedback adaptation rate can be increased so that whatever the improved tuning parameters might be, they are found faster. During normal operation the adaptation rate can be dropped back to the nominal value or even disabled completely.

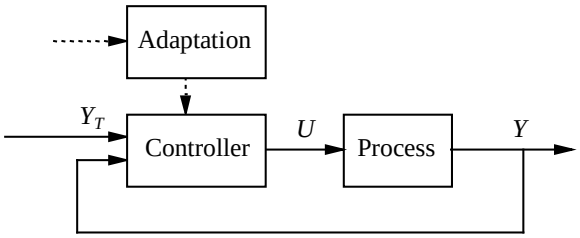

Fig. 5.16: Forced adaptation.

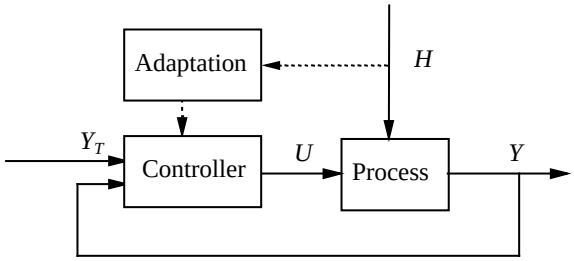

Fig. 5.17: Feedforward adaptation.

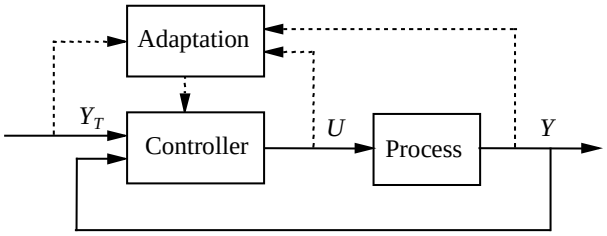

Fig. 5.18: Feedback adaptation (direct).

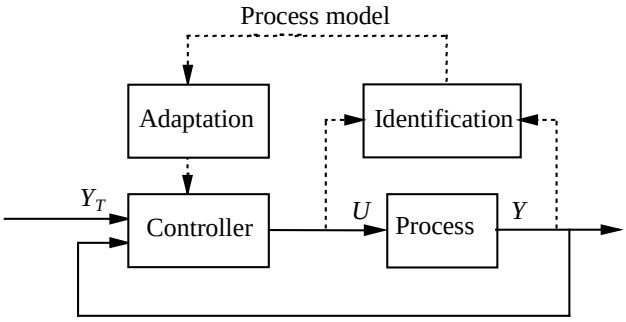

Fig. 5.19: Indirect feedback adaptation.

Another way of categorising is to divide the adaptive systems according to the learning procedure:

- adaptive systems that learn the process behaviour on-line from samples
- adaptive systems that learn the process behaviour off-line from samples
- adaptive systems that do not learn the process behaviour from the samples

The systems that learn process behaviour on-line collect data during the normal operation. The learning takes place all the time as long as the system is running. In off-line learning the data is collected either beforehand or from a special tuning sequence. The data collection is followed by a learning sequence, after which the tuning is assumed to be learned and the controller is fixed until the data collection is activated again. Those adaptive systems that do not learn the process

behaviour from the data usually rely on the principles of theoretical modelling (in process industry typically material and energy balances).

As a rule, there are more risks with adaptive controllers than with conventional controllers and feedback adaptive controllers are more riskier than other adaptive controllers. The adaptation is driven by measurements and if measurements are not in operation (due to maintenance, mechanical breakdown or some other reason) a learning controller will try to learn things from data that does not describe the process in any way. As a result the controller may operate arbitrarily.

The crucial skill for the designer is to know, when an adaptive controller is required and what kind of adaptation is suitable. For an adaptive controller to be beneficial particular emphasis has to be laid on reliable operation and safety because they are vitally important in industrial control. Many of the adaptive (and nonlinear) controllers use the basic structure of the PID-controller that is well-known and understood in process industry.

5.3 Different approaches to advanced pH control

In practice a fixed PID-controller and its modifications are the most common controllers for pH-control and that is hardly surprising because most of the practical pH processes are heavily buffered, approximately linear and very robust. However, there is a significant number of difficult, practical pH processes that can benefit from advanced control strategies. In addition to practical applications, there are also many pilot processes that are designed intentionally to be challenging for research purposes.

A good review of different nonlinear and adaptive control strategies for pH is given by Gustafsson and Waller, [29]. An earlier review of pH control, with emphasis on practical pH control, is given by McMillan, [85]. Different practical pH-control strategies are also reviewed by Rys, [108]. This survey emphasises the practical benefits of feedforward-feedback structure as well as the ratio-control (an effective an simple method for performing the flow compensation). A more recent review of practical pH-control strategies can be found in [49].

5.3.1 Model based controllers

Many early model based controllers assumed a simple Wiener-type model for the pH process. The dynamic part was usually a simple first order dynamic model with unit gain, time constant and delay (e.g., Rand, [105] and Welfonder *et al.*, [130], [131]). The nonlinearity was introduced as a fixed titration curve or in more advanced models with changing buffering a time-variant titration curve. In some cases the nonlinearity was incorporated as a time-varying gain of the first order dynamic model (Gupta and Coughanowr, [26]).

It could well be said that the advanced pH control begun with first successful pH models. McAvoy *et al.*, [84], who developed the first physico-chemical model of a pH process, used the model for time-optimal control design. Gustafson and Waller, [30] and Jutila and Visala, [52] developed controllers in which the model was incorporated to the controller. Both research groups used hypothetical species estimation for explaining instantaneous nonlinearity in the process. With the help of hypothetical species an inverse titration curve was obtained that was be used for pseudo-linearisation of the control loop so that linear controllers could be used. Gustafsson and Waller used least squares method and Jutila and Visala Kalman filter for estimation of unknown parameters.

There is an easily modified pilot scale pH process at UCSB that has been used as a test bench in several different applications of adaptive and non-adaptive control strategies (e.g., [36], [33], [39], [38]). The concept of reaction invariants was used by Henson and Seborg, [39], [38] in their

research of different model reference adaptive controllers in which the adaptation could be based on direct or indirect parameter estimation.

Jacobs and a group of researchers ([42], [103] and [102]) did several industrial implementations of pH control. They used general model of first order dynamics with titration curve as the nonlinearity, [42]. They applied conventional and adaptive control strategies on a process that appeared to be a strong acid – strong base system with some minor buffering (due to, e.g., carbon dioxide or the chemicalisation of municipal water). The implementation of self-tuning PI controller proved to be significantly better than an optimally tuned fixed PI controller, [102]. In this application the process model was a simple first order time series model with two unknown parameters that were identified on-line. The results were good but, on the other hand, the buffering remained constant during the test runs thus creating a rather simple control problem.

Several researchers have chosen more experimental structures instead of a physico-chemical model. Pajunen, [94] and Norquay *et al.*, [88], [89] both used Wiener model assumption (linear dynamics and static nonlinearity) in their research. They used a linear ARX-model structure for the dynamic part and different approaches for the static nonlinearity. Pajunen used a piecewise linear approximation for the titration curve whereas Norquay modelled the nonlinearity with cubic splines. In both cases the inverse of the nonlinearity (corresponds to inverse titration curve) was used for pseudo-linearisation of the control loop. Pajunen used a model reference algorithm and Norquay a model predictive algorithm as the actual controller.

Williams *et al.*, [132] developed a rather complicated pH measurement, control and reagent injection system. They divided the reagent feed into two separate injection points and measured the pH-value at three different positions (prior any injection, between the injections and after both injections). They identified hypothetical acids and bases from data and used them in a model that was incorporated into the controller, which calculated the required feed of reagent. They only presented simulation results and their pH-controller was criticised by, e.g., Gustafsson and Waller, [29] and Waller, [127].

Internal model control has been extensively applied to the strong acid – strong base system by a Singaporean group of researchers, [65], [114], [133], [86], [87], [12], [41], [118]. They estimate the strong acid concentration in the inflow and use the calculated concentrations in the control law. In [118] a fuzzy tuning was combined to the model and in [41] the augmented internal model controller was tested with a laboratory scale pH pilot process (in this practical application buffering was added) In pilot experiments the internal model controller outperformed the conventional PI-controller. Edgar and Postlethwaite, [16] developed an internal model control, in which the internal model was a fuzzy relation map generated by least squares minimisation described in detail in [99]

Bucholt and Kümmel, [7] used a linear self-tuner in a sensitive pH pilot process and Goodwin *et al.*, [24] a nonlinear self-tuner in a similar simulated process. The results by Goodwin *et al.* were excellent but they can be criticised because an exact model that was used for simulation was also used in the controller. Experiences with commercially available self-tuners, such as ASEA-Novatune, have also been documented. Jutila and Jaakola, [50] installed ASEA-Novatune in a pilot scale process and Piovoso and Williams, [98] in a larger scale pH process.

Dumont *et al.*, [15] presented an interesting industrial application of adaptive pH control based on Laguerre functions. What makes it even more interesting in view of this thesis, is the fact that the application was an industrial bleach plant that contains pulp (fibres). The Laguerre based selt-tuner improved the pH control significantly in real situation at the plant. The slow pH phenomena were not discussed in this paper.

Lee *et al.*, [70] used a model with one hypothetical component of unknown dissociation constant and concentration, both of which were estimated from the on-line data with a recursive least squares method. After the estimation a nonlinear self-tuner was used for the actual control.

Gain-scheduling strategy applied to a laboratory-scale pH process was studied by Chan and Yu, [9] as well as Klatt and Engell, [63]. Chan and Yu used a high-frequency square wave for titration curve slope identification and the PI-controller parameters. The experimental results were

good and the autotuning procedure quite simple. Klatt and Engell defined a desired nominal trajectory. They generated several linear approximations at suitable operating points throughout of the nonlinear pH range and developed a linear controller that would achieve the desired trajectory for each of these operating points. The experimental results showed improvement when compared to conventional controllers.

Maiti *et al.,* [79] extended the traditional dynamic matrix control and developed an adaptive version of the basic algorithm. They applied the controller to a laboratory-scale pilot plant, in which acidic effluent is neutralised with sodium hydroxide. The adaptive version is only sequentially adaptive as the adaptation (learning) is done by an operator command. Maiti *et al.* suggest that the adaptation is performed once a day, which indicates that the controller can not adapt to sudden changes in the buffering.

Palancar *et al.,* [95] applied model reference adaptive control for a pilot-scale pH process and received good results. They emphasised the practical points of the control strategy and concluded that the controller performance was greatly affected by longer time delays, and control valve nonideality. They criticised that even though the results were good the controller required careful tuning and if the process conditions changed significantly the controller had to be retuned.

Kavšek-Biasizzo *et al.,* [59] generated a fuzzy predictive control of a pH process. They used a known simulation model, generated data and used that data for developing a corresponding fuzzy model by using nonlinear least squares. The fuzzy model was then used as the model in conventional model-predictive controller. They simulated the controller with the original pH system and the performance was good. The point of the research was to prove that a general fuzzy model can be generated without any prior knowledge of the pH-process and this model can be used in a model-predictive controller. On the other hand, the buffering remained constant in the simulations and any nonlinear, time invariant modelling technique could have been used as well.

Model-predictive pH control was applied on a small pilot scale pH process by Pröll and Karim, [104]. They used on-line recursive identification for a NARX-model with the conventional model-predictive structure and applied the controller to a pilot-scale wastewater process. The results were significantly better that the ones received with a similar controller using linear model structure.

Tadeo *et al.,* [122] developed l_1-optimal regulation of a pH control plant and received good results in a simulation study. Later they tried the methods they developed in a pilot-scale pH-process and got practical experimental results (pilot-scale pH-process, [123]). They applied robust loopshaping for a pH process, in which a flow of liquid of varying pH and varying buffer was controlled with a strong hydrochloric acid. The robustness was improved with the new controller.

Some researchers have used several local models instead of one global model. Nyström *et al.,* [91], [90] constructed five different linear models for pH range 3 to 7 and designed an optimal controller (linear quadratic minimisation subject to H_∞ constraint) for a simulated process that consisted of phosphoric acid and calcium hydroxide. Only simulation results were presented.

Ylöstalo and Hyötyniemi, [147] developed a gain scheduled multi-model pH controller for a pilot scale neutralisation process that was, in fact, the same process that was used as an application in this thesis (Chapter 6, section 6.1). They gathered a model library for various buffer and acidity load changes and studied how to perform smooth transform between different submodels. A conventional PID controller was used as the controller with different tuning parameters for each submodel.

A recent paper by Wright and Kravaris, [135] presented an industrial application of the strong acid equivalent approach that was developed in [134] and [138]. The industrial process is a lime-slurry neutralisation of acidic flow of unknown contents and drastically changing acidic load. They used an on-line identification method for unknown chemical species developed in [136]. Once the identification is realised the strong acid equivalent (SAE) controller can be used. The results are very good and the controller has been in continuous operation for more that four years (in 2001).

The approach given in [135] is very similar to the adaptive physico-chemical modelling method by Jutila and Visala, [52] or the adaptive reaction invariant modelling method by Gustafsson and Waller, [30]. Jutila and Visala used Kalman filter for hypothetical species estimation whereas Gustafsson and Waller identified the reaction invariants with the help of least squares method.

The application process and its problems are rather similar to those presented in the ammonia scrubber application (section 6.2.1) of this thesis. Let us take a closer look at the differences between SAE, [135] and the modified SOC-algorithm presented in this thesis. A fundamental difference between the two methods is that SAE uses indirect feedback adaptation (the process model is first identified and then used in the control law) and SOC direct feedback adaptation (control law is directly manipulated based on the control performance).

The SAE approach uses the inverse of the identified (adaptive) titration curve in the pseudo-linearisation of the control loop but the slave controller (fixed PI-controller) is not adapted. SOC, on the other hand, changes directly the control rule tables (proportional vs. derivative rules and the local integral gain) that corresponds to adapting the controller gains. As a result, if flow and volume changes are large enough for the process time constant to change significantly, the SAE approach can not adapt to compensate the changes but SOC approach can. If the flow and volume are measured, the parameters of the PI-controller of SAE could be made adaptive with feedforward adaptation as shown in Fig 5.10. and documented in Zenger, [151].

A very good and detailed application of model-based pH-control in an actual industrial precipitation/cementation process is given by Støle-Hansen, [117]. What makes the application even more interesting is the fact that the model contained slow precipitation phenomena that were included in the model by combining reaction invariants to reaction variants. A very realistic case in a sense that after all the careful modelling, simulation, analysis, controller development and actual experiments the new controller gave approximately as good performance as a conventional PI-controller. The reason for that was that the pH-value behaved almost linearly in the particular pH control range.

5.3.2 Non-model-based controllers

In many practical pH processes time delays, time constants, gains and sensitivities change over a wide range mainly due to varying flows and their chemical contents. A fixed model (off-line modelling) can not adjust to variations in the process and an adaptive model (on-line modelling) has many practical problems. Unbiased and efficient model identification within a control loop is difficult. The controlled signal can also be poor in many frequencies i.e. the system is not persistently exciting. From control point of view keeping the pH value constant at reference value is in many cases the objective of control whereas from modelling point of view system identification from practically constant signals is impossible or at least inefficient.

A poor process model can have serious effects for model based controllers and fixed controllers are often more robust and reliable even though they might not give the best performance in every situation. However, if an adaptive controller is required, many modelling problems can be avoided by using direct adaptive controllers instead of a combination of on-line modelling and model based control. Indirect adaptive controllers evaluate the performance of the control loop and modify the controller when needed.

Shinskey, [113] developed an adaptive analogue controller that consisted of a conventional PID controller combined with a nonlinear gain shaping element. The controller was commercially available and it was used in many practical applications. The algorithm was later improved by Foxboro Inc. [21] and the improved controller is known as Foxboro Exact autotuner. It evaluates the control performance with respect to periodic oscillations and slow creeping behaviour. There is also a dead band for error signals close to zero that prevent adaptation for small errors.

Other instrument manufacturers, e.g. Yokogawa Inc. and Honeywell Inc., developed their own versions of autotuners. Kao *et al.,* [57] tested the Yokogawa autotuner in a difficult pilot plant. They studied the effect of adaptation dead band and they found that by using the dead band the control action became more stable but the momentary maximum control deviation increased as well.

Kurz, [66] developed an adaptive PID-controller especially for rapid buffering changes in a pH process. The controller has a predefined trajectory as a tuning parameter and at every time instant the controller tries to force the error to follow this trajectory. The algorithm is easy to realise and it was tested in an actual industrial scale pilot plant. Jutila and Jaakola, [50] performed a comparative simulation test for different adaptive PID controllers in a challenging laboratory-scale pH process and Kurz algorithm performed very well.

pH processes are nonlinear by nature and nonlinear controllers have proved successful in controlling the pH value. Soft computing methods are suitable for nonlinear control. Especially fuzzy control has made a breakthrough in process industry and there are many documented practical applications, e.g. by Heckenthaler and Engell, [35] to name but a one. The self-organising fuzzy controller based on the original work of Procyk and Mamdani, [101] is presented in detail in next section with modifications by the author. There is a successful implementation of the basic algorithm in a pH control problem documented by Shah [111]. Fuzzy rule base can be generated with a number of methods and in many commercial controllers there are tools for that. Karr and Gentry, [58] used genetic algorithms for generating the fuzzy rule base.

Maron and Burgert, [82] developed an adaptive fuzzy controller for wastewater neutralisation with hydrated lime. Their controller constructed of a conventional PI-controller in feedback loop and of a feedforward adaptive fuzzy part. The new controller proved to outperform the earlier conventional controller in simulations. Garrido *et al.,* [23] developed a conventional one-level, fixed fuzzy controller for wastewater neutralisation simulator. The results were good as long as the buffering did not change significantly, as can be expected.

Neural networks have not had a similar commercial breakthrough as fuzzy logic and practical applications in pH control are more scarce. Loh *et al.,* [78] viewed different approaches to neural network modelling and control in a pH process. Palancar *et al.,* [96] developed a neural controller that consisted of two artificial neural networks, the first of which described the plat model and the second the plant inverse model. By combining these two the neural controller could calculate the required reagent flow for pH control. The controller was first tested with simulations and then implemented on a pilot-scale neutralisation process. The neural networks learned the plant on-line, i.e., the controller was adaptive. The buffering was changed during the test runs and the controller adapted to small and gradual buffer changes. Unfortunately the learning was not efficient enough for sudden and significantly big changes in the buffering.

Artificial neural networks have also been used for pseudo-linearisation of the control loop. Kim *et al.,* [62] used a radial basis network that learned to compensate the nonlinearity of the process. The radial basis net used process output (pH) and controller output (reagent flow) as inputs as it generated an additive compensation signal that was added to the original control signal. This combined control signal, which was thus pseudolinearised, was an input for the actual process. The pseudolinearisation worked well in the simulation study. A similar approach was presented by Boozarjomehry and Svcek, [6]. They developed two different pseudolinearisation schemes for a simple pH process (these include state feedback linearisation and output feedback linearisation) with both direct and indirect training methods. The most general approach is the output feedback linearisation scheme with indirect training. The results are good, but again, the buffering did not change during the test runs and only simulation results were presented.

5.4 Self-organising fuzzy controller

Self-organising controller (SOC) is a term used by numerous researchers in different contexts and most of them have a strong opinion of what the term signifies. Unfortunately the opinion of one researcher varies significantly from the opinion of another. Self-organisation is often understood to be connected only to self-organising maps (and in most cases to Kohonen self-organisation).

The idea that a fuzzy logic controller could learn from past performance and generate required rules on-line was first proposed by Mamdani and Baaklini, in 1975 [81]. Procyk and Mamdani, [101] presented the original, linguistic self-organising controller as well as the abbreviation SOC in 1979. In this thesis the term self-organising controller and the abbreviation SOC is used as a general term for a family of adaptive fuzzy controllers that are based on the original idea by these authors and, in particular, as the controller developed in the course of the rest of this chapter.

There are also other interpretations of definitions, e.g. Kazemian, [60] uses the term self-organising fuzzy controller for a gain scheduling PID – controller, in which the tuning parameters of a continuous PID-controller are modified with a supervisory fuzzy logic system, which is, in turn, modified by another even higher hierarchy fuzzy logic that uses a fuzzy look up table as a rule base. On the other hand, Lee *et al.*, [71] use the term self-organising fuzzy controller as they developed a controller, which was constructed from fuzzified radial basis network that autonomously organised its network structure to the required size and parameters. They applied this controller for position control in a servomechanism with asymmetrical loading and changes in the load.

These two applications serve only as an example of what can be meant by a self-organising fuzzy controller; there are many others. In this thesis the scope is restricted to a fuzzy logic controller with a base level fuzzy controller which uses a rule table that is modified by a higher hierarchy adaptation as shown in Fig. 5.20 (the definition given in [101]).

Self-organisation is understood as the autonomous organisation of the positions of the fuzzy inference output membership functions as shown in Fig. 5.21. The membership functions are singletons that are spread in the fuzzy output space P_u. Initially all rules can be "empty", i.e., all singletons are at zero point (Fig. 5.21a) and whatever values the fuzzy input may have, the output stays at zero. The performance of the controlled system is poor and the higher hierarchy, that is responsible for the adaptation or learning, changes the singleton positions so that the control performance improves (the singletons have organised in Fig. 5.21b).

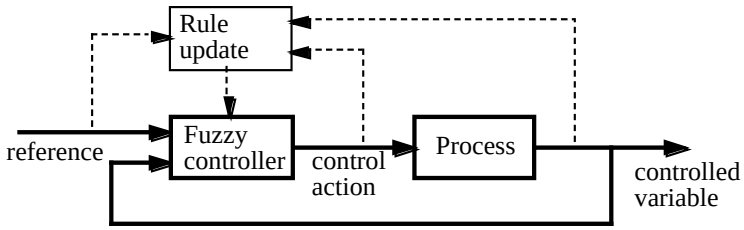

Fig 5.20: The block diagram of the self-organising controller

The original idea and structure by Mamdani and Baaklini, [81] was sound and understandable but the actual mechanisms of self-organisation and rule correction were rather undeveloped. These points were improved by Procyk and presented in great detail in his Ph.D thesis in 1977, [100]. He simplified the rule structure into a standard two-dimensional rule table of unit depth, that uses only AND-rules (earlier work also included more complicated rules with THEN IF and OR – structures). He also introduced the performance criterion rule table for the control performance evaluation. Procyk and Mamdani later revised few small inconsistencies of [100] (such as asymmetry problem in the error regions) in their paper in 1979, [101].

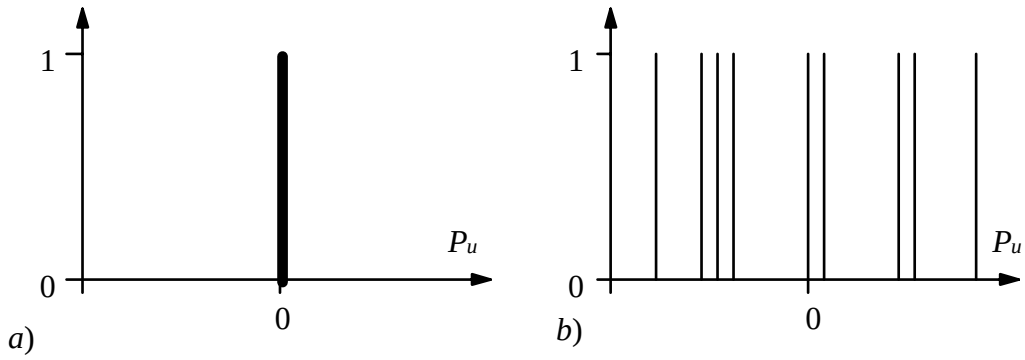

Fig. 5.21: The membership singletons of the controller output a) the initial rule base (all rules at zero), b) the final self-organised rule base.

After all this pioneer work, the SOC-algorithm was further developed in the course of three more Ph.D thesis: Yamazaki, [139], Lembessis, [72] and Sugiyama, [119]. The main contribution of these researchers was in the area of scaling parameter selection, different quantisation and defuzzification methods, different performance decision table entries, etc. All the processes (with different orders, time constants and time delays) were simulated and the aim of the controller was always to solve a simple servo problem. A clear shortcoming was that the SOC-algorithm was not tried on any actual process and the subject of time-varying characteristics was not considered.

All this research effort was done at the University of London, Queen Mary College, Dept. of Electrical and Electronic Engineering under the supervision of prof. Mamdani who wrote his personal experiences of the research period in an article, suitably named, “Twenty Years of Fuzzy Control: Experiences Gained and Lessons Learnt”,. [80]. The article was published in 1993.

In 1988 Shao, [112] introduced a novel performance criterion formulation, in which the $e/\Delta e$-plane performance criterion was based on the minimum acceptable distance diminishing rate. This variable could be directly, experimentally determined from an acceptable control behaviour. Criterion by Shao is also used throughout this thesis.

An interesting application of the basic SOC algorithm was presented by Shah, [111] in 1991. He did not use the performance criterion structure suggested by Shao, [112] but instead he hold to the original criterion developed in Queen Mary College, [81]. The interesting fact in this application was that the complex, real process Shah chose for SOC testing ground was a laboratory scale pH process, which consisted of one ca. 4 l vessel with a mixture of acids (sulphuric, hydrochloric and acetic acids) to be controlled with sodium hydroxide.

The initial results with the basic SOC algorithm did not show good control performance; the pH value was very oscillatory and damping was poor. He concluded that the performance criterion did not take the specific nature of the pH process into consideration and so he decided to compensate the nonlinearity in the system by having a special coefficient multiplier for particular pH-areas. The response using this approach still oscillated but it dampened much better that the original response.

Encouraged by this success, Shah created several different performance coefficients for other specific pH areas (4 different pH areas) effectively creating a line approximation of the nonlinear titration curve. He also developed a varying coefficient multiplier and the results improved still. He concluded that the original performance table by Procyk, [100] was not particularly suitable for highly nonlinear processes (such as a pH process) but that the performance could be improved significantly by introducing the performance coefficient multipliers.

The results achieved by Shah were good and a practical application gave validity to the results. The only drawback was that the approximate titration curves were used as a priori knowledge for performance coefficient multiplier determination. In fact, from general point of view this approach is similar to a classical pseudolinearisation of a control loop with an inverse

titration curve. Once the linearisation is done, the controller is then self-organised on-line. This also indicates that the controller could only be used for time-invariant nonlinearities that are determined from fixed titration curves. The performance criterion developed by Shao, [112] would have suited much better for this application.

In 1991 Zhang and Edmunds, [152] improved the complicated and inefficient rule adaptation mechanism so that the performance criterion directly gives an output correction factor that is transformed into an input correction factor that is then divided for each of the activated membership functions with respect to their activation levels. Laurikkala used the performance criterion by Shao, [112] and the rule update mechanism by Zhang and Edmunds, [152] in his Mc.S. thesis [69] (a simulation study of the learning capabilities of SOC). This was the initial SOC-algorithm that was considered as a base level for all the modifications in this thesis.

Other early applications of SOC on real processes include a yaw control for a Royal Navy warship by Sutton and Jess, 1991, [121]. The application created a difficult control problem because of the highly nonlinear yaw dynamics. In this application the SOC-argorithm was compared against a conventional self-tuning algorithm. An interesting fact was that they originally developed a conventional self-organising PI-table and after preliminary tests found that derivative action is also required and incorporated an additional derivative action to the control algorithm creating effectively a PI+D-controller. In this thesis a self-organising PD-controller is incorporated with an integral action (PD+I). Sutton and Jess also developed a higher hierarchy set of rules they called “over rules” that held a priori knowledge of the nonlinear yaw model and guaranteed that the controller did not learn stupid things in view of the yaw model.

The comparative evaluation between an optimally tuned fixed PID, a self-tuning PID and the SOC-algorithm showed that SOC gave a sluggish response whereas the other controllers reached the target value quickly. Sutton and Jess concluded that this is mainly due to the fact that SOC-algorithm was time-discrete with relatively high sampling time and the other controllers were analogue. The comparison of analogue controllers to discrete in terms of quick performance is somewhat questionable as well as the idea of incorporating a priori known nonlinear model into a learning controller. If a crude nonlinear model is known beforehand there are other model-based solutions for controlling the system.

In 1991 Linkens and Abbod applied the basic SOC-algorithm to a simple laboratory-scale flow system that consisted of two interconnected tanks, [76]. The level of the second tank was affected with load disturbances (manipulation of the valve opening in leaving flow pipe) and the level was controlled with a pump that fed water to the first tank. They introduced an extended SOC-algorithm, in which the scaling coefficients for error and change of error were different when the level was close to the target value and when the level was far from target.

Linkens and Abbod also documented a SOC application in the control of tension and speed of a coupled electric drives apparatus that consists of two D.C. servo motors which drive, via a continuos belt, a jockey pulley, [76]. They applied the same extended SOC-algorithm with the switch for coefficient change and the results were good. However, it is to be noted, that no comparisons were made with any other controllers and it is open to suggestions whether other strategies would operate as well or even better.

In 1992 Linkens *et al.* applied SOC-algorithm to nonlinear multivariable anaesthesia problem, [77], in which two drugs, atracurium and isofluorane are used for achieving the required levels muscle relaxation and unconsciousness. The objective is to get a smooth level of anaesthesia so that the patient is sedated heavily enough for the operation but as lightly as possible for safety and fewer complications. An additional difficulty is that every patient’s reaction to the drugs is somewhat unique.

In that research a generalised predictive controller (GPC) and the extended SOC-algorithm were compared in simulations. GPC performed better when a detailed model was available but the SOC operated even when there was no prior knowledge about anaesthesia with an empty initial rule base (sounds rather dangerous in real anaesthesia). GPC performance settled better as the SOC-

algorithm was inclined to small amplitude limit cycle oscillations. The results were mere simulations; no real anaesthesia applications were considered in the paper.

Jan Jantzen collected together the current state (current at 1998) of the basic SOC algorithm in a tutorial rapport, [43], that he used as a teaching material for undergraduate students. The rapport is very illustrative and gives excellent guidelines for tuning the free parameters of the basic SOC-algorithm. He simulated the controller behaviour with simple examples. He and Olivares, [92] applied the basic SOC-algorithm to an inverted pendulum system (cart with an iron ball).

More recent real applications of SOC include a laboratory scale flow process that consists of two coupled vessels (Singh, [115]), a laboratory scale heating process (Dias and Dourado, [13], a two link manipulator (Lin and Tsai, [74]) and a circular inverted pendulum system (Kim and Bien, [61]). With an adaptive autopilot for bank-to-turn missiles (Lin and Wang, [75]) and a nuclear steam generator level control problem (Park, and Seong, [97]) only simulations were presented.

The SOC-algorithm has gone through many modifications and changes by several researchers since the early days of Procyk and Mamdani, [101]. Lin and Wang, [75] integrated fuzzy reasoning and radial basis function networks into fuzzy basis function networks. This extension enabled the adaptation of input membership function shapes in addition to the output singleton positions. Park and Seong, [97] compared the controller performance with traditional performance table and a performance cost function they developed.

Kim and Bien, [61] were concerned about the SOC robustness (the original SOC algorithm is rather sensitive to external signals) and so they proposed that the learning and modification of the controller is made in consideration of the motional trend of the error state vector as well as its locational information. Their proposal did improve the robustness in simulations.

5.4.1 Low level fuzzy controller

As explained in the previous section, the basic algorithm that was used as a foundation for all the modifications, was a combination of the basic structure (by Procyk and Mamdani, [101]), the rule update mechanism (by Shao, [50]) and performance criterion (by Zhang and Edmunds, [152]). It is presented in, [69] and also, in detail, in this section.

Self-organising fuzzy controller (SOC) consists of two hierarchies, as shown in Fig. 5.20. The lower hierarchy is an ordinary fuzzy logic controller with a rule base that is modified by the higher hierarchy. Generally, the membership functions of the fuzzy labels can have a variety of shapes and the rule base update could change the actual rules or the membership functions of the input signals or the output signals. For practical purposes, some restrictions had to be made.

The traditional SOC-controller uses only two signals (error and change of error) and uses a two dimensional rule table for calculating either control action or the change of control action (Fuzzy PD and Fuzzy PI controller structures correspondingly). However, the application processes gave the best control performance (with conventional PID-controllers) when both integral and derivative actions were included and therefore the basic SOC-algorithm was modified to include both of them as well. The modified low level fuzzy controller has a (PD+I)-type rule base where the self-organising PD-table is adjusted and the linear integration eliminates the steady-state error. The integration gain tracks the average gain changes in the PD-table (Fig. 5.22).

The input variables of the fuzzy PD-controller (error and change of error) both have normalised and triangular membership functions that become linearly more dense towards the zero values as shown in Fig. 5.23. Traditionally a fuzzy controller uses significantly fewer membership functions and the reason for such a large number of labels in this application is twofold. Firstly the number of membership functions depend on the complexity of the nonlinearity and the industrial ammonia scrubber application presented in Chapter 6, section 6.2 is very nonlinear. As can be seen from Fig. 6.30 (pH controlled with a fixed PID controller) when the pH value changes slightly the behaviour changes significantly.

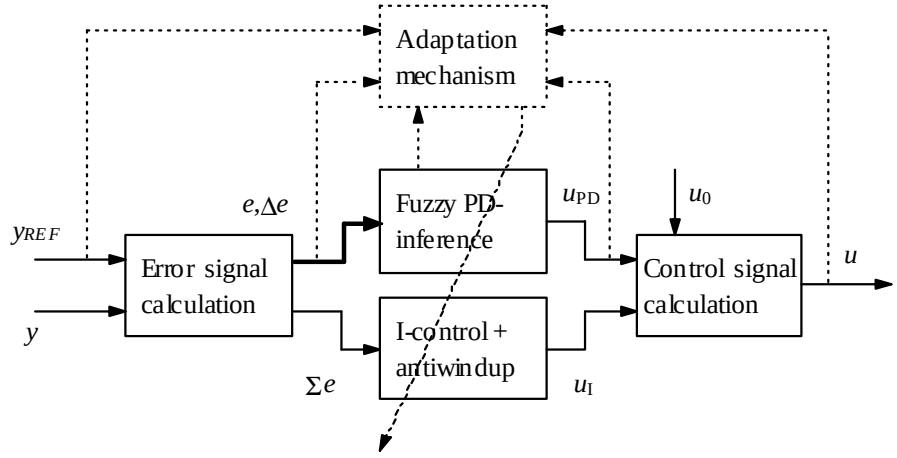

Fig. 5.22: Block diagram of the control signal calculation

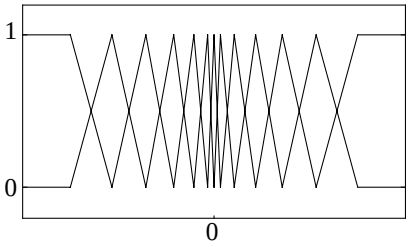

Fig. 5.23: Input membership functions

Each rule was designated to a specific output membership function (singleton). The performance indicators correspond to acceptable process behaviour from deterministic and stochastic point of view and the places of output singletons are changed in the rule update procedure if the performance criteria are not satisfied.

The controller input signals are scaled with constants G_e and $G_{\Delta e}$ ($y(k)$ is the process output, $y_{ref}(k)$ is a reference signal for the output and k is the discrete time instant).

$$\begin{cases} e(k) = G_e \cdot (y_{ref}(k) - y(k)) \\ \Delta e(k) = G_{\Delta e} \cdot ((y_{ref}(k) - y(k)) - (y_{ref}(k-1) - y(k-1))) \end{cases} \tag{5.4}$$

The signals are fuzzified (μ_{ei} and $\mu_{\Delta ei}$ are the ith membership function of the error signal and the change of error respectively, while N and M are the total numbers of membership functions).

$$\begin{cases} \hat{\mathbf{e}}(k) = \left[\mu_{e_1}(e(k)) \quad \mu_{e_2}(e(k)) \quad \cdots \quad \mu_{e_{Ne}}(e(k))\right]^T \\ \Delta\hat{\mathbf{e}}(k) = \left[\mu_{\Delta e_1}(\Delta e(k)) \quad \mu_{\Delta e_2}(\Delta e(k)) \quad \cdots \quad \mu_{\Delta e_{M\Delta e}}(\Delta e(k))\right]^T \end{cases} \tag{5.5}$$

The fuzzy rules follow the format:

$$\text{IF} \quad e(k) = \mu_{e_i} \quad \text{AND} \quad \Delta e(k) = \mu_{\Delta e_j} \quad \text{THEN} \quad u(k) = \mu_{u_l} \tag{5.6}$$

which is calculated as a minimum:

$$\mu_{u_i}(u(k)) = \min\left\{\mu_{e_i}(e(k)), \mu_{\Delta e_j}(\Delta e(k))\right\}. \tag{5.7}$$

The output singleton positions (constant at the low level) are presented as a vector $\mathbf{p}_u$, and their activation levels, calculated according to equation (5.7), are collected into a fuzzy vector:

$$\hat{\mathbf{u}}(k) = \left[\mu_{u_1}(u(k)), \mu_{u_2}(u(k)), \cdots, \mu_{u_k}(u(k)), \cdots, \mu_{u_{Nu2}}(u(k))\right]^T. \tag{5.8}$$

Because each rule is designated to one particular output singleton, the same output singleton cannot be activated by separate rules and the fuzzy inference is simplified. With normalised triangular membership functions, only four rule activate simultaneously and the rest of the singletons can be excluded at that particular one time instant. The output u is de-fuzzified using a centre-of-gravity method that corresponds with the singletons in the calculation of the weighted mean.

$$u(k) = \frac{\mathbf{p}_u^T \hat{\mathbf{u}}(k)}{\begin{bmatrix}1 & 1 & \cdots & 1\end{bmatrix}\hat{\mathbf{u}}(k)} \tag{5.9}$$

The normal operating level and the integral part are added to the scaled output.

$$u_{TOT}(k) = \bar{u} + \sum K_i \cdot e(i) + G_u u(k) \tag{5.10}$$

5.4.2 Adaptation mechanism

The adaptation criterion is based on the phase plane behaviour of the error signal. Fig. 5.24 shows the trace of a disturbance in phase plane. The switching line describes optimal (e,Δe) –pairs (from the controller point of view). Due to the disturbance, the actual process behaviour deviates from the switching line. This happens with all controllers and it should not be considered as an indication of bad tuning of the controller. However, if the controlled system does not recover well from the disturbance (persistent oscillation, too slow transient response or even instability), then the controller tuning has to be improved.

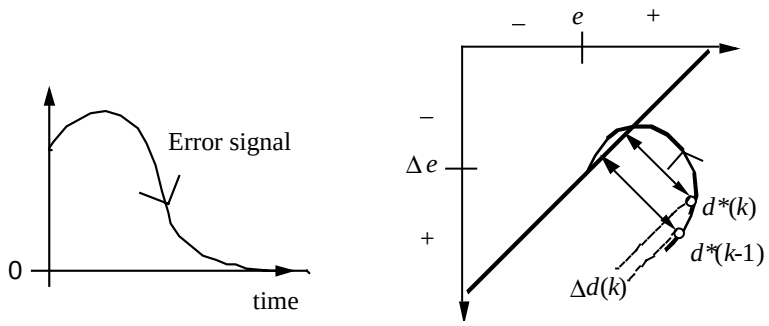

Fig. 5.24: Error signal behaviour in phase plane (d* is the geometric distance from the switching line and Δd the decrease of the distance)

If the distance from the optimal line does not decrease (instability) or if the decrease of the distance is too slow (sluggish transient response) the fuzzy rule base has to be improved. There is a

threshold limit for adaptation and if this threshold for acceptable controller performance is not met, a corrective action p_1 is calculated. p_1 is proportional to the difference between the acceptable and actual controller performance in phase plane.

The performance criterion, described above, tends to allow oscillating behaviour and in order to avoid oscillations another criterion is needed. The second criterion is based on the stochastic behaviour in the phase plane. The variance of Δd is calculated recursively with an exponential forgetting factor and compared to variance threshold value. An increase in the Δd variance indicates oscillation and a corrective action p_2 is needed.

The actual correction to the rule base p is calculated as an ordinary sum of the two different corrective actions p_1 and p_2. With this kind of construction both instability, slow response and oscillation in the controller performance is punished.

5.4.2.1 Deterministic behaviour criterion

A simple error signal does not describe the control performance adequately. If there is a large deviation from the reference but the error is diminishing rapidly, the controller is operating satisfactorily. In the $e/\Delta e$-plane this optimal performance is described by a straight line, as shown in Fig. 5.24. The distance $d^*(k)$ between the actual output $(e(k),\Delta e(k))$ and the optimal line is calculated, as well as the change in the distance $\Delta d^*(k)$ in one sampling period.

$$d^*(k) = \frac{1}{\sqrt{2}}\left|e(k) + \Delta e(k)\right| \tag{5.11}$$

$$\Delta d^*(k) = d^*(k) - d^*(k-1) \tag{5.12}$$

Diminished distance is defined as $\Delta d = -\Delta d^*$, and the required output correction $p(k)$ is calculated as follows

$$p(k) = \begin{cases} 0 & , \Delta d \geq q(e, \Delta e) \\ L \cdot \left(q(e,\Delta e) - \Delta d(k)\right) \cdot \operatorname{sign}\left(e(k) + \Delta e(k)\right) & , \Delta d < q(e, \Delta e) \end{cases} \tag{5.13}$$

where L is a learning factor and q the required distance diminishing rate as a function of e and Δe. There are many suitable choices for the structure of q. It can be chosen to imitate a process of first order dynamics and a time delay. A highly nonlinear pH-process is very far from first order dynamics and superfluous effort is needed for forcing a needlessly strict first order response instead of an adequate nonlinear response. An experimental approach proved to be more suitable for the pH-process.

The experimental approach calls for either simulated or real plant data of satisfactory responses. $\Delta d(k)$ can be calculated from the data in accordance to (5.12) and the resulted values can be considered as a basis for q in different situations. The calculated values of q can be further modified and smoothed and collected in, e.g., a fuzzy rule table.

The output correction $p(k)$ describes the extent to which the controlled variable needs to be corrected. The input correction $r(k)$ describes what kind of additional control action is needed to achieve the required output correction. $r(k)$ can be calculated from $p(k)$ with the help of an inverse model M^{-1}. For SISO processes the model is 1 if a positive change in the control action produces a positive response, and -1 if a negative response results. The input correction is calculated simply as follows:

$$r(k) = M^{-1} p(k). \tag{5.14}$$

The only thing that has to be known about the process in addition to the response sign, is the average time constant in discrete time instances, $\overline{n}_\tau$. This knowledge is used when determining which control action has resulted in the present situation, and consequently which rules need to be corrected. The control value that would have achieved the acceptable output u^* can be calculated from the actual control value u and the input correction r:

$$u^*(k-\overline{n}_\tau) = u(k-\overline{n}_\tau) + r(k). \tag{5.15}$$

All rules that were activated when the control value u was calculated are now updated in proportion to their activation levels, so that the entire control action adds up to u*. For the two-dimensional rule table with membership functions chosen as in Fig. 5.23, a maximum of four rules are activated simultaneously.

A simplified numerical example of the self-organising algorithm is presented in Appendix 2 in order to clarify the basic structure of the algorithm.

The adaptation has to be halted during a set-point change. The output evaluation would recommend a radical change to the rule base, even though the increasing error is only the result of a stepwise change in the reference signal. The halting of the adaptation is taken care of by setting the output correction p to zero. The adaptation can be started with an empty rule base, but in that case the convergence will take some time and there will be empty holes in the rule base corresponding to $e/\Delta e$-plane areas where the state seldom goes.

As there was an adequate PID-tuning available, a full rule base, that operates exactly like the PID-controller, was generated. With this rule base as the initial value for the SOC, there is always the PID-algorithm in the no-go areas to guarantee performance at all instances.

5.4.2.2 Stochastic behaviour criterion

The deterministic evaluation of the closed loop performance operated well in cases where the noise ratio was small and there were no high frequency oscillations. In many practical test runs with actual pH-processes this requirement was not fulfilled and problems occurred.

In addition to deterministic evaluations also stochastic measures were called for. A suitable indicator of good performance from the stochastic point of view was the variance of Δd. The estimated variance avoided saturation and tracked the changes of the actual variance with the introduction of exponential forgetting factor λ (N indicates the number of samples). This and all the other modifications on the basic SOC-algorithm are also presented in [140].

$$\sigma^2_{\Delta d}(N) = \frac{\sum_{i=1}^{N} \lambda^{N-i} \Delta d^2(i)}{\sum_{i=1}^{N} \lambda^{N-i}} \tag{5.16}$$

With the definition of

$$P(N) = \sum_{i=1}^{N} \lambda^{N-i} \tag{5.17}$$

the equation (5.16) could be modified into a recursive algorithm

$$\sigma^2_{\Delta d}(N+1) = \sigma^2_{\Delta d}(N) + \frac{1}{\lambda P(N)+1}\left(\Delta d^2(N+1) - \sigma^2_{\Delta d}(N)\right) \tag{5.18}$$

$$P(N+1) = \lambda P(N) + 1 \tag{5.19}$$

A suitable output correction p_V was determined from the variance estimate as follows

$$p_v(k) = \begin{cases} 0 & ,\sigma^2_{\Delta d} < q_v \\ \alpha \cdot \left(\sigma^2_{\Delta d}(k) - q_v\right) \cdot \operatorname{sign}\left(e(k) + \Delta e(k)\right) & ,\sigma^2_{\Delta d} \geq q_v \end{cases} \tag{5.20}$$

where α is the variance weighting factor and q_V is the acceptable variance limit value.

Instead of using merely the equation (5.13) to define the output correction, a combination of (5.13) and (5.20) was used. The combined output correction $p_{TOT}(k)$ was then used in equation (5.14) instead of $p(k)$.

$$p_{TOT}(k) = p(k) + p_v(k) \tag{5.21}$$

The required distance diminishing rate q of equation (5.13) is also modified to include even small negative values of Δd to acceptable behaviour near the origin.

The algorithm can be initialised if the parameters of an adequate PID-controller are available. In this case the initial rules were calculated from an initial PID-algorithm. This caused the controller to operate initially as a fixed PID-controller.

5.4.2.3 Adaptation of the integral action

The test runs showed that even though the PD-adaptation was successful a fixed integral gain was not a suitable choice for the applications. With sensitive systems the integral gain was too high causing oscillations and with well buffered systems the elimination of the steady state error was too slow.

A good indication of the average gain change of the PD-table was the relative change from the initial values. The integral adaptation was calculated as follows

$$K_I(k) = \left(\frac{u_{PD}(k)}{u_{PD}(0)}\right) K_I(0) \tag{5.22}$$

where the initial values corresponded to the same tuning parameters that were used for generating the initial rule base.

5.4.3 Practical modifications

There are several practical modifications that can be divided into following categories:

- limitations in the control signal (one-sided control action, antiwindup) adaptation maintenance (evaluation and monitoring of pathological process situations (step changes, fault diagnosis)
- safety issues (initial PID-tuned rule bases, limitations on the rule update)
- knowledge upkeep (saving and loading of rule bases)
- hardware, software and communication aspects (construction of the actual unit controller)

These modifications are crucial to the satisfactory operation of the adaptive controller in a practical application.

5.4.3.1 Initial values

Initial rule base is calculated from a cautiously tuned PID-algorithm and if the adaptation mechanism is disabled the SOC-algorithm (now a fixed fuzzy controller) operates identically to a fixed PID-controller. The controller-PC contains a C-program for generating rule bases to correspond any PID-tuning.

During start-up the adaptation is disabled for a short time period and only after the fixed fuzzy controller proves to operate during the test period the self-organisation is started.

The adaptation parameters correspond initially to slow learning rate but as most of the parameters they can also be changed by operator command at any time (e.g. during a grade change or other predictable disturbances that affect the process behaviour).

The benefits of full rule table as initial starting point are self-evident. The controller can be started from zero values (all output singletons at zero) but then the SOC operates poorly until the sufficient rules have been learned. The rule table is updated only in situations that have actually taken place in the real process and when an unprecedented situation occurs the controller has no rule for controlling it. The full initial rule table always provides at least a careful PID-control action and the operation of SOC-algorithm becomes more reliable in rare situations and when the algorithm is started.

5.4.3.2 Improved performance by limited rule bases

As SOC-algorithm is both nonlinear and adaptive no guarantee of good closed-loop performance can be given especially when the pH-process is also nonlinear and time variant.

Some general process knowledge can be utilised in controller design. Determination of the titration curve is a standard analysing method and during long term plant operation this data has been collected. From titration curves the average sensitivity changes were calculated and the sensitivity range around an average sensitivity indicates the needed controller gain variation around the average gain.

The gain variation was inserted to the SOC-algorithm in the form of limited minimum and maximum values for output membership function positions (e.g. the singleton output membership function of any rule could only be changed from the initial position x to x/n or $n \cdot x$, where n is a pre-specified parameter). In addition to the PD-rule table the same limitation was stated for the integral part.

The extreme rule bases that can be achieved with maximum and minimum limits now correspond to two extreme PID-controllers that can be used for rough controlled system evaluation. The actual controller however is a nonlinear combination of the two extreme linear controllers and the evaluation is more accurate, if the limit values are close to each others.

Another benefit of the limited rule bases is the improved tolerance of bad data. During normal operation some of the actuators or measuring probes can be out of order in which case the control signal and the actual input of the process or the measured output and true output do not correlate. If the collected input/output data is used for self-organisation the algorithm learns erroneous control behaviour. If the rules are not limited the results can be poor.

5.4.4 The tuning of adaptation

The tuning of the adaptation mechanism is relatively easy to begin with and the controller-program makes it even more effortless. Most of the tuning parameters are closely related to good closed-loop performance which makes the physical interpretation possible. Performance criteria are:

- If the (e/Δe)-plane speed Δd is greater than minimum requirement q no adaptation is needed, else the correction factor is proportional to (q-Δd).
- If the speed variance $\sigma^2_{\Delta d}$ is smaller than maximum limit q_V no adaptation is needed, else the correction factor is proportional to ($\sigma^2_{\Delta d}$ - q_v).

Speed Δd and variance $\sigma^2_{\Delta d}$ are performance indicators that can be calculated from data collected from any specific situation. with or without controller The SOC-algorithm shows these and other variables related to tuning to operator who can change tuning parameters while the controller is running.

5.4.5 Comments on the modified SOC algorithm

The modified SOC algorithm contains deterministic and stochastic performance criteria. The deterministic criterion improves the transient speed whereas stochastic criterion diminishes oscillations and high frequency noise. Both aforementioned criteria adapt the PD rule base and the integral adaptation, as name implies, adapts the integral action.

Initial rule base calculation from an existing PID algorithm and the rule base limitation are necessary for safety and reliability issues as they guarantee that there are no holes in the rule base and that there is a limit how far the membership singletons can self-organise.

There are also numerous other modifications but they are more application dependent and therefore they are presented in section 6.2.

Chapter 6

Practical applications

Jarrow (n.)

An agricultural device which, when towed behind a tractor, enables the farmer to spread his dung evenly across the width of the road. [1]

The methods developed in earlier chapters are applied to different practical processes including a pilot scale neutralisation process, an industrial ammonia scrubber and acidification of thick deinked pulp. The aim in every application is to control the pH value but in most cases the pH manipulation was only an indirect tool for achieving the ultimate target, e.g. avoiding the dissolution of calcium carbonate or washing the ammonia from gas phase.

In every application the process is modelled by combining theoretical and experimental modelling methods and simulations. The simulators are fitted to correspond to the actual process adequately (keeping the model objectives in mind). Controllers are evaluated with the simulated models.

The pilot scale neutralisation plant is an excellent test process because the number of unaccounted disturbances is minimised. Theoretical models and the simulator match the actual process accurately and load and process changes are easily generated when required. The self-organising fuzzy controller (SOC) is constructed to the neutralisation problem in order to test and further improve the SOC-algorithm in a difficult real process but under controlled conditions.

The industrial ammonia scrubber is obviously much more complex than the laboratory scale neutralisation plant but despite the complexity the process can still be described with a Wiener type model and consequently traditional pH-modelling methods are used. Even though the obtained models are traditional the process is both nonlinear and timevariant so traditional controllers could not operate satisfactorily. Self-organising fuzzy controller is implemented and it proved to adapt to process changes reliably and efficiently. After the test period the developed controller is installed permanently to the process.

The acidification of thick deinked pulp is a very different process compared to the ammonia scrubber. The pH measurement is troublesome and the optimal pH value is not known beforehand, but once the measurement problem is solved, good control performance is achieved with a conventional PID-controller. Modelling and simulation of the process proved helpful in determining what kinds of phenomena take place within the system and how to prevent unfavourable and promote favourable ones. The pH value was the most important factor in achieving this.

6.1 Neutralisation pilot plant

There is a pilot scale pH-neutralisation process (Fig. 6.1) in the Control Engineering laboratory of Helsinki University of Technology. It provides a good test bench for various different control strategies. In fact, it was also used as an application test process in [50], [147] and [148].

All the modifications and improvements to the SOC-algorithm are developed simultaneously with the test runs and simulations with this neutralisation pilot plant. The ultimate target, however, was the control of the industrial ammonia scrubber presented section 6.2. The application described in this section was considered to be the final test before industrial application.

The modified SOC algorithm of section 5.3 was applied and was structurally identical in both applications. The industrial ammonia scrubber is more interesting and challenging application as a control problem and several safety and maintenance features had to be added to the industrial implementation that would make little sense in the laboratory scale process.

So why is this pilot application included in the thesis when the essential details are explained with the industrial application? Well, the neutralisation pilot plant is definitely not an uninteresting application. As a process it is completely different from the ammonia scrubber and even the control objectives do not coincide. There is validity in the fact that the modified controller does not perform well with just one application but also with a completely different process.

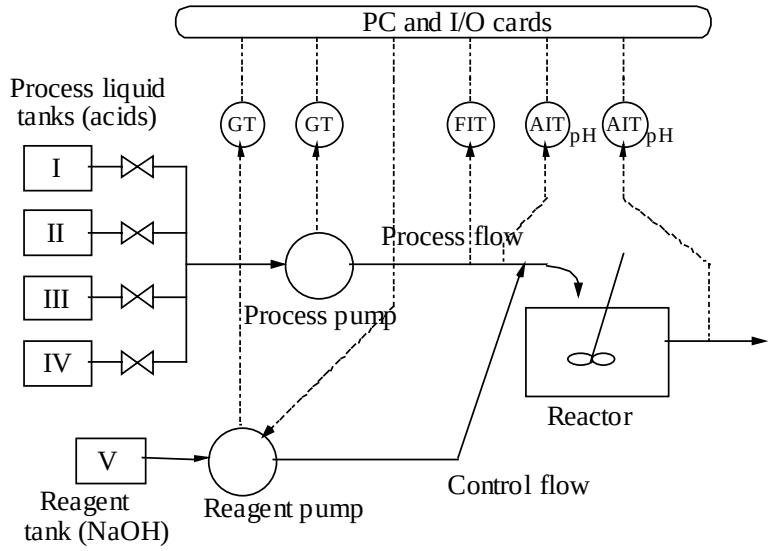

Fig. 6.1: Laboratory pilot equipment.

6.1.1 Basic process construction

Acidic process liquid (pH < 7) that consists of different acids, salts, bases and municipal water is neutralised with sodium hydroxide solution. There are four source tanks (I – IV, each ca. 2 m^3) for the acidic flow and one smaller tank (V, ca. ½ m^3) for the concentrated sodium hydroxide. The volume, flows and inflow source can easily be changed during the operation. There are also different reactors available (such as a plug flow reactor) but in these experiments only a well-mixed reactor (practically an ideal mixer) is used.

In this experiment the volume was kept constant (0.75 l) by taking the outflow from the overflow pipe. The nominal value for the inflow was 1 l/min but it was dropped down to 0.5 l/min during the test run.

In the pilot test the inflow is changed between strong acid - strong base and weak acid - weak base systems of different acidity loads. The inflow source tanks contain hydrochloric acid and ammonium acetate with various amounts so that the concentrations follow those given in Table 6.1.

Table 6.1: Concentrations (moles/litre) of liquid tanks

		Tank number				
Component		I	II	III	IV	V
Hydrochloric acid	$[A_P]$	0.003	0.010	0.003	0.010	0.000
Ammonia	$[\beta_P]$	0.000	0.000	0.010	0.017	0.000
Acetic acid	$[\alpha_P]$	0.000	0.000	0.010	0.017	0.000
Sodium hydroxide	$[B_C]$	0.000	0.000	0.000	0.000	0.143

The inflow source tanks I and II contain only strong acid (hydrochloric acid) and the only buffering elements in those tanks originate from municipal water and surrounding air. Tanks III and IV also contain ammonium acetate that buffers the system above and below the neutral point. The titration curves of the source samples are shown in Fig. 6.2.

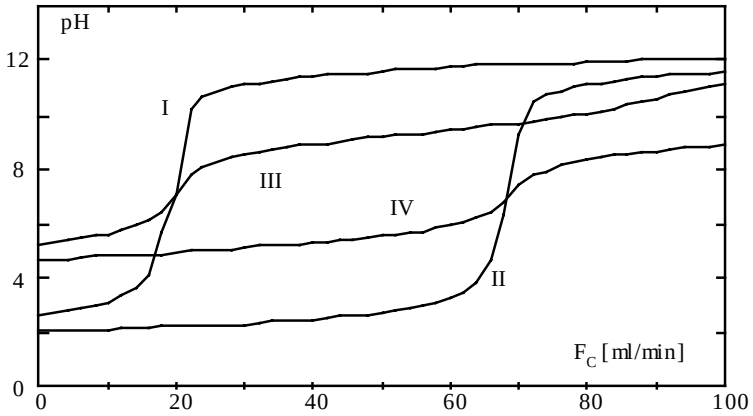

Fig. 6.2: Titration curves of the inflow source samples.

Titration curves are usually constructed for batch processes, but for control purposes they should be converted into CSTR-titration curves for a CSTR-process (as in Fig. 6.2). The difference is that in batch processes there are no flows in or out of the system except the reagent addition (that increases the total volume and dilutes the original sample), whereas in CSTR-titration the volume can be kept at a constant value and there are continuous in- and outflows as well as a reagent flow. The driving force of the pH-value is cumulative reagent addition in batch titration and momentary reagent flow rate in CSTR-titration.

The benefits of the CSTR-titration curves are self-evident as there is the actual reagent flow rate on the x-axis and the control signal steady-state value can be read directly from y-axis. For instance, the acidic loads of samples I and III are equal (reagent flow of approximately 20 ml/min should neutralise them) and the same applies for samples II and IV that have a higher acidic load (neutralisation takes ca. 70 ml/min of reagent).

There are also some benefits in performing an actual CSTR-titration (such as perfect irreversibility and no dilution), but from purely practical point, they are not economical and rather laborious (special instrumentation is needed) and therefore seldom performed. This is not a serious shortcoming as batch titration curves and CSTR-titration curves can be calculated from each other mathematically.

Additional nonlinearity is caused by the reagent pump as its speed of rotation can only change with a constant slope. This is clarified in Fig. 6.3 in which the control signal (target value for the

speed of rotation) in shown in the left and the actual realised speed of rotation on the right. For sudden large changes in the control signal there is a notable lag, but the small changes are tracked down almost to perfection.

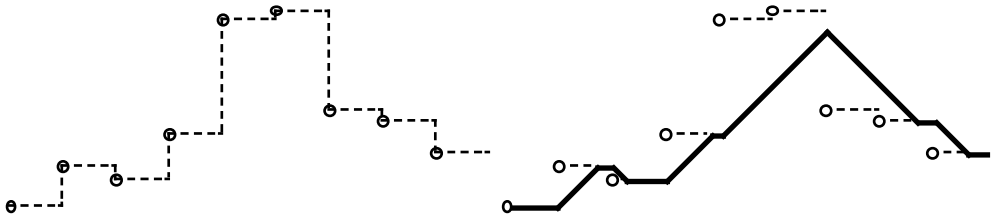

Fig. 6.3: The target value (left) and the realised (right) speed of rotation for the reagent pump.

6.1.2 Unaccounted disturbances

By manipulating the inflow source tank valves and the inflow pump, a variety of deterministic disturbances can be generated. During the test runs these disturbances were assumed to be unknown and no on-line information about them was included in the controller. Despite the voluntary ignorance concerning these disturbances, they and their effect on the pH-value were actually well-known and the disturbance sequence was carefully planned during the test runs.

In addition to the self-inflicted disturbances, there are a number of disturbances present that can not be manipulated and that are not exactly known. Compared to the planned disturbances their effect is minor and approximately constant during one test run. These disturbances are discussed in the following.

Table 6.1 contains only the concentrations of chemicals that are intentionally added to the system. In the system there are several compounds that are not exactly known as the municipal water contains odds and ends and it is even chemicalised against corrosion and bacterial growth and such. What is more, the consistency of municipal water changes with seasons of the year and weather (on warm weather, the bacterial growth is more of an issue and consequently municipal water contains more chemicals).

Another important factor is the dissolution of carbon dioxide. The inflow source tanks and the reagent tank contain covers but they are, by no means, airtight. Carbon dioxide of the surrounding air will gradually dissolve to the liquids in the system adding buffering and even precipitates in the system (carbon dioxide reacts with water and numerous cations forming carbonic acid and different carbonates of poor solubility, e.g. calcium carbonate).

The pilot equipment is located indoors, so basically there are only minor temperature changes (couple of degrees centigrade). However, on a sunny day there might be an increase in the temperature (compared to the regular conditions) that would have some influence on the chemical equilibria.

At times the process liquids consist of only hydrochloric acid and sodium hydroxide creating basically a strong acid – strong base system that is extremely sensitive to the smallest variations in the concentrations. The instrumentation (e.g. pumps) has limited accuracy and resolution in resulting notable high-frequency oscillation that is typical for sensitive neutralisation processes such as this one.

All these effects could be decreased with slight modifications in the process construction (e.g., by using distilled water instead of municipal water and by using pure nitrogen atmosphere, using cooling and heating for guaranteeing isothermic environment, etc) and for extremely accurate experiments some of these steps would be taken in order to get better repeatability on the results. In the neutralisation experiments, instead of constructing an unrealistic and expensive disturbance-free ideal process, a more natural approach was adopted.

All test-runs were carried out under normal disturbances and sufficient repeatability was achieved by performing the final comparative experiments within couple of days and by using freshly prepared chemicals in each case. In modelling, the unknown components were taken into consideration as “dummy species”. The buffering effect of municipal water and carbon dioxide has practical significance especially on the strong acid system (source tanks I and II).

6.1.3 Modelling of the flow and mixing characteristics

The assumptions made of the pilot process model are:

- All chemical reaction are instantaneous, the equilibrium assumption is valid and there are no limiting phenomena
- All events related to the pH-value take place in the aqueous phase
- The concentrations are sufficiently low in the operating region so that concentrations can be used instead of activities
- The system is at constant room temperature
- The neutralisation vessel is an ideal mixer and the flows are perfect plug flows without diffusion or dispersion.
- The unaccounted disturbances remain constant during the test runs
- The nonlinearity of the reagent pump is not modelled (the model describes the process without instrumentation)

The indices indicate the source and the property of the component:

A	Strong acid (hydrochloric acid)
B	Strong base (sodium hydroxide)
α	Weak acid (acetic acid)
β	Weak base (ammonia)
P	Process flow
C	Control flow

All flows contain also disturbance components from tab water or carbon dioxide. The pilot process is shown in Fig. 6.4 and the flow diagram of an individual component in Fig. 6.5.

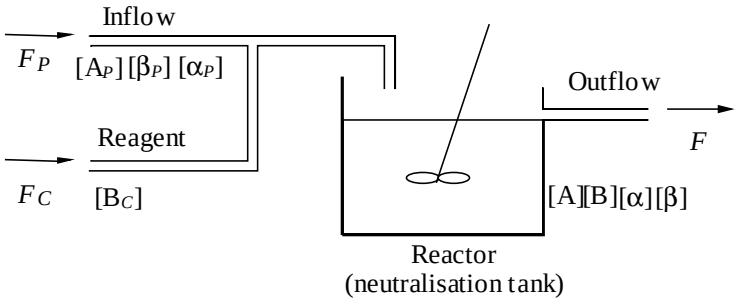

Fig. 6.4: Neutralisation pilot plant

As there is no information about the contents of the inflow, the time-delay caused by the pipe can be neglected in the model. However, there is a small time-delay in the reagent flow from the point, in which the reagent is mixed to the inflow to the neutralisation vessel. Otherwise, the flow models of all components are identical from the mixing point to the outflow. There is also a small time delay (plug flow) from the ideal mixer to the point in which the pH-value is measured.

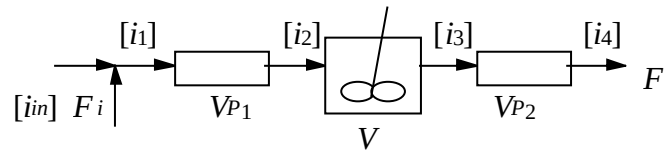

Fig. 6.5: The flow diagram of an individual component

The concentration of one individual component through the neutralisation process is described in detail. F_i is the respective flow to the mixing point (either inflow or control flow), V_{P1} is the volume of the pipe before the neutralisation vessel and V_{P2} the pipe volume after it. The quantities that change as functions of time are indicated with *t*.

The inflow and reagent flow mixing point (dilution):

$$[i_1](t) = \frac{F_i(t)}{F(t)}[i_{in}](t) \tag{6.1}$$

The plug flow from the mixing point to the neutralisation vessel:

$$[i_2](t) = [i_1]\left(t - \frac{V_{P1}}{F(t)}\right) \tag{6.2}$$

The neutralisation vessel:

$$\frac{dV[i_3](t)}{dt} = F[i_2](t) - F[i_3](t) \tag{6.3}$$

The plug flow from the vessel to the measurement:

$$[i_4](t) = [i_3]\left(t - \frac{V_{P2}}{F(t)}\right) \tag{6.4}$$

The equilibrium is valid at every point in the system and it is explicitly defined by the concentrations at that point. pH value can be calculated at any point of the process but the most interesting one is the pH-measurement point in the outflow.

6.1.4 Modelling of the chemical equilibrium

The principal chemical compounds in the system are as follows:

Sodium hydroxide (strong base, complete dissociation) $\mathrm{NaOH \rightarrow Na^+ + OH^-}$ (6.5)

Hydrochloric acid (strong acids, complete dissociation) $\mathrm{HCl + H_2O \rightarrow Cl^- + H_3O^+}$ (6.6)

Ammonia (weak base, partial dissoc. as function of the pH-value) $\mathrm{NH_3 + H_2O \Leftrightarrow NH_4^+ + OH^-}$ (6.7)

Acetic acid (weak acid, partial dissoc. as function of the pH-value) $\mathrm{HAc + H_2O \Leftrightarrow Ac^- + H_3O^+}$ (6.8)

In addition to the principal compounds there is a great number of secondary compounds originating mainly from municipal water and surrounding air. Strong acids and bases are not significant because they dissociate completely and as they do not affect the buffering, they can be combined together and included in other strong acids and bases. The weak buffering compounds

are of more interest as they change the sensitivity of the process significantly, especially in the strong acid – strong base case in which there is no other buffering elements present.

There is most definitely dissolved carbon dioxide present, but there are also many other components and instead of taking a priori knowledge into account the unknown buffering effect was modelled completely using hypothetical compounds. The reason for this is that even though some of the components are known their concentrations are not. A better result with fewer parameters can be achieved by experimental modelling with hypothetical components. In this case (by trial and error), the buffering was modelled with a two-valued weak acid (a), a two valued weak base (b) and a one-valued weak base (β).

$$\begin{aligned} &H_2a + 2H_2O \Leftrightarrow Ha^- + H_3O^+ + H_2O \Leftrightarrow a^{2-} + 2H_3O^+ \qquad K_{a1}, K_{a2} \\ &b + 2H_2O \Leftrightarrow Hb^+ + H_3O^+ + OH^- \Leftrightarrow H_2b^{2+} + 2OH^- \qquad K_{b1}, K_{b2} \\ &\beta + H_2O \Leftrightarrow H\beta^+ + OH^- \qquad K_\beta \end{aligned} \tag{6.9}$$

The buffering elements from municipal water and air are assumed to be constant in the system during one test run and therefore present at every point of the system with identical concentrations. For this reason they can be omitted from the flow model even though they are present at the chemical equilibrium model. The chemical equilibrium is determined by the charge balance (the liquid does not have any charge so the sum of all charged ions, weighted with the charges, must be zero).

$$\begin{aligned} &\left[H_3O^+\right] - \left[OH^-\right] - \left[Cl^-\right] + \left[Na^+\right] - \left[Ac^-\right] + \left[NH_4^+\right] \\ &- \left[Ha^-\right] - 2\left[a^{2-}\right] + \left[Hb^+\right] + 2\left[H_2b^{2+}\right] + \left[H\beta^+\right] = 0 \end{aligned}$$

$$\begin{aligned} &\left[H_3O^+\right] - \frac{K_W}{\left[H_3O^+\right]} - \left[Cl^-\right]_{TOT} + \left[Na^+\right]_{TOT} - \frac{K_{Ac}}{K_{Ac} + \left[H_3O^+\right]}\left[HAc\right]_{TOT} \\ \Rightarrow \quad &+ \frac{K_{NH_3}\left[H_3O^+\right]}{K_W + K_{NH_3}\left[H_3O^+\right]}\left[NH_3\right]_{TOT} - \frac{K_{a1}\left[H_3O^+\right] + 2K_{a1}K_{a2}}{\left[H_3O^+\right]^2 + K_{a1}\left[H_3O^+\right] + K_{a1}K_{a2}}\left[Ha\right]_{TOT} \\ &+ \frac{K_{b1}K_W\left[H_3O^+\right] + 2K_{b1}K_{b2}\left[H_3O^+\right]^2}{K_W^2 + K_{b1}K_W\left[H_3O^+\right] + K_{b1}K_{b2}\left[H_3O^+\right]^2}\left[b\right]_{TOT} + \frac{K_\beta\left[H_3O^+\right]}{K_W + K_\beta\left[H_3O^+\right]}\left[\beta\right]_{TOT} = 0 \end{aligned} \tag{6.10}$$

This is a ninth order equation (with respect to the oxonium ion concentration $[H_3O]^+$) that is solved iteratively at each simulation step. All the total concentrations (referred with sub-index *TOT*) are determined by the flow model. K_W is the ion product of water, K_{Ac} is the acid constant of acetic acid K_{NH3} is the base constant of ammonia, all the other acid and base constants (K_{a1} ,K_{a2} ,K_{b1}, K_{b2} and K_β) are fitted to match the experimental titration curve of the system.

A sample from the inflow source tank consisting mainly of hydrochloric acid (tank I) is titrated with sodium hydroxide (control reagent) and the result is compared to theoretical pure water titration curve. The curves are shown in Fig. 6.6.

There is a slight increase in the buffering of the system around the neutral point and some offset at high and low values (with pH-values less than two or more than twelve). The offset at high and low pH-values is very typical (effect of increased ionic strength leading to activities) and at first glance the buffering appears to be insignificant but a closer look will show some notable differences. The buffer indices and higher resolution titration curves are shown in Fig. 6.7.

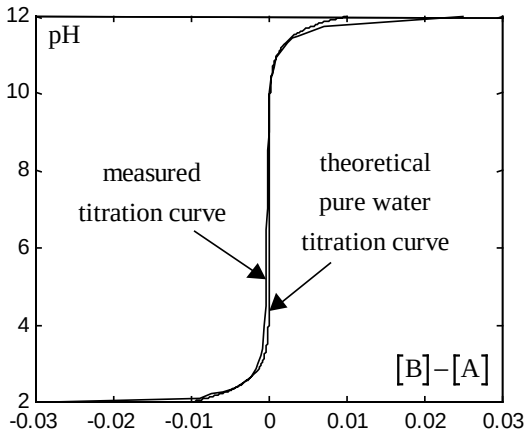

Figure 6.6: Measured and theoretical titration curve for strong acid – strong base system.

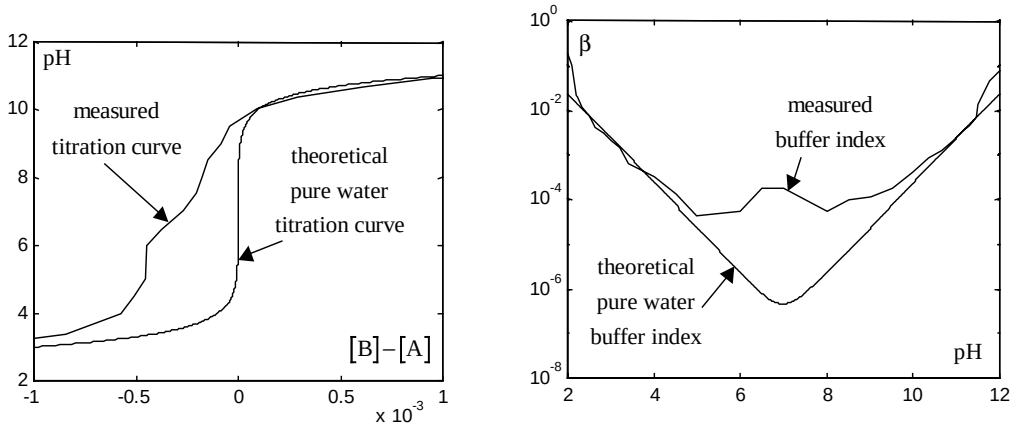

Fig. 6.7: The titration curves and the buffer indices of a theoretical system and a measured sample.

The buffer index is inversely proportional to the sensitivity of the system and therefore the theoretical system is ca. 1000 times as sensitive as the actual process (that itself appears to be sensitive as well). The tuning parameters of a controller depend on the sensitivity of the process and therefore a theoretical system is not suitable for controlled system simulations without adding some kind of a model for the buffering. Fig. 6.8 shows two simulations with the same PID controller tuning for water, strong acid and strong base system (one without and one with municipal water buffering). The reference value of the controller was changed at time instant one from seven to six.

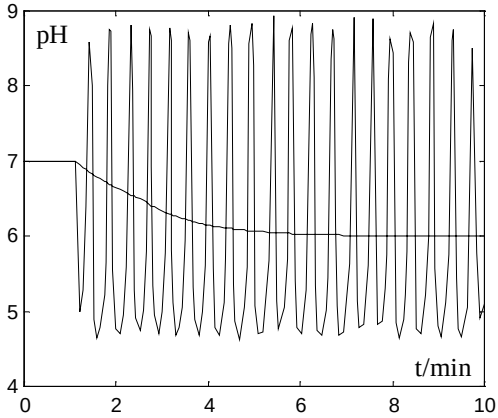

Fig. 6.8: PID-control performance for unbuffered (oscillatory response) and buffered (non oscillatory response) water process with the same controller tuning.

The step response changes drastically when the buffering of the municipal water is included in the model. Without any buffering the system is extremely sensitive and oscillatory but with just a hint of buffering the response appears to be over damped and unnecessary slow.

The buffering of the system can be fitted experimentally using either titration curves or buffering indices. In principle, every equilibrium constant *K* creates a protuberance at the p*K*-value position on the pH-scale. The total concentration of the buffering compound defines the magnitude of the protuberance. The fitting can be automated (numerical optimising, least squares) or it can also be done by hand. Fig. 6.9 shows the hand-fitted buffering effect on a titration curve and a buffering index.

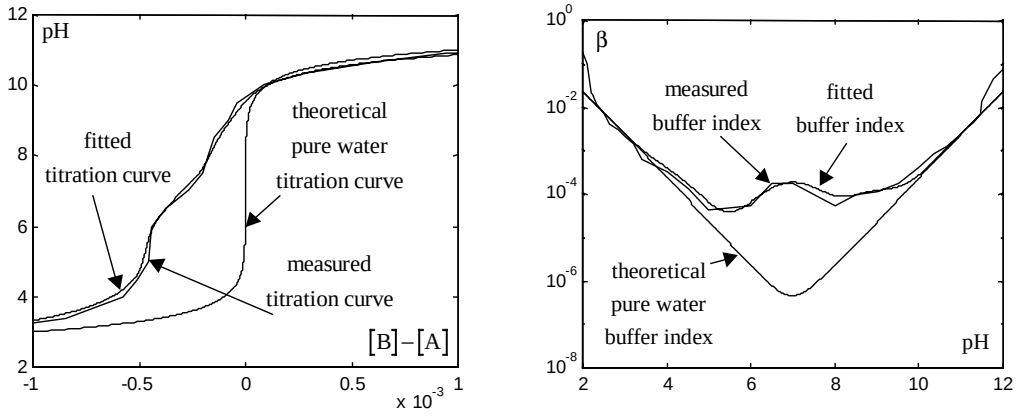

Fig. 6.9: The experimentally fitted buffering (titration curves and buffering indices are compared).

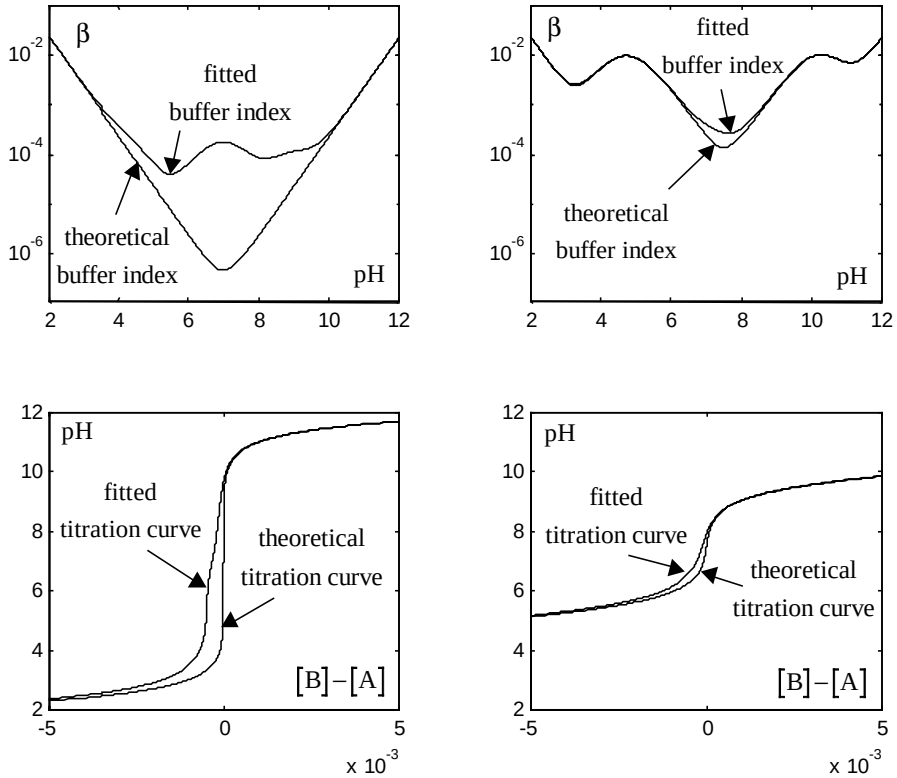

Fig. 6.10: Buffer indices (top row) and titration curves (lower row) of a strong acid – strong base system (left column) and a weak acid – weak base system (right column).

Buffering (and process sensitivity) obey the rule of the weakest link in a chain. If the system has no buffering compounds, then even the weakest effects have significant effect on the behaviour,

but if the system is well buffered, any small amounts of impurities have no effect on the behaviour. This can be illustrated by comparing how the buffering effect of municipal water and surrounding air affects the behaviour of liquids inside tanks (I – no buffering and III notable buffering from ammonia and acetic acid). The titration curves and buffer indices are shown in Fig. 6.10.

6.1.5 Test runs

The pilot process was used for testing the SOC-algorithm and for tuning up the adaptation features in practice. The convergence speed and reliability were tested by changing the process abruptly between strong acid - strong base (SASB) and weak acid - weak base (WAWB) systems by changing the source of process flow from either tanks I or II to III or IV. Load changes are generated in SASB neutralisation by changing the source of process flow between tanks I and II and correspondingly WAWB uses tanks III and IV.

The initial situation consists of SASB-process and a controller (PID or SOC) that is tuned well for the initial process. After a load change the process is changed to WAWB and after four load changes back to SASB. The sequence of input flow source tanks is: II - I - IV - III - IV - III - II - I - II - I. At this point the inflow flow rate was dropped to half of the original and the same sequence was repeated. Sample time for the process is one second and the measurement is filtered with an analogue filter. The PID-controlled pH-value is shown in Fig. 6.11 and the SOC-controlled pH-value in Fig. 6.12.

The objective of the controller was to be as fast as possible with the cost of increased high frequency variations as indicated earlier. The SOC operated well both in strong and weak acid systems. Even the changing flow rate that caused variations in the time delay of the system was not affecting the performance of the controlled system notably. The PID controller allows large pH deviations for weak acid systems with the optimal tuning for strong acids. If the tuning is corrected to operate well in weak acid systems, the system becomes unstable when strong acids are neutralised.

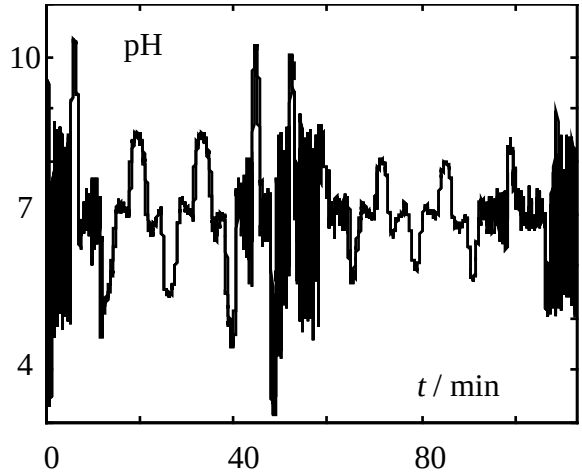

Fig. 6.11: Fixed PID-control performance for the neutralisation process

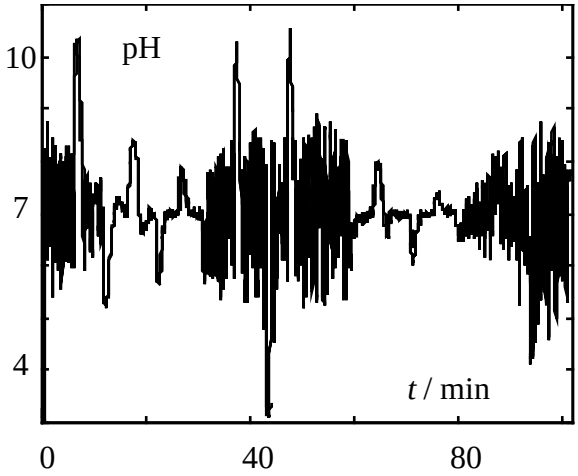

Fig. 6.12: SOC performance for the neutralisation process

6.1.6 Comments on the neutralisation application

The test run of the neutralisation plant was designed to contain both process changes and load changes. The process changes include variations in the flow and mixing characteristics (flow variations affect time constants and time delays) and variations in the buffering (sensitivity of the

process). The sensitivity changes were rather extreme as a well-buffered robust process abruptly turned into a very sensitive process of practically no buffering at all. It could be argued that these changes reflect poorly to real processes but as a test of adaptation efficiency and process stability the test run proves the point.

The self-organising fuzzy controller operated satisfactorily in the neutralisation application. The pH-process is particularly suitable for this kind of approach; nonlinear, time-variable process with few measurements and with no fixed model structure. Many of the critical points of traditional adaptive controllers are avoided, e.g. the algorithm is not sensitive to incorrect measurements and changing time delays.

SOC algorithm was tested against other advanced controllers in the same pilot process in 2001 (results are published in Ylöstalo *& al.,* [148]). In this comparison SOC gave a good control performance but not as good as the algorithm based on a model library, implementation of which was documented in [147]. The basic structure of the winning approach consists of a conventional controller and a model library. The higher hierarchy adaptation continuously compares the actual process against the model library in order to find the best match (with respect to time constant, delay and buffering) and the controller parameters attached to the particular model in the library. These parameters are then updated in the controller with smooth switching procedure.

6.2 An industrial ammonia scrubber

Gas scrubbers are two-phase processes, where one or more components in the gas phase are dissolved into the liquid phase; ammonia scrubber removes ammonia from gas. The scrubbing efficiency is a function of the wash water consistency. In general, gases that tend to have acidic water solutions are easily removed with alkalinic washing and vice versa. As a base component ammonia can be washed with acidic wash water. This application is also documented in [144].

6.2.1 Process description

Kemira, chemical company produces fertilisers in its Uusikaupunki plant in Finland. The fertiliser production process generates reactor gas containing, among other things, ammonia. Before the gas is released into atmosphere, ammonia has to be removed for environmental reasons. Ammonia is also one of the raw materials in fertiliser production and returning it back to the production is a good idea also from the economical point of view. All this leads to a closed ammonia circulation operating similarly to a kidney system.

The ammonia scrubbing system of Kemira Uusikaupunki fertiliser plant consists of several scrubber units (see Fig. 6.13) that operate in series with the counter-current principle (the raw gas enters the first and the fresh water the last scrubber unit). Depending on the fertiliser grade recipe, different acids are added to the wash water tanks. The aim is to achieve a specified combination of ammonia sulphate, ammonia nitrate and ammonia phosphate (the required acids are sulphuric, nitric and phosphoric acid respectively).

The scrubbing efficiency and the operation of the scrubber depends mainly on the pH of the scrubbing water; with too high pH all of ammonia is not recovered and with too low pH the scrubber equipment and instrumentation is vulnerable to corrosion and chemical strain.

The main disturbances in the scrubber come with raw materials (gas, water and acid feeds). There are varying amounts of numerous substances that affect the behaviour of the pH-value in different ways. The changes in the acid and base concentrations naturally create load changes but what is more crucial to pH-control is the fact that they also generate changes in the buffering of the process and therefore create a time-varying system. This point is clarified with an example. Fig.

6.14 shows the pH-trend of the same scrubber with the same constant tuning parameters of a fixed, nonlinear PID-controller in three different occasions.

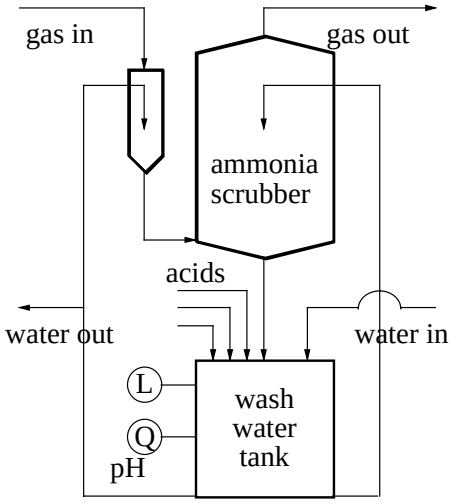

Fig. 6.13: One ammonia scrubber unit

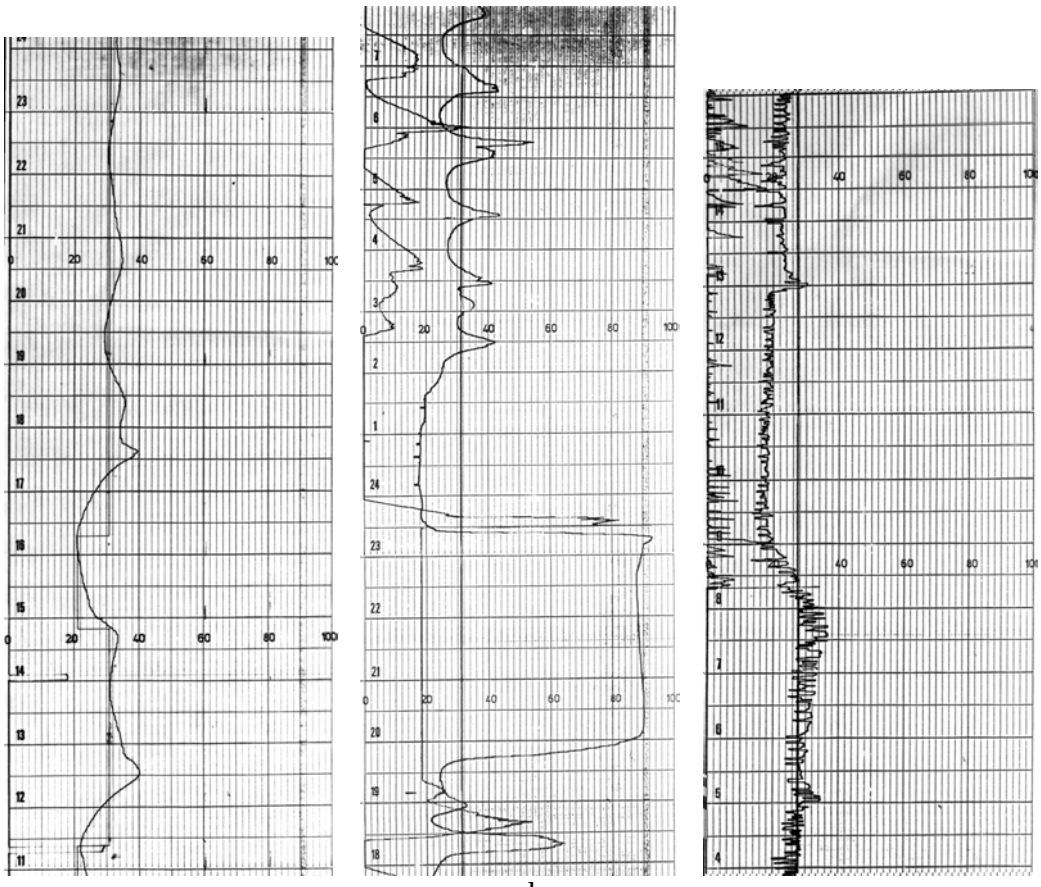

a b c

Fig 6.14: The behaviour of the controlled pH-value on three different occasions. y-axis is time in hours and x-axis contains the pH-value and its reference in percentage of the range (pH:1 – 8)) as well as the control signal (combined acid load) in percentages.

Fig. 6.14(a) describes a situation, where the controller operates satisfactorily. Fig. 6.14(b) describes a tendency to a highly nonlinear oscillation and Fig. 6.14(c) variations on a very high

frequency range. If the apparent nonlinearity is ignored at this point, it is still obvious that all three situations would require very different tuning for the controller; integral part would have to be decreased for the second case and the derivative part for the third case.

The ammonia scrubber clearly offers good grounds for an adaptive control strategy. Especially Fig. 6.14(b) indicates that a nonlinear controller strategy might prove to be beneficial. This is also verified by titration curves made from five random wash water samples (Fig. 6.15). The slope of the titration curve corresponds to process sensitivity (with respect to control signal changes). There is clearly a significant change of slope in the operation area, which indicates that an optimal controller should operate differently in different pH-regions, i.e. a nonlinear controller can perform better than a linear controller. The titration curves also show that the slopes vary with different samples, which indicates that the nonlinearity is timevariant.

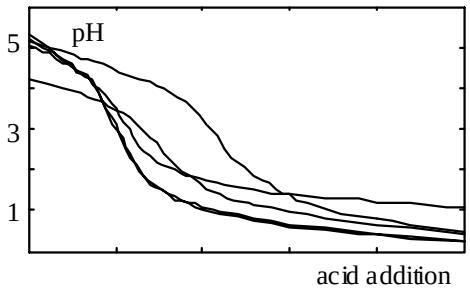

Fig. 6.15: Titration curves of five random samples

There are also several other difficulties in the ammonia scrubber process. The process operates under such a severe conditions that the instrumentation is under heavy mechanical and chemical wear; even to that extent that there has to be automatic sample collection and analysis for pH-measurement alone (long sample times). Furthermore, the control action consists of acids alone, which can create problems when there is not enough alkaline substances in the gas or there are significant unaccounted acidic substances in one of the feed flows. In these cases, there is a risk of acidic saturation that in practice means that the pH-value is much too low for long time periods and there is no control action available that can correct the situation. The acidic saturation can also be seen from Figs. 6.14(b) and 6.14(c).

There are several fertiliser grade changes during one week and this is a priori knowledge that could be used in the control strategy. The fertiliser grade defines many of the participating components and once an optimal controller for one particular grade has been learned, it would be practical to remember how the system was controlled, the next time the same grade is comes up. However, there are still many other factors that affect the behaviour of the system; factors that can not be tracked down to one grade or any other known phenomena (e.g., the chemical content of the raw water and the conditions under which it is stored).

The ammonium, nitric, sulphate, phosphate, fluoride, chloride and potassium contents are analysed in laboratory regularly from wash water samples. Unfortunately the concentrations in the process change considerably in a short time and therefore the analysis can not be used in on-line control. The analysis of the reactor gas is very time-consuming and it is done only in special cases. The temperatures, flows and levels of the wash water tanks are measured continuously. The level control is very efficient with relatively small volume changes, that do not affect pH-control.

6.2.2 Simulation model

There are no on-line analysis available from the reactor gas or the plant water and the chemical contents of both vary continuously and significantly. As these changes are the main

reasons for both pH variations and process buffering changes, there is no change of predicting the process behaviour on-line no matter how good the model is.

There is, however, a possibility of collecting samples from the process and analysing them, collecting data from all the available on-line measurements and developing a model that corresponds to that one particular test period under those specific conditions in the plant. This model could then be used for testing different controllers and comparing the results.

Rather than being satisfied with only one interesting test period in the plant, five different instances were chosen for closer study in order to get somewhat larger validity to the model. A chemical analysis and experimental titration curve were determined for each sample.

Based on the analysis, a theoretical model structure was chosen with the components that dominate the buffering of the sample. The titration curves were used for determining the parameters within the theoretical models so that theoretical and experimental titration curves coincided.

Flow dynamics of the process contained many non-ideal features such as stagnant regions, channelling, etc., that could not be analysed theoretically. In addition the circulation speed between the wash water tank and the gas scrubber was high enough compared to the time constants of the unit processes that even theoretically the circulation could not be separated from ideal mixing. Due to these facts, the flow dynamics was modelled with tracer tests.

6.2.2.1 Theoretical model structure

The neutralisation reaction is very quick compared to the time constant of the flow dynamics. As a result, the flow dynamics can be modelled separately from the chemical characteristics, which can be considered as static nonlinearities. If the flow dynamics were linear, the overall system would be a typical Wiener-process.

Chemical model is based on the charge balance (4.2)

$$\left[\mathrm{H_3O^+}\right]-\left[\mathrm{OH^-}\right]+\sum_i z_i\left[\mathrm{H_{z_i}B_i^{+z_i}}\right]-\sum_i z_i\left[\mathrm{A_i^{-z_i}}\right]+\sum_i\sum_n z_{ni}\left[\mathrm{H_{z_{ni}}b_i^{+z_{ni}}}\right]-\sum_i\sum_n z_{ni}\left[\mathrm{a_i^{-z_{ni}}}\right]=0 \qquad (6.11)$$

For acids that have several dissociation steps, all charged ions have to be taken into account. Weighted sum of all charged ion concentrations for an acid with N dissociation steps is as follows

$$\sum_n z_{ni}\left[\mathrm{a_i^{-z_{ni}}}\right]=\left(\sum_{j=1}^{N} j\cdot\prod_{k=1}^{j}\frac{K_{aik}}{\left[\mathrm{H_3O^+}\right]}\right)\cdot\left[\mathrm{a}_{i,TOT}\right]\Bigg/\left(1+\sum_{j=1}^{N}\prod_{k=1}^{j}\frac{K_{aik}}{\left[\mathrm{H_3O^+}\right]}\right) \qquad (6.12)$$

where K_{aik} is the acid constant.

The analysis of samples showed that the theoretical model includes ammonia, fluoride, sulfates, phosphates and many other components that would behave as strong acids and bases within the interesting operating region. When the charge balance is applied to the ammonia scrubber, an equation for the oxonium ion concentration becomes

$$\left[\mathrm{H_3O^+}\right]-\frac{K_W}{\left[\mathrm{H_3O^+}\right]}+\left[\mathrm{K^+}\right]-\left[\mathrm{NO_3^-}\right]-\left[\mathrm{Cl^-}\right]+\frac{K_{\mathrm{b,NH_3}}\left[\mathrm{H_3O^+}\right]}{K_w+K_{\mathrm{b,NH_3}}\left[\mathrm{H_3O^+}\right]}\left[\mathrm{NH}_{3,TOT}\right]$$
$$-\frac{K_{\mathrm{a,F}}}{\left[\mathrm{H_3O^+}\right]+K_{\mathrm{a,F}}}\left[\mathrm{HF}_{TOT}\right]-\frac{K_{aS1}\left[\mathrm{H_3O^+}\right]+2K_{aS1}K_{aS2}}{\left[\mathrm{H_3O^+}\right]^2+K_{aS1}\left[\mathrm{H_3O^+}\right]+K_{aS1}K_{aS2}}\left[\mathrm{H_2SO}_{4,TOT}\right]$$

$$-\frac{K_{aP1}\left[\mathrm{H_3O^+}\right]^2+2K_{aP1}K_{aP2}\left[\mathrm{H_3O^+}\right]+3K_{aP1}K_{aP2}K_{aP3}}{\left[\mathrm{H_3O^+}\right]^3+K_{aP1}\left[\mathrm{H_3O^+}\right]^2+K_{aP1}K_{aP2}\left[\mathrm{H_3O^+}\right]+K_{aP1}K_{aP2}K_{aP3}}\left[\mathrm{H_3PO_{4,TOT}}\right]=0 \quad . \tag{6.13}$$

Equation (6.13) applies when concentrations are low. In the ammonia scrubber the concentrations are very high and activities have to be used instead. The activity was assumed to have a direct dependency on concentration

$$\{i\}=f_i\cdot[i] \tag{6.14}$$

where $\{i\}$ is activity of i and λ is the activity coefficient. With this assumption equation (6.13) can still be used, if the actual equilibrium constants are replaced with constants that have been corrected to include the activity coefficients. This method is illustrated with a simple example. Consider the dissociation of a 1-valued weak acid Ha:

$$\mathrm{Ha+H_2O\Leftrightarrow a^-+H_3O^+} \tag{6.15}$$

The equilibrium coefficient is defined as:

$$K_a^*=\frac{\left\{\mathrm{a^-}\right\}\left\{\mathrm{H_3O^+}\right\}}{\left\{\mathrm{Ha}\right\}} \tag{6.16}$$

If concentrations could be used instead of activities, the equilibrium coefficient could be expressed as:

$$K_a=\frac{\left[\mathrm{a^-}\right]\cdot\left[\mathrm{H_3O^+}\right]}{\left[\mathrm{Ha}\right]}. \tag{6.17}$$

With the assumption (6.14) the equilibrium coefficients of (6.16) and (6.17) are linearly dependent:

$$K_a^*=\frac{\left\{\mathrm{a^-}\right\}\cdot\left\{\mathrm{H_3O^+}\right\}}{\left\{\mathrm{Ha}\right\}}=\frac{f_{\mathrm{a^-}}\cdot f_{\mathrm{H_3O^+}}}{f_{\mathrm{Ha}}}\cdot\frac{\left[\mathrm{a^-}\right]\cdot\left[\mathrm{H_3O^+}\right]}{\left[\mathrm{Ha}\right]}=\frac{f_{\mathrm{a^-}}\cdot f_{\mathrm{H_3O^+}}}{f_{\mathrm{Ha}}}\cdot K_a\,. \tag{6.18}$$

The pH-value is determined by definition from the oxonium ion activity

$$\mathrm{pH}=-\log_{10}\left\{\mathrm{H_3O^+}\right\} \tag{6.19}$$

Thus, for equilibrium modelling (6.13) (6.14) and (6.19) define the pH value as long as theoretical acid and base constants are modified to include activity coefficients.

6.2.2.2 Experimental modelling

The fitting of the flow and mixing characteristics

The radioactive tracers (measured impulse response is shown in Fig. 6.16) proved that the complicated flow phenomena can be approximated with a simple model structure consisting of ideal

mixers and plug flows (Fig. 6.17). The flow pattern was checked with different flow rates and volumes to validate the model over the whole operating area.

The total volume V_{TOT} is defined by the flow out of the system, F_{out}, and the flows to the system, reagent acid $F_{1,in}$ and wash water $F_{2,in}$ (the volume flow of particles from the gas is assumed negligible).

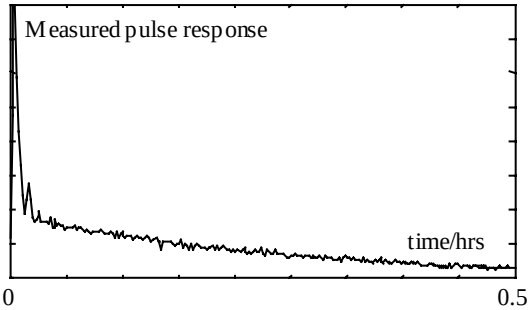

Fig. 6.16: The radioactive tracer test

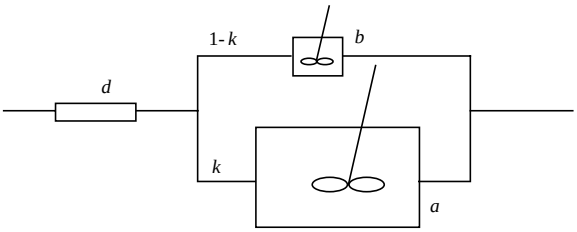

Fig. 6.17: The approximated flow model

$$\frac{dV_{TOT}(t)}{dt} = F_{1,in}(t) + F_{2,in}(t) - F_{out}(t)\,. \tag{6.20}$$

The total volume is divided into two partial volumes, V_1 and V_2, by a ratio factor K_V:

$$V_1(t) = \frac{K_V}{K_V+1}V_{TOT}(t), \quad V_2(t) = \frac{1}{K_V+1}V_{TOT}(t), \quad V_1(t)+V_2(t) = V_{TOT}(t)\,. \tag{6.21}$$

Consider a general ion *i* that can correspond to any of the compounds present. The total molar amount of that ion entering the system in a time unit is defined as $\dot{n}_{i,TOT}$:

$$\dot{n}_{i,TOT}(t) = \dot{n}_{i,gas}(t - T_{Dgas}) + F_{1,in}(t)[i]_{1,in}(t - T_{D1}) + F_{2,in}(t)[i]_{2,in}(t - T_{D2}) \tag{6.22}$$

where $\dot{n}_{i,gas}$ is the molar amount of *i* from the gas and $[i]_{1,in}$ and $[i]_{2,in}$ refer to concentrations of *i* in the arriving reagent and water flows respectively. Time delays T_{Dn} correspond to plug flow delays in each arriving stream *n*. The flow dynamics is then described as

$$\begin{cases} \dfrac{d[i]_1(t)V_1(t)}{dt} = k\cdot\dot{n}_{i,TOT}(t) - k\cdot F_{out}(t)\cdot[i]_1(t) \\ \dfrac{d[i]_2(t)V_2(t)}{dt} = (1-k)\cdot\dot{n}_{i,TOT}(t) - (1-k)\cdot F_{out}(t)\cdot[i]_2(t)\,, \\ [i]_{out}(t) = k\cdot[i]_1(t) + (1-k)\cdot[i]_2(t) \end{cases} \tag{6.23}$$

where *k* is the bypass constant, $[i]_1$ and $[i]_2$ are intermediate concentrations and $[i]_{out}$ is the outflow concentration of ion *i*. The free parameters of the flow model (K_V, *k*, T_{Dn}) were identified using the nonlinear least-squares method as shown in Fig 6.18.

The optimisation and simulation were performed in MATLAB/SIMULINK environment (Matlab, windows version 5.1). Nelder-Mead –algorithm was used for numerical optimisation

(**fmins**-command) and Runge-Kutta 45 for integration (simulation). The trajectory fitting is shown for one pulse response sample in Fig. 6.19.

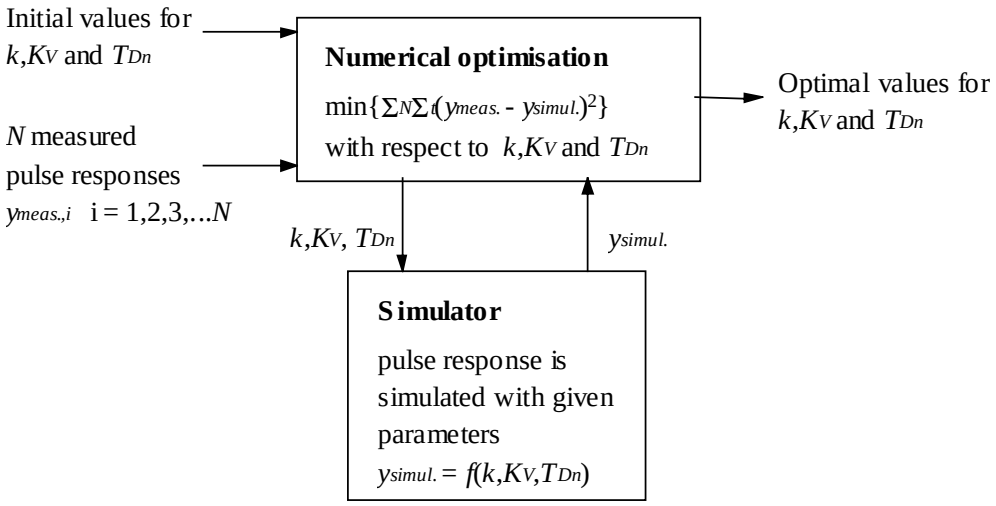

Fig. 6.18: The parameter estimation of the flow model

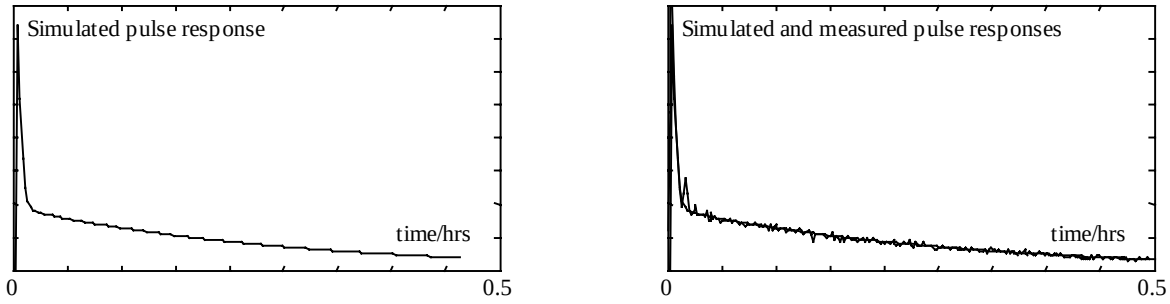

Fig. 6.19: Trajectory fitting for one pulse response sample

One benefit of this kind of parametrisation is that the parameters can be easily found for nonlinear systems when the input data is poor, e.g., only one pulse. The static gain is also automatically set to one, which fact is physically sensible for a flow model.

The fitting of the chemical equilibrium

Because all reactions were considered to be instantaneous and the equilibrium assumption valid, the flow dynamics and the chemical equilibrium could be modelled separately. The basis for the equilibrium matching were component analysis and titration curves of the wash water samples.

The basic structure of the chemical model was derived theoretically in the previous section 6.2.2.1. The important buffering components contain sulphuric, phosphoric and fluorhydric acids as well as ammonia. Strong acids and bases , such as nitric and hydrochloric acid and potassium hydroxide do not need individual treatment as they dissociate completely and can be combined into one variable (weighted sum of the total concentrations of strong acids and bases).

There are also many unknown components that have an effect on the chemical properties of the scrubber and they can not be included in the model as known compounds. Their effect, however, is taken into account as the chemical characteristics of the model are matched to those of analysed samples. The various ion concentrations are relatively high and the pH value is usually very low (above one) in the scrubber. The increased ionic strength makes it necessary to use activities instead of concentrations in the equilibrium equations and in the pH determination. It was shown in section

6.2.2.1 that the activity coefficients can be included in the equilibrium constants so that the model can still be constructed for concentrations.

The temperature is notably higher than the room temperature and so the equilibrium constants have to be corrected in any case from the room temperature values found in the literature to coincide the higher process temperature. The temperature correction can be performed by, e.g., Gibbs's function minimisation.

The complexity of the system and the above mentioned difficulties (unknown components, the effect of activities and the temperature correction) make it unrealistic to model the chemical parameters of the system from purely theoretical point of view. Temperature corrected equilibrium constants were used as initial values for the parameters, but they were fitted with numerical optimisation, very similarly to the pulse response fitting (Fig. 6.20).

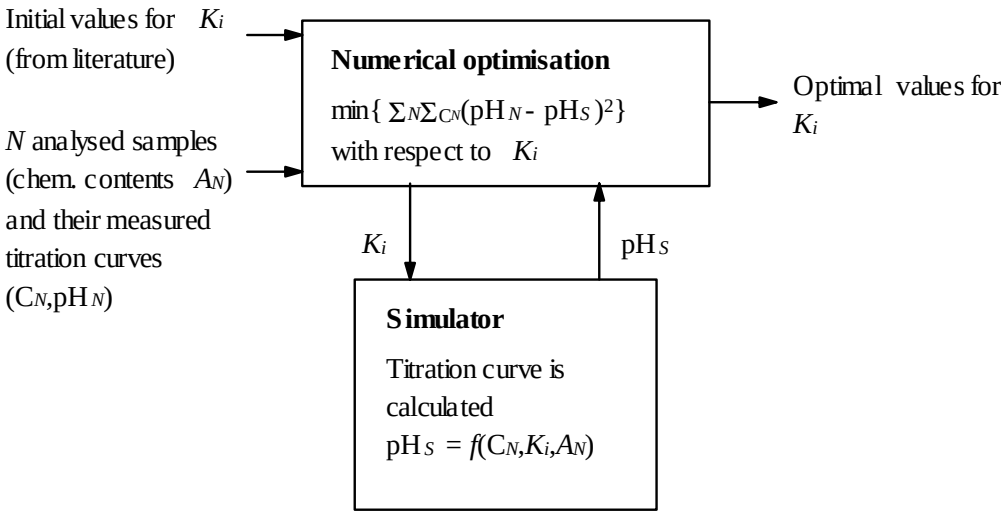

Fig. 6.20: The titration curve fitting (*C* is the reagent concentration, *N* refers to samples and *S* to simulations, *i* is a running index)

Fig. 6.21 show the titration curves of two different samples. The measured titration curve is indicated by *m*, and the theoretical curve is marked with *t* when the theoretical parameters were used without fitting, and with *a* when the fitting was performed.

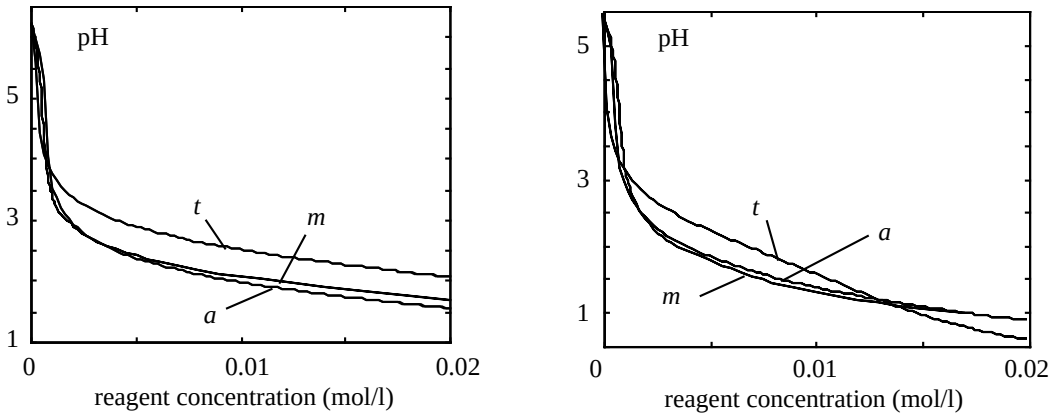

Fig. 6.21: Titration curves of two different samples (*m* refers to measured, *t* to non-fitted theoretical and *a* to experimentally fitted curve)

It is to be noted that the fitted chemical parameters were general constants that adequately suited all given samples with the same numerical values. The fact that the experimental titrations were

performed in the process temperature is also essential, because otherwise the fitted chemical characteristics would not correspond to the conditions in the process. The actual temperature variations in the process are relatively small, so the chemical parameters can well be assumed to be constant in the operation range.

There are some limitations in the chemical model and they have to be considered when the model is used. All samples were explained satisfactorily, but the main factor for this was that the same samples were analysed and there was reliable information on the actual concentrations. In the real process, the concentrations change constantly and rapidly and there is no possibility for on-line analysis. Furthermore, the titration curves are fitted so that the model and the sample react similarly to acid additions in each case, but there is no real information concerning the unknown components.

However, the model includes the most important disturbance (ammonia content variation) and the control reagents (acids) and it describes accurately the pH responses to acid feed changes in different distinct cases (samples). It is therefore ideal for controller performance evaluation, which is actually the main purpose of this model.

The model describing the physical and chemical phenomena in the scrubber is achieved by combining the flow model and the chemical model.

6.2.2.2 The realisation of the simulator

A flexible simulator was constructed in MATLAB/SIMULINK environment (Appendix1, Figs. A1.10 and A1.11). The simulator and simulation results are also documented in [146]. All flows, volumes and concentrations were treated as possible variables in order to make the simulator as versatile as possible. Fig. A1.10 shows the highest hierarchy of the model with the connections to measurement, controller and actuators. Fig. A1.11 gives a more detailed description of the process. Block *C* (Fig. A1.11) contains the flow dynamics and the block marked with *pH* (Fig. A1.11) the nonlinear chemical dependency.

pH is determined from equations (6.13), (6.14) and (6.19). The flow dynamics resolves the total ion concentrations in equation (6.13) and the only unknown parameter is the oxonium ion concentration that determines the pH-value.

The high order equation has several roots but as proven by Richter & al. [106], only one positive real solution. This solution is found iteratively at each simulation step with *regula falsi* - method (also known as the secant method).

The simulation model was validated with step responses that proved the model to be accurate enough for testing different controllers. The simulator was used for repeating a particularly difficult eight-hour-period at the plant. All measurable variables (e.g. valves, flows, volumes etc.) were recorded. The ammonia content of the gas could not be measured during the run and therefore an estimator was built to calculate its estimate with the help of other measurable variables. This estimate was then used in the simulator as the main disturbance.

PID-controller with and without nonlinear conversion (modified counter titration curve) were studied in simulations as well as a self-organising fuzzy logic. For pH-control Foxboro Exact (a commercial adaptive controller) has been successful and it was also tested with the simulator.

Foxboro Exact operates in real time and therefore simulations had to be made in real time as well. Input/output routines were constructed to the simulator PC and corresponding *C-language/S-file* blocks to SIMULINK environment. The simulator operated in simulated time and in real time by user option. A controller (another PC or unit controller) communicated with the simulator via voltage signals and D/A - A/D cards.

6.2.2.4 Simulation tests for controllers

The adaptive controllers were all PID-type and most of them required initial values. A poorly tuned PID-controller (simulated control performance shown in Fig. 6.22) was chosen as initial tuning for all of them.

A reference to all other algorithms was a well tuned PID-controller (simulated behaviour in Fig. 6.23). It is however to be noted that a fixed PID can not operate, if the buffering effect changes drastically. The inverse titration curve improved the performance only if pH changed over a wide area and if the buffering effect was known a priori well enough. Foxboro Exact improved the original tuning (Fig. 6.24). However, the algorithm was continuous and for discrete measurements with this high sampling interval, some problems occurred. The self-organising fuzzy controller (SOC) gave the best performance (Fig. 6.25).

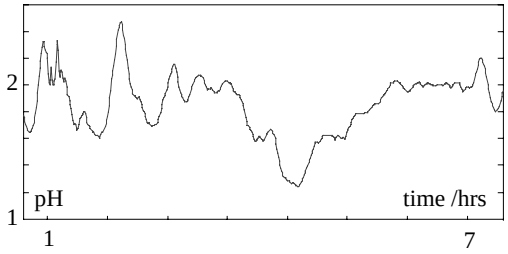

Fig. 6.22. A poorly tuned PID (initial values)

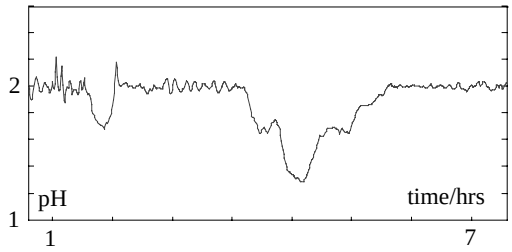

Fig. 6.23. A well tuned PID

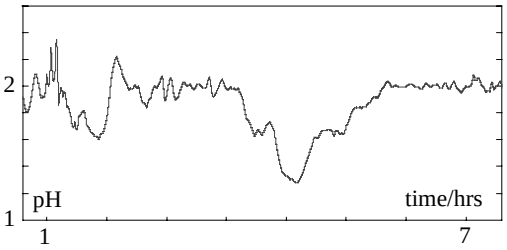

Fig. 6.24. Foxboro Exact

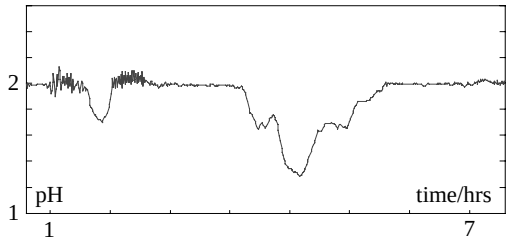

Fig. 6.25. Self-organising fuzzy controller

6.2.3 Particular SOC-modifications for the ammonia scrubber

The previous section 6.2.1 described the specific problems of the ammonia scrubber application. In this chapter these problems are discussed further and particularly how they contribute to the controller selection.

The objective of the pH control of the ammonia scrubber is very different from the neutralisation process application (section 6.1), where the average pH has to be kept at seven at the cost of increased high frequency oscillations (that could be filtered with a levelling vessel). In ammonia recovery the scrubbing efficiency is directly related to the correct pH-value and the variance of pH changes has to be kept low. The objective is to get more careful and smooth control.

As indicated earlier, the controller should be both nonlinear and adaptive. It would also be good to have an option to use a priori knowledge concerning the different grades and grade changes. There are several benefits from the PID-type controller structure, such as the ease of implementing practical PID-modifications, e.g., antiwindup and the compensation of the one-sided control action (integral reduction and derivative dead zones). There is also a lot of experience on PID-controlled ammonia scrubber and reasonable initial tuning parameters can be derived from existing control strategies.

The adaptation should ideally be local as the buffering components cause local changes in the titration curve and subsequently local changes in the nonlinearity (every component in the process creates its personal fingerprints in the pH-behaviour in its specific equilibrium area defined by the

equilibrium constant). The buffering changes are also relatively rapid and the adaptation mechanism should be effective enough to follow the time-varying phenomena.

All this points to the use of an adaptive fuzzy controller that can easily be constructed in a way that it combines all the requirements discussed above. The simulation results of the previous section 6.2.2.4 were favourable to SOC-algorithm and consequently SOC-algorithm was installed to the pH-control of the ammonia scrubber. The basic modifications of the SOC-algorithm were presented in Chapter 5 and they will not be repeated here. However, there are particular modifications for the ammonia scrubber application mainly due to process specific problems or safety and reliability issues and they are illustrated in the following.

6.2.3.1 Implementation of the SOC-algorithm

pH-value was earlier controlled by a fixed PID-controller of the distributed control system (DCS) named ALTIM. C-algorithm was installed to a separate controller-PC that communicated with the automation system that realised the control actions and provided measurements. Practical aspects of the implementation are discussed in [142]. The plant operator only needs to work with the DCS system. Therefore the controller-PC is located in a separate building. In case the SOC-algorithm needs attention, the automation maintenance staff can deal with the problem.

The DCS system (ALTIM)

The SOC-algorithm was programmed with C-language to operate in 386PC on DOS. The controller-PC communicates with the plant DCS system (ALTIM) via analogue currents (4 - 20 mA) and binary signals.

On DCS system, the operator can choose from three options for the pH-control: manual, automatic or computer. Automatic mode corresponds to a fixed PID-controller of ALTIM-system and computer mode to the SOC-algorithm in the controller-PC (and manual mode to manual control actions done by the plant operators). If the communication between the DCS system and the controller-PC encounters any difficulties the controlling task is automatically returned to ALTIM (the computer mode is changed to automatic mode.

In case the controller PC encounters a power failure, the SOC-algorithm is interrupted and after the power has returned the PC starts the controller program by itself. Because of the communication lapse ALTIM has taken over the pH-control and the operator has to change the controlling option to computer mode manually. The plant operators only task with respect to the SOC-controller is to monitor the controller-mode (manual/automatic/computer) and change it if necessary.

The communication procedure

Three analogue signals (measured output, previous control action and reference signal) are passed from the DCS system to the controller-PC and one signal (the present calculated control action) is returned back. There are variations on the measurement cycle period and a binary signal indicates when a new measurement has been received. Same binary signal lets the DCS know that the controller-PC has read the analogue signal.

Another binary signal tells ALTIM that SOC-algorithm has calculated the new control action and correspondingly it also tells controller-PC when ALTIM has read (and used) the calculated control action.

This simple communication procedure is supervised by both ALTIM and controller-PC. If new control actions are not calculated ALTIM bypasses the controller-PC and uses a fixed PID-controller instead. If ALTIM does not send new measurements or the calculated control actions are not used, the controller-PC still calculates new control values but the adaptation mechanism is disabled so that the last updated rule base is used as a fixed fuzzy controller.

The controller-PC is designed to operate continuously. After power failures the SOC-algorithm is started automatically with the initial rule base. Any other rule base (e.g. the last saved rule base) can be loaded by operator command from an ASCII- file even while the SOC-algorithm is running.

6.2.3.2 Disabling the adaptation

There are numerous situations where the adaptation should be disabled by the operator or the controller-PC. The operator may want to disable the adaptation whenever learning of the present situation is not favourable, e.g. starting or shutdown of the process, broken actuators or measuring probes, etc...

The controller-PC automatically disables the adaptation temporarily when there are communication problems with the automation system (ALTIM is not sending measurements or nor using the calculated control actions), when there are reference changes (system performance deteriorates suddenly without specific control signal changes) and when the control action is outside of the operating range (the control action could not be realised to the fullest).

6.2.3.3 The operator/SOC -interface

The SOC-controller was made as flexible as possible for research and tuning purposes. At the same time the interface was designed to be easy to use for everyday operators because the controller was installed for permanent use. The PC-monitor shows graphically which rules have been activated, and which rules are corrected according to adaptation. The last measurement, adaptation correction and the calculated control action are shown numerically at one ascii line. One line is reserved for operator input (commands that are typed). The upper section of the monitor shows a number of parameters and intermediate variables by user selection. Some of the pre-specified selections include:

- tuning mode	tuning parameters and variables
- control mode	low hierarchy control action calculation
- adaptation mode	high hierarchy adaptation procedure
- communication mode	communication (with ALTIM) procedure

On normal operation the SOC-algorithm does not save anything on a file automatically, instead the user can save any data on an ASCII-file by option. Similarly parameter files or rule bases can be saved or loaded at any time. The saving and loading of rule bases can also be automated by e.g. grade changes. Once a good controller for one grade has been learned it can be loaded automatically when the automation system indicates that the same grade is produced again.

6.2.3.4 Modifications to compensate the one-sided control action

The one-sided control action (pH is controlled only by acids) causes particular difficulties for control. The pH-value is often too low while the acid flow is already at zero. When this happens there is no additional control action that can be realised for increasing the pH-value and the only thing that can be done is to wait until the ammonia in the gas and in the inflows makes pH higher. There are also several ammonia scrubbers in series and when the acidity in a scrubber series becomes high the pH tends to be too low for long time periods.

As the control signal hits often the lower operation limit (acid flows at zero) an integral anti-wind-up is needed. In the rule-table (PD+I) the integral term is separate and thus the integral wind-up can be easily prevented by traditional methods.

In order to prevent excessive acidity (low pH values) and to make the pH increase easier two practical modifications were implemented. These modifications are called *integral reduction* and *one-sided derivative action*.

The idea of integral reduction is shown in Fig. 6.26. If the pH-value is close to reference value and at the same time it goes down rapidly with relatively high control values the integral in reduced recursively.

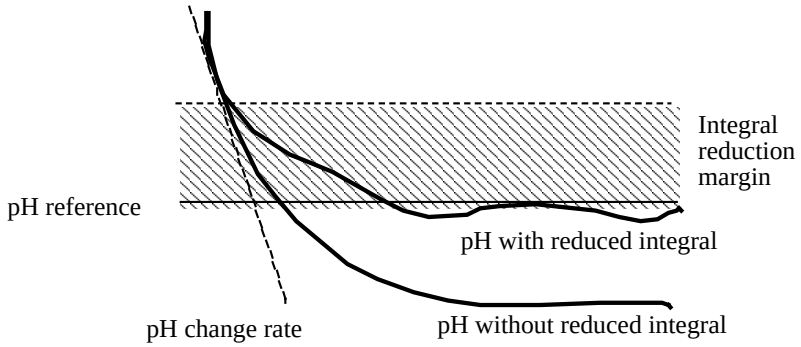

Fig. 6.26: The effect of integral reduction

The derivative-action in PID-type controllers reacts to increasing pH-values by suggesting increases in acid flows. By preventing the increase of control action until the pH is too low but sufficiently close to the reference value, the rise of pH is eased as shown in Fig. 6.27.

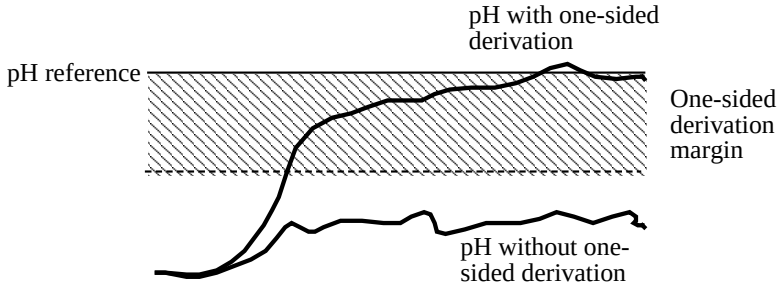

Fig. 6.27: The effect of one-sided derivation

6.2.4 Results

After the simulation study, the self-organising fuzzy controller was validated successfully with laboratory-scale pilot tests, and then implemented on the industrial ammonia scrubber for a test trial. Before the trial, the scrubber was controlled with a fixed PID-controller with a modified pH-signal that was filtered with a general inverse titration curve. In order to use the existing PID-controller as the source for initial values, the SOC-controller also uses the same filtered signal.

During this test trial two different fertiliser grades were selected for a closer inspection. Two step changes were inserted in the pH-reference signal, and the responses were collected, with both controllers and both grades (shown in Figs. 6.28 – 6.31). The SOC-controller proved to perform well for all grades.

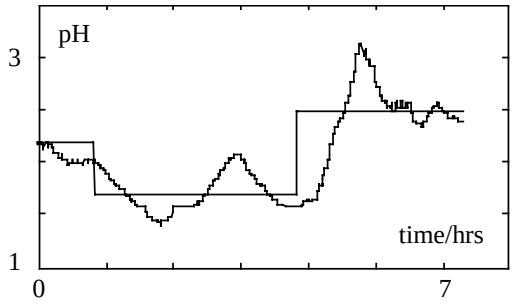

Fig. 6.28: PID performance for grade A

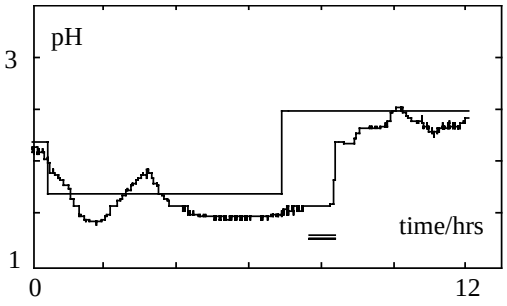

Fig. 6.29: SOC performance for grade A

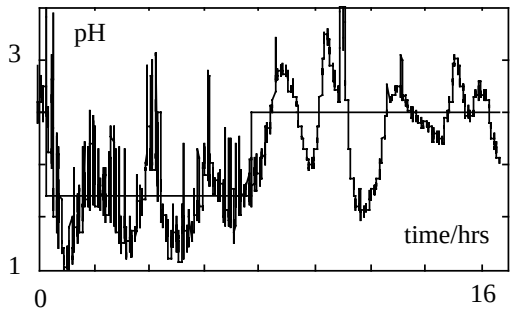

Fig. 6.30: PID performance for grade B

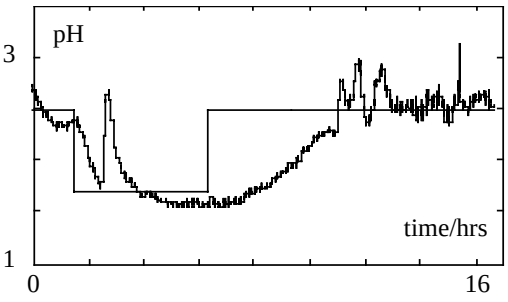

Fig. 6.31: SOC performance for grade B

Grade A is considered by the operators as an easy grade to control. Grade B is very sensitive to disturbances, and the variations in pH are large. During the test run shown in Fig. 6.29, the process waters contained lots of acids while the gas contained very little ammonia. The pH cannot be raised with one-sided control action (as indicated earlier). During the same test period, the pH probe was out of order for approximately an hour (the double line in the figure) while the adaptation algorithm was receiving incorrect information. The general behaviour of the controlled system is still not much affected, because of the local adaptation mechanism. Grade A is controlled without difficulties by either of the controllers, but the grade B pH-value is significantly smoother with SOC-adaptation.

6.2.5 Comments on the ammonia scrubber

The self-organising fuzzy controller operated well, both in simulation and in industrial application. The application was particularly suitable for this approach; a nonlinear, time-variable process with few measurements. The algorithm offers several benefits over traditional adaptive controllers: no model structure is required, the time delays do not have to be known exactly, it is easy to insert expert knowledge, the existing controller can be used for initial values, nonlinearities can be learned (local convergence), and the PID structure (easy-to-implement practical modifications, e.g. anti windup). After the permanent installation of the SOC-algorithm the ammonia emission values have diminished at the fertiliser plant and the steady-state variance is significantly lower.

6.3 pH value and dynamic chemical state in paper and pulp processes

The chemical state of pulp has recently become a key factor in explaining variations in paper quality and problems in paper machine operability, even though the entire concept of “chemical state” is rather vague and as such can not be measured. However, there are several on-line and off-

line measurements available that are closely connected to paper chemistry and consequently to the chemical state of the paper. These issues are discussed in e.g., [141].

Off-line measurements are very important but they can only describe the equilibrium conditions of the samples i.e. the state the system would reach if there was adequate time for the chemical reactions to reach their equilibrium. In pulp there are numerous slow phenomena that limit the equilibrium, e.g. precipitation, dissolution, evaporation, mass transfer between the fibres and the liquid phase, etc. Furthermore, the conditions (temperatures, pressures) between the actual plant and the sample are not identical and there might be erroneous sample taking, preparation or storing of the sample, for instance, the sample may react with surrounding carbon dioxide.

On-line measurements, unlike off-line measurements, can capture an instantaneous situation on the actual plant under the real process conditions. Unfortunately, many of the essential measurements can not be performed on-line due to number of reasons such as cost, too severe conditions, difficult maintenance, etc. Some of the traditional chemical on-line measurements in paper and pulp processes are κ-number, conductivity, redox-potential and the pH-value. Sometimes there are also more advanced (and expensive) on-line measurements; different selective analysators but they are more scarce.

A good example of chemical state tracking based on on-line measurements was performed at UPM-Kymmene Kaipola paper machine 7. There were operational problems that were assumed to be result of chemical state variations caused by changes in raw materials; recycled paper in particular. An abnormal process situation is first indicated by a pH shock in the pulp (an alkalinity pulse). According to the operators whenever the pH shock presented itself there was an 80% probability of a break in the paper machine after the regular transport delay. Abnormal situations and paper breaks were more common when the recycled paper feed consisted of paper of high calcium carbonate content.

In order to test different hypothesis and pinpoint the actual cause of paper breaks a disturbance test was performed. In the test a natural chemical state disturbance was deliberately created by feeding office paper of high calcium content for half an hour to the deinking process while all the major chemical flows were kept at constant values manually. There were several pH-measurements in different process stages and a commercial X-ray fluorescence on-line equipment (Courier by Outokumpu Mintec) for the elemental calcium measurement. Pulp samples were also taken at different stages from both the normal and abnormal situation for off-line analysis (one sample before, one during and one after the pulse). The on-line measurements are shown in Fig. 6.32.

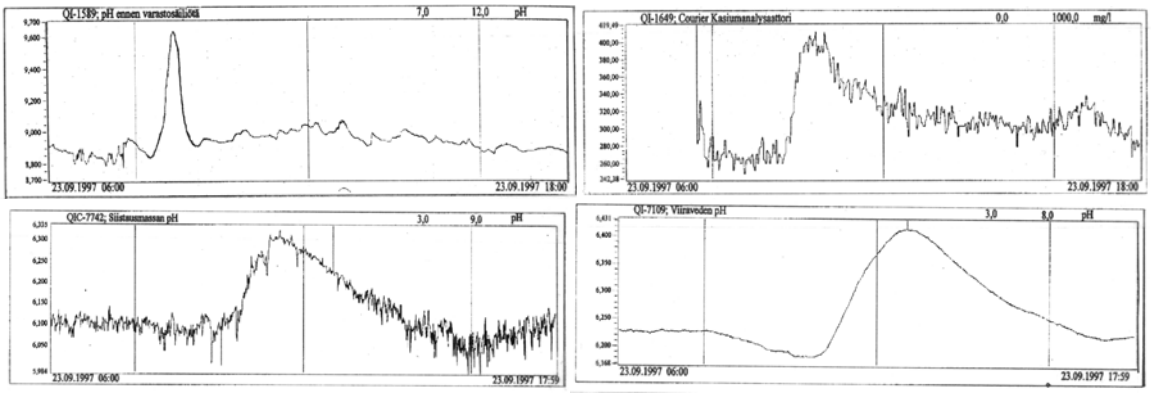

Fig. 6.32: . Four responses to a single raw material pulse (top left – pH at an early process stage / range 8.7-9.7, top right – elemental calcium content by Courier / range 240-420 ppm, bottom left – pH at a late process stage / range 5.95-6.35, bottom right – tail water pH / range 6.15-6.45)

The on-line measurements show that the pH pulse is caused by the increased calcium content. The reason for paper breaks was slow calcium dissolution caused by a faulty control action based on erroneous consistency measurement. The optical consistency measurement was calibrated under normal operation (i.e., normal calcium carbonate content) but optical properties are, in fact, strongly affected by calcium carbonate. Sulfuric acid was fed to the pulp based on the consistency measurement and as a result of erroneous acid flow the calcium carbonate was still dissolving even after the head box causing paper breaks. By changing the chemical state control strategy the problems were avoided and the number of paper breaks was decreased significantly.

6.3.1 pH measurement and control in thick pulp systems

Another application of the chemical state determination is the pH-measurement and control of thick deinked pulp (c.a. 10 % thickness). This application is also presented in [53]. The problematic part of process is shown in Fig. 6.33. The pH-value of the thick pulp is lowered by using a sulphuric acid flow.

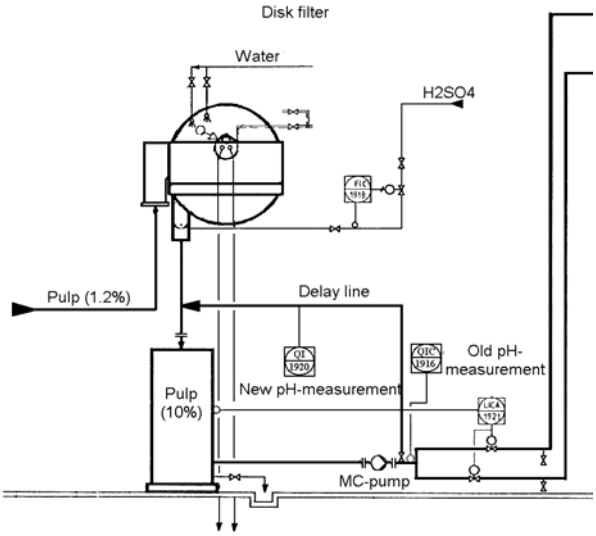

Fig 6.33: The acidification of thick pulp

The pH-measurement is situated next to a MC-pump after which the pulp is pumped into two tanks. The pH sensor is too close to the pump (pressure and flow disturbances that cause variations to the measured pH) and too close to the sulphuric acid addition (slow pH-phenomena that cause systematically too low measured pH-values). pH-measurement from two-day period is shown in Fig. 6.34. A batch experiment, in which sulphuric acid is added batchwise to an ideally mixed, isothermal, hermetical vessel (Genencor Quantum Mark V Mixer) containing pulp sample, is shown in Fig. 6.35.

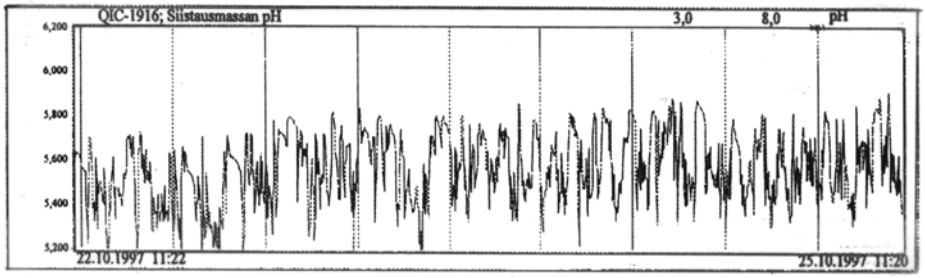

Fig. 6.34: Old pH-measurement from a two-day period

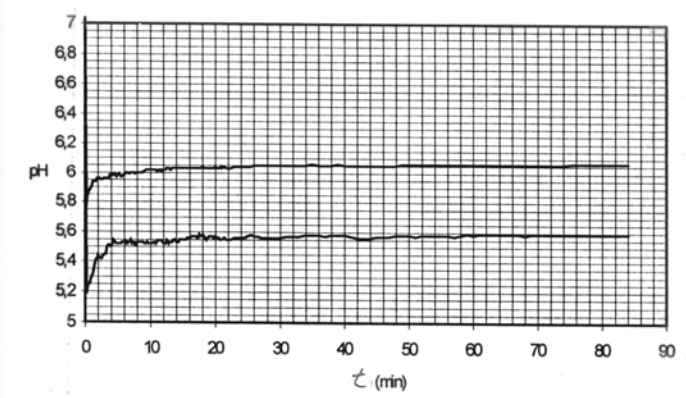

Fig. 6.35: The measured pH-value from the batch equipment

The batch experiment indicated that the delay from the acidification to the pH-measurement was too short and a delay line was constructed to improve the process noise filtering and to increase the delay. A pH-electrode was fitted to the delay line. Both the old and the new pH-measurement operated side by side for a trial period and Fig. 6.36 presents the pH-measurement from the same time period as in Fig. 6.34.

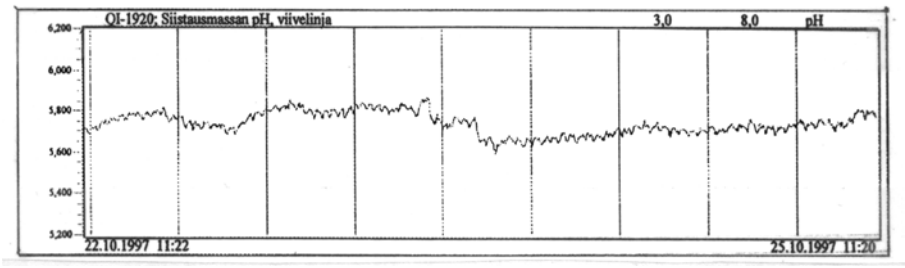

Fig. 6.36: New pH-measurement from a two-day period

When the old and the new measurement are compared the improvement with the new concept is evident; both the measurement noise and the systematic error are eliminated. The old pH-measurement was (even after filtering the signal) either too noisy or sluggish for control but with the improved measurement a feedback control could be easily realised.

Before the improved pH-measurement the pH control was performed from a later process stage (closer to head box) with more dilute pulp. Because of the slow transient kinetics, the acid addition close to the head box was not ideal. By reliable pH measurement the control could be performed satisfactorily from the thick pulp and the last controller before the head box could be removed. A conventional PI-controller was used for the pH control. The performance of the controller is shown in Figs. 6.37 and 6.38.

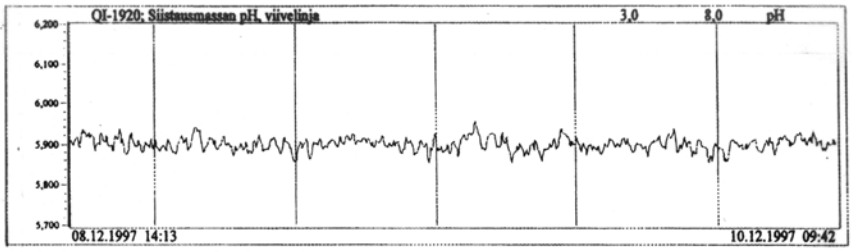

Fig. 6.37: The controlled pH-value

This application shows a pH control problem where the actual problem is the poor pH measurement. Flow and pressure variations are avoided by using a recirculation line and the required reaction time (delay) is determined by batch experiments. The required reaction time is

actually the transient of the dynamic chemical state but in this application theoretical pH modelling was not needed as an experimental transient is sufficient for the determination of suitable delay.

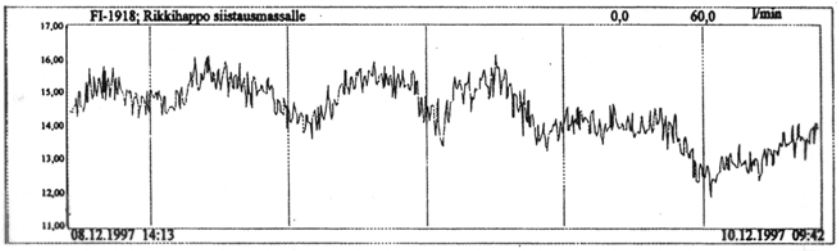

Fig. 6.38: The sulphuric acid flow

From control point of view the deliberate increase of time delay inside the control loop is not good control engineering. The time delay would be avoided by a predictive scheme where the final pH-value would be calculated based on the knowledge of the transient. However, there are problems with that approach as the shape of the transient is affected by numerous components (e.g., calcium carbonate) that are not measured in the application. Time delay can also be compensated inside the control loop by using a Smith predictor and that was actually tried on the application. Smith predictor improved the control performance but the improvement was not significant enough to justify more complicated control strategy. Despite the increased time delay a conventional PI-controller performed satisfactorily as can be seen in Figs. 6.37 and 6.38.

6.3.2 Dynamic chemical state modelling for deinked pulp

Previous applications (calcium carbonate pulse in section 6.3 and pH measurement and control in section 6.3.1) dealt with dynamical chemical state of pulp but the approaches relied heavily on experimental modelling and low level targets such as fault diagnosis, measurement and low level pH-control. Once the pH control problem is solved and pH value can be controlled to an arbitrary value, there still exists the fundamental question of what is the target of pH control and what is the optimal value for pH. In pulp and paper processes answering these questions is not easy. There are many contradicting objectives and reactions take place if there are certain components present in the pulp, components that seldom can be measured on-line. As a result the phenomena related to the chemical state of pulp in many cases remain a mystery.

The chemical and physical phenomena in the pulp can be divided into three categories: the double-sided, one-sided and negligible phenomena. Double-sided phenomena contain e.g. ionic reactions, precipitation and dissolution, etc. For instance the dissolution of calcium carbonate depends on the pH-value but on the other hand dissolution also affects the pH value so the dependency between dissolution and the pH-value is double-sided. One-sided phenomena include resin stability as well as many microbiological and polymerisation reactions. These phenomena are important for either paper quality or the operability of the paper machine and they depend strongly on the pH value but their effect on the overall chemical state or pH value is often insignificant. Negligible phenomena do not have significant effect on the overall chemical state and including them in the model would just complicate the model without notable improvement on the model.

In this section the dynamic chemical state is delimited to double-sided phenomena as one-sided significant phenomena can always be modelled separately and added to the overall chemical state when required. The model is generated for Keräyskuitu deinking plant. This application is also documented in [143].

There is extensive literature on paper chemistry and especially on the pH dependency of many key phenomena of papermaking. Excellent reference is given by e.g. Eklund and Lindström [17]. Several commercial simulation tools exist for paper and pulp processes that are capable of

managing large systems accurately. These simulators usually concentrate on total mass and energy balances as the more complex chemical, physical and biological phenomena are difficult to measure and consequently to model satisfactorily in a dynamic process.

Static measurements (e.g., analysing a sample) are easier to make and many of the important phenomena of pulp have been modelled with static dependencies. Static models are excellent tools for process optimisation, plant design, etc, but care must be taken when they are combined together in a dynamic simulator in an attempt to describe the actual dynamic situation in the plant. Most of the phenomena that affect the chemical state of the pulp are fast, some even instantaneous but with fibres and precipitates there are always slow events that limit the overall reaction speed. For instance, acid – base neutralisation can be considered instantaneous but when acid is added to alkalinic pulp in a closed vessel the pH-value drops fast and then creeps slowly close to the original value as acidity slowly dissolves precipitates and affects the liquid phase inside the fibres. Fig. 6.39 shows a measured pH and calcium (2+) -ion concentration [Ca^{2+}] responses to three consecutive acid additions.

The dynamic transients take place during several hours and traditional "analysing of a sample" describes only the final equilibrium state. As machine speeds increase and the volumes of unit processes decrease, the pulp remains shorter and shorter time periods inside one vessel and chemical equilibrium is not reached even though the process is at steady state. If the equilibrium assumption is applied to the dynamic total mass and energy balances, there will be considerable differences between the actual process and the model describing it. For instance, if acid in Fig. 6.39. is added to a continuous flow vessel that has a mean residence time of twelve minutes, the equilibrium model predicts that the pH-value measured at the vessel output will be about eight when in fact it will be close to six and inside the vessel even less. If there are irreversible side reactions that take place under acidic conditions the final pulp will not be what can be expected if static models are used for describing the acidification.

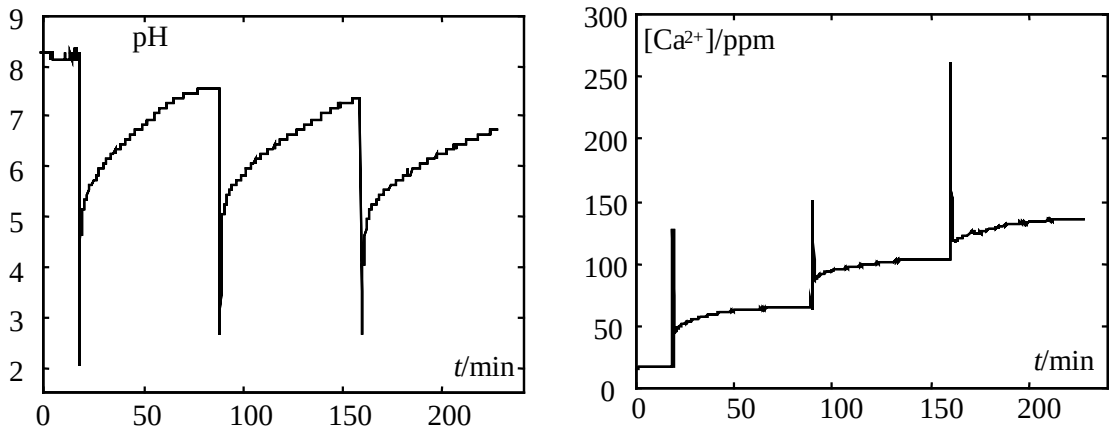

Fig. 6.39: Measured pH and [Ca^{2+}] responses to three consecutive acid additions

Another example will clarify the different modelling approaches. A simple chain reaction as shown below is assumed to take place.

$$A \Leftrightarrow B \Leftrightarrow C \tag{6.24}$$

The reactions between A and B are very fast (instantaneous) and the reactions between B and C are considerably slower. An analogy to pulp systems could be, e.g., that the first phase describes acid-base reactions and the second phase precipitation-dissolution phenomena or the mass transfer between the fibres and the surrounding liquid phase. Fig. 6.40. shows the pH-responses with three different modelling approaches.

Curve c1 gives the response when the slower second phase of the chain reaction is totally omitted, curve c3 contains all the reactions but they are considered to be very fast or instantaneous (corresponds to the equilibrium assumption) and curve c2 consists of a fast first phase and a slow second phase. The model c2, that corresponds to reality, is a combination of the models c1 and c3 that are simplifications of the actual behaviour. In static modelling the reaction rates do not have any effect on the steady state values and the models c2 and c3 that contain the same reaction structures, also have the same steady states. The dynamic behaviour of models c1 and c2 is identical initially i.e. they have similar immediate responds to changes, but their steady states are very different because the slow reactions have been omitted altogether in model c1.

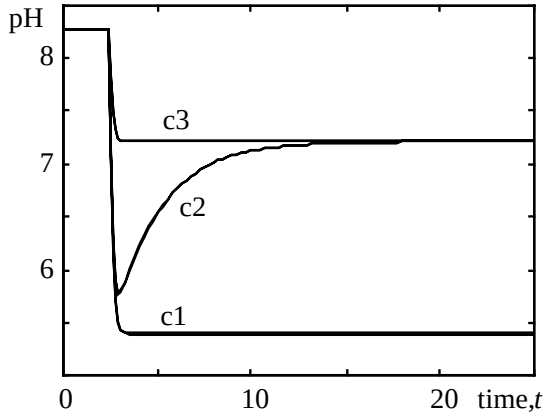

Fig. 6.40: pH responses with three different modelling approaches

6.3.2.1 Three phase pH process model (dissolution/precipitation/evaporation)

Calcium carbonate is a typical compound in many paper and pulp processes and its reaction chain is spread into three phases. Calcium carbonate can enter the process with the recycled paper (deinked pulp), water contains calcium (especially in the hard water areas), carbon dioxide dissolves from air into the pulp and reacts further into carbonates, the use of calcium carbonate as a filler increases as paper processes become more neutral and the micro-organisms in the pulp produce carbon dioxide in their metabolism. Furthermore, calcium variations and calcium compounds are often connected with product quality variations, breaks in the paper machine and other problems with paper machine operation.

The process contains three major factors that limit the overall reaction rate; two phase change phenomena: gas-liquid, liquid-solid and the reactions with fibres.

The phase change is governed by e.g. the surface area between the two phases (the porosity of the solid particles, the size distribution of the particles and the relative mixing of the two phases). The dissolution and precipitation phenomena are presented with detail in section 4.2.2.6.

6.3.2.2 The effect of fibres

Calcium ions, calcium carbonate, acids and bases interact with fibres. These interactions are governed by complex molecular micro phenomena that are difficult to model and combine with other macro models. For this reason, simple macro models are used that describe the effect of fibres adequately for chemical state modelling and simulation. These models are often experimental. The population principle is still valid as long as the new populations are included in the model.

From theoretical point of view there are several important populations that can be added to the calcium carbonate model presented in section 4.2.2.7 for fibre systems. If the sorption mechanism is well known (whether adsorption and/or absorption takes place, what is the extent of physical and chemical sorption, etc.), each component in each sorption can be added as their own population. There would be separate populations for calcium ion that is adsorpted to the surface of the fibre and calcium ion that is inside the fibre, Calcium carbonate would precipitate and dissolve inside the fibre and outside the fibre and it would also adsorpt to the surface of the fibre with physical adsorption (in accordance to the van der Waals equation) and there would be separate populations for each of the stages.

The issue of sorption is essential to paper production (retention, optical properties, swelling of fibres, etc) but it is not as essential to dynamic chemical state modelling as many of the sorption mechanisms can be considered to be a one sided phenomena. Omitting the sorption altogether is also a mistake as systems with and without fibres behave very differently when chemical state is concerned. On the other hand, including all the populations related to sorption into the model is not practical because all the transport mechanisms between the different populations have to be modelled experimentally as they depend strongly on the particular fibres and the resulted complicated model would have huge amount of free parameters.

The practical solution is to combine all the different sorption mechanisms together and model the fibre system with as few sorption populations as possible because, in any case, they will have to be modelled experimentally. The deinked pulp of Keräyskuitu plant was modelled with only one sorption population; calcium carbonate sorpted to fibres.

6.3.3 General modelling procedure

It is rather obvious that a purely theoretical modelling procedure is not sound for real applications. Even if all the chemical compounds and reactions could be determined, the resulted model would be much too complex for any practical purpose. Therefore all the phenomena have to be divided into two categories; the phenomena that are inseparably interconnected with the overall chemical state and the phenomena that depend on the chemical state but that do not affect it significantly.

E.g., the carbon dioxide content is inseparably interconnected with the overall chemical state of the pulp. If, for some reason, there is an increase in the carbon dioxide content, it quickly reacts into carbonic acid that dissociates resulting a drop in the pH-value and variations in all the reaction products that are pH-dependent (which include most of the reactions). On the other hand, the carbon dioxide bubbles in the pulp can collect hydrophobic compounds together into clusters causing spots in the paper. The formation of the spots depends on the chemical state but it does not affect any other reactions significantly.

Also many reactions that depend on the chemical state (e.g., pH) but which in turn have only a minor effect on the chemical state can be included in the latter category. These phenomena can include e.g. resin and polymer reactions. It is to be noted that these elements can have a severe influence on the paper quality and on the smooth operation of the paper machine even though they do not have similar influence on the overall inorganic chemical state.

After determining the phenomena that have significant effect on the chemical state of the system, they can be further divided on e.g., three subcategories; the white box, grey box and black box phenomena (terminology corresponds to identification and modelling theory). White box phenomena include accurate crystal clear theory, in which reactions and their parameters can be modelled with precision and no experiments are needed (e.g. inorganic unit reactions in room temperature). With grey box phenomena the structure of reactions is assumed to be known but the parameters have to be estimated experimentally (e.g. temperature corrections on some parameters, equilibrium constants of specific organic reactions, etc.). A wide variety of parameter estimation

algorithms are useful in grey box modelling. In black box phenomena there is a relation between the quantities but the structure of this relation is not known nor the parameters.

Another categorisation that could be used is to divide the significant phenomena into general and application specific. General phenomena models can be easily transferred from one application to another whereas application specific phenomena, as their name implies, have to be modelled in each application separately. If the terminology of the previous paragraph is used, then the general phenomena correspond to white box and the application specific phenomena to black box. The grey box phenomena lay somewhere between the two extremes, the model structures are general and easily transferred to other applications but the parameters are application specific. The categorization of phenomena is a vital stage at understanding the resulted models and their validity. It also makes the transfer of models from one application to another simple.

A similar modelling procedure can be performed for static and dynamic models. The static models are better known and they avoid many of the problematic areas of the dynamic models (such as the phase change kinetics). The static diagrams also serve as the fingerprints of the system. Based on the static model matching, significant phenomena can be included and insignificant phenomena excluded from the system model, static parameters can be estimated to meet steady-state specifications, etc.

Because of all this, a static model matching is usually done as the first step even in cases where a dynamic model is the final goal. As a rule, the modelling should be started from simple general phenomena. The model can then easily be expanded when that is needed. Suitable static chemical models for model matching are e.g. titration curves, distribution diagrams, phase diagrams, etc.

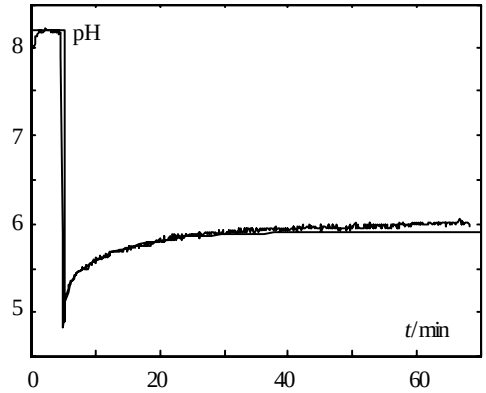

Fig. 6.41. An actual and a simulated acidification transient

The dynamic transients can usually be determined from batch experiments by matching the simulated and the actual transient and minimising, e.g. the squared error with a suitable optimisation method. An actual transient vs. simulated transient matching is shown in Fig. 6.41. A deinked pulp sample (8 % thickness) is treated with sulphuric acid in a closed vessel under fluidising mixing. The matching is done for several dynamic and static model structures and numerous different samples simultaneously in order to achieve a model that, instead of matching one specific transient accurately, matches all transients and static conditions adequately to a required extent. The resulted models are also cross-validated with independent samples.

Different samples (3%, 8% and 12% thickness) were collected from the Keräyskuitu deinking plant and the dynamic transients were modelled experimentally.

6.3.4 Comments on dynamic chemical state modelling

The dynamic chemical state of paper and pulp systems can be modelled to a certain degree. It has to kept in mind that things that can not be measured can not be modelled and many on-line measurements are required. There are many problems in modelling wet end chemical state. Inorganic and organic reaction kinetics are combined with biological and physical phenomena as well as flow and mixing characteristics. The entire process can not be modelled theoretically and pure experimental black-box models are either very case specific or inefficient. The models are also very stiff as there are instantaneous and slow reaction kinetics with different time constants for flow and mixing characteristics. The stiffness of the models can be avoided by reconstructing the system with population model structures so that the resulting model can be considered as extensions of Wiener-models or reaction invariant models.

The combination of theoretical structures with experimental modelling (grey-box modelling) makes efficient models. With only a few free parameters the models fit the validation data satisfactorily. In most cases the models predict the chemical state of pulp satisfactorily but there are instances when there are drastic unaccounted disturbances, the effects of which can not be modelled. Nevertheless, the understanding of the process with respect to different substances, their kinetic behaviour and the approximate time constants makes it possible to optimise process conditions, to modify the processes, to avoid unwanted phenomena and to improve the operability and efficiency of the process.

Chapter 7

Conclusions

Eakring (ptcpl. vb.)

Wondering what to do next when you've just stormed out of something. [1]

The pH control problem is a good example of the law of the weakest link in a chain. It is obvious that poor controller gives a poor performance but it should be equally obvious that if the measurement is poor, no controller can make up for that. Bad control performance can also be result of inadequate actuator choice; for highly nonlinear pH process the actuator has to realise both very small and large control actions accurately and many single actuators are not up to this challenge. A typical example of the "difficult measurement – easy control" case is the acidification of the thick deinked pulp.

In some cases the measurement and actuator are satisfactory and the controller is tuned well for one operating point at one time instant but the nature of the controlled pH process is forgotten. For nonlinear process the controller may perform well only in some operating ranges and for timevariant process the controller may perform well only for some periods of time. An example of a very difficult process that is both nonlinear and timevariant is the industrial ammonia scrubber.

Another instance where the nature of the pH application has to be taken into consideration is the question of what is actually good control performance. In many biological processes the pH value can deviate from the reference value for long time periods as long as the error is not too large and the are no sudden acid-base shocks. Whereas, in some sensitive neutralisation processes controllers have been deliberately tuned for high frequency oscillation because then low frequency disturbances are efficiently eliminated. If there are two vessels in series and the controller is in the first vessel, the second vessel operates as a levelling tank that will filter the high frequency oscillation. The pilot neutralisation plant is a good example of the that kind of a process.

Even when all of the low level problems of the pH control loop have been solved, sometimes there is still the fundamental question of what is the optimal pH range for the process and the reference value of the pH control loop. This is often the situation when pH value is an indirect quantity that is used for manipulating some other phenomena, e.g. precipitation. Finding an answer to this question requires good understanding of the process and, in many cases, trial and error. Modelling and simulation can be an invaluable tool for this procedure as can be seen in the deinked pulp application.

To summarise, the strongest theoretical contribution of this thesis is the introduction of the population principle and the modifications of the SOC-algorithm. The population principle can be

used as a simple mechanical tool for dividing a complex stiff system into several smaller subgroups with different kinetic properties. This kind of kinetic division is essential, e.g., for parallel computing solution of stiff systems. However, in this thesis the population principle was applied exclusively to pH models. The structure of the developed models is such that advanced methods for solving pH by the use of the thermodynamic equilibrium (Gibbs free energy minimisation) can be used as well. The models generated with the population principle are also very suitable for dynamic simulations as can be seen from the examples.

A great deal of research and numerous thesis have been dedicated to the pH control problem and the modified SOC-algorithm that was presented in Chapter 5 is one approach among many others. However, among nonlinear and adaptive controllers it has a couple of benefits. The adaptation is local and limited; a fact that guarantees stability even when the pH measurement is out of order. It also generates a characteristic rule base that can be saved and loaded either manually or automatically and these learned rule bases can operate as fixed controllers if that is required. Compared to many adaptive algorithms that perform well in simulations or during short supervised pilot runs the SOC algorithm has operated satisfactorily for years in permanent industrial installation adapting continuously without any supervision from the plant personnel.

The minor contribution to pH measurement is more of a practical nature. The recirculation structure presented in Chapter 6 is particularly suitable for systems that contain high solid content combined with significant pressure and flow variations. However, the achieved benefits of the re-circulation measurement structure are notable as the pH measurement was the crucial factor before the control loop could be realised.

pH process and its control is an interesting and challenging area for researchers and for anyone in process industry. Because of its diversity it is a subject that no one can give definitive solutions or absolute truths as every application is somewhat unique. The methods derived in previous chapters can be applied for a number of practical applications but not for every pH problem. It is a comforting thought that there are many cases where a simpler solution is adequate; a PID algorithm operates well for most pH applications. But it is equally comforting to know that there still are challenging pH processes that require every bit of insight and skill from the person who tries to measure, model and control them...because who wants to live in a perfect world anyway?

Bibliography

Bathel (vb.)

To pretend to have read the book under discussion when in fact you've only seen the TV series. [1]

Whasset (n.)

A business card in your wallet belonging to someone whom you have no recollection of meeting. [1]

[1] Adams, D., Lloyd, J., The deeper meaning of liff, Pan Books limited, 1992.

[2] Ala-Kaila, K., A dynamic model for calculating pH inside kraft pulp fibers, Paper and Timber, 81(3), 202-209, 1999.

[3] Ala-Kaila, K., Nordén, H. V., Application of a film model to the multicomponent mass transfer of ions into kraft pulp fibers, Acta Polytechnica Scandinavica, Chemical Technology series, Espoo, 255, 1998.

[4] Ashour, S. S., Hanna, O. T., A new implicit backward mid-point rule for highly-stiff systems of ordinary differential equations, Comput. Chem. Eng., 15(2), 125-32, 1991.

[5] Bates, R.G., Determination of pH, theory and practice, 2nd edition, John Wiley & Sons, New York, 1973.

[6] Boozarjomehry, R. B., Svcek, W. Y., Output feedback neurolinearization, ISA Transactions, 40, 139-154, 2001.

[7] Bucholt, F., Kümmel M., Self-tuning control of a pH neutralization process, Automatica, 15, 665-671, 1979.

[8] Butler, J. N., Ionic equilibrium - a mathematical approach, Addison-Wesley Publishing Company inc, 1964.

[9] Chan, H.-C., Yu, C.-C., Autotuning of gainscheduled pH control: An experimental study, , Ind. Eng. Chem. Res., 34, 1718-1729, 1995.

[10] Compton, R., Daly, P., The dissolution/Precipitation Kinetics of Calcium Carbonate: An Assessment of Various Kinetic Equations Using a Rotating Disk Method, J. of Colloid and Interface Sci., 115(2), 493-498, 1987.

[11] Cremer, M., On the reason of electromotoric properties of textures, Z. Biol., 47, 562-608, (in German), 1906.

[12] De, D. S., Loh, A.-P., Krishnaswamy, P. R., A nonlinear adaptive controller of pH neutralization process, Proc. Am. Contr. Conf, 2250-2254, Chicago, 2000.

[13] Dias, J. M., Dourado, A., A self organizing fuzzy controller with a fixed maximum number of rules and an adaptive similarity factor, Fuzzy Sets and Systems, 103, 27-48, 1999.

[14] Docherty, P. J., Automatic pH control: neutralization of acid wastes by addition of lime slurry, M.Sc thesis, Dartmouth College, Thayer School of Engineering, Hanover, New Hampshire, 1972.
[15] Dumont, G. A., Zervos, C. C., Pageau, G. L., Laguerre-based adaptive control of pH in an industrial bleach plant extraction stage, Automatica, 26(4), 781-787, 1990.
[16] Edgar, C. R., Postlethwaite, B. E., MIMO fuzzy internal model control, Automatica, 34, 867-877, 2000.
[17] Eklund, D., Lindström, T., Paper Chemistry – An Introduction, Kauniainen, DT Paper Science Publications, 1991.
[18] Emara-Shabaik, H. E., Bomberger, J., Seborg, D. E., Cumulant/bispectrum model structure identification applied to a pH neutralisation process, IEE Control 1996, Conference publication, 427, 1046-1051, 1996.
[19] Fjeld, M., Asbjørnsen, O. A., Åström, K. J., Reaction invariants and their importance in the analysis of eigenvectors, state observability and controllability of continuos stirred tank reactor, Chem. Eng. Sci., 29, 1917-1926, 1974.
[20] Foxboro Inc., 870/TPH intelligent electrochemical transmitter for pH, ORP and ion selective measurements, 1997.
[21] Foxboro Inc, PID algorithm with self tuning, Technical information, 1984.
[22] Gadewar, S. B., Doherty, M. F., Malone, M. F., A systematic method for reaction invariants and mole balances for complex chemistries, Comp. & Chem. Eng., 25, 1199-1217, 2001.
[23] Garrido, R., Adroer, M., Poch, M., Wastewater neutralization control based in fuzzy logic simulation results, Ind. Eng. Chem. Res., 36, 1665-1674, 1997.
[24] Goodwin, G. C., McInnis, B., Long, R. S., Adaptive control algorithms for waste water treatment and pH neutralization, Optimal Control Appl. & Methods, 3, 443-459, 1982.
[25] Great Lakes Inst. International Inc., What is pH and how is it measured, Tecnical handbook for industry, 1997.
[26] Gupta, S. R., Coughanowr, D. R., On-line gain identification of flow processes with application to adaptive pH control, AIChE J., 24(4), 654-664, 1978.
[27] Gustafsson, T. K., A study of modeling and control of pH in fast acid-based reaction processes based on chemical reaction invariance, Ph.D thesis, Deparment of Chemical Engineering, Åbo Akademi, 1984.
[28] Gustafsson, T.K., Skrifvars, B. O., Sandström, K. V., Waller, K. V., Modelling of pH for control, Ind. Eng. Chem. Res., 34, 820-827, 1995.
[29] Gustafsson, T.K., Waller, K. V., Nonlinear and adaptive control of pH, Ind. Eng. Chem. Res., 31, 2681-2693, 1992.
[30] Gustafsson, T. K., Waller, K. V., Dynamic Modelling and Reaction Invariant Control of pH, Chem. Eng. Sci, 38(3), 389-398, 1982.
[31] Haber, F., Klemensiewicz, Z., On the electrical phase limit powers, Z. Physik. Chem., 67, 385-431, (in German), 1909.
[32] Hach Inc., Hach systems for electrochemical analysis, 1997.
[33] Hall, R. C., Development of a multi-variable pH experiment, M.Sc thesis, University of California, Santa Barbara, 1987.
[34] Hall, R. C., Seborg, D. E., Modelling and self-tuning control of a multivariable pH neutralization process. Part I: Modelling and multiloop control, Proc. Am. Contr. Conf., Pittsburg, 2, 1822-1827, 1989.
[35] Heckenthaler, T., Engell, S., Fuzzy-logic controller-design for pH-control in a CSTR, Proc. of 4th IFAC DYCORD Symp, Pergamon Press, New York, U.S.A., 27-32, 1995.
[36] Henson, M. A., Feedback linearization strategies for nonlinear process control, Ph.D thesis, University of California, Santa Barbara, 1992.

[37] Henson, M. A., Seborg, D. E., A critique of exact linearization strategies for process control, AIChE J., 36, 1753-1757, 1990.
[38] Henson, M. A., Seborg, D. E., Adaptive nonlinear control of a pH neutralization process, IEEE Trans. on Control Syst. Tech, 2, 169-182, 1994.
[39] Henson, M. A., Seborg, D. E., Nonlinear adaptive control of a pH neutralization process, Proc. of the American Control Conf., Chicago, Illinois, U.S.A., 4, 2586-2590, 1992.
[40] Honeywell Inc., pH analysis and control solutions, 1997.
[41] Hu, Q., Saha, P., Rangaiah, G. P., Experimental evaluation of an augmented IMC for nonlinear systems, Contr. Eng. Prac., 8, 1167-1176, 2000.
[42] Jacobs, O. L. R., Hewkin, P. F., While, C., On-line computer control of pH in an industrial process, IEE Proc. D, 127, 1980.
[43] Jantzen, J., The Self-Organising Fuzzy Controller, Tech. report no 98-H 869, Technical University of Denmark - Department of Automation, 1998.
[44] Johansen, T. A., Operating regime based process modeling and identification, Ph.D: thesis, Department of Engineering Cybernetics, Norwegian Institute of Technology, University of Trondheimn Norway, 1994.
[45] Johansen, T. A., Foss, B. A. Identification of non-linear system structure and parameters using regime decomposition, Automatica, 31, 321-326, 1995.
[46] Johansen, T. A., Foss, B. A., ORBIT - Operating Regime Based Modeling and Identification Toolkit, Contr. Eng. Prac., 6, 1277-1286, 1998.
[47] Joshi, P. V., Kumar, A., Mizan, T. I., Klein, M. T., Detailed kinetic models in the context of reactor analysis: Linking mechanistic and process chemistry, Energy Fuels, 13(6), 1135-1144, 1999.
[48] Junhong, N., Loh, P. A., Hang, C. C., Modeling pH neutralization processes using fuzzy-neural approaches, Fuzzy Sets and Systems, 78(1), 5-2259, 1996.
[49] Jutila, P., Hyötyniemi, H., Ylén, J.-P., Problems and practice of pH process modelling and control in stirred tank reactors, Arch. Contr. Sci. 9(XLV)3-4, 5-31, 1999.
[50] Jutila, P., Jaakola, P., Tests with five adaptive pH-control algorithms in laboratory, Helsinki Univ. Tech., Control Eng. Lab., Report 65, 1986.
[51] Jutila, P., Orava, J., Control and Estimation Algorithms for Physico-Chemical Models of pH-Processes in stirred Tank Reactors, Int. J. Systems Sci., 12(7), 1981.
[52] Jutila, P., Visala, A., Pilot plant testing of an adaptive pH-control algorithm based on physico-chemical modelling, Math. and Comp. in Simulation, 26, 523-533, 1984.
[53] Jutila, V.-P., Jutila, P., Ylén, J.-P., The measurement and control of the pH of thick deinked pulp., 3rd Asia-Pacific Conference on Control and Measurement (APC CM'98), Dunhuang, P. R. China, August 31-September 4, 1998. Nanjing, Jiangsu, China, China Aviation Industry Press, 326-330, 1998.
[54] Kaesser, R., Adaptive continuous pH-control monitored by on-line gain identification, IFAC PRP, 4, 285- 293, 1980.
[55] Kalafatis, A., Arifin, N., Wang, L., Cluett, W. R., A new approach to the identification of pH processes based on the Wiener model., Chem. Eng. Sci., 50(23), 3693-3701, 1995.
[56] Kalafatis, A., Wang, L., Cluett, W. R., Identification of Wiener-type nonlinear systems in noisy environment., Int. J. Contr., 66(6), 923-941, 1997.
[57] Kao, P., Popham, L., Walker, W. A., Evaluation of a self-tuning regulation, In prep. Of IFAC Conference on Intelligent Tuning and Adaptive Control, Session one, Singapore, 1991.
[58] Karr, C. L., Gentry, E. J., Fuzzy control of pH using genetic algorithms, IEEE trans. on Fuzzy Syst., 1, 46-53, 1993.

[59] Kavšek-Biasizzo, K., Škrjanc, I., Matko, D., Fuzzy predictive control of highly nonlinear pH process, Comp. Chem. Eng., 21(Suppl.), S613-S618, 1997.

[60] Kazemian, H. B., Comparative study of a learning fuzzy PID controller and a self-tuning controller, ISA Transactions, 40, 245-253, 2001.

[61] Kim, Y.-T., Bien, Z., Robust self-learning controller design for a class of nonlinear MIMO systems, Fuzzy Sets and Systems, 111, 117-135, 2000.

[62] Kim, S.-J., Lee, M, Park, S., Lee, S.-Y., Park, C. H., A neural linearizing control scheme for nonlinear chemical processes, Comp. Chem. Eng., 21(2), 187-200, 1997.

[63] Klatt, K.-U., Engell, S., Nonlinear control of neutralization processes by gain-scheduling trajectory control, , Ind. Eng. Chem. Res., 35, 3511-3518, 1996.

[64] Knio, O. M., Najm, H. N., Numerical simulation of unsteady reacting flow with detailed kinetics, Comput. Fluid Solid Mech., Proc MIT Conf, Elsevier Science Ltd., 2, 1261-1264, 2001.

[65] Kulkarni, B. D., Tambe, S. S., Shukla, N. V., Deshpande, P. D., Nonlinear pH control, Chem. Eng. Sci., 46, 995-1003, 1991.

[66] Kurz, H., Adaptive control of a waste water neutralization process, Proc. of 9th IFAC World Congress, VI, Pergamon Press, New York, U.S.A., 3257-3261, 1995.

[67] Kässer, R., Adaptive pH-Regelung des Abwassers aus Chemischer Produktion, Regelungstechnische Praxis, 23(9), (in German), 321- 328, 1981.

[68] Laidler, K. J., Meiser, J. H., Physical Chemistry, Benjamin/Cummings Publishing Company inc., 1982.

[69] Laurikkala, M., Self-organising fuzzy controller, M.Sc. thesis, (in Finnish), Tampere Univ. of Tech., 1993.

[70] Lee, S. D., Lee, J. Park, S., Nonlinear self-tuning regulator for pH systems, Automatica, 30, 1579-1586, 1994.

[71] Lee, T. H., Nie, J. H., Tan, W. K., A self-organising fuzzified basis function network control system applicable to nonlinear servomechanisms, Mechatronics, 5(6), 695-713, 1995.

[72] Lembessis, E., Dynamic learning behaviour of a rule-based self organising controller, Ph.D. thesis, Queen Mary College, Dept. of Electrical and Electronic Engineering, London, UK, 1985.

[73] Levenspiel, O., Chemical reaction engineering, 2nd edition, John Wiley & Sons, 1972.

[74] Lin W.-S., Tsai, C.-H., Self organizing fuzzy control of multi-variable systems using vector quantization network, Fuzzy Sets and Systems, 124, 197-212, 2001.

[75] Lin C.-K., Wang, S.-D., A self organizing fuzzy control approach for bank-to-turn missiles, Fuzzy Sets and Systems, 96, 281-306, 1998.

[76] Linkens, D. A., Abbod, M., Self-organising fuzzy logic control for real-time processes, IEE Control, 971-976, 1991.

[77] Linkens, D. A., Mahfouf, M., Abbod, M., Self-adaptive and self-organising control applied to nonlinear multivariable anaesthesia: a comparative model-based study, IEE Proc. D, 139(4), 381-394, 1992.

[78] Loh, A. P., Looi, K. O., Fong, K. F., Neural network modelling and control strategies for a pH process, J. of Process Control, 5, 375-386, 1995.

[79] Maiti, S. N., Kapoor, N., Saraf, D. N., Adaptive dynamic matrix control of pH, , Ind. Eng. Chem. Res., 33, 641-646, 1994.

[80] Mamdani, E. H., "Twenty Years of Fuzzy Control: Experiences Gained and Lessons Learnt," Proc. of IEEE International Conf. on Fuzzy Systems, pp. 339-344, 1993.

[81] Mamdani, E. H., Baaklini, N., Prescriptive method for deriving control policy in a fuzzy-logic controller, Electronic letters, 11(25/26), 625–626, 1975.

[82] Maron, C., Burgert, K., Adaptive pH-Wert-Regelung in einer Neutralisationsanlage mit Hilfe von Fuzzy-Logik, Automatisierungstechnische Praxis, 35(12), 666-672, (in German), 1993.

[83] Martinez, E. C., Drozdowicz, B., Multitime-scale approach to real-time simulation of stiff dynamic systems, Comput. Chem. Eng., 13(7), 767-78, 1989.

[84] McAvoy, T., Hsu, E., Lowenthal, S., Dynamics of pH in Controlled Stirred Tank Reactor, Ind. & Eng. Chem., Process Descr. & Develop. 11(1), 67-70, 1972.

[85] McMillan, G. K., pH Control, Instrument Society of America, 1984.

[86] Narayanan, N. R. L., Krishnaswamy, P. R., Rangaiah, G. P., An adaptive internal model control strategy for pH neutralization, Chem. Eng. Sci., 52, 3067-3074, 1997.

[87] Narayanan, N. R. L., Krishnaswamy, P. R., Rangaiah, G. P., Use of alternate process variables for enhancing pH control performance, Chem. Eng. Sci., 53(17), 3041-3049, 1998

[88] Norquay S. J., Palazoglu, A., Romagnoli, J. A., Model predictive control based on Wiener models, Chem. Eng. Sci, 53, 75-84, 1988.

[89] Norquay S. J., Palazoglu, A., Romagnoli, J. A., Application of Wiener Model Predictive Control (WMPC) to a pH neutralisation experiment, IEEE trans. on Control Syst. Tech., 7(4), 437-445, 1998.

[90] Nyström, R. H., Sandström, K. V., Gustafsson, T. K., Toivonen, H. T., Multimodel robust control applied to a pH neutralization process, Comp. Chem. Eng., 22(Suppl.), S467-S474, 1998.

[91] Nyström, R. H., Sandström, K. V., Gustafsson, T. K., Toivonen, H. T., Multimodel robust control of nonlinear plants: A case study, J. of Process Control, 9, 135-150, 1999.

[92] Olivares, M., Some experiments with the self-organising controller, Tech. report no 99-E 882, Technical University of Denmark - Department of Automation, 1999.

[93] Orava, P. J., Niemi, A. J., State model and stability analysis of a pH control process, Int. J. Control, 20, 557-567, 1974.

[94] Pajunen, G., Adaptive control of Wiener type nonlinear systems, Automatica, 28(4), 781-785, 1992.

[95] Palancar, M. C., Aragón, J. M., Miguéns, J. A., Torrecilla, J. S., Application of a model reference adaptive control system to pH control. Effects of lag and delay time, Ind. Eng. Chem. Res., 35, 4100-4110, 1996.

[96] Palancar, M. C., Aragón, J. M., Torrecilla, J. S., pH-control system based on artificial neural networks, Ind. Eng. Chem. Res., 37, 2729-2740, 1998.

[97] Park, G. Y., Seong, P. H., Application of a self-organizing fuzzy logic controller to nuclear steam generator level control, Nucl. Eng. and Des., 167, 345-356, 1997.

[98] Piovoso M. J., Williams, J. M., Self-tuning pH control, A difficult problem. an effective solution, In tech, 32(5), 45-49, 1985.

[99] Postlethwaite, B. E., Brown, M, Sing, C. H., A new identification algorithm for fuzzy relational models and its application in model-based control, Trans. Inst. Chem. Eng., 75(A), 453-458, 1997.

[100] Procyc, T. J., A self-organizing controller for dynamic processes, Ph.D. thesis, Queen Mary College, Dept. of Electrical and Electronic Engineering, London, UK, 1977.

[101] Procyk, T. J., Mamdani, E. H., A linquistic self-organizing process controller, Automatica, 15, 15-30, 1979.

[102] Proudfoot, C. G., Gawthrop, P. J., Jacobs, O. L. R., Self-tuning PI-control of a pH neutralisation process, IEE Proc. D, 130, 1983.

[103] Proudfoot, C. G., Industrial implementation of on-line computer control of pH, Ph.D. thesis, University of Oxford, 1983.

[104] Pröll, T., Karim, N., Model predictive pH-control using real-time NARX approach, AIChE J., 40(2), 269-282, 1994.

[105] Rand, E. R., Application of the Popov criterion to pH neutralization control, ISA AC., 764(1)-764(4), 1975.
[106] Richter, J. D., Fournier, C. D., Ash, R. H., Marcikic, S., Waste neutralization control - digital simulation spots nonlinearities, Ins. Tech., 21, 35-40, 1974.
[107] Ross, T. J, Fuzzy logic with engineering applications, 183-210. McGraw-Hill, U.S.A., 1995.
[108] Rys, R. A., Advanced control methods, Chem. Eng., Aug. 20, 151-158, 1984.
[109] Sandström, K. V., Gustafsson, T. K., A study of the dynamics of calcium-phosphate precipitation in pH control systems, Åbo Akademi process control laboratory report, 94-5, 1994.
[110] Seborg, D. E., Edgar, T. F., Shah, S. L., Adaptive control strategies for process control: A survey, AIChE J., 32(6), 881-913, 1986.
[111] Shah, I. M., Application study of a fuzzy self-organizing process controller: control of pH in stirred tank, Ph.D. Thesis, University of Utah, U.S.A., 1991.
[112] Shao, S., Fuzzy self-organizing controller and its applications for dynamic processes, Fuzzy Sets and Systems, 26, 151-164, 1988.
[113] Shiskey, F. G., Adaptive pH controller monitors nonlinear process. Control Eng., 57, 57-59, 1974.
[114] Shukla, N. V., Deshpande, P. D., Kumar, V. R., Kulkarni, B. D., Enhancing the robustness of internal-model-based nonlinear pH controller, Chem. Eng. Sci, 48, 913-920, 1993.
[115] Singh, Y. P., A modified self-organizing controller for real-time process control applications, Fuzzy Sets and Systems, 96, 147-159, 1998.
[116] Sjöberg, E. L., A fundamental equation for calcite dissolution kinetics, Geochimica et Cosmochimica Acta, 40, 441-447, 1976.
[117] Støle-Hansen, K., Studies of some phenomena in control engineering projects – with application to precipitation and cementation processes, Doctoral thesis, Norwegian university of science and technology – department of engineering cybernetics, Report 98-5-W, 1998.
[118] Subramani R., Krishnaswamy P. R., A fuzzy adaptive internal model control strategy for pH neutralization, Proc. of Iasted Int. Conf. Control and Applications, Honolulu, Hawaii, U.S.A.,189-193, 1998.
[119] Sugiyama, K., Analysis and synthesis of the rule-based self-organising controller, Ph.D. thesis, Queen Mary College, Dept. of Electrical and Electronic Engineering, London, UK, 1986.
[120] Sun, P., Chock, D. P., Winkler, S. L., An implicit-explicit hybrid solver for a system of stiff kinetic equations, J. Comput. Phys., 115(2), 515-23, 1994.
[121] Sutton, R. Jess, I., Real-time application of a self-organising autopilot to warship yaw control, IEE Control, 827-832, 1991.
[122] Tadeo, F., Holohan, A., Vega, P., l_1-optimal regulation of a pH control plant, Comp. Chem. Eng., 22(Suppl.), S459-S466, 1998.
[123] Tadeo, F., López, O. P., Alvarez, T., Control of neutralisation processes by robust loopshaping, IEEE Trans. Contr. Sys. Tech., 8(2), 2000.
[124] TBi Bailey Inc., pH/ORP sensors for process monitoring, 1994.
[125] TBi Bailey Inc., Model TB82 advantage series two-wire pH/ORP transmitter, 1997.
[126] Tyreus, B. D., Luyben, W. L.. Schiesser, W. E., Stiffness in distillation models and the use of an implicit integration method to reduce computation times, Ind. Eng. Chem., Process Des. Dev., 14(4), 427-33, 1975.
[127] Waller, K. V., Comments on “In-line process-model-based control of wastewater pH using dual base injection”, I&EC Res., 30, 2238-2239, 1991.

[128] Waller, K. V., Mäkilä, P. M., Chemical reaction invariants and variants and their use in reaction modeling, simulation and control, Ind. Eng. Chem. Process Des. Dev., 20, 1-11, 1981.

[129] Walsh, S., Perkins, S., Application of integrated process and control system design to waste water neutralisation, Comp. Chem. Eng., 18(Suppl.), S183-S187, 1994.

[130] Welfonder, von E., Beyerle, T, Alt, M., Kontinuierliche Abwasserneutralisation mittels eines Kleinprozessrechners, Regelungstechnische Praxis, Heft4, (in German), 116-120, 1978.

[131] Welfonder, von E., Beyerle, T, Alt, M., Kontinuierliche Abwasserneutralisation mittels eines Kleinprozessrechners, Regelungstechnische Praxis, Heft5, (in German), 151-154, 1978.

[132] Williams, G. L., Rhinehart, R. R., Riggs, J. B., In-line process-model-based control of wastewater pH using dual base injection, Ind. Eng. Chem. Res., 29, 1254-1259, 1990.

[133] Wong, Y. H., Krishnaswamy, P. R., Teo, W. K., Kulkarni, B. D., Deshpande, P. D., Experimental application of robust nonlinear control law to pH control, Chem. Eng. Sci, 49(2), 199-207, 1994.

[134] Wright, R. A., Kravaris, C., Nonlinear control of pH processes using the strong acid equivalent, Ind. Eng. Chem. Res., 30, 1561-1572, 1991.

[135] Wright, R. A., Kravaris, C., On-line identification and nonlinear control of an industrial pH process, J. Proc. Cont., 11, 361-374, 2001.

[136] Wright, R. A., Kravaris, C., On-line identification and nonlinear control of pH processes, Ind. Eng. Chem. Res., 37, 2446-2461, 1998.

[137] Wright, R. A., Kravaris, C., pH control in the presence of precipitation equilibria, Preprints from DYCORD+'95, Helsingør, Denmark, 1995.

[138] Wright, R. A., Soroush, M., Kravaris, C., Strong acid equivalent control of pH processes: an experimental study, Ind. Eng. Chem. Res., 30, 2437-2444, 1991.

[139] Yamazaki, T., An improved algorithm for a self-organising controller and its experimental analysis, Ph.D. thesis, Queen Mary College, Dept. of Electrical and Electronic Engineering, London, UK, 1982.

[140] Ylén, J.-P., Improved Performance of Self-Organising Fuzzy Controller (SOC) in pH Control, IEEE World Congress on Computational Intelligence (WCCI98), Anchorage, Alaska, USA, May 4-9, 1998. USA, ALTEC/IEEE, pp. 258-263, 1998.

[141] Ylén, J.-P., pH-value and the dynamic chemical state of wet end. Scientific & Technological Advances in the Measurement & Control of Papermaking, Edinburgh, UK, 9th & 10th November 1998. UK, Pira International, 1998.

[142] Ylén, J.-P. Practical Aspects of Self-Organising Fuzzy Controller (SOC) Implementation, FUZZIEEE 1997, Proc. of 6th IEEE Conf. on Fuzzy Systems, 1, 483-488, 1997.

[143] Ylén, J.-P., Jutila, P., Dynamic Chemical State Modelling in Paper and Pulp Processes., 4th Asia-Pacific Conference on Control and Measurement (APCCM'2000), July 9-12, 2000., Guilin China, 27-34, 2000.

[144] Ylén, J.-P., Jutila, P., Fuzzy Self-Organising pH Control of an Ammonia Scrubber, Contr. Eng. Prac., 9, 1233-1242, 1997.

[145] Ylén, J.-P., Jutila, P., pH control, Wiley Encyclopedia of Electrical and Electronics Engineering, 16, 225-239, 1999.

[146] Ylén, J.-P., Jutila, P., Traditional and Modern Methods in pH Control of an Ammonia Scrubber - A Simulation Study, EUROSIM '95, Proc. of EUROSIM Conference, Vienna, Austria, 1995.

[147] Ylöstalo, T., Hyötyniemi, H., Model library based adaptive control – implementation aspects, Proc. of the European Control Conf. (ECC99), Karlsruhe, Germany, (CD-ROM format), 1999.

[148] Ylöstalo, T., Hyötyniemi, H., Jutila, P., Ylén, J.-P., Comparison of practical adaptive algorithms in pH control, To be published in Europ. J. Contr., 2001.
[149] Yokogawa Inc., pH in theory and practice, 1997.
[150] Yokogawa Inc., Model pH18 differential pH sensor: general specifications, 1997.
[151] Zenger, K., Analysis and control design of a class of time-varying systems, Licenciate thesis, Control engineering laboratory Report 88, Helsinki University of Technology, 1992.
[152] Zhang, B. S., Edmunds, J. M., A self-organising fuzzy logic controller, Report 744, UMIST, Control Systems Centre PO Box 88, Manchester, England, 1991.
[153] Åström, K. J., Wittenmark, B., Adaptive control, Addison-Wesley, Reading, MA, 1989.

Appendix 1

Simulink models

Kirby (n.)
Small but repulsive piece of food prominently attached to a person's face or clothing. [1]
Wawne (n.)
A badly suppressed yawn. [1]

This appendix contains all Simulink models of Chapters 4,5 and 6

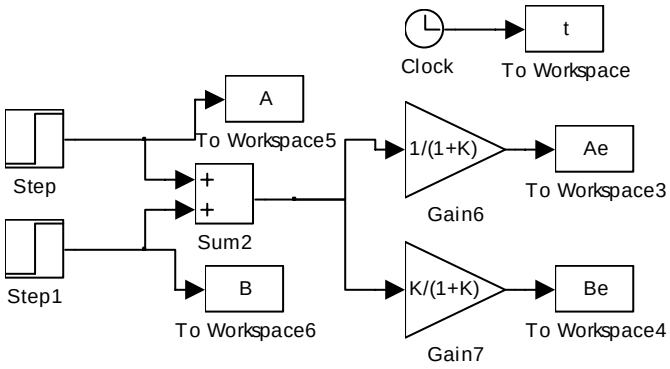

Fig. A1.1: The simulation model for instantaneous reactions in the batch process.

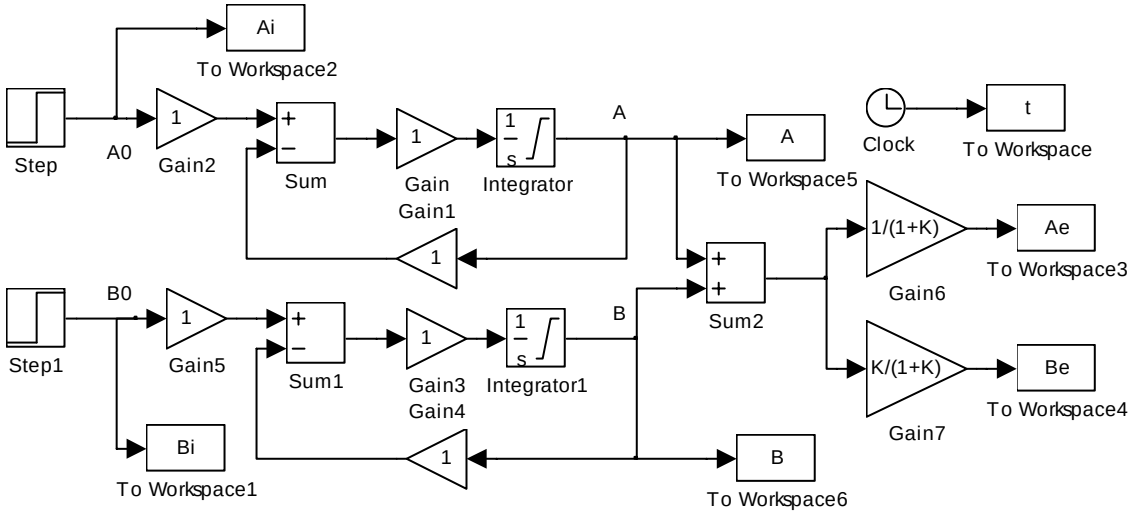

Fig. A1.2: The simulation model for the continuous flow process (instantaneous equilibrium).

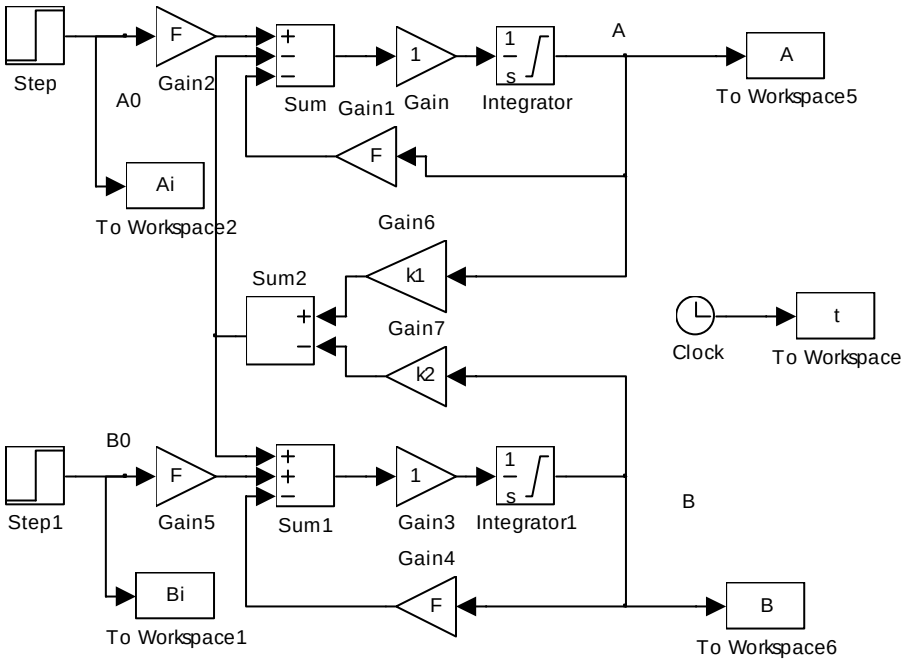

Fig. A1.3: Simulation model of the continuous flow process with slow reaction dynamics.

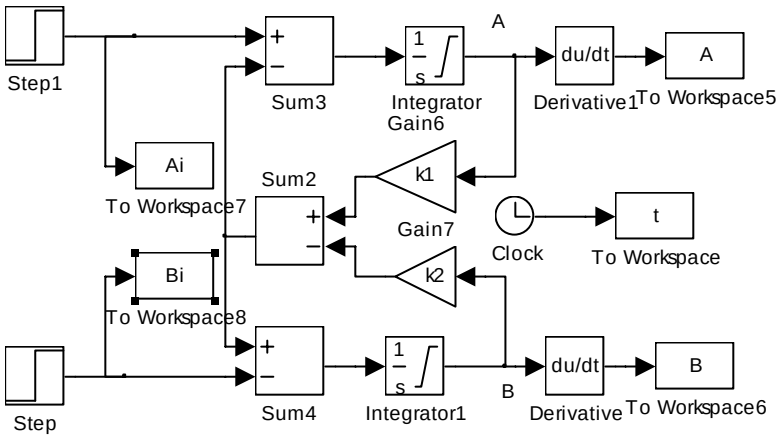

Fig. A1.4: Simulation model of the batch process with slow reaction dynamics.

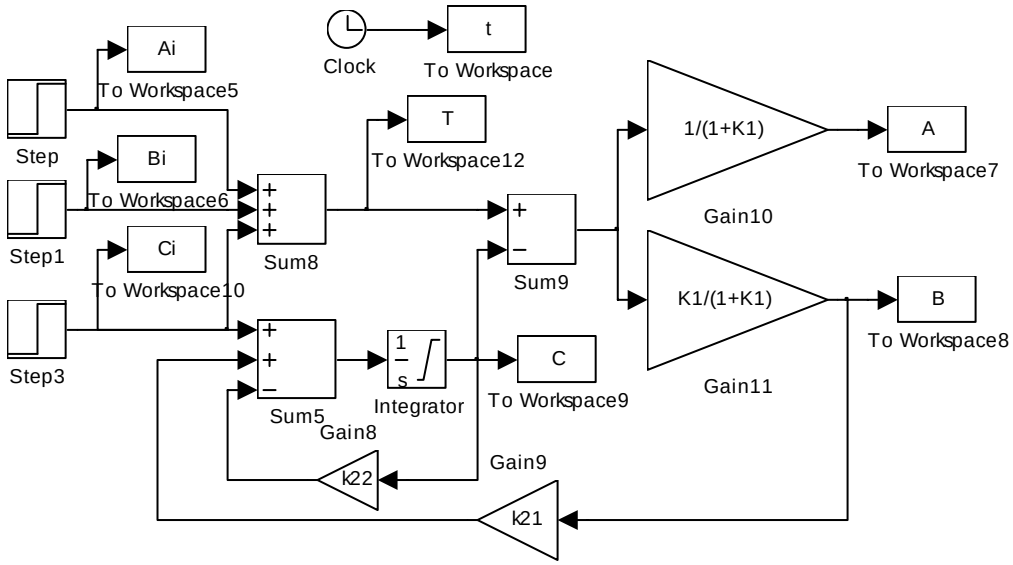

Fig. A1.5: Simulation model for the batch process with combined instantaneous and slow dynamics.

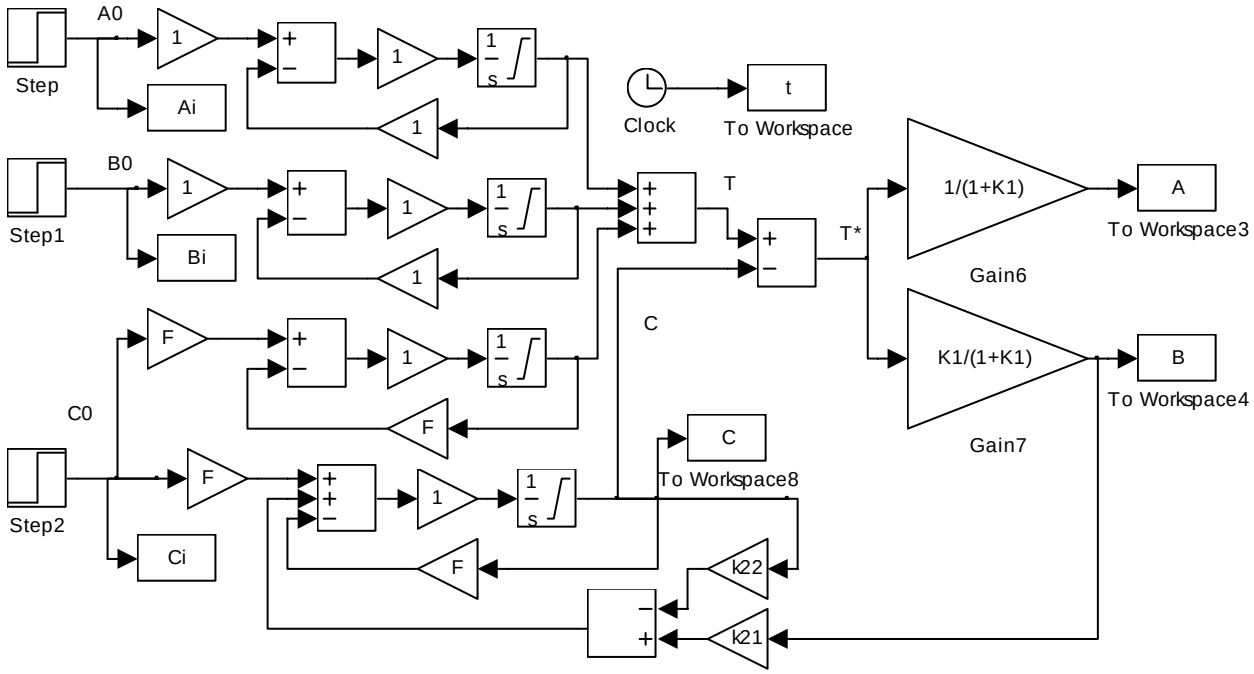

Fig. A1.6: Simulation model for the continuous flow process with combined instantaneous and slow dynamics.

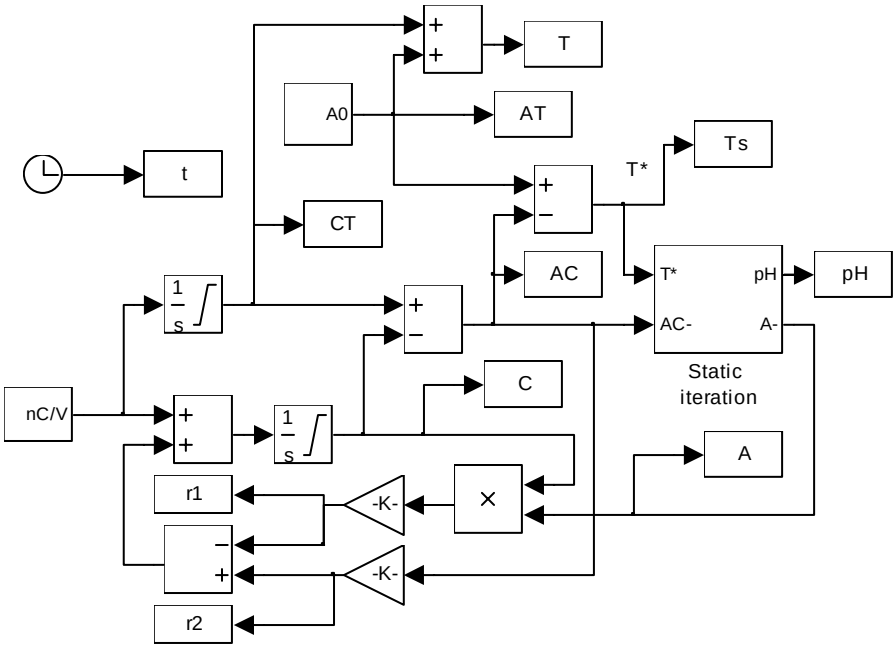

Fig. A1.7: The simulation model for the batch pH process.

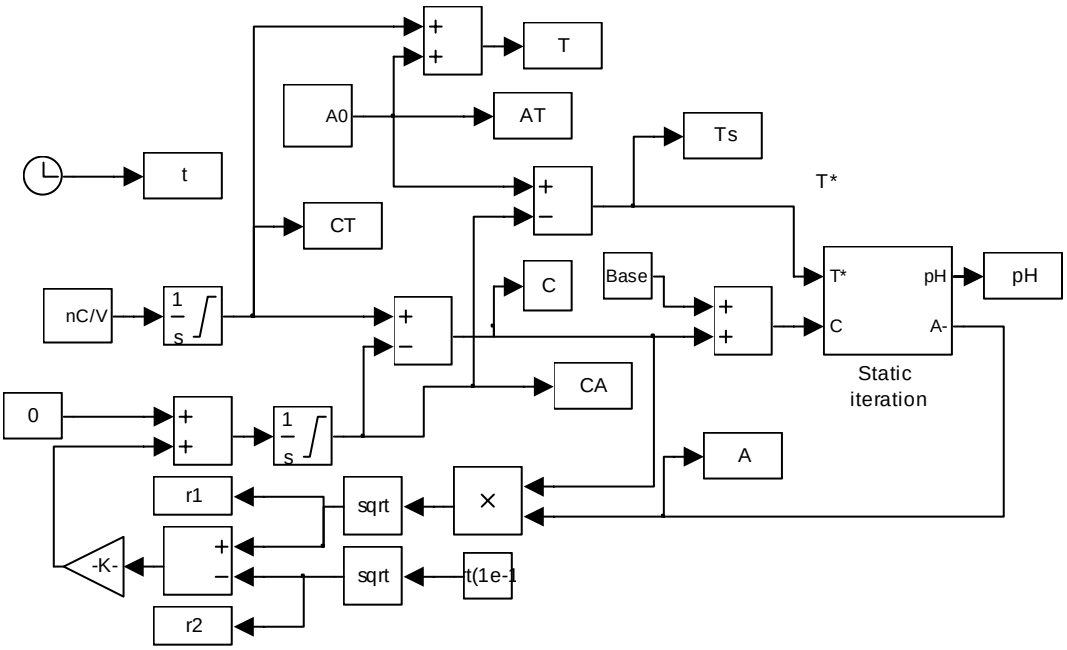

Fig. A1.8: Simulation model for the titration process with precipitation/dissolution phenomena.

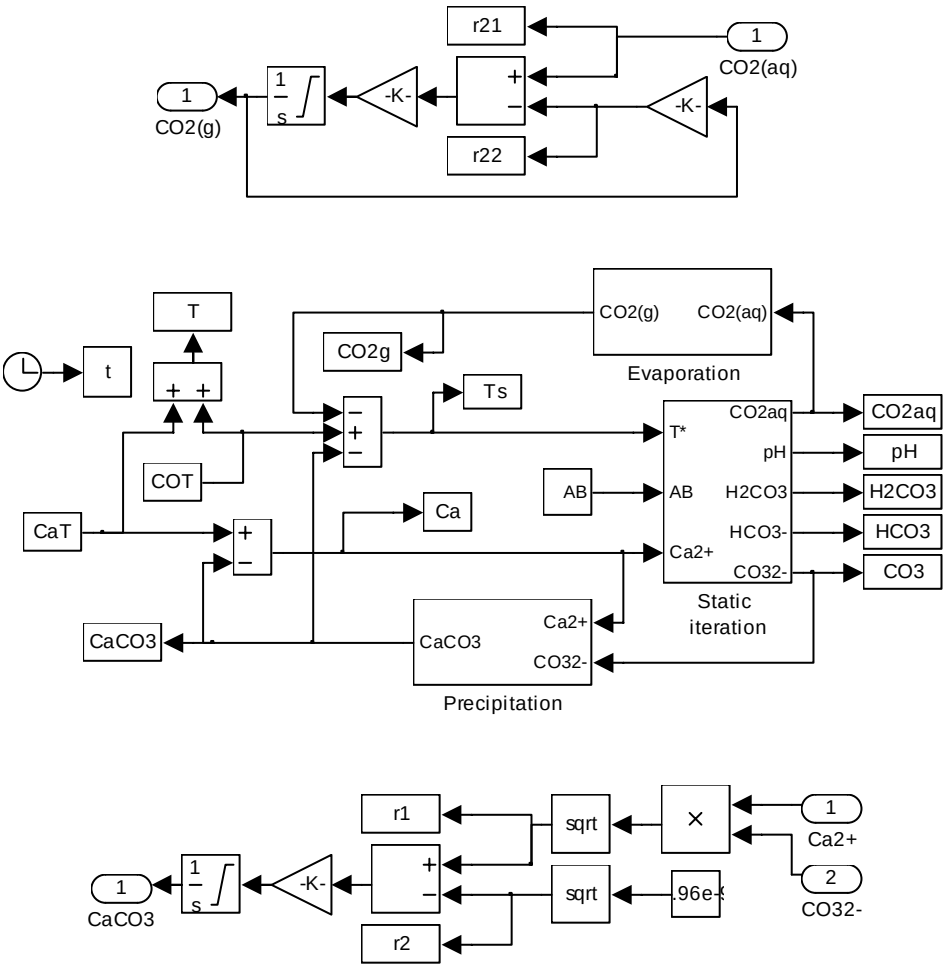

Fig. A1.9: Simulation model for the calcium carbonate process.

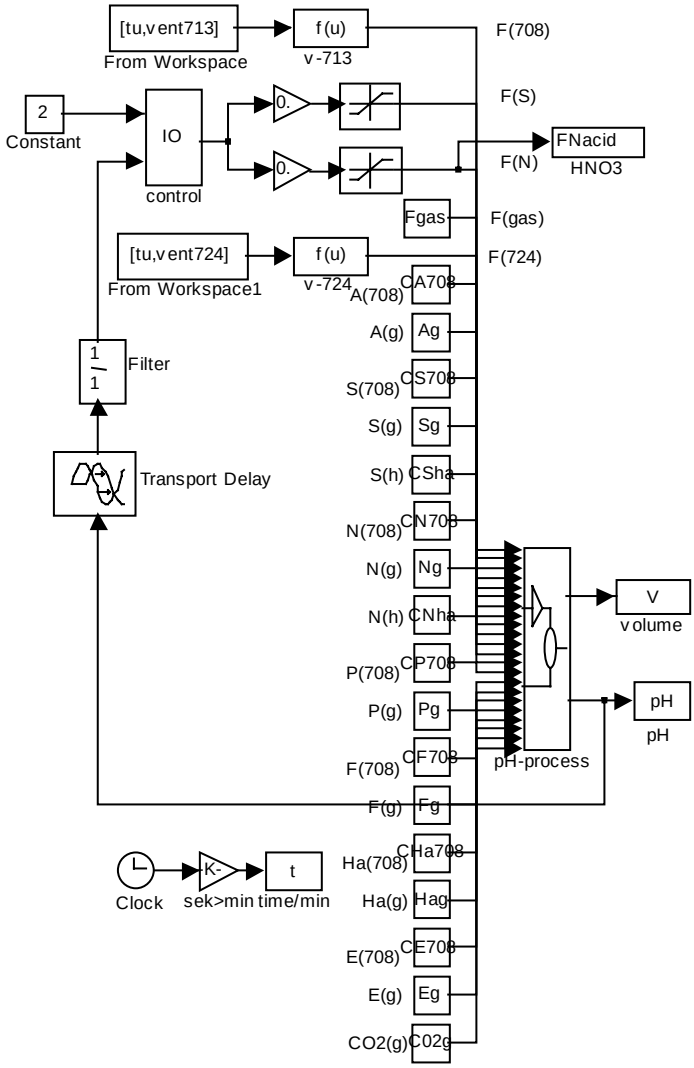

Fig. A1.10: Top level of the ammonia scrubber simulator

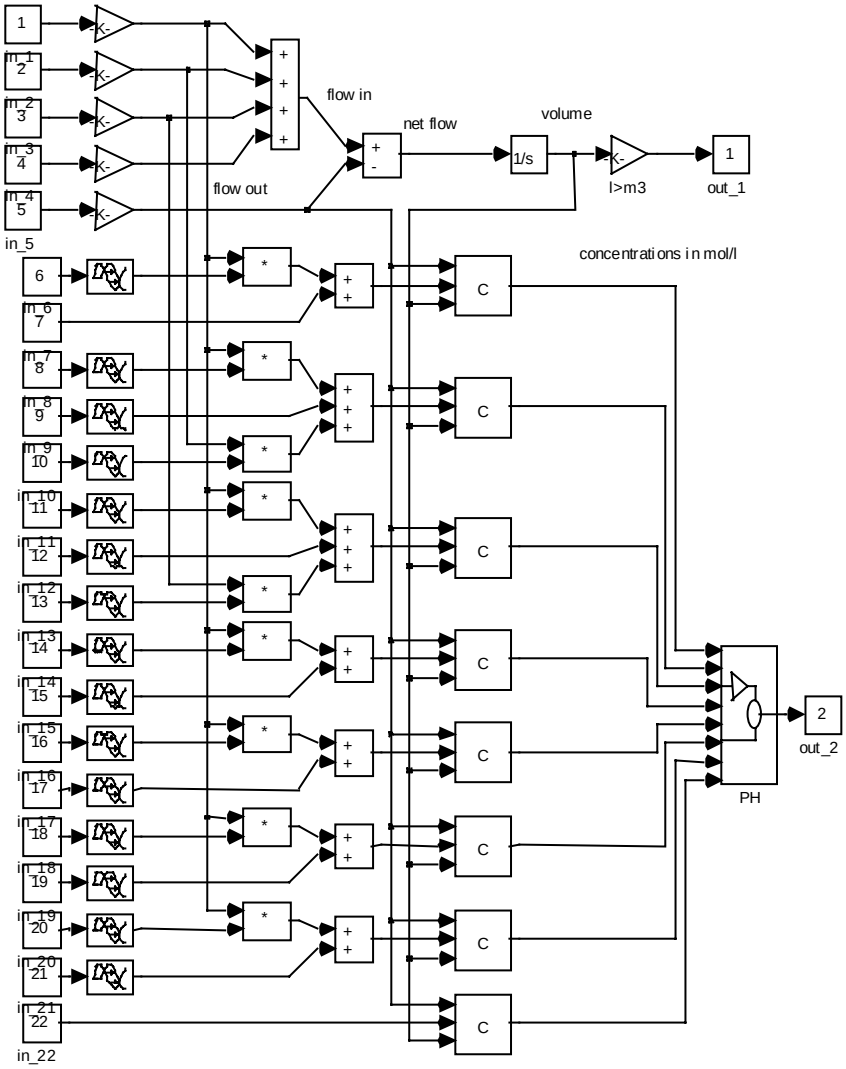

Fig. A1.11: Lower level of the ammonia scrubber simulator

Appendix 2

Numerical example of the SOC low level adaptation

Scremby (n.)

The dehydrated felt-tip pen attached by a string to the "Don't forget" board in the kitchen which has never worked in living memory but which no one can be bothered to throw away. [1]

Nome (sfx.)

Latin suffix meaning: question expecting the answer "Oh really? How interesting." [1]

This appendix contains a simple numerical example of the basic self-organising algorithm. The rule update at one time instant is calculated in detail.

The output behaviour is given in Table A2.1. The reference signal is constantly kept at seven and the scaling factors are G_e = 0.2 and $G_{\Delta e}$ = 0.5. The errors and change of errors are calculated according to (5.4) and distances and diminishing of distances in accordance to (5.11) and (5.12). All the calculated values are presented in Table A2.1.

Table A2.1 The output signal, calculated scaled errors and change of errors, calculated distances and diminishing of distances at discrete time instances *k*.

k	y	e	Δe	d^*	Δd
i-4	7.0	0.0	-	-	-
i-3	7.5	-0.1	-0.25	0.2475	-
i-2	8.0	-0.2	-0.25	0.3182	-0.0707
i-1	7.0	0.0	0.5	0.3536	-0.0354
i	6.0	0.2	0.5	0.4950	-0.1414

The membership functions of both e and Δe are in this example exactly the same and they are shown in Fig. A2.1. The original controller rule base is shown in Fig. A2.2 and the performance criterion q rule base in Fig. A2.3.

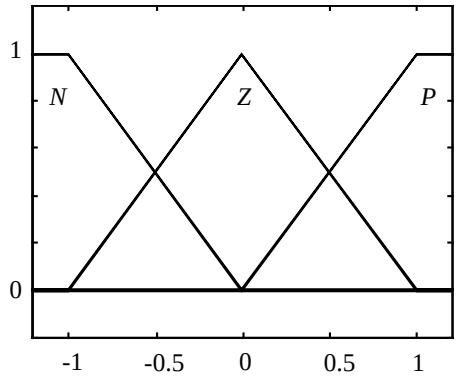

Fig. A2.1: The membership functions of e and Δe

		e		
		N	Z	P
	N	-16	-3	0
Δe	Z	-2	0	1
	P	0	2	14

Fig. A2.2: The controller rule base

		e		
		N	Z	P
	N	Q_2	Q_1	Q_0
Δe	Z	Q_1	Q_0	Q_1
	P	Q_0	Q_1	Q_2

Fig. A2.3: The performance criterion rule base

The membership functions of the performance criterion rule base are singletons. Their numerical values are $Q_0 = 0$, $Q_1 = 0.3$ and $Q_2 = 1$. The required process parameters are the average time constant $\overline{n}_\tau = 2$ and the process gain sign $M = 1$. The learning factor $L = 1$.

The evaluation of the performance begins by fuzzyfying the variables

$$\begin{cases} \hat{\mathbf{e}}(k) = \begin{bmatrix} 0 & 0.8 & 0.2 \end{bmatrix}^T \\ \Delta\hat{\mathbf{e}}(k) = \begin{bmatrix} 0 & 0.5 & 0.5 \end{bmatrix}^T \end{cases}$$

The lower right hand square is activated in the performance criterion rule base.

		e		
		N	Z	P
	N	Q_2	Q_1	Q_0
Δe	Z	Q_1	Q_0	Q_1
	P	Q_0	Q_1	Q_2

The activation level of each of the output singletons is calculated with the basic max-min composition that is explained in detail in e.g. (Ross [107])

$$\mu_{Q_0}(q) = \min\left\{\mu_{e_Z}(e(i)), \mu_{\Delta e_Z}(\Delta e(i))\right\}$$
$$= \min\{0.8, 0.5\} = 0.5$$
$$\mu_{Q_1}(q) = \max\left\{\min\{0.2,0.5\}, \min\{0.8,0.5\}\right\}$$
$$= \max\{0.2,0.5\} = 0.5$$
$$\mu_{Q_2}(q) = \min\{0.2,0.5\} = 0.2$$

The output of the fuzzy inference is a fuzzy variable

$$\hat{\mathbf{q}} = \left[\mu_{Q_0}(q), \mu_{Q_1}(q), \mu_{Q_2}(q)\right]^T = [0.5,0.5,0.2]^T$$

that is defuzzified with the centre of gravity method in accordance to (5.9)

$$q = \frac{\begin{bmatrix} Q_0 & Q_1 & Q_2 \end{bmatrix}\begin{bmatrix} 0.5 \\ 0.5 \\ 0.2 \end{bmatrix}}{\begin{bmatrix} 1 & 1 & 1 \end{bmatrix}\begin{bmatrix} 0.5 \\ 0.5 \\ 0.2 \end{bmatrix}} = \frac{0 + 0.15 + 0.2}{0.5 + 0.5 + 0.2} \approx 0.2917$$

With the given values of e and Δe the distance from the optimal line should be diminishing at rate q = 0.2917, but in fact the distance is increasing and the performance criterion is not fulfilled

$$\Delta d(i) = -0.1414 < q = 0.2917$$

and therefore the controller rule base needs updating. The required correction is calculated according to (5.13) and (5.14)

$$r(i) = 1 \cdot p(i) = L \cdot \left(q - \Delta d(i)\right) \cdot \text{sign}\left(e(i) + \Delta e(i)\right)$$
$$= 1 \cdot (0.2917 + 0.1414) \cdot 1 = 0.4331$$

The average time constant describes the discrete time interval of the maximum correlation from input changes to output changes. In this example the control actions two time instances earlier have the maximum effect in the present state. The rules that were activated at time instant i-2 have to be corrected if the state at time instant i does not meet the performance criterion.

When $\{e(i-2), \Delta e(i-2)\} = \{-0.2, -0.25\}$ is fuzzified, this results in

$$\begin{cases} \hat{\mathbf{e}}(i-2) = \begin{bmatrix} 0.2 & 0.8 & 0 \end{bmatrix}^T \\ \Delta\hat{\mathbf{e}}(i-2) = \begin{bmatrix} 0.25 & 0.75 & 0 \end{bmatrix}^T \end{cases}$$

and the upper left hand square is activated

		e		
		N	Z	P
Δe	N	−16	−3	0
	Z	−2	0	1
	P	0	2	14

The activation levels of the control action singletons are as follows

		μ_e		
		N	Z	P
$\mu_{\Delta e}$	N	0.2	0.25	0
	Z	0.2	0.75	0
	P	0	0	0

The defuzzified control action at time instant i-2 is calculated according to (5.9)

$$u(i-2) = \frac{\begin{bmatrix}-16 & -3 & -2 & 0\end{bmatrix}\begin{bmatrix}0.2\\0.25\\0.2\\0.75\end{bmatrix}}{\begin{bmatrix}1 & 1 & 1 & 1\end{bmatrix}\begin{bmatrix}0.2\\0.25\\0.2\\0.75\end{bmatrix}} \approx -3.1056$$

Based on the correction factor calculated earlier, the control action should have been

$$u(i-2)^* = r(i) + u(i-2) = 0.4331 - 3.1056 = -2.6725$$

The positions of the activated singletons are changed in order to achieve the corrected control, if the same process situation occurs again. Each singleton is changed with respect to its activation level. The following notation is used for singletons and their activation levels:

$$\begin{matrix}u_{11} & u_{12}\\ u_{21} & u_{22}\end{matrix} \quad \text{and} \quad \begin{matrix}\mu_{11} & \mu_{12}\\ \mu_{21} & \mu_{22}\end{matrix}$$

and for the defuzzification of the control action:

$$u = \frac{\begin{bmatrix}u_{11} & u_{12} & u_{21} & u_{22}\end{bmatrix}\begin{bmatrix}\mu_{11}\\\mu_{12}\\\mu_{21}\\\mu_{22}\end{bmatrix}}{\begin{bmatrix}1 & 1 & 1 & 1\end{bmatrix}\begin{bmatrix}\mu_{11}\\\mu_{12}\\\mu_{21}\\\mu_{22}\end{bmatrix}}.$$

Each singleton is corrected

$$\begin{bmatrix}u_{11}^*\\u_{12}^*\\u_{21}^*\\u_{22}^*\end{bmatrix} = \begin{bmatrix}u_{11}\\u_{12}\\u_{21}\\u_{22}\end{bmatrix} + \begin{bmatrix}r_{11}\\r_{12}\\r_{21}\\r_{22}\end{bmatrix}.$$

The individual correction factors are calculated as follows

$$\begin{bmatrix} r_{11} \\ r_{12} \\ r_{21} \\ r_{22} \end{bmatrix} = \begin{bmatrix} \mu_{11} \\ \mu_{12} \\ \mu_{21} \\ \mu_{22} \end{bmatrix} \cdot \frac{\mu_{11} + \mu_{12} + \mu_{21} + \mu_{22}}{\mu_{11}^2 + \mu_{12}^2 + \mu_{21}^2 + \mu_{22}^2} \cdot r \approx \begin{bmatrix} 0.1719 \\ 0.2321 \\ 0.1719 \\ 0.6447 \end{bmatrix}$$

It can be easily verified that the correction factors and the activation levels of the singletons have the same ratios with respect to each others

$$r_{11} : r_{12} : r_{21} : r_{22} = \mu_{11} : \mu_{12} : \mu_{21} : \mu_{22}$$

The rules are corrected

$$\begin{bmatrix} u_{11}^* \\ u_{12}^* \\ u_{21}^* \\ u_{22}^* \end{bmatrix} = \begin{bmatrix} u_{11} \\ u_{12} \\ u_{21} \\ u_{22} \end{bmatrix} + \begin{bmatrix} r_{11} \\ r_{12} \\ r_{21} \\ r_{22} \end{bmatrix} = \begin{bmatrix} -16 \\ -3 \\ -2 \\ 0 \end{bmatrix} + \begin{bmatrix} 0.1719 \\ 0.2321 \\ 0.1719 \\ 0.6447 \end{bmatrix} = \begin{bmatrix} -15.8281 \\ -2.7679 \\ -1.8281 \\ 0.6447 \end{bmatrix}.$$

If the same process situation is repeated and the corrected rules are used for fuzzy inference, the desired control action is achieved

$$u(i-2)^* = \frac{\begin{bmatrix} -15.8281 \\ -2.7679 \\ -1.8281 \\ 0.6447 \end{bmatrix}^T \begin{bmatrix} 0.2 \\ 0.25 \\ 0.2 \\ 0.75 \end{bmatrix}}{\begin{bmatrix} 1 & 1 & 1 & 1 \end{bmatrix} \begin{bmatrix} 0.2 \\ 0.25 \\ 0.2 \\ 0.75 \end{bmatrix}} \approx -2.6725.$$

It is to be noted that the correction calculated above would change the position of the origin (e,Δe) = [0,0) of the rule base. The pH application controller contains an external integral action that eliminates the steady state error and as a result there is no need to change the origin. The change would only cause unnecessary problems and therefore the origin is fixed in the real controller. This means that the rule

IF $e(k) = Z$ AND $\Delta e(k) = Z$ THEN $u(k) = 0$

cannot be changed by the self-organisation algorithm. If the same rule would be fixed in this example, the final corrected rule base would be

		e		
		N	Z	P
Δe	N	−15.8281	−2.7679	0
	Z	−1.8281	0	1
	P	0	2	14

Coodardy (adj.)

Astounded at what you've just managed to get away with. [1]

Beppu (n.)

The triumphant slamming shut of a book after reading the final page. [1]

HELSINKI UNIVERSITY OF TECHNOLOGY CONTROL ENGINEERING LABORATORY

Editor: H. Koivo

Report 114 Hasu, V.,
Design of Experiments in Analysis of Flotation Froth Appearance. April 1999.

Report 115 Nissinen, A. S., Hyötyniemi, H.,
Analysis Of Evolutionary Self-Organizing Map. September 1999.

Report 116 Hätönen, J.,
Image Analysis in Mineral Flotation. September 1999.

Report 117 Hyötyniemi, H.,
GGHA Toolbox for Matlab. November 1999.

Report 118 Nissinen, A. S.
Neural and Evolutionary Computing in Modeling of Complex Systems. November 1999.

Report 119 Gadoura, I. A.
Design of Intelligent Controllers for Switching-Mode Power Supplies. November 1999.

Report 120 Ylöstalo, T., Salonen, K., Siika-aho, M., Suni, S., Hyötyniemi, H., Rauhala, H., Koivo, H.
Paperikoneen kiertovesien konsentroitumisen vaikutus mikrobien kasvuun. September 2000.

Report 121 Cavazzutti, M.
Fuzzy Gain Scheduling of Multivariable Processes. September 2000.

Report 122 Uykan, Z.
Intelligent Control of DC/DC Switching Buck Converter. December 2000.

Report 123 Jäntti, R.
Power Control and Transmission Rate Management in Cellular Radio Systems - A snapshot analysis approach. May 2001.

Report 124 Uykan, Z.
Clustering-Based Algorithms For Radial Basis Function and Sigmoid Perceptron Networks. June 2001.

Report 125 Hyötyniemi, H.
Multivariate Regression - Techniques and tools. July 2001.

Report 126 Kaartinen, J.
Data acquisition and analysis system for mineral flotation. October 2001.

Report 127 Ylén, J.-P.
Measuring, modelling and controlling the pH value and the dynamic chemical state. November 2001.

ISBN 951-22-5782-3

ISSN 0356-0872

Picaset Oy, Helsinki 2001